A STATISTICAL INVESTIGATION OF EL. BREAKDOWN IN ASKAREL

VICTOR EDWIN RUDINSKAS
ELECTRICAL ENGINEERING
M. ENG.

A STATISTICAL INVESTIGATION OF ELECTRIC BREAKDOWN IN ASKAREL

by

Victor Edwin Rudinskas B.Eng. (Electrical)

A thesis submitted to the Faculty of Graduate Studies in partial fulfilment of the requirements for the degree of Master of Electrical Engineering.

Department of Electrical Engineering
McGill University
Montreal October 1977

ACKNOWLEDGEMENTS

I would like to express my deep gratitude and appreciation to:

Dr. F. Spitzer for his support, guidance, unending patience and understanding throughout the course of the work and his assistance in the preparation of this thesis

Mr. J. Földvári of the Electrical Engineering Mechanical Workshop to whom goes my heartfelt thanks, whose expert advice and prompt work helped overcome many difficulties with the experimental apparatus

Prof. Thorpe of the Computing Center who generously provided computer time

Dr. L.E. St. Pierre, Chairman of the Chemistry Department, who provided the services of his department's glass blower when no other was available

Dr. P. Bélanger, who on behalf of the Electrical Engineering Department kindly gave me some financial assistance.

M. Eng. Electrical Engineering

Victor E. Rudinskas

A STATISTICAL INVESTIGATION OF ELECTRIC BREAKDOWN IN ASKAREL

ABSTRACT

Electrical breakdown experiments were conducted in liquid dielectrics under uniform field conditions. A synthetic dielectric (Monsanto 7030) was mainly used but a few experiments were conducted in mineral oil. The liquid was carefully prepared by degassing and filtration through glass sintered filters which formed an integral part of the test cell apparatus. Steadily rising d.c. voltages at rates ranging from 0.3 kV $sec.^{-1}$ to 30 kV $sec.^{-1}$ were applied to two spherical nickel electrodes of 5 mm. diameter at separations of 100 to 250 microns. The rate of voltage rise and the time delay between successive voltage applications were automated to eliminate observer bias.

The appropriateness of the extreme value distributions and the log-normal distribution in describing the observed distributions of breakdown voltages was tested by calculating the parameters of these distributions from the observed data by numerical methods and applying the Kolmogorov-Smirnov Goodness-of-fit test. It was found that the Weibull distribution was best, the log-normal second. The shape parameter of the Weibull distribution increased with increasing gap length.

Computer produced breakdown voltage density plots accurately made by using the "pile of sand" technique, showed multiple peaks for breakdown voltages above 5 kV, indicating the existence of several different breakdown mechanisms. The effect of the rate of rise of voltage on the breakdown probability was studied. The probability of breakdown for a particular voltage was found to increase with the rate of voltage rise.

RESUMÉ

Expériments du claquage électrique des diélectriques liquides ont été faits sous condition de champ uniform. Une diélectrique synthetique (Monsanto 7030) ont été employé pour la plupart des expériments mais il y en avait aussi des expériments de comparison fait avec huile mineraie. La liquide a été preparée soigneusement par un extraction de l'air èt la filtration par des filtres composés du verre sintré le tout qui a fait partie intégral de la cellule d'essaie. Tension continue qui croissait à l'ordre de 0.3 kV $sec.^{-1}$ jusqu'à 30 kV $sec.^{-1}$, a été appliquée aux deux electrodes sphericals de nickel de diamétre de 5 mm. avec une séparation de 100 microns jusqu'à 250 microns. La montée continue de la tension et le délai entre les applications successives de voltage étaient automatisés dans le but d'éliminer le biais d'observateur.

L'applicabilité des lois de probabilités des valeurs extrêmes et de la distribution log-normal comme un description des distributions de voltage du claquage observées a été examinée par la calculation des paramètres de ces distributions par méthodes numerical et l'application du "Kolmogorov-Smirnov Goodness-of-fit test". Il était constaté que la loi de Weibull était le mieux, celle du log-normal était seconde. La paramètre de forme de la loi Weibull a crûe avec une augmentation de la distance entre les électrodes.

Courbes de la densité de la voltage du claquage produisées par un ordinateur en employant la mèthode du "tas de sable" (pile of sand) ont montrées des pointes multiples pour des voltages de claquages au-dessus 5 kV, démonstrant ainsi l'existence de plusieurs mécanismes du claquage differénts. L'effet de la vitesse de la montée de la tension a été étudié. Il était constaté que la probabilité de claquage a crûe avec la vitesse de la montée de la tension.

To my Parents

and

my sister, Leona

TABLE OF CONTENTS

APPENDICES

LOCATION OF FIGURES AND TABLES

TABLE OF SYMBOLS

a = a constant not dependent on voltage

a' = a constant

B = $\delta_o/(a+1)$

b' = a constant

B_j' = event due to a particular type of flaw in dielectric

c = parameter of type II distribution

c_a = $a+1$

c' = $c_o \sum_{j=1}^{n} w_j^{b'} n_j$, a constant

c'' = $c_o \int_{\text{whole volume stressed}} w^{b'}\,du$

c_j = a constant

C_o = constant $\bar{t}^R \bar{E}^R$

c_o = c_j/n_j

D = Deviation of actual distribution function from the assumed distribution function for a particular random variable

E = electrical stress

E' = notional electrical breakdown stress due to only one factor

$\bar{E}$ = particular value of electrical stress

E_1 = arbitrarily chosen value of electric stress

$\bar{E}$ = particular value of stress

E_B = applied field between electrodes away from the tip of a particle bridge

E_d = randomly distributed part of the breakdown stress

E_j = applied stress in a small volume element of the system

E_m = an electric stress at which breakdown occurs

ΔE = increment of electric field

E_o = a refernece electrical stress

E_T = a threshold field strength, below which no electrons are emitted

F(x) = cumulative probability function according to different conditions set on x

f(x) = probability density of x according to different conditions set on x

f_a = "after effect" function

F_B = probability of breakdown

$F_o(x)$ = assumed or null distribution function

F_p = probability of failure of entire system

f_p = failure probability for small volume dielectric liquid

$g(E-E_d)$ = non-random component of breakdown voltage

G_n = moment generating function

H(x) = cumulative hazard function

h(x) = hazard function

I = number of electrons emitted per second

I_m = number of electrons emitted per second at stress E_m

k = shape parameter of type III extreme value distribution (Weibull)

1/k' = a nondimensional constant

k_B = Boltzmann constant

k_c = constant depending on deviation from symmetry in the process of attracting particles

K_s = ratio of gap spacing to sphere electrode radius

L = length of cable sample

m = a number of sample observations such that m is less than n

N = constant Q/R

n	=	sample size of observations
n_j	=	V_j / V_o
N_R	=	Reynolds number
$P(x)$	=	cumulative probability function according to different conditions
$p(x)$	=	probability density of x according to different conditions on x
$P_B(E,r_a)$	=	Breakdown probability distribution obtained by convolution of $T(E,r_a)$ and $q(E_d)$, the distributed part of ${}^{a}\Upsilon$
$P_f(E)$	=	probability of breakdown occurring within a time interval t to t + dt after the instant a step function voltage is applied.
P_j	=	probability of survival of a small volume element
P_l	=	hydrostatic pressure
P_m	=	probability of breakdown occurring within a time interval t to t + td after the instant a step function voltage E_m is applied
P'_m	=	probability of breakdown when a train of N pulses at stress E_n are applied
P_s	=	survival probability
Q	=	constant not dependent on voltage
$Q(E)$	=	continuous variable equivalent of Q_n
Q_n	=	probability of breakdown at a level E_n in any succession of pulses
$q(E_d)$	=	first asymptotic distribution of stress E_d
R	=	constant not dependent on voltage
dR	=	incremental portion of radius R
r	=	root of an equation
r'	=	a dummy variable
r_a	=	a particular rate of rise of voltage

r_p = particle radius

R_1 = the outer radius of two concentric cylinders modeling a length of cable

$R_1(r_a)$ = probability distribution of the occurrence of breakdown due to a rate of voltage rise r_a

$R_k(r_a)$ = distribution of breakdown due to a multiple k of voltage rise r_a

R_o = the inner radius of 2 concentric cylinders modelling a length of cable

r_s = sphere radius

s_x^2 = standard deviation

T = absolute temperature

t = time

$\bar{t}$ = particular value of time

$T(E,r_a)$ = time dependent component of the breakdown probability distribution function obtained from $g(E - E_d)$, the nonrandom component of Υ

$T_C(E,r_a)$ = cumulative distribution function of $T(E,r_a)$

t_f = formative time of breakdown

t_p = voltage pulse duration

t_s = statistical time lag

U = average breakdown stress

u = variable of integration

u_1 = characteristic smallest value

u_e = mean of the logarathms of random variable x

u_i = i^{th} central moment of sample values x_i

u_m = characteristic m^{th} smallest value

v = voltage

dV = incremental volume element

v' = parameter associated with type III extreme value distribution

v_1 = characteristic smallest value associated with type II extreme value distribution

v_f = forward velocity of fluid

ΔV_j = a small volume element under uniform electric stress

ΔV_o = small element of volume used as a reference volume

v_p = velocity of particle relative to fluid containing it.

x = random variable; initial variate

$\bar{x}$ = mean of the type III (Weibull) distribution

$\bar{x}_o$ = average of sample values x_i

x_1 = the smallest value of x among n independent observations

X' = minimal value of x from among n independent observations

y = reduced variate

$\bar{y}_n$ = mean of reduced variate

$\overline{y^2}$ = mean squares of reduced variate

W = probability of electron initiating a breakdown

W_j = a parameter used to describe electric field and dependent on the geometry of the system

W_m = probability that an electron has of initiating a breakdown process when at stress E_m

z = random variable representing sample values distributed according to type II extreme value distribution

α = a constant employed in a linear transformation

α' = Weibull scale parameter

α_m = extremal intensity function

β = a constant employed in a linear transformation

β' = shape parameter

Γ = gamma function

γ = Euler's constant (0.57721.....)

γ' = location parameter

Δ = incremental amount

δ = breakdown frequency

δ_o = a constant not dependent on voltage

ϵ = location parameter of type III extreme value distribution

ϵ_e = permittivity of the liquid dielectric

ϵ_o = permittivity of free space

ϵ_p = permittivity of particles in dielectric liquid

ζ = θ^k, a dummy variable

η = viscosity

η' = a non-uniformity coefficient

θ = $(x - \epsilon)/(v_1 - \epsilon)$

Λ = number of pulse applications in a unit interval of stress

λ = dummy variable of integration

ν = notational superscript indicating the order of the derivative

ξ = particular observed sample value

π = pi (3.1416....)

ρ = skewness

ρ' = density of fluid

σ^2 = variance of the type III (Weibull) distribution

σ_e = standard deviation of the logarithms of the random variable x

σ_n^2 = standard deviation of reduced variate

σ_s = surface tension of the liquid

Υ (E) = Breakdown probability per unit time

$\Phi(\omega)$ = probability integral $\int_0^{\omega} \exp(-\omega^2/2)\, d\omega$

$_1\Phi(\ )$ = first asymptotic distribution function; also referred to as type I extreme value distribution, or double exponential distribtuion

$_2\Phi(\ )$ = second asymptotic distribution of smallest values, or type II extreme value distribution

$_3\Phi(\ )$ = third asymptotic distribution of smallest values, also called type III extreme value distribution or Weibull distribution

$_1\phi(\ )$ = density function corresponding to $_1\Phi(\ )$.

$_2\phi(\ )$ = density function corresponding to $_2\Phi(\ )$.

$_3\phi(\ )$ = density function corresponding to $_3\Phi(\ )$.

Ψ = particle flux in vicinity of electrode

ω = variable of integration

CHAPTER I

BREAKDOWN IN LIQUID DIELECTRICS

INTRODUCTION

CHAPTER I

BREAKDOWN IN LIQUID DIELECTRICS - INTRODUCTION

1.1 INTRODUCTION

There are many different theories concerning electrical breakdown in dielectric liquids. In general it can be said that some of them explain the breakdown mechanism using a macroscopic interpretation, such as, heat production in certain places in the liquid, especially at the cathode, irregularities on the cathode surface, the presence of impurities, colloidal suspensions, gas bubbles and vapour bubbles, non-uniform distribution of the electrical field, etc. Other theories consider the mechanism of breakdown from a microscopic point of view and derive the breakdown criterion on the basis of molecular structure.

The first group of theories refer to experimental conditions in which liquids of a commercial grade are used, which are not properly cleaned and degassed, and large fields of long duration are applied. Such conditions are used in most of the industrial and commercial work, and for this reason these theories are acknowledged and find application.

Theories connecting the phenomenon of breakdown with molecular structure of the liquid tested refer to experimental conditions where it is possible to observe the physical mechanism of breakdown regardless of the purity of the liquid. Under such conditions it is possible to measure various physical quantities for different types of liquids, even for small variations in the properties. Results obtained using liquids of high purity in this manner furnish the basis for a physical theory (1).

However, the breakdown of liquid dielectrics is now regarded inherently a statistical phenomenon (99) and the general concept of an 'intrinsic electric strength' is both unrealistic and incompatable with the probablility approach to dielectric failure. That there is a dominant random element is indicated indirectly by the fact that refinements of experimental technique and use of highly purified liquids have failed to reduce scatter of results, or to give results which could be reproduced by other workers. By using carefully controlled experimental technique, however, it is possible to identify those parameters which significantly affect the probability distribution of breakdown measurements and relate them to the statistical behavior (99).

1.2 PREBREAKDOWN PHENOMENA

Under experimental conditions, various pre-breakdown phenomena can be observed: light emission, acoustical disturbances, cavitation, dark spots and current pulses. To gain better insight into the breakdown mechanism, the progress of the breakdown must be observed carefully before, during and after its occurrence.

1.2.1 Light Emission

When a hydrocarbon insulating liquid is stressed, points of light or luminescent zones are observed within the stressed volume (40,102). The same phenomenon occurs in hexachlorodiphenyl (84). Smith and Calderwood (138) report that with a point-plane system in hexane, the point electrode being the cathode, light emission in the form of flashes from the tip of the point electrode was observed to take place at voltages within 20% of the breakdown voltage. These light flashes appeared at intervals ranging from seconds to minutes with a tendency to become less frequent and less intense with increase in the duration of time for which the slowly rising d.c. voltage was applied.

These observations constitute evidence for the presence of electrons with an energy of at least 2.5 eV in these liquids at high stress (139). In transformer oil this phenomenon has been interpreted as involving the acceleration of electrons and the resulting excitation of polycyclic aromatics. (13). On the other hand, the emission of prebreakdown light is also thought to arise from a gas discharge in a bubble in the liquid (50). For example, the light emitted from hexane is likely to result from such a microdischarge because it is only after the onset of cavitation that light is emitted in any significant amount (103). In contrast, not only are light levels in transformer oil greater than those in hexane, but there is significant emission prior to cavitation inception in non-uniform fields, as well as for sphere-sphere electrode configuration tests for which no bubbles were detected (103).

Another explanation is that light emission is due to microdischarges when charged particles approach an electrode (15). In support of this explanation, proponents observed photographically microdischarges when a metal sphere (about 3 mm in diameter) was placed between two planar electrodes, 8 mm apart, in transformer oil.

1.2.2 Shaded Areas

Under direct voltage conditions, a spray of bubbles and an intermittent blue light appear at the point cathode when the applied voltage is of the order of 10 kV with a gap length of several millimeters (29). As the direct voltage is further increased to approach the direct breakdown voltage of the system, a dark diffuse region is observed in the vicinity of the cathode (85, 135). This region, which is called the discharge region, bears resemblence to regions of reduced density produced under pulse conditions (28). The nature of the shaded areas has not been clarified experimentally and opinion regarding their nature is divided. One hypothesis ascribes the phenomenon to bubbles too minute to be seen and which scatter the light, causing appearance of a darker area. The time required to build up bubbles makes this model questionable because the shaded areas have always appeared instantly, or at least within a time much too short to be measured (62). However, Krasucki, by his theory, has showed that in liquids like n-hexane, breakdown due to the formation and growth of a vapour bubble should occur in times of about 0.14 microsecond. This time is of the same order of magnitude as the formative time lags* in n-hexane which have been measured. Another explanation is that the shaded areas contain high local concentrations of charges of both signs like a plasma, in which case the light is scattered by fluctuations in the refractive index (86).

* (When a dielectric liquid is suddenly subjected to a high electric stress, it retains its insulating properties for a time before the formation of a low impedance path between electrodes. The statistical model divides this time into two components, a statistical lag t_s and a formative lag t_f. The time t_s is defined as the period between the application of stress and the appearance of an initiating event which will eventually lead to breakdown; t_f is the time required to complete a breakdown after the appearance of the critical initiating

event. These definitions are quite general, and no physical processes need be postulated for them. The only assumption required is that initiating events occur randomly at a mean rate f(E) when a stress E is applied to the electrode-liquid system.)

1.2.3 Cavitation

Cavitation occurs under non-uniform high field conditions. There is evidence that this results in such fields from the rapid collapse of a cavity or microbubble produced by electrostatic or thermal conditions. Detection of both sound at sonic and supersonic velocities and optical emissions are characteristic of cavitation, the onset of which is strongly temperature dependent (38).

1.2.4 Shock Waves

The generation of shock waves is believed to play an important role in the propagation of prebreakdown disturbances. It has been stated that the breakdown voltage of the system is raised by conditioning (see section 1.3.3) This suggests that the growth at the discharge region is related to the injected charge. The onset of growth is heralded by a weak shock wave indicating an abrupt energy change to the system (30). The presence of rapidly moving particles probably provides the necessary nucleation centers for the precipitation of cavities in their wake (16,2).

1.2.5 Current Fluctuations

In very high fields single large current pulses can be observed before breakdown occurs, as if local breakdowns occurred which do not pass the whole way between the electrodes. These are sometimes called microbreakdowns. The frequency of such ionizing pulses and their value depend on field intensity, the type of liquid and its purity, the presence and nature of gas dissolved in the liquid, electrode material, the condition of the electrode surfaces and temperature (2).

It is the motion of the charge carriers in the liquid which is responsible for the random nature of the conduction current and its fluctuations. It is reasonable to assume that at low fields, ions will play an important part. Ions can originate in the bulk liquid either by dissociation of impurities or by absorption of external radiation, while the electrons result from cathode emission. There are at least three ways in which electrons can contribute to conduction:

1) They may become attached to molecules and the resulting ions will move under the influence of the applied field.
2) They may jump from molecule to molecule in the field direction.
3) They may be accelerated by the applied field

and move through inter-molecular spaces, suffering elastic or inelastic collisions.

Which of these mechanisms is operative in a particular case will depend on the liquid itself and its temperature. (140).

1.2.6 Ion-induced Liquid Motion

Experiments in hexane using sphere-sphere 1/4" electrodes of stainless steel were done by Smith and Calderwood during which a dye stream flowed under gravity over each electrode (gap length = 2 cm.). When a steady 200 volts d.c. was applied to the gap, each dye stream was deflected away from its respective electrode. At 1,000 volts globules of the dye moved right across the gap in either direction alternately. By 2000 volts there was a general turbulence of the liquid between electrodes and the dye stream in this region was completely dispersed. By 20 kV the turbulence was visible as rippling at the free surface of the hexane. The effects were more pronounced when a higher purity hexane (suitable for spectroscopy) was used (138).

Ostroumov (1954) presented a theory based on a hydrodynamic interpretation of the conduction current in highly stressed liquid dielectrics, from which a conclusion is that highly stressed liquid dielectrics cannot be stationary (141). Nelson and

McGrath observed that circulating transformer oil produced an oscillating autocorrelation function of pre-breakdown conduction current pulses, whereas, stationary oil produced only a simple exponentially decaying ACF. Oscillating and non-oscillatory ACF's for gas-saturated and degassed oil respectively were found, leading them to conclude that the presence of gas in solution is a factor affecting liquid motion. It was inferred that positive gaseous ions are responsible for the drag mechanism bringing about motion (104).

1.3 OTHER FACTORS AFFECTING BREAKDOWN STRENGTH OF A LIQUID

1.3.1 Electrode Effect

There are strong reasons for supposing that it is the value of the stress at the electrode surface which is critical in determining the probability of breakdown (95):

1) the measured strength is somewhat smaller than might be reasonable as an 'intrinsic' strength on the basis of knowledge of gases and solids
2) the breakdown probability is dependent on the nature of the electrode material
3) virtually all the physical models that have been proposed for liquid breakdown depend upon an initiatory mechanism at the electrode surface.

Electron emission from the cathode and the mechanism of the formation of an avalanche of electrons and ions greatly influence the breakdown strength. Consequently this strength shows dependence on the electrode material used. This is accounted for by the variation in the gas absorbance of the metals. Charge carriers in the liquid, will drift to the electrode of sign opposite to that of the charge, creating a space charge. Some of the carriers, having given up their charge to the electrode,may continue to adhere there forming an insulating layer which may greatly affect the subsequent formation of space charge at or near the electode (142). Such a layer on the cathode makes the process of neutralization of positive ions arriving at the cathode difficult, and the space charge produced increases the electrical stress in the layer. This may result in a microbreakdown and in the creation of a microbubble of plasma (60). The presence of a layer of gas on the surface of the electrode influences the emission of electrons (61). By initiating a microbreakdown at the surface of an electrode , Gzowski et al. (59) found that the average electrical stress which resulted in breakdowns was several times smaller than the breakdown stress without triggering. Thus, a breakdown of the insulating film on the occasion of a microbreakdown provides a smaller effective gap and increases available free charge.

Kao(90) has proposed a new theoretical model for impulse high-field conduction and breakdown in liquids based on the idea that high-field conduction is due mainly to electron emission from unavoidable asperities on the metallic cathode. The current, however is mainly confined to one or more filamentary paths, in which the current density is much larger than that in other regions instead of being uniform as previous theories have assumed. There is at least one filamentary path in which the current density may reach a critical value so that the joule heating produced in it is sufficient to initiate thermal instability and hence the onset of the breakdown process. The mathematical expressions developed take account of the temperature, hydrostatic pressure, gap length, molecular structure and applied voltage waveform. Computed results are reported to be in good agreement with currently available experimental results for saturated hydrocarbon liquids and aromatic hydrocarbon liquids.

1.3.2 Effect of Bubbles on the Breakdown Process

Since the electric field in a bubble will be greater than the average field in the liquid, owing to the different permittivities, a bubble on the electrode surface would likely enhance the emission of electrons from the underlying metal (61). Because of the build-up of space charges, the gap will be non-uniformly stressed. Positive and negative space charges will enhance fields in the cathode and anode regions respectively. It is therefore more likely that a discharge will be initiated inside a bubble formed in one of those regions rather than in a bubble formed in the bulk of the liquid (160).

Krasucki (84) developed a theory of breakdown in uniform fields by assuming that the dark regions observed (see section 1.2.2) in breakdown experiments were bubbles of vapour which were at a pressure close to zero. This would account for the quick disappearance of these regions with the removal of the electric field. Under the effect of the field, electrical energy injected into the growing bubble is converted into heat which vapourizes the liquid. Once formed, the vapour regions grew until breakdown. Points of zero pressure, according to the theory, are most likely to form in the presence of particulate impurities. The condition for the development of a point of zero pressure at the surface of the particle is:

$$E = 358\sqrt{(1/\epsilon_1)(P_1 + 2\sigma_s/r)} \quad \text{V/cm} \quad (1)$$

where

ϵ_1 = relative permittivity of the liquid
P_1 = (dyne/cm^2) hydrostatic pressure of the liquid
σ_s = (dyne/cm) surface tension of the liquid
r = (cm) radius of the particle.

Whenever this condition is satisfied, it is assumed that the vapour bubble grows to a size at which breakdown occurs.

It was shown that this expression gave good predictions for the known dependencies of breakdown strength of n-hexane on both temperature and pressure and for the observed increase in the breakdown strength of aliphatic hydrocarbons with increasing molecular weight. Though the molecular weight does not appear in the equation, any variations on breakdown strength must be due to variations in surface tension and permittivity between the different liquids in the aliphatic series.

1.3.3 Effect of Additives

Water added to very pure transformer oil causes a considerable decrease in the breakdown strength This effect is explained by the great ability of water to dissociate and produce a large quantity of ions in the bulk of the liquid as well as in the vicinity of the electrodes. Addition of iodine to an oil in the amount of 0.01 g per liter increased the breakdown stress value by 18% but greater doses reduced it (3). The addition of p-nitrotoluene to petroleum derived oil increases its electric strength by 48% (3). The effect of selenium is very pronounced in improving the breakdown strength and is attributed to the formation of a protective layer on the electrode surfaces (3).

When an electric discharge takes place in an insulating liquid, gas is evolved, which may or may not be absorbed by the liquid. In mineral oil the gas produced is mainly hydrogen and gaseous hydrocarbons and the amount absorbed improves both with increasing aromatic content and volume of oil (119).

An electric discharge in askarel, however, produces hydogen chloride which is corrosive to metals and attacks cellulosic insulation. To prevent such deterioration a compound known as a "scavenger" is added to basic askarel to react with and absorb any dissolved hydrogen chloride. Tin tetraphenyl is used as a scavenger (see Table 2-1). It reacts with the hydrogen chloride to form benzene and non-ionizing complex tin chlorides. Though this compound can effectively eliminate occasional minor arcing occurring under normal operating conditions, it may be unable to cope with the larger quantities of gas produced by heavy arcing (9).

Zaky et al. (158) found that the same additive concentration which gave a maximum in the breakdown characteristics, gave a minimum in the gas evolving characteristics of the oil and vice versa. This correlation provides further experimental evidence in support of the theory that the breakdown process, particularly in its later stages, is governed by the presence of a gaseous phase; that the breakdown of an insulting liquid is initiated and governed by a gaseous discharge inside gas bubbles formed in the liquid.

For additive-free oil the most effective of the dissolved gases in increasing the electric breakdown strength of oil is oxygen and the least effective is hydrogen.

1.3.4 Effect of Particles

Particles exist in the liquid either because they are too small to be filtered out during the initial purification of the liquid, or are produced during "electrode conditioning". For example, it has been shown that in the breakdown of liquid argon, metal particles, ranging in diameter from 200-500 Å are produced (84).

When voltage is applied to the electrodes, the particles move toward the electrodes where there exist regions of maximum field strength. Some particles settle out on the electrode and recoil from it as a result of puncturing the oil film on the electrode surface and becoming charged. The higher the electric field strength, the more probable it becomes that particles will recoil from the surface. This process has a random nature. The particles may finally form a bridge between the electrodes if they are permanent dipoles. After the permanent dipoles form a bridge, electrons may be shown to move with relative ease along this bridge although permanent dipoles are essentially internally non-conducting particles (81). Admixtures of particle bridges simultaneously grow and breakdown. Volkov and Mit'kin (46) developed a statistical theory of bridge formation and derived the following formula for the growth of a single bridge:

$$\psi = \frac{4k_c}{3}\left[\frac{\epsilon_p - \epsilon_1}{\epsilon_p + 2\epsilon_1}\right]\frac{\eta_o r_p E_B}{\eta\Phi_{(z)}}\sqrt{k\ T_r}\ \text{particles/sec} \quad (2)$$

where

$$\Phi(\omega) \quad \frac{2}{\sqrt{2\pi}}\int_0^{\omega} \exp\left(\frac{\omega^2}{2}\right) d\omega \quad (3)$$

$$\omega = \frac{\epsilon_p - \epsilon_1}{\epsilon_p + 2\epsilon_1}\ r_p^2 E_B \sqrt{\frac{\epsilon_o \epsilon_1 \pi}{k\ T_r}} \quad (4)$$

where

k_c = a constant depending on deviation from symmetry in the process of attracting particles. (e.g. if it can be assumed all the particles are directed to the tip of the bridge from a half space, k =0.5)

ϵ_1 = permittivity of the liquid

ϵ_p = permittivity of the particles

η_o = particle concentration in the outer region

r_p = particle radius

E_B = the external field, not that near the top of the particle bridge

k_B = Boltzmann constant

T = temperature

η = viscosity of the liquid

Assuming that the particles in the liquid have an exponential size distribution as is suggested by Epstein's paper (42), it would be interesting to examine whether the above equation provides a criteria of breakdown when the gap length and particle distribution are known. The same authors have also formulated a theory on the growth of bridge systems. Their work is based in part, on that of Kok (81) who assumes that breakdown is caused by the formation of a bridge. Disruptive forces of diffusion due to the thermal energy of the particles, when equated to the electric force acting on the particles tending to concentrate them in the region of maximum field, provide a condition above which breakdown will sooner or later occur:

$$\frac{\epsilon_p - \epsilon_o}{\epsilon_p + 2\epsilon_o} \epsilon_1 r_p^3 E_B^2 > 1/4 \, k_B T \qquad (5)$$

where r_p = particle radius

E_B = field strength

T = absolute temperature in degrees Kelvin

ϵ_p = permittivity of the particle

ϵ_1 = permittivity of the liquid

How quickly a bridge can form is indicated by Kok (81) who speculated that the time t in which a particle could cross a gap d with constant velocity was:

$$t = 6\pi\eta / E_B^2 \qquad (6)$$

where η = viscosity (poise)

E_B = electric field strength (e.s.u.)

If the field is 10 kV/mm, in the c.g.s. system of units which applies to (6) corresponds to:

$$q = E_B(4\pi\epsilon_o)\, r_q^2 \text{ coulombs} \times 3 \times 10^9 \frac{\text{e.s.u.}}{\text{coulomb}}$$

where r_q is the distance of the test charge from charge q:

$$= \frac{10^7 \times (10^{-2})^2 \times 3 \times 10^9}{9 \times 10^9}$$

$$= 330 \text{ e.s.u.}$$

Thus for a viscosity for askarel where η = 0.146 poise* a particle would be able to cross the gap in 30 micro-seconds.

*Note: The kinematic viscosity of a liquid is the ratio of its viscosity to its density. The c.g.s. unit of kinematic viscosity is the "stoke". The c.g.s. unit for viscosity is the "poise". Therefore to convert from "stokes" to "poise", the figure in stokes for the kinematic viscosity is multiplied by its density. To convert from the unit of kinematic viscosity called "Saybolt Universal Seconds" which is often employed in giving viscosity data in North America, and as appears in Table 2, the following formula is used (144):

$$\eta_{Stokes} = 0.00226t_s - 1.95/t_s$$

where t_s = kinematic viscosity (Saybolt Universal Second)

η_{Stokes} = kinematic viscosity (Stokes)

The conversion to viscosity is, therefore:

$$\eta = \eta_{Stokes}/\rho'$$

where η = viscosity (poise),

η_{Stokes} = kinematic viscosity (Stokes)

ρ' = density (gm/cc^3)

It is not known how well this agrees with reality because it is usually assumed that Stoke's formula $F = 6\pi\eta r_p v_p$ (where η = viscosity, r_p = radius of a spherical particle , v_p = velocity of particle relative to the fluid.) agrees better with experimental data for large particles than for small ones (82). Also Stokes formula is valid only for slow uniform motions of spherical particles on which the forces of inertia acting on the particles and in the liquid may be neglected and only viscous friction forces in the liquid play a part. From a Reynolds number ($N_R = \rho' v_f / \eta$, where ρ' = the density of the fluid, v_f is its forward velocity and η = viscosity) of 5 onwards the forces of inertia in the flowing liquid begin to play a part and then Stoke's formula is no longer applicable, not even for shperical particles (83).(For water at 20°C flowing in a tube of 1 cm diameter with an average velocity of 10 cm/sec, the Reynolds number is about 1000.) This cause of deviations becomes even more important if the shape of the particles may not be assumed to be spherical (83).

1.3.5 Dependence of Electric Strength on the Number of Breakdowns

Breakdown values are lower for the first few breakdowns and increase systematically with the number of breakdowns and only after a certain number of breakdowns reach a steady mean value. This phenomenon is known as "conditioning". After this conditioning the breakdown stress of the liquid may have increased by 50-100%. This may be explained by assuming that the first breakdowns remove gas bubbles and impurities from the liquid and the surface of the electrodes (4). Nelson carried out experiments with large electrode areas of up to 2 m^2 and nevertheless found rapid conditioning despite their large area and capacitance. It may be supposed that the larger bubbles were removed by mechanical shock forces caused by the discharge of the cell capacitance (105).

Chadband (31) explains conditioning as an initial progressive decrease in the quantity of charge stored per pulse as pulsing of the system proceeds, The process is regarded as complete when a smaller, but relatively constant charge per pulse is obtained. The conditioning process is both time and voltage dependent (31). Conditioning using short duration pulses requires a greater number of pulses than is the case when longer pulses are employed. A system is conditioned to a particular voltage. Below this level of voltage reproducible results are obtained; however, if higher voltages are then employed, further conditioning occurs.

Shaded areas in connection with regions of reduced density which form at the point in liquid dielectrics has been already mentioned (sec. 1.2.2). These regions originated at the cathode and grew towards the anode to a distance dependent upon the magnitude of the applied voltage, so long as the pulse duration was sufficient to allow full growth. With a constant pulse amplitude, the maximum size of this region was observed to decrease with continued pulse application until a smaller but reproducible size was obtained coinciding with a conditioned state (31).

1.4 SKETCH OF PROBABLE EVENTS LEADING TO BREAKDOWN

The liquid in the gap is in turbulent motion and unless it is perfectly filtered there will also be movement of particles. (If the field is relatively slowly rising, a system of bridges between the electrodes may have developed). There will be an injection of electrons from any sharp points or protuberances at a negative potential followed by a corona and a spray of bubbles from negative points and subsequently from any positive points which are sharp enough (136). Sparks can be observed which do not bridge the gap but occur within the gas bubbles (137). At the onset of the spray, high values of conduction current appear. A dark region at the tip of the needle can be seen. Electrical discharges in bubbles cause the bubbles to grow due to vaporization and develop into a gas channel which propagates. This ultimately determines the breakdown strength. If these discharges are regarded as regions of highly conducting plasma in contact with the electrode, the breakdown of the gap seems to be due to the propagation of the plasma in the direction of the electric field (136). The breakdown tracks tend to follow lines of electric field along a path which can be represented as the surface of a cone describing the limit of the extent of the spray (136). If conditions are not propitious for propagation, the bubble may disintegrate into several smaller ones (159).

1.5 STATISTICAL APPROACH TO DESCRIBING BREAKDOWN

1.5.1 The Weak Link Concept

From a statistical point of view, the problems associated with the term "strength" as applied to different states of matter and phenomena, such as mechanical strength, electrical strength etc. are all essentially equivalent if we conceive of materials as being permeated by small defects spread in a random way throughout the body. These defects give rise to local weaknesses which may reduce the strength of a specimen locally to a value which is considerably smaller than the theoretical strength of the specimen. Assuming that the randomly distributed flaws have a certain density per unit volume (or unit area or unit length), the statistical nature of the problem becomes evident (42).

Assumptions on which the weakest link concept is based are:

1) A certain number of physical imperfections or other initiating events exist or are created within the material under investigation (99,25).
2) These flaws are randomly distributed throughout the material
3) These flaws are also randomly distributed with respect to size (99).
4) A breakdown is possible for a certain range of experimental values.
5) Each flaw can be the cause of a breakdown. Thus the probability of being the cause of a breakdown is the same for each flaw.
6) Flaws act independently of each other; the effect of the imperfections is not cumulative. This

idealization is a good approximation when the distance between the flaws is large as compared to their region of influence, and in the case of liquids, when the time intervals between breakdowns are large enough to ensure the return to normal of the test sample.

7) No one flaw is dominant, so that the probability that a certain predetermined flaw will cause breakdown is very small.
8) Breakdown of a part of the system coincides with the breakdown of the whole.

In liquid breakdown work, such flaws may be solid or gaseous impurities or other phenomena contributing to failure. Liquids offer the experimental advantage of a high degree of recovery, which, in conjunction with rapid discharge suppression circuits, permits the study of long sequences of measurements on a single sample. Having established the statistical properties of such a sequence, we can investigate the effect of a change in an experimental parameter, without having to consider the pronounced variations which are found in suposedly identical samples (19).

Experimental factors, some of which have already been examined, such as the correlation between impulse strength and the degree of oxidation of the electrodes, contribute to the breakdown probability in a trial. In some early experiments, manual control was used. The introduction of such arbitrary variations alter the statistical nature of the results. The resulting scatter of the results in a sequence of breakdown measurements can be analysed into four components (20):

a) a random component which is characterised by particular distribution properties determined by the physical nature of the breakdown process.

b) systematic component due to the deliberate variation of an experimental factor during the sequence, appearing as a change in the distribution parameters of (a).

c) systematic variation between different samples, which have received nominally identical preparation - i.e. the factor which has encouraged the study of breakdown sequences on a single sample.

d) a systematic variation in a sequence associated with the passage of time and the damage caused by previous discharges.

Unfortunately, (b) is often the smallest of these components; (c) and (d) are of little interest, and one attempts to eliminate them by adopting a test procedure in which the experimental parameter is alternated during a sequence of measurements on a single sample. The existence of (d) raises the question of the statistical stationarity of the sequence. If the random process is stationary, the mean and variance of of the distribution are independent of time (114). Strict stationarity requires that distribution parameters should remain unchanged throughout the sequence. There is a nonstationary region at the start of a breakdown experiment that is called "conditioning". This is followed by a "stable" region and then by another region called the "well sparked region" in which the strength deteriorates into wild erratic behavior (51). With efficient discharge suppression, the length of the stable region varies from about 15 breakdowns in the degassed liquid to several hundred in air saturated liquid (20).

1.5.2 Dependence of Dielectric Strength on Stress and Time

If the expected breakdown or failure probability of a volume of dielectric liquid in the interval of voltage from v to v $+\Delta v$ may be assumed to be (111):

$$f_p = \delta \, \Delta v \qquad (f_p \ll 1) \tag{6}$$

see 1.5.1 assumption #7

where δ is the breakdown frequency of the system depending in general on both time and voltage, then, the corresponding survival probability is:

$$1 - f_p = 1 - \delta \, \Delta v \tag{7}$$

If the entire voltage change is assumed divided into n intervals, the survival probability over the whole voltage change is:

$$p_s = \prod_{i=1}^{n} (1 - \delta_i \Delta v_i) \tag{8}$$

where δ_i represents the average value of δ over the interval of Δv_i. Consequently

$$\text{Log}_e\, p_s = \sum_{i=1} \log_e (1 - \delta_i\, \Delta\, v_i) \tag{9}$$

Making use of the expansion

$$\log_e x = \frac{x-1}{x} + \frac{1}{2}\left(\frac{x-1}{x}\right)^2 + \frac{1}{3}\left(\frac{x-1}{x}\right)^3 + \ldots.$$

and by neglecting all but the first term, we can approximate (9) by :

$$\log_e P_s \simeq -\sum \delta_i\, \Delta\, v_i \tag{10}$$

As $\Delta\, v_i \rightarrow 0$

$$\log_e P_s = -\int_0^v \delta_i(t,v)\,dv \tag{11}$$

Therefore, the probability of breakdown of the system can be written as

$$F_p(t,v) = 1 - \exp\left[-\int_0^v \delta\ (t,v)\,dv\right] \tag{12}$$

A small change in stress corresponds to several orders of time (21).

It will be seen in the next chapter that equation (12) is the general form of the distribution of extreme values. Depending upon the form that the expression

$$\int_0^v \delta(t,v)\,dv$$

in equation (12) takes, we may have the first, second, or third type of extreme value distribution.

A complete knowledge of the dependence of δ on time and stress cannot be obtained only by means of statistical considerations, as δ depends essentially on the physical considerations of the delectric and on the breakdown mechanism involved. The dielectric system cannot be considered as homogeneous when dominating effects occur such as ageing or when some parts of the system are subjected to strong partial discharges while other parts are ionization free, or if there are differences in the system environment so that single regions are differently stressed by chemical, mechanical or thermal agents. The statistical considerations should then be only separately applied to the single parts of the system under the same conditions or having the same environment (112).

If it is assumed that the dominating characteristics on the ageing of the dielectric are not present, then, if

$$\delta = \delta_0 v^a \qquad (13)$$

where δ_0 and a are parameters not depending on v, then if this is applied to equation (12) the Weibull distribution is obtained:

$$F(v) = 1 - \exp(-Bv^{c_1}) \tag{14}$$

where $B = \delta_o/(a+1)$; $c_1 = a + 1$

If we take account of assumption number 9 of the weak link concept (see section 1.5.1) - i.e. that the breakdown of a part of the system coincides with the breakdown of the whole system, then it follows that if P_s is the survival probability of part of the system for a time t and at a stress E, and the system is composed of n equal parts, the survival probability of the whole system for the same time and stress will be P_s^n. Therefore the joint distribution function must be so defined that the transformation of P_s into P_s^n does not change its character either with regard to time or stress. Assuming the condition that P = 1 for either t = 0 or E = 0, the most simple two dimensional distribution of survival probability satisfying these conditions is (112):

$$P_s(t,E) = \exp(-Kt^R E^Q) \tag{15}$$

where K, Q, and R are constants independent of t and E. This is consistent with equations (12) and (14) and the expected breakdown frequency would be:

$$\delta(t,E) = KRt^{R-1}E^Q \tag{16}$$

This can be written as:

$$P_s(t,E) = \exp\left[-\left(\frac{t}{\bar{t}}\right)^R \left(\frac{E}{\bar{E}}\right)^Q\right] \tag{17}$$

or, introducing the "breakdown or failure probability"

$$F_p(t,E) = 1 - \exp\left[-\left(\frac{t}{\bar{t}}\right)^R \left(\frac{E}{\bar{E}}\right)^Q\right] \qquad (18)$$

where $\bar{t}^R\bar{E}^Q = 1/C_o$ (19)

If a stress $\bar{E}$ is applied to the system, its survival probability after a time $\bar{t}$ according to (18) is:

$$P_s(\bar{t},\bar{E}) \cong 1/e = 0.365 \qquad (20)$$

If C_o is already known, by assuming a chosen value for $\bar{t}$, equation (19) makes it possible to determine the value of $\bar{E}$ corresponding to this time. Equation (19) can be written in the following way:

$$\bar{t}\,\bar{E}^N = \text{constant} \qquad (21)$$

where $N = Q/R$ (22)

Equation (21) is a relation between time and stress: the 'life function'.

The assumption that the breakdown of a volume element causes the breakdown of the whole system has been introduced as a general hypothesis (seq. 1.5.1). Therefore assuming that an insulating system can be divided into volume elements having different stresses, it follows that a joint time and stress distribution can be attributed to each element, the stress and time distribution of the whole system being the composition of all the single volume element distributions (113).

Let E_j be the value of the applied stress in an element j of the system, having volume V_j small enough so that the stress can be assumed to be uniform within it. The survival probability of this element will be (113):

$$P_j = \exp\left(-c_j t^{a'} E_j^{b'} \right)$$

The survival probability of the whole system composed of n elements will then be obtained by

$$P_s = \prod_{j=1}^{n} \exp(-c_j t^{a'} E_j^{b'})$$

$$= \exp\left(-t^{a'} \sum_{j=1}^{n} c_j E_j^{b'} \right) \qquad (23)$$

If E_o is a reference stress, then

$$E_j = E_o w_j \qquad (24)$$

where w_j is a parameter depending only on the geometry of the system. For example, the electric field near a rounded corner surface can be expressed as (74):

$$E = \frac{U}{X_G} \eta'$$

where U = the average breakdown stress, X_G = the gap distance and η' = a nonuniformity coefficient. Similarly, for concentric conducting cylinders, the electric stress between them can be expressed as a function of their respective radii.

Therefore, substituting in equation (23):

$$P_s = \exp\left(-t^{a'} E_o^{b'} \sum_{j=1}^{n} c_j w_j^{b'} \right) \qquad (25)$$

On the other hand, taking an element V_o as a refernce, c_j can be expressed as a function of the ratio:

$$n_j = V_j / V_o \qquad (26)$$

so that

$$c_j = c_o n_j \qquad (27)$$

Therefore,

$$P_s = \exp(-c_o t^{a'} E_o^{b'} \sum_{j=1}^{n} w_j^{b'} n_j)$$

$$= \exp(-c' t^{a'} E_o^{b'}) \qquad (28)$$

having assumed

$$c' = c_o \sum_{j=1}^{n} w_j^{b'} n_j \qquad (29)$$

If the system is continuous the preceding relation can be written:

$$c'' = c_o \int w^{b'} dn \qquad (30)$$

the integral being extended to all the stressed volume.

These relations find practical application where the volume has a simple geometrical shape. In the case of a cable, volume ΔV_j would be written as:

$$\Delta V_j = \pi L (R_{j+1}^2 - R_j^2) \; ; \quad R_o \leq R_j < R_1 \qquad (31)$$

where L is the length of a cable sample; R_o is the inner radius or the conductor and R_1 the radius over the insulation. Therefore

$$dV = 2\pi LRdR \qquad (32)$$

and from (26)

$$dn = \frac{2\pi LR}{\Delta V_o} dR \qquad (33)$$

If the stress E_o at the inner conductor is assumed as reference stress, then $w = R_o/R$. Occhini (111) has determined that for a cable to have a constant survival probability,

$$LR_o^2 t^{a'} E_o^{b'} \left[1 - \left(\frac{R_o}{R_1} \right)^{b'-2} \right] = \text{constant} \qquad (34)$$

$$b \neq 2$$

Tsumoto and Okai (148) described, with good experimental agreement, the impulse breakdown of oil-filled cable by a Weibull distribution.

1.5.3 Ward-Lewis Statistical Theory of Impulse Voltage Breakdown

Ward and Lewis (149) proposed a statistical interpretation of the breakdown mechanism in hexane based on the concept of electron availability. This concept is dependent only upon the assumption of a constant breakdown probability per unit time. They proposed that electrons are ejected randomly from the cathode at a mean rate I per second and that each electron has a probability W of initiating a breakdown process having a formative time t_f which is small. I is determined by cathode surface conditions and is likely to be a field aided thermionic process according to a Schottky law, and liquid properties determine W and t_f. All three quantities were considered dependent on field strength. If a step function voltage is applied, creating a mean stress E in the liquid, the probability of breakdown occuring within a time interval t to t + dt after the instant of voltage application is:

$$P_f(E)dt = W\,I\,\exp(\,-W\,I\,(t_p - t_f)\,)dt \qquad (35)$$

where t_p = the duration of a rectangular pulse, and $P_f(E) = 0$ if $E \leq E_T$ where E_T is a threshold field strength. The expression is valid only if $t_p \geq t_f$.

In a study of impulse breakdown strength, it is normal to apply a succession of pulses of duration t and increase their magnitude in steps of ΔE until the value of E_m is reached at which breakdown occurs. If at each level of stress N pulses are applied, the probability of breakdown at a stress E_m is then(150):

$$P'_m = 1 - (1 - P_f)^N \qquad (36)$$

$$= 1 - \exp(-I_m W_m tN) \qquad (37)$$

and the probability of a breakdown first occuring at a level E_n in any succession of pulses is:

$$Q_n = P_f n \prod_{m=0}^{n-1} (1 - P'_m) \qquad (38)$$

It is more convenient to express the breakdown probability Q_n by a continuous variable Q(E)dE which is defined as the probability of a first breakdown in the interval E to E + dE and writing Λ instead of n as the number of pulse applications in a unit interval of stress:

$$Q(E) = \Lambda P_f \exp(-\Lambda \int_{E_o}^{E} P_f dE \qquad (39)$$

It can be seen that this probability function does not vary in time.

Experiments were carried out by Ward and

Lewis with hexane, using stainless steel electrodes separated at a distance of 5 x 10^{-3} cm and voltage step function pulses lasting not more than 10^{-4} sec. at maximum stress (about 1.4 MV/cm).

The experimental curve obtained of average breakdown voltage plotted against pulse duration (10^{-4} sec.), bore striking resemblance to the sharply descending initial curvature of the theoretical curve. The sharp curvature was attributed not to a formative time but to the statistical requirements and the shape of the IW curve (151).

In a later paper (89) a modification of the physical interpretation of I, the number of electrons emitted per second, was presented: that since the first stage in a breakdown event in the light of further experiments showed it to be the occurrence of an extra large localized burst of electrons from the cathode, I represented the rate of occurrence of these bursts rather than a mean rate of I electrons per second. A freshly prepared cathode might have many active sites for these large bursts and conditioning could occur by successive removal of these. Each emitted electron has a certain probability of initiating a breakdown. Different electrode materials would give different values of I.

1.5.4 Continuous Voltage Application Case

For ramp function tests, one might be

tempted to treat these as a limiting case of impulse breakdown strength tests where the sequence of short rectangular pulses are merged and the waveform is a finite ascending staircase. However, once the time of stress application becomes appreciable, the effect of prestressing, plus several other slower processes, dominate the breakdown probability(22).

1.5.4.1 Rate of Rise Effect

Similar to the Ward and Lewis statistical model, Brignell suggests a model for ramp-function measurements by dividing the breakdown probability function per unit time Υ into two parts, a constant part $g(E - E_d)$ and a distributed part E_d such that:

$$\text{Probability } (E_1 < E_d < E_1 + E_d) = q(E_1)dE_d \qquad (40)$$

E_d has a Type I Extreme Value distribution (161) represented by $q(E_d)$. E_1 is an arbitrarily chosen electric stress. Division of the breakdown probability function is illustrated in Figure 1-1.

Suppose that the distribution for a rate r_a is given by $R_1(r_a)$, then the distribution for a rate kr_a can be obtained by application of the binomial distribution as follows. Let the probability that the effect occurs at rate r_a be termed a failure and be given by $R_1(r_a)$, that the event does not occur be termed a success and is given by $1-R_1(r_a)$. Hence the probability for 0 successes and k failures, in any

Υ(E) THE RAMP FUNCTION DISTRIBUTION OF BREAKDOWN VOLTAGES PER UNIT TIME SHOWN BROKEN INTO TWO COMPONENTS, q(E) and g(E). (23)

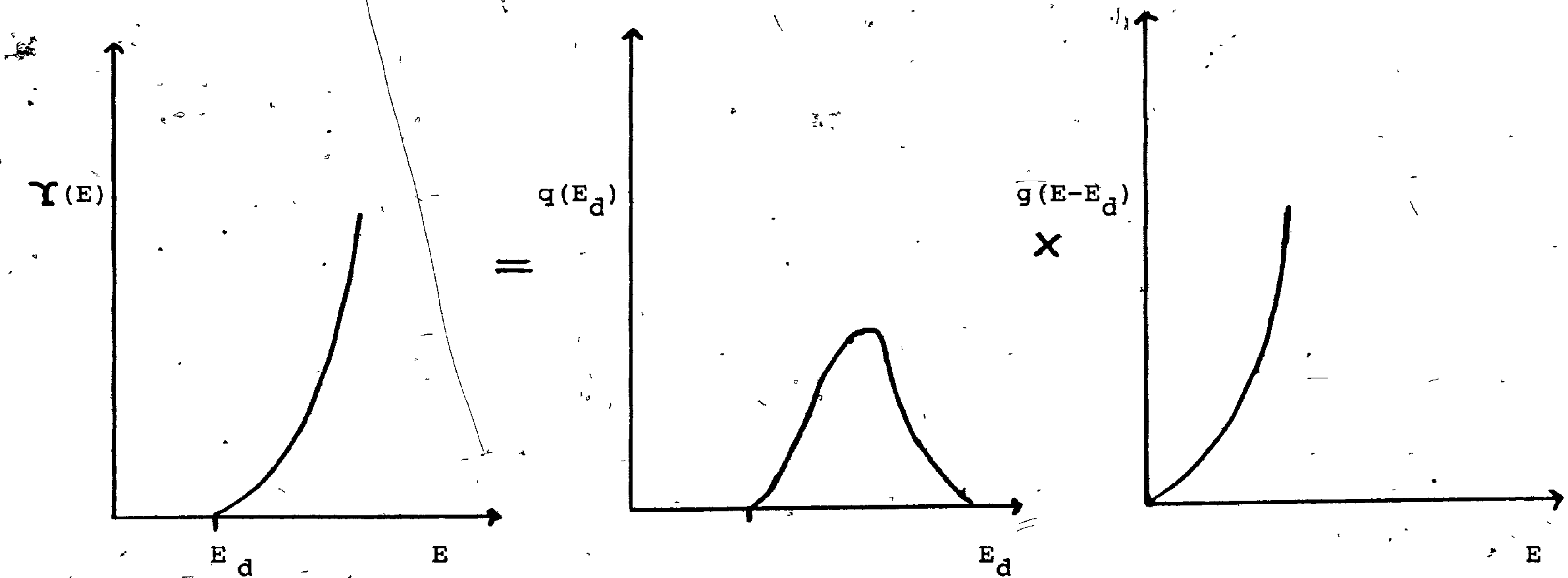

FIGURE 1-1

order is:

$$b(0;k,R_1(r_a)) = \frac{k}{k\ 0} R_1(r_a)\ \ 1 - R_1(r_a)^{\ k} \qquad (41)$$

Consequently, the probability distribution of an event occuring in k trials is:

$$R_k(kr_a) = 1 - (1- R_1(r_a))^k \qquad (42)$$

If the performance of the k individual trials at rate r_a can be considered to yield the same results as a single trial at the rate kr_a on the assumption that no new physical phenomena present themselves at the higher rate, then equation (42) corresponds to that given by Brignell (23) whereby the distribution for a rate kr is obtained from that at a rate r. In practice, however, Eq. (42) gives a difference larger than is observed experimentally.

From g(E) can be obtained a distribution function $T(E,r_a)$ whose dependence on the ramp rate r_a is given by equation (42). The distribution of the ramp function breakdown measurements is given by (23):

$$P_B(E,r_a) = T(E,r_a) * q(E)$$

where * signifies convolution with respect to E. The effect on the cumulative distribution of $T(E,r_a)$, namely $T_C(E,r_a)$, of changing the ramp rate is r_a, is illustrated in Figure 1-2b. The distribution of breakdown stress which takes account of the rate of rise effect is represented by the shaded area.

MODEL FOR RAMP FUNCTION MEASUREMENTS (23)

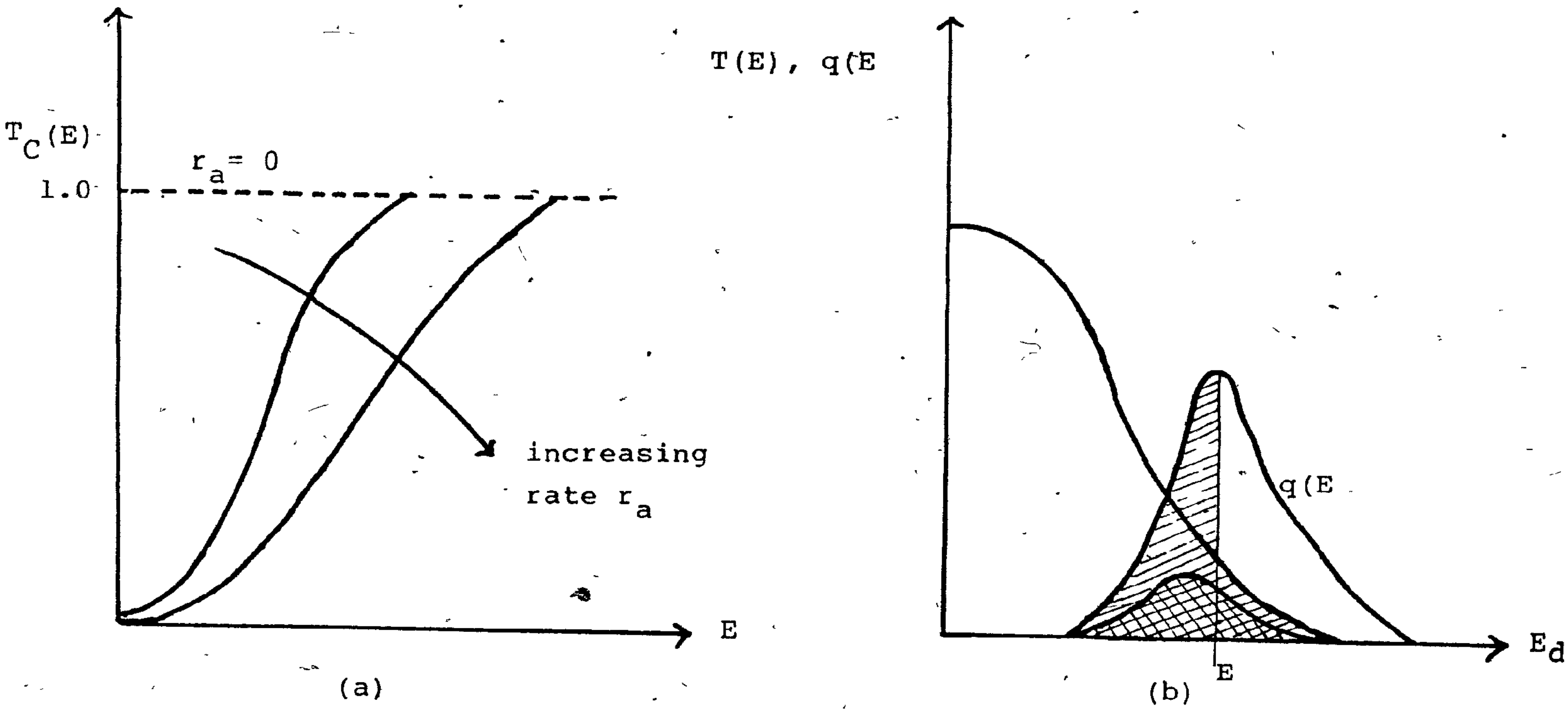

Convolution of Distributions due to Rate of Rise of Voltage T(E), and Extreme Value Distribution of Threshold Breakdown Stress

FIGURE 1-2

In conventional treatment of direct-stress breakdown r_a corresponds to zero - i.e. the rate effect is ignored. However if r_a is treated as non-zero, it can be shown by a series of sketches similar to that of Figure 1-2, that with increasing rate r_a, there is a dilution of the rate dependence. This would explain why in practice it is found that there is an over-estimation made by equation (42). Furthermore, in the same manner it can be seen that if r_a is significant, equation (42) will always produce a smaller value at a particular stress and $T(E,r_a)$ will decrease as r_a increases, thus giving an explanation for the observed phenomena that the cumulative distribution for a higher rate lies to the right of that for the lower rate (24).

Brignell(25) carried out 100 breakdown measurements at 2 different rates of rise, with trials at these two rates interlaced in groups of 10. He observed that not only variations of rate within the trial, but also variations in the sequence affect the probability of breakdown. An explanation for the rate of rise effect is that it is caused by the greater pre-stressing with the lower rate, or by a longer time between discharges allowing discharge products more time to disperse. Although the stress dependence is dominant, the observation of a rate of rise effect suggests the existence of a slow process in the chain of events leading to breakdown, for example, thermal processes or motion of ions or particles or of the liquid itself (21).

1.5.4.2 Statistical Effect of Environmental Factors

While the bulk liquid breakdown can be characterised by a weak link concept having an external distribution, Nelson (99) proposed that the probability of breakdown will be the result of a second random process due to random enviromental errors with an assumed Gaussian distribution. He produced a "hybrid distribution" by carrying out a convolution of the first asymptotic smallest value distribution with the normal distribution.

The new distribution is given by

$$F_B(E) = \frac{1}{x\sigma\sqrt{2}\,\pi} \quad f_a\left(\frac{1}{x}, \frac{1}{k'}\right) \qquad (44)$$

where f_a is the "after-effect function" tabulated by Jahnke and Emde (100). The parameter k' is a nondimensional constant relating standard deviation with the extremal intensity of the component extreme-value distribution.

Nelson analysed oil breakdown data for slowly rising 50 Hz voltages was carried out on the basis of the proposed hybrid distribution. For the particular volume of circulating oil and electrode configuaration (31), k' was found to be 5.1. In contrast, stationary liquid yielded a value of 0.7, indicating a lack of dilution of the extremal distribution. Normalization took place gradually with increasing speed and not abruptly at a transition velocity.

The hybrid parameters for the case of stationary and circulating oil subjected to 1/50 μ sec surges revealed insignificant change in the form of the distribution as a result of liquid motion; only partial normalization had taken place in these cases.

It is suggested that a clean dielectric liquid will exhibit an extremal distribution if (101):

(a) 'idealized' electrodes are used

(b) time effects are permitted to influence the breakdown

(c) the liquid is homogeneous and stationary

(d) the testing technique is exactly reproducible

(e) there are no errors of measurement

To some extent these conditions will be met in a practical testing system or service environment.

It is reasonable to suppose that there will be several mechanisms contributing to the breakdown of a liquid, but that one of these mechanisms will dominate under the idealised conditions mentioned above. If the environmental factors are not 'ideal', this dominance would be partially destroyed, bringing about normalization. Since the dilution of the extreme value distribution is almost unchanged if fast ramp voltages were used, the transition would appear to occur primarily in the long-time region. As soon as the influence of the experimental variations exceeds that of the weakest point in the insulation, the Gaussian distribution best describes the distribution of breakdown voltages. This would explain why some workers (108)have found the normal distribution suitable to describe the breakdown voltage distributions. It has also been observed that the distribution type seems to be affected by the quantity of stressed oil volume(73). The smaller the volume, the more closely does the distribution resemble the Gaussian distribution. The greater the quantity, the more closely does it appraoch an extreme value distribution. Environmental factors such as the rate of flow of oil can be expected to be more pronounced for a smaller volume.

CHAPTER II

DESCRIPTION OF EQUIPMENT AND METHOD OF DATA COLLECTION

CHAPTER II

DESCRIPTION OF EQUIPMENT AND METHOD OF DATA COLLECTION

2.1 DIELECTRIC LIQUIDS USED

2.1.1 Chlorinated Hydrocarbons

These are the group of synthetic aromatic liquids, notably the chlorinated diphenyls and benzenes, which have been developed for capacitor and transformer insulation. These compounds are several times more expensive than mineral oils but they possess a combination of characteristics which make them suitable and economically practicable for particular applications(10):

(a) excellent resistance to fire hazards since they are not readily ignited and they do not give off inflammable or explosive gases under arcing conditions.

(b) High dielectric strength, comparable with that of mineral oils.

(c) Adequate thermal, chemical, and electrical stability under normal operating conditions.

(d) A relatively high dielectric constant (approximately double that of mineral oils).

Thus, they are used in capacitors where, for equal capacitance, units can be half the size of mineral oil.

The diphenyl molecules ($C_6H_5C_6H_5$) contains

10 hydrogen atoms for which chloride atoms may be substituted. The properties of the chlorinated diphenyls depend on the degree of chlorination. The viscosity, pour point, temperature, distillation temperature, density and related properties increase with the degree of chlorination. Because of the alternative substitution positions in the diphenyl molecule, there are a number of isomers for each molecular composition. The commercial materials consist of mixtures of these different isomers and are classified in terms of the percentage of chlorine by weight which is present. Therefore the "Aroclors" manufactured by Monsanto Chemicals are graded as types 1242, 1248, 1254, 1260 etc., the last two figures representing the precentage of chlorine by weight. In the experiments, Askarel 7030, which is 70% Aroclor 1254 and 30% trichlorobenzene, was used.

The diphenyl molecule is non-polar due to its symmetrical charge distribution. Where electronegative chlorine atoms are substituted for hydrogen atoms in an asymmetrical arrangement, the resultant charge distribution gives rise to a permanent dielectric moment, the magnitude of which depends on the degree of asymmetry. Because of the 10 available substitution positions, many isomers are possible, and most of these isomers are asymmetrical and polar. The average degree of asymmetry and hence the average dipole moment of the

'Aroclors' decreases with increasing chlorine content.

With the chlorinated hydrocarbons, the principal arc decomposition product is hydrogen chloride, which is non-flammable and non-explosive. No chlorine or phosgene is evolved. Small amounts of hydrogen chloride that are evolved by occasional minor arcing under normal operating conditions can be absorbed by suitable non-ionizing additives.(1.3.3)

Askarels have until very recently been widely used in practice but from an experimental and research viewpoint, they leave much to be desired. They are more difficult to handle and are less stable than mineral oil. The higher chlorodiphenyls are photochemically stable but trichlorodiphenyl (Aroclor 1242). for example, shows an increase in conductivity when exposed to strong sunlight (9). A similar effect occurs if the liquid is heated above 80°C. However, the higher "Aroclors" are suitable for use at higher temperatures (9).

Properties of typical transformer Askarel are shown in Table 2-1.

2.1.2 Mineral Oil

The chemical constitution of a hydrocarbon insulating oil, derived from a given crude, determines its physical properties (18). The electrical properties are more affected by non-hydrocarbon contaminants, and

TABLE 2-1

Typical Transformer Askarel (97,123)

PROPERTY	TYPICAL
Viscosity at 37.8°C(ASTM D88)	56-61 Saybolt Univ. sec.
Spec. Gravity at 15.5°C(ASTM D287)	1.563-1.571
Condition	Clear
Acidity, mg.KOH/g(ASTM D974,D644)	0.014 max.
Pour Point, °C(ASTM D-97)	-35°C or lower
Inorganic Chlorides,ppm.	0.10 max
Refractive Index at 25°C	1.6075-1.6085
Boiling point at 1 atm,°C	302
Water content, ppm	30 max.
Resistivity,100°C,500v,0.1"gap	100 x 10^9 ohm-cm., min.
Dielectric Strength, 25°C(ASTM D877)	35 kV,min.
Dielectric Constant, 100°C., 1000 cycles	3.8-4.2
Tin Tetraphenyl	0.125% ± 0.01% by wt.
Burn Point (ASTM D92)	None up to boiling pt.
Flash Point,°C	None

differ but slightly at ordinary temperatures from ultra-pure oils. The electrical properties depend almost completely on whether or not it contains polar or dielectric ionizing materials causing dilectric losses (11). Such materials can be due to insufficient refining, or be picked up during transportation, processing, and service. In addition polar materials may develop as a result of degradation of the oil itself.

When an insulating liquid is subjected to an arc discharge, decomposition generally occurs. With hydrocarbon mineral oils, the decomposition products are largely hydrogen and gaseous hydrocarbons. Where the hydrogen may become mixed with air, it can constitute a fire and explosion hazard (12). The properties of typical mineral oil are shown in Table 2-2.

2.1.3 Alternative Dielectric Fluids

Although askarel is among the best liquid man-made insulations (17), they are, because of their chemical stability not biodegradable, and hence, are a major environmental concern. In the past, the chlorinated biphenyls have all been used in a wide variety of applications including food packaging materials, lubricants and insecticides. Until a suitable substitute can be found for them, their continued use is necessary because of the increased risk of fire and explosion, and the disruption of electrical service that

TABLE 2-2

Typical Mineral Oil (123)

PROPERTY	TYPICAL
Viscosity at 37.8°C(ASTM D446)	58 Saybolt Univ. sec.
Spec. Gravity (ASTM D1250)	0.885
Acidity,mg KOH/g(ASTM D974)	0.02
Pour Point,°C (ASTM D-97)	-45
Refractive Index at 25°C	1.48
Boiling point at 1 atm,°C	greater than 150
Resistivity at 100°C,(ASTM D1169)	35×10^{12} ohm-cm.
Dielectric Strenght, kV (ASTM D877)	30
Dielectric Constant at 60 Hz,100°C(ASTM D924)	2.25
Burn Point °C,(ASTM D-92)	148
Flash Point, °C (ASTM D-92)	135

might result from an outright ban. Also, continued use of chlorinated biphenyls in transformers and capacitors presents minimal environmental risk (18).

Many are working on the problem of finding fluids having the attractive characteristics of askarel without its environmental and health drawbacks. Monsanto has introduced Aroclor 1016 for capacitors and it has found growing use. This fluid retains the high dielectric properties of traditional askarel but is also partially biodegradable. Silicone oil is another potentially useful liquid in transformers. Its autoignition point is about 318^{o}C (124). If the heat source is removed or fluid temperature drops below the autoiginition point, burning will cease. Thus the fluid is self-extinguishing (17). The main decomposition products are silicon dioxide, water and carbon dioxide. Temperatures as high as 200^{o}C can be maintained with little decomposition of the silicone fluid, but gradual polymerization does occur and viscosity approaches that of a gel in long exposure to heated air (125). The fluid however costs twice as much as askarel.

The fluorinated hydrocarbon liquids, as a group, are available in great variety. So far they have been mainly used in electronic transformers where because of their high dielectric strength, high voltages are possible in a minimum of space. For example, $(C_3F_3O)_5C_2H_5$ has no flash point, a dielectric strength of 50 kV/cm and a boiling point of $224^{o}C$ (113).

The fluorocarbons are excellent in cooling electrical apparatus but because of their low boiling point and high cost, they are not a serious competitor of chlorinated diphenyls (127). For ecological reasons, however, some of the exotic liquids will find increased use in the future.

Other alternatives are use of electronegative gases and the development of non-liquid transformers.

2.2 GENERAL EXPERIMENTAL ARRANGEMENT

The purpose of the arrangement was to measure the magnitude of the breakdown voltage caused by applying a d.c. potential (range 3 - 15 kV), rising at a predetermined rate, to a pair of electrodes separated by a known distance, and immersed in a dielectric fluid. The breakdown voltage was by a chart recorder. A block diagram illustrating the experimental arrangement appears on page 52. The general experimental set-up was arranged in the following way:

(a) The dielectric fluid was passed through a filtration column.

(b) The liquid was degassed.

(c) A quantity of delectric liquid was admitted to the test cell.

(d) Voltage breakdown experiments were conducted.

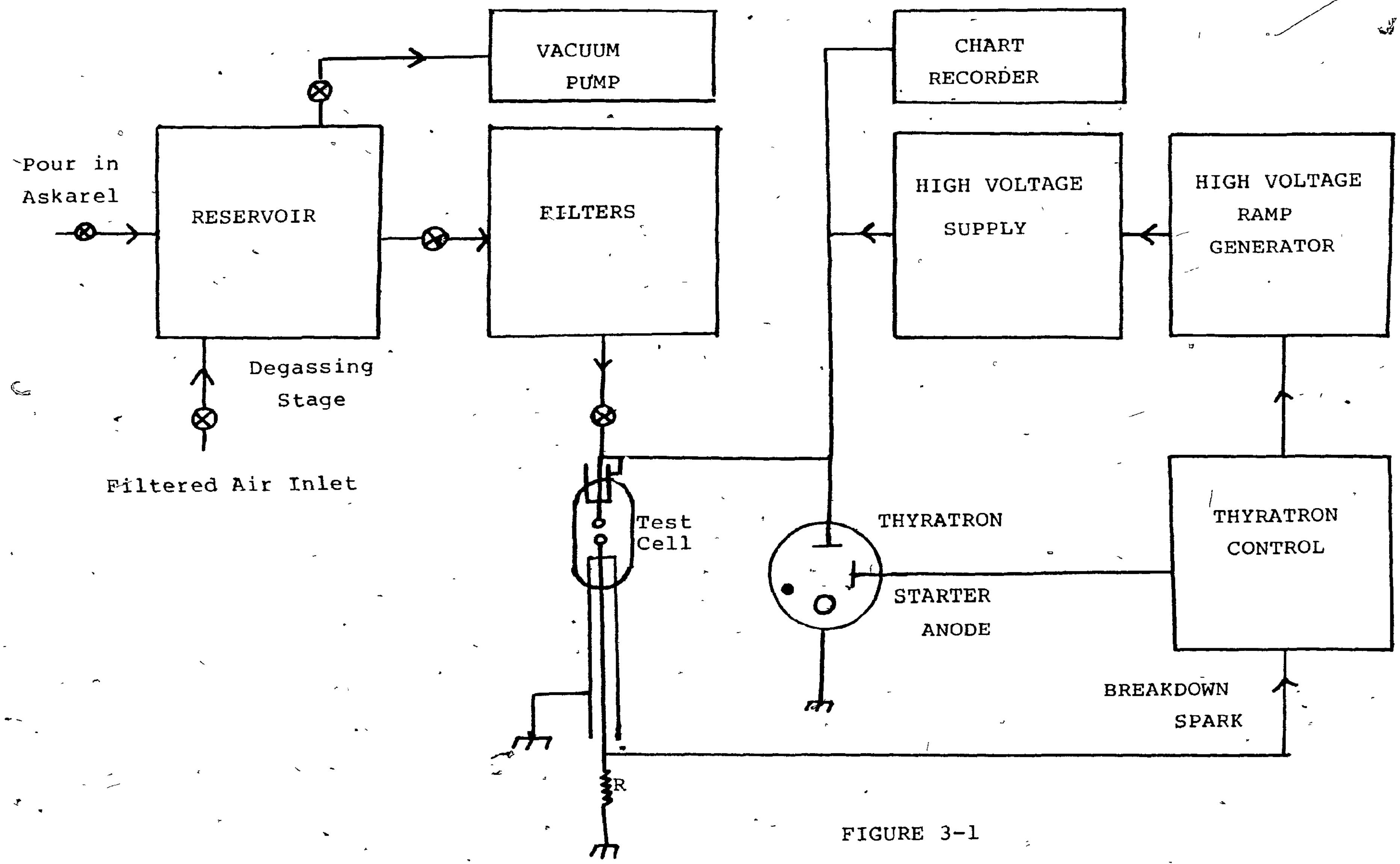
VACUUM PUMP
CHART RECORDER
Pour in Askarel
RESERVOIR
FILTERS
HIGH VOLTAGE SUPPLY
HIGH VOLTAGE RAMP GENERATOR
Degassing Stage
Filtered Air Inlet
Test Cell
THYRATRON
STARTER ANODE
THYRATRON CONTROL
BREAKDOWN SPARK
R

FIGURE 3-1

(e) The electrodes and test cell are prepared for a new cycle of experiment and the dielectric fluid is changed.

2.2.1 Test Sample Preparation

The filtration column, which is depicted by a line diagram in Figure 3-2A served two purposes:

1) To degas the dielectric liquid to be tested.
2) To filter the fluid.

It was composed of a two-stage system, each composed of a reservoir of about 900 ml. capacity and a glass sintered filter, positioned on the glass line draining the bottom of the reservoir. By means of the filters, whose pore size is known, an attempt was made to put an upper limit on the maximum size of the particles present in the liquid.

To minimize any possible photochemical deterioration of the askarel, the filtration column was shrouded in heavy opaque black paper.

Air that was let into the system, passed through a round bottom liter flask filled with silica gel and then was filtered through a glass sintered filter.

Contol of the flow of liquid through the system was controlled by means of greaseless stopcocks. See figure 3-2.The stopcocks consisted of a rubber (Viton) diaphragm which pressed against the inner outlet.

It is acknowledged that plasticizers in

TEST SAMPLE PREPARATION COLUMN

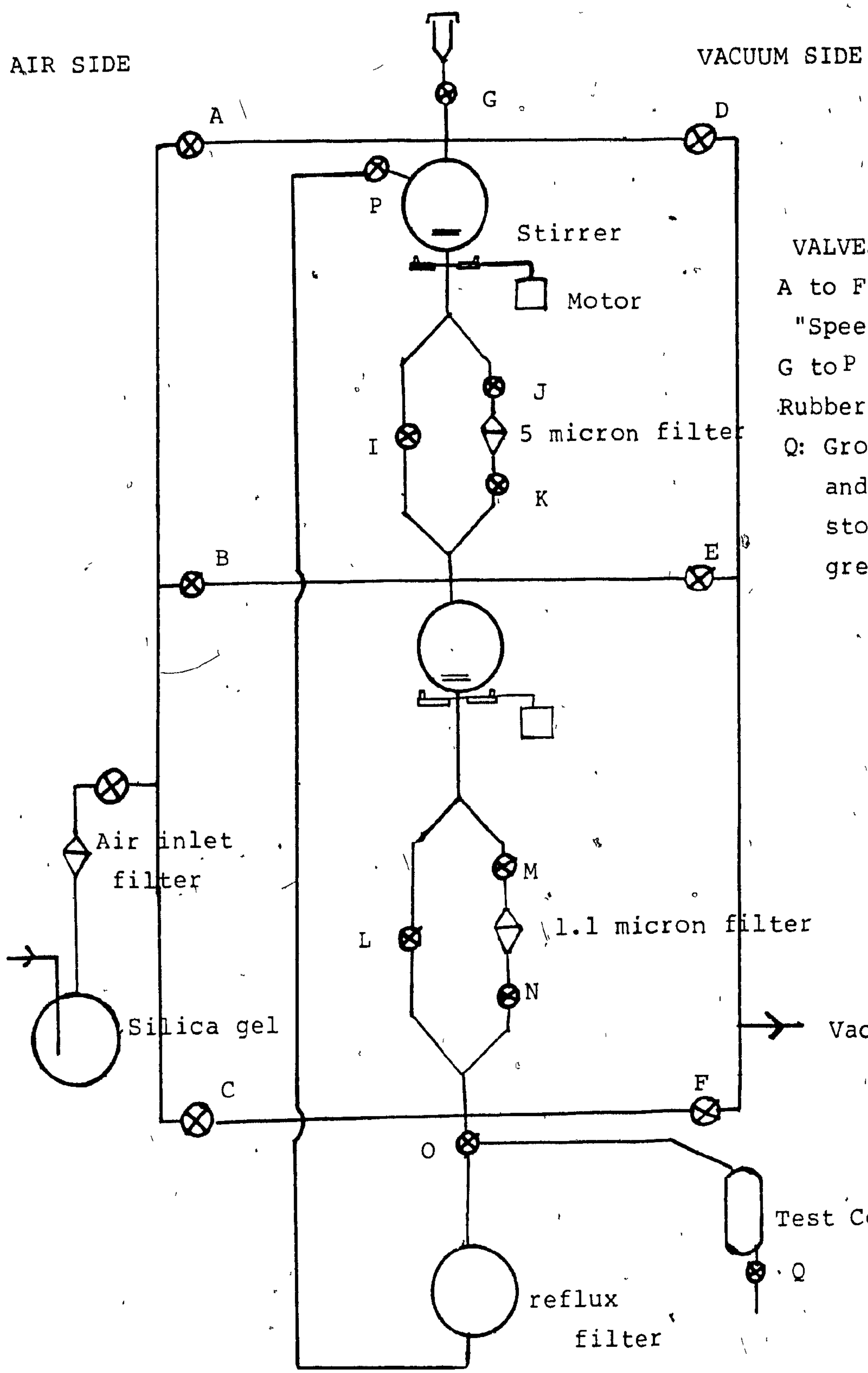

VALVES:
A to F: Edwards "Speedivalve"
G to P : Viton Rubber Diaphram
Q: Ground glass and Teflon stopcock (no grease)

FIGURE 3-2 A

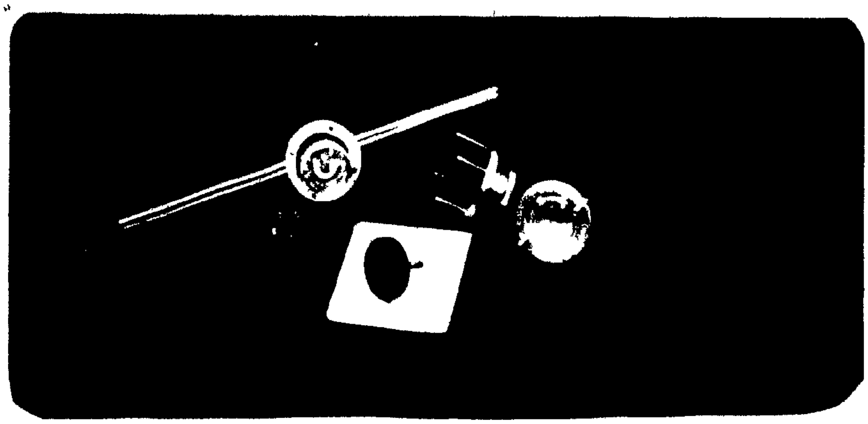

Two Greaseless Stopcocks in Various Stages of Disassembly.
A Viton rubber diaphragm is on the white square card.

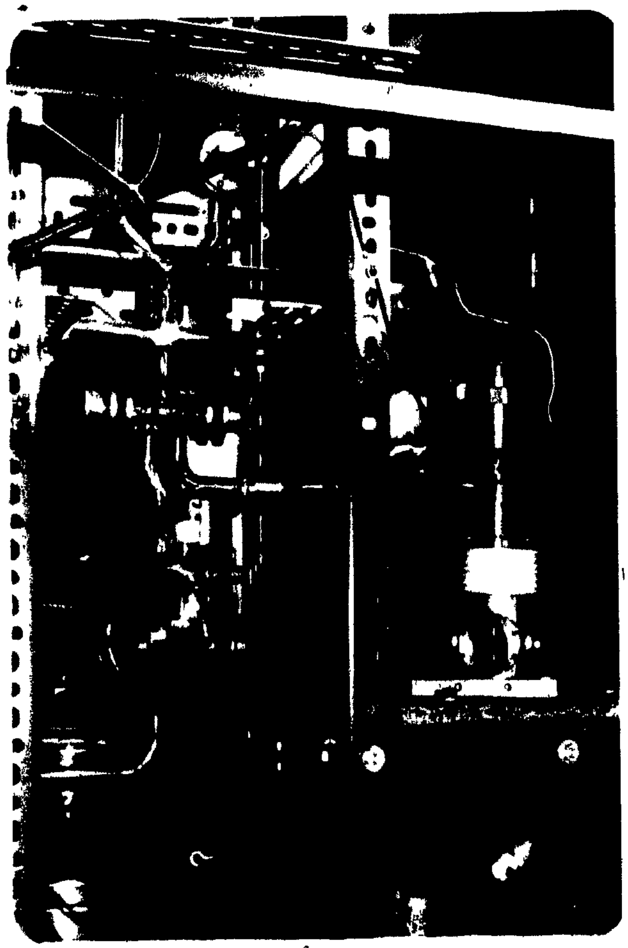

Fig. 3-2B

The Assembled Sample Preparation Column
The test cell is on a small platform to the right, with the red wires.

the rubber were a potential source of contamination, however, the rate at which the fluid was passed through the system while the tests were conducted, the high resistance of Viton to deterioration and the relatively small area of rubber actively in contact with the fluid, minimized this source of contamination.

2.2.2. The Test Cell

The particular design of the test cell (see figures 3-3 and 3-4) which is based primarily on the type of cell used by Dr. F. Spitzer(143), was such that the rigidity and accuracy of electrode position would be maintained despite continual disassembling of the cell for electrode maintenance.

The test cell, a cylinder of 3.2cm.(inside diameter) and a length of 8.9 cm., with a volume of about 72 ml. was machined out of a single tube of stainless steel, its midsection encircled by four evenly spaced observation ports. The ports were fitted with optically flat glass which were seated by ring flanges encircling the windows and bearing down on Teflon 'O' rings between the glass and inside metal surface of the window sockets. The partially disassembled test cell is shown in Figure 3-5 .

The top and botton electrode holders were stainless steel shafts, separated from one another and the body of the cell by means of glass loaded Teflon spacers. The Teflon provided rigidity and was

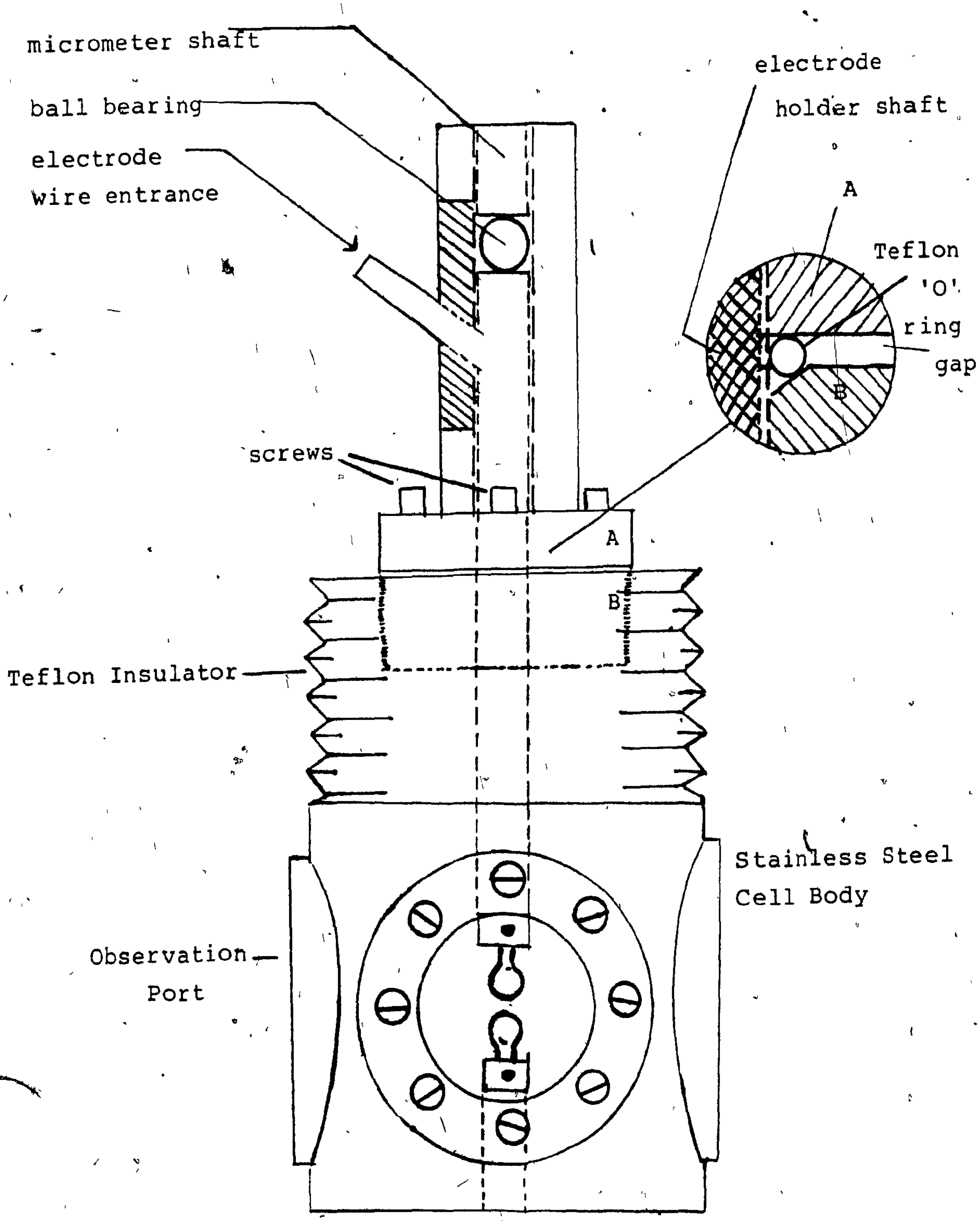

A PORTION OF THE TEST CELL FIGURE 3-3

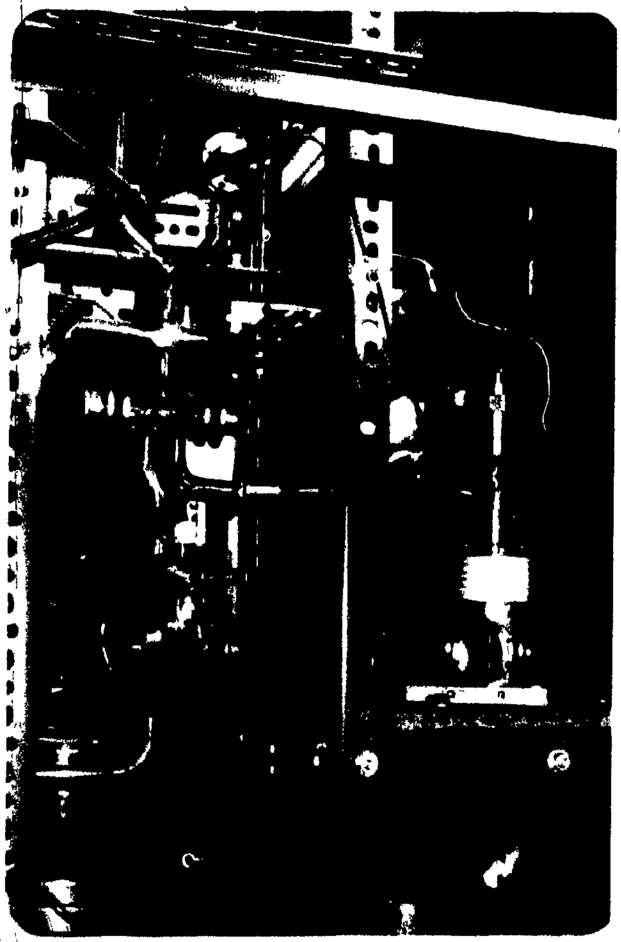

Two Different Views of the Test Cell

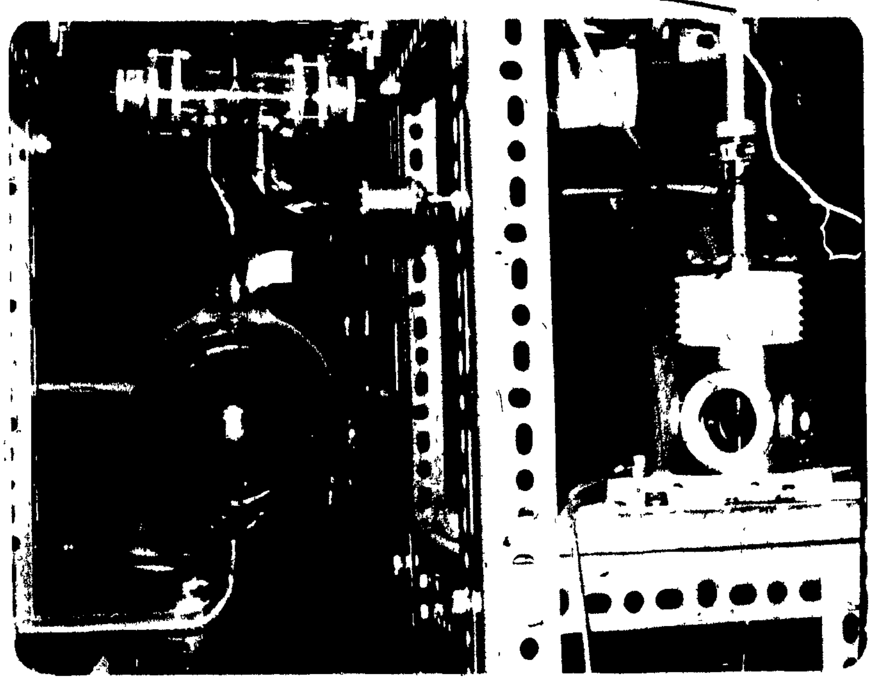

FIGURE 3-4

FIG. 3-5

Test cell partially disassembled

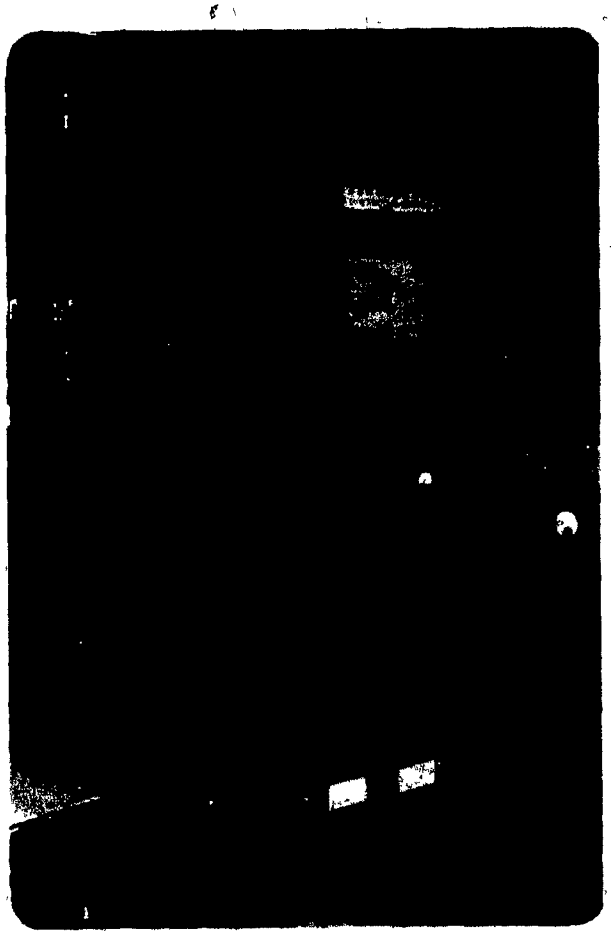

FIGURE 3-6

Chart recorder, High Voltage Supply, and High Voltage Ramp Controller (on table). Thyratron control panel is just below the chart recorder.

chemically inert. On the outer side of the Teflon spacers,V-shaped grooves were cut circumferentially to increase the surface distance the electrical leakage would have to pass before reaching any other portion of the test cell. The tip of the electrode holder had a hole into which the mounting stem of the electrode was inserted and secured to the holder by means of a small grub screw. The top electrode was moveable. The gap distance was set by adjusting a micrometer attached to this electrode holder. Teflon 'O' rings on the electrode holder provided a seal around the point where their shafts entered the test cell. Pressure was applied to these 'O' rings by the flanges at the base of the electrode holders. In order to permit tests with different polarities, both electrode assemblies were insulated from the cell body.

The test cell was fed by a length of stainless steel tubing which was connected to the filtration column glass tubing by means of a short length of stainless steel tubing. This connection was made vacuum tight by means of a Viton 'O' ring at either end of the short steel tubing. Pressure on the 'O' ring around the circumference of the feed tube was accomplished with a metal ring with a bevelled inner edge pressing against the bevelled circumference of the connector. See Figures 3-4 and 3-5.

When the electrodes were in position for a test, they were co-axial with one another and positioned centrally within the cell, in plain view of the observation windows.

The cell could be emptied of its contents by means of a stainless steel spout set into the cell's base fitted with a glass and Teflon stopcock joined to it by a glass-to-metal seal.

2.2.3 Estimation and Control of Electrical Stress

The gap distances used in the experiments were 100,125,150,250 microns. The field between two equal and separate spheres is symmetrical about a plane situated midway between them (5). The expression for the ratio of maximum to mean stress for the sphere-sphere electrode configuration used throughout the experiments is (6).

$$\frac{E_{max}}{E_{av}} = \frac{1}{4}\left[k_s + \sqrt{k_s^2 + 8}\right]$$

with $k_s = \frac{X_G}{r_s} + 1$, where X_G = gap spacing and r_s = radius of the sphere.

The diameter of the spheres was 5mm. With this value Table 2-3 was prepared.

Table 2-3

Gap spacing (microns)	100	125	150	250
E_{av}/E_{max}	1.013	1.017	1.020	1.034

This small degree of non-uniformity should not unduly obscure the nature of any statistical distribution which the breakdown voltages should take. Greater distortion of the field is to be expected from the effect of space charges, and the presence of particles of appreciable size.

The gap distances were set by using an "Etalon" screw micrometer adjustable to within 2 microns. The actual setting was made by noting the micrometer reading when the electrodes were just touching as indicated by the vacuum tube ohmeter (Voltohmyst by RCA). To minimize possible damage to the electrodes caused by the small measuring current of the ohmeter, the ohmeter was set to its highest range.

2.2.4 Electrical Connection of the Test Cell

The entire system was evacuated by an Edwards double stage rotary pump which under ideal conditions is capable of a vacuum of 0.001 torr.

When the experiments were first begun it was noted that spurious breakdowns were occurring, although no breakdown spark could be observed between the electrodes. The largest possible gap lengths did not change these observations. The test cell and electrode holder were dismantled and it was discovered that there were breakdown punctures on the Teflon insulated wire running along the inside of the electrode shaft to the electrode itself. Furthermore the stainless steel electrode holder shaft was discolored, indicating that there were breakdowns occuring between points A and B of Figure 3-3. The problem was due to the fact that the moving portion of the top electrode (A) was separated from the stationary portion by the Teflon 'O' ring through which the shaft part slides. Both these portions were held together originally by stainless steel screws. However, the oxide layer on the stainless steel screws which held both these portions together was sufficient insulation for points on A and B to be at different potentials and thus suffer an occasional breakdown as the voltage increased. This preliminary problem was overcome by replacing the stainless steel screws with polished brass screws which were then afterwards repolished every third day of experimental work. This ensured good electrical connection between portion A and B of the upper electrode to which the high voltage was applied.

As a result of this experience, the upper electrode holder, the feed pipe, and the connector from the feed pipe to the glass filter column, the latter two which were also slightly separated due to the 'O' ring in the connector, were each solidly joined together electrically (i.e. with electric wires).

2.2.5 Vacuum System

The vacuum system was primarily intended to maintain the pressure over the dielectric liquid surface at a constant reproducible value.

The vacuum pump was an Edwards 75 which was a double stage mechanical rotary pump equipped with a gas ballast. This latter feature of the pump was particularly useful. The volatile components of the Askarel became dissolved in the vacuum pump oil thus degrading the ultimate vacuum possible. The volatile component which is taken out of the askarel by the pumping is mainly trichlorobenzene, which is used to achieve desired viscosity-temperature characteristics for the particular variety of askarel used, but does not affect dielectric strength. Vapours condensed in the vacuum pump oil are removed by the ballast facility of the vacuum pump. Integral to the pump was protection against oil suck-back into the system in the event of a power or belt failure.

The pump was connected to the glassware by 0.5 inch O.D. copper tubing with soldered connections. The copper tubing was joined to the glassware by Edwards manual pipeline valves ("Speedivalve") having a flexible rubber diaphragm seal. The glass tubing which was also of 0.5 inch O.D. fitted into one end of the valve and the copper tubing went into the other side.

The pressure was monitored by a Edwards

Pirani Guage, model no. 8/2 with Edwards Pirani gauge head model no. M5C.

2.2.6 Apparatus Support Frame

The entire system, that is, the filtration unit, the test cell and vacuum system were built on a mobile platform and secured to a metal frame made of Dexion, the trade name of lengths of prepunched structural steel.

2.3 THE CONTROL UNIT AND HIGH VOLTAGE SUPPLY

2.3.1 General

The purpose of the high voltage controller, a block diagram of which appears on page 64 was:

1) To periodically produce linear voltage increases measured against time in the high voltage output at a preselected rate.
2) To trigger the thyratron at the instant of breakdown to minimize excessive electrode damage.
3) To stop application of the ramp high voltage upon breakdown, and return to normal conditions.

2.3.2 Ramp Generator

A block diagram of the circuit is shown in Figure 3.8 Any one of 11 ramp rates could be selected:

CONTROLLER FUNCTIONING FIGURE 3- 7

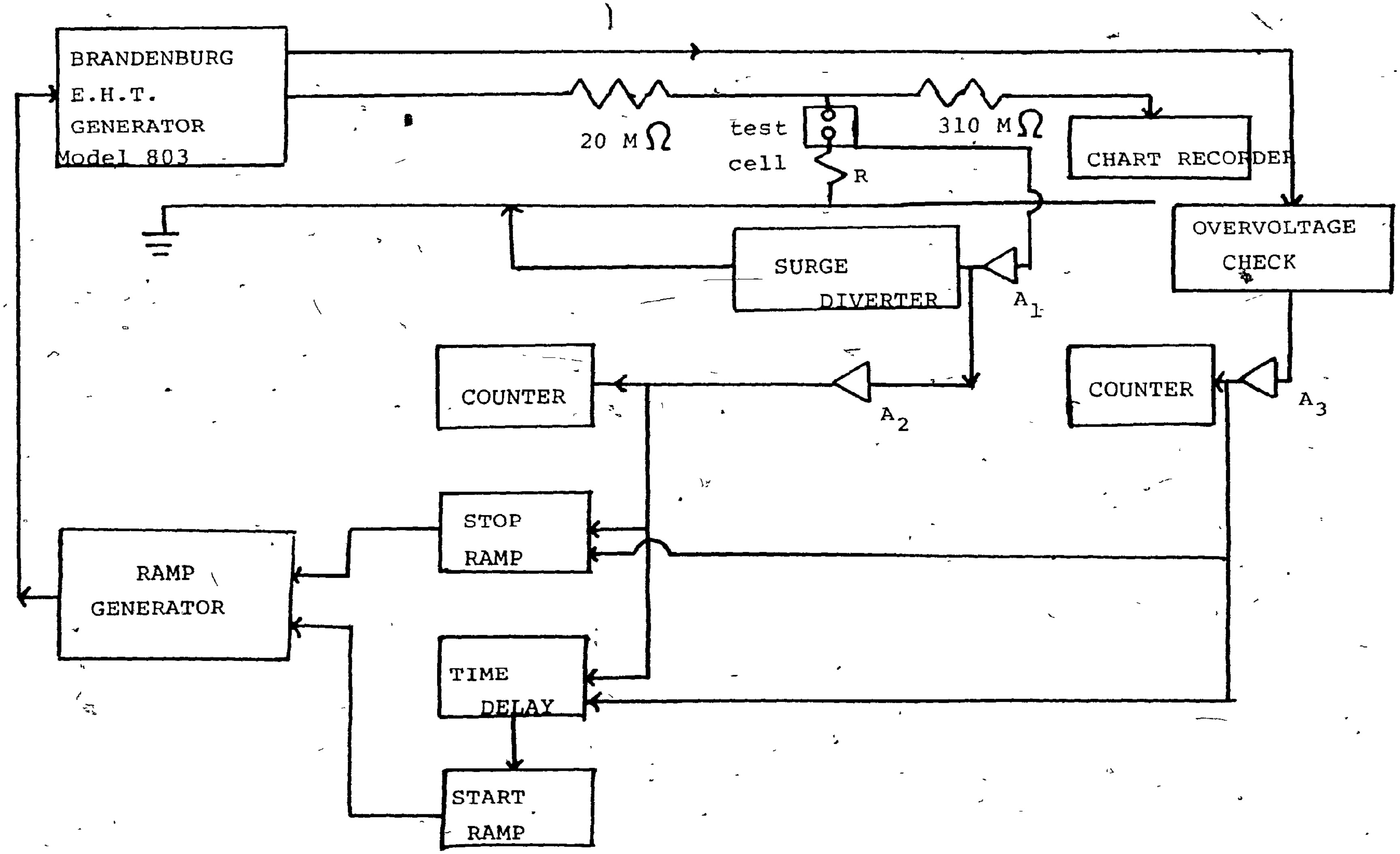

-64-

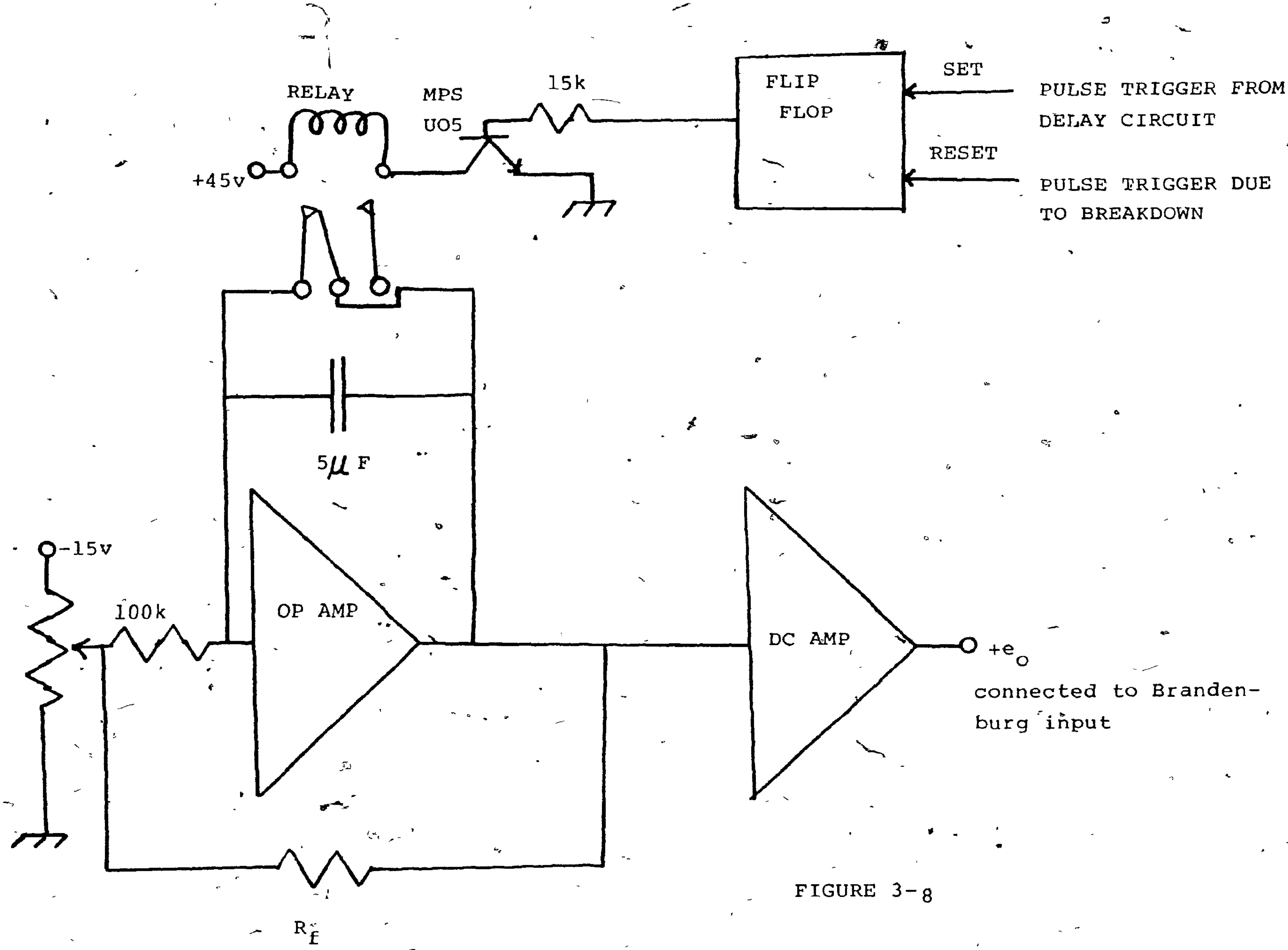
RELAY
MPS
UO5
15k
FLIP
FLOP
SET
RESET
PULSE TRIGGER FROM
DELAY CIRCUIT
PULSE TRIGGER DUE
TO BREAKDOWN
+45v
5μ F
-15v
100k
OP AMP
DC AMP
$+e_o$
connected to Branden-
burg input
R_f

FIGURE 3-8

0.25kV/sec., 0.3, 0.375, 0.5, 0.75, 1.0, 1.5, 3.0, 6.0, 12.0 and 30.0 kV/sec. At the instant of breakdown, the relay (see figure3-8)would discharge the integrating capacitor of the operational amplifier thereby causing the output of the high voltage generator to fall to its quiescent base voltage. This capacitor would remain shorted until a delay period had expired and another pulse from the delay circuit would reset the flip flop, opening the relay contacts shorting the integrating capacitor, and allow that capacitor to charge at a pre-selected rate. Its output is amplified by a direct coupled amplifier whose output was directly connected across a 100kΩ resistor inserted in the output adjustment circuit of the Brandenburg high voltage generator. The direct coupled amplifier is required in order to change the voltage over the complete range of the high voltage generator's capability. The relatively small output swing of the operational amplifier would not be sufficient to cause an appreciable voltage change at the output of the high voltage supply.

2.3.3 <u>Overvoltage Check Circuit</u>

The purpose of this circuit was to prevent the output of the high voltage generator from exceeding some prespecified high voltage level if no breakdown had occurred up to that time. The front panel was provided with a number of such selections of voltages from 5 kV to 30 kV in steps of 5 kV. The overview of its place in the system is shown in Figure 3-9.

If an overvoltage occurred, i.e. when the output of the high voltage generator has reached a certain predetermined voltage level and yet for some reason, no breakdown had occurred, then the comparator (see Fig 3-9 ?) would deliver a pulse to the flip flop controlling the integrating capacitor of the ramp generator's op amp. The relay bridging this capacitor would close, discharging it and a fresh delay period would commence. The inverting transistor at the output of the time delay unijunction transistor was necessary to provide the proper voltage polarity to reset the flip flop.

This monitoring feature which prevents excessive voltages, is realized by connecting the output of the ramp generator's op amp integrator to the inverting terminal of another operational amplifier which serves as a comparator (Fig 3-10). The noninverting terminal of this operational amplifier is connected to one of several preselected points on a resistive divider chain which provides reference voltages corresponding to the various preselected voltages to correspond to the limiting output voltage of the ramp generator. The selected voltage is connected to the non-inverting terminal of the op amp (Figure 3-10).

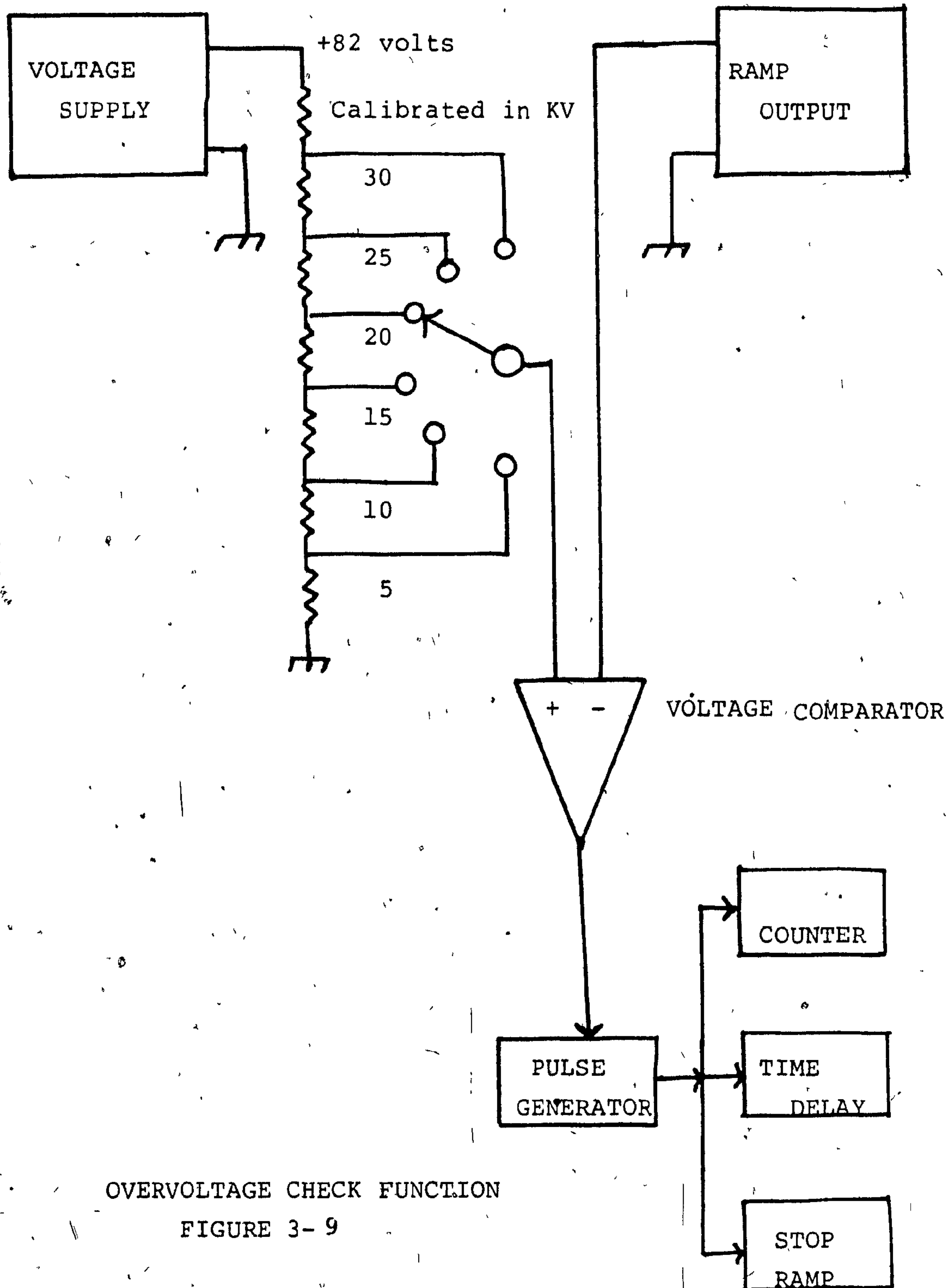

OVERVOLTAGE CHECK FUNCTION
FIGURE 3- 9

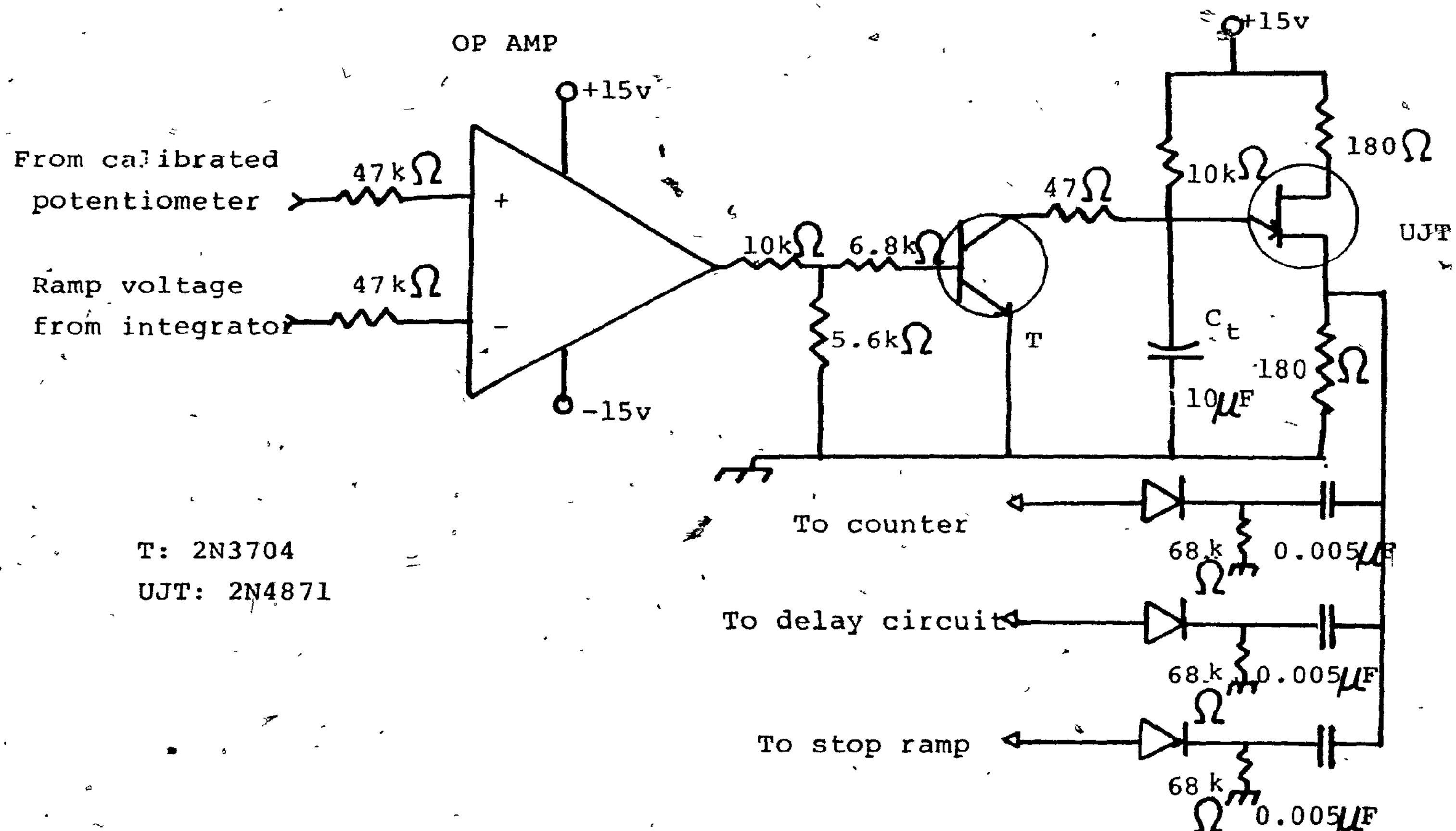

OVERVOLTAGE CHECK CIRCUIT
FIGURE 3-10

Initially while the output of the integrator is quiescent or is still rising the output of the comparator is positive, at a value close to its positive supply voltage. At such time the voltage on the noninverting terminals from the potentiometer selecting the particular overvoltage level exceeds that voltage appearing at the inverting terminal of the integrator. Because the output of the comparator is positive, the transistor T (Figure 3-10) is "on" thereby maintaining the capacitor C_t of the unijunction transistor in this circuit, discharged. As the output of the integrator continues its rise, it will reach the preset voltage on the non-inverting terminal. Immediately the output of this comparator op amp will switch to a negative voltage close to its negative supply voltage value. Transistor T is now in its nonconducting state. The unijunction transistor will then deliver a pulse which will stop the ramp, begin the time delay circuit by changing the state of the flip flop controlling its timing capacitor (Figure 3-11), and this pulse will also cause a counter keeping count of the number of overvoltages to increment its count by one.

2.3.4. The Time Delay Circuit

In order to create as identical conditions as possible for each breakdown event, the ramp voltage should be applied commencing at the expiry of equal time periods. The time base used is a relaxation oscillator constructed around a unijunction transistor (labelled UJT in Figure 3-11). At the expiry of the preselected delay period, the output pulse at its base was transmitted to a flip flop and to an inverting transistor T_4 (Figure 3-11). Upon reception of the pulse, the flip flop (T_1 and T_2) changed states, causing T_3, which during the delay period had been off, to turn on and discharge the timing capacitor and maintain it that way until the flip flop again changed state. This change of state occurred whenever a breakdown pulse was received, or when an over-voltage had occurred.

2.3.5 Surge Diverter

The other unit which the breakdown pulse activates is the surge diverter unit. The thyratron is

TIME DELAY CIRCUIT

FIGURE 3-11

TRANSISTORS

T_1, T_2, T_3 - 2N3704
T_4 - 2N3702
UJT - 2N4871
Diodes - 1N4001
(D_1, D_2)

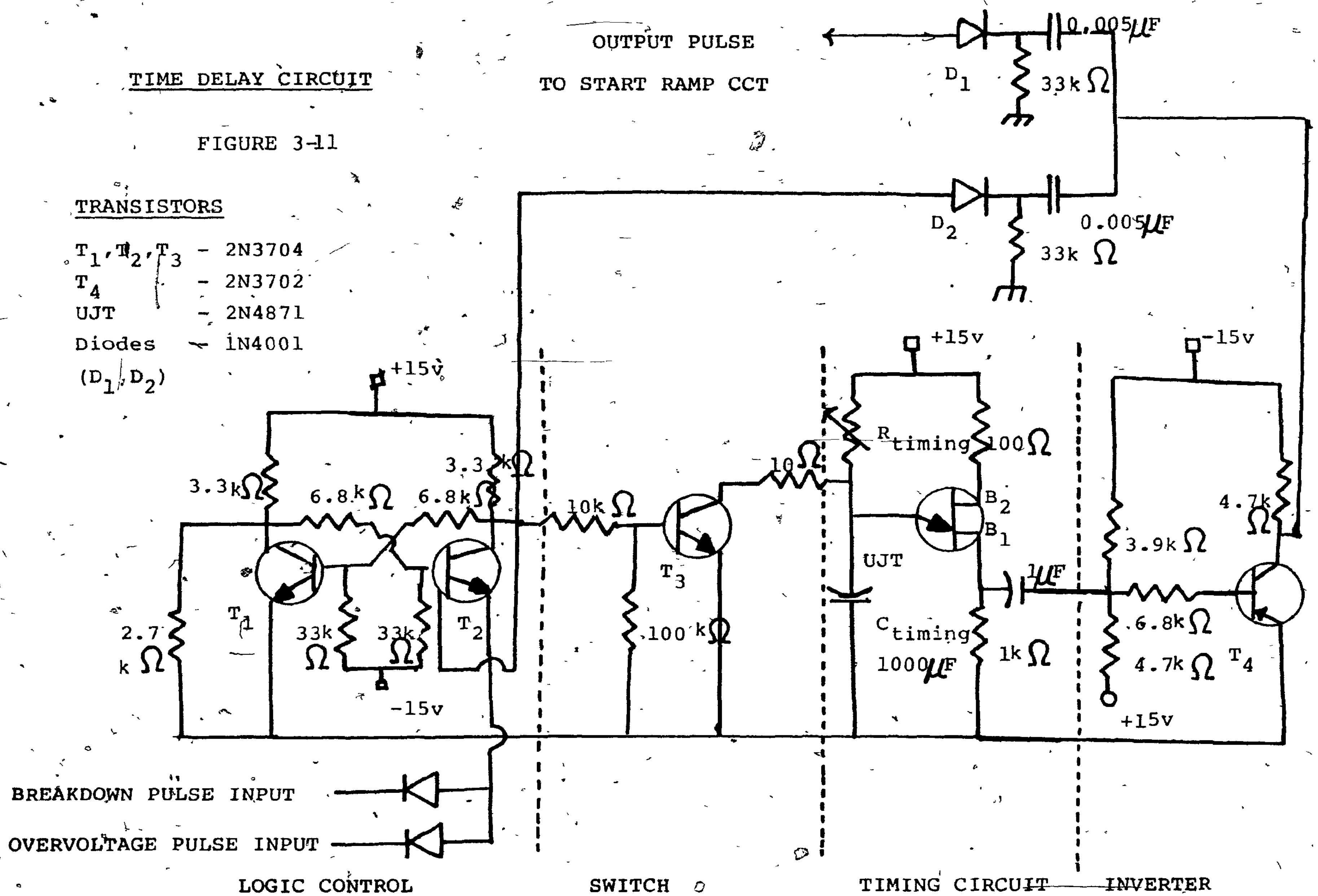

a hydrogen filled tetrode (CX1140) manufactured by the English Electric Company. This tube contains hydrogen to neutralize the space charge which would otherwise severely limit the amount of current which it could carry. Its peak forward voltage is 25,000 volts and its recovery time is in the order of 100 microseconds. Its purpose was to protect the electrodes from excessive pitting by providing a low resistance path to the breakdown current at the moment of breakdown. It was triggered at the instant of breakdown by a voltage pulse which appeared across the resistor connected between ground and the bottom electrode. This voltage pulse would trigger the thyratron and reset the high voltage supply to its base voltage.

2.3.6 The High Voltage Generator

The high d.c. voltage was supplied by a Brandenburg Model 803. Its miminum/maximum output was 3/30 kV. Stability against a 10% mains change is better than 0.1% at full load, while the output ripple is 0.5% at full load. Regulation to full load is better than 0.5% at full output.

2.3.7 Interconnection of the Control System With the High Voltage Generator

The power supply of the control unit is floating with respect to ground. When the output of the direct coupled amplifier of the ramp generator circuit is connected to the external control input of the high voltage generator, the ground reference of the control system is about 240 volts below zero potential ground. This negative d.c. voltage shifts steadily as the output of the high voltage generator increases until it reaches about -290 volts when the output of the generator is 30 kV.

The breakdown voltage pulse from across the resistor connected to the bottom electrode of the test cell (see Figure3-1) is about 20 volts positive and consequently it is not capable of triggering the various control circuits. A pulse d.c. shift amplifier corrects this deficiency by bringing the lowest level of the breakdown to about -290 V. This amplifier is illustrated in Fig. 3-12. Point P is normally at -290 V due to the voltage divider arrangement: -350 x 58/70 = -290 The output transistor T of the amplifier is, in the abscence of any breakdown pulse, in its "Off" state because the output of the operational amplifier is slightly positive due to a d.c. bias voltage on the noninverting terminal of the op amp. Thus, point P on the voltage divider arrangement is normally at -290 V, the lowest value possible corresponding to conditions when the output of the generator is maximum (30 kV) should that be required. When the breadkown is transmitted to the inverting input of the operational

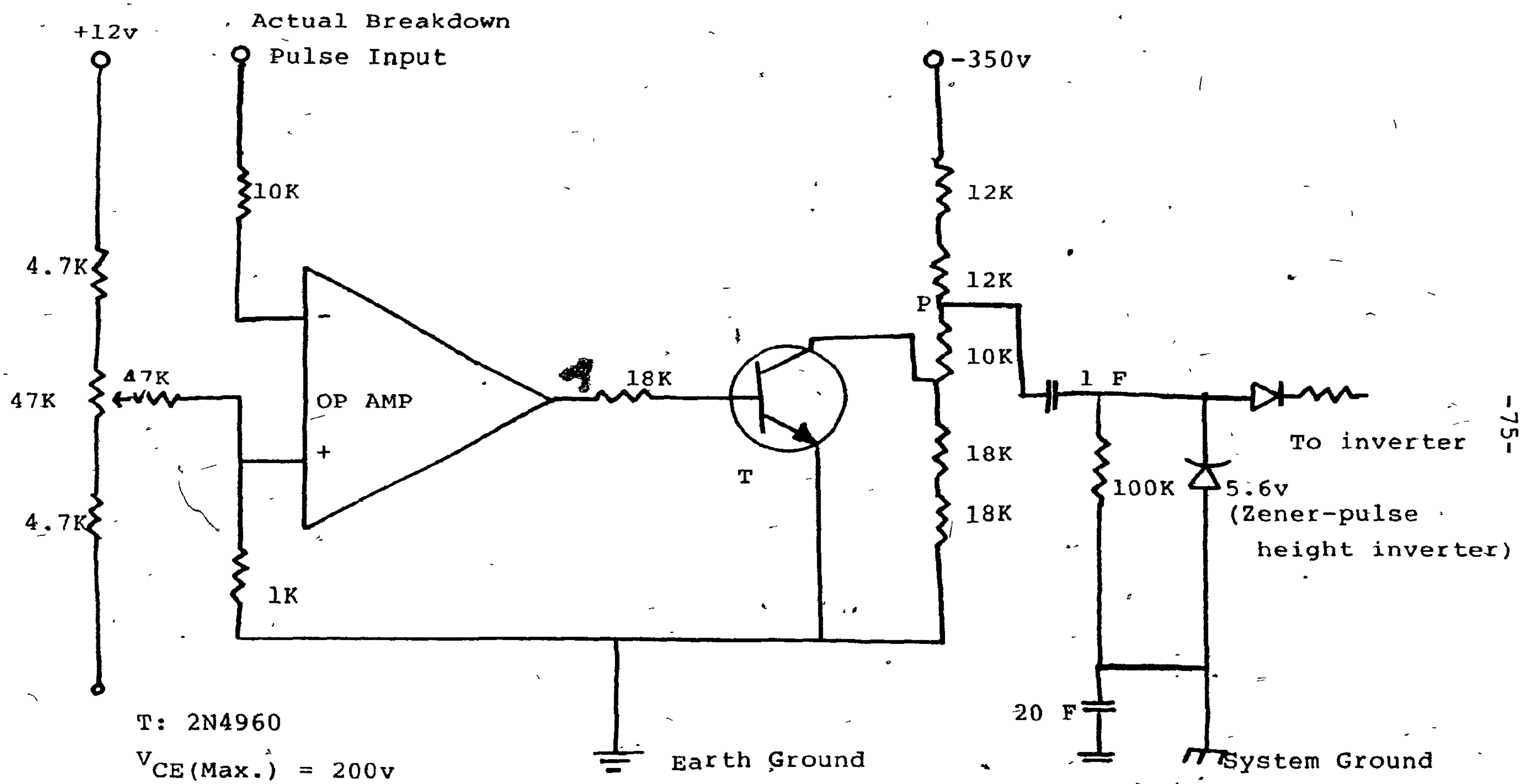

D.C. PULSE SHIFT AMPLIFIER

FIGURE 3-12

amplifier, the amplifier will momentarily switch to -12 V, the supply voltage, and then back to its initial state. At the instant of switching, the high voltage transistor (T) is momentarily saturated. When this happens, the voltage at point P drops to:

$$-350 \times 24/34 = -245$$

Thus, the pulse has been shifted down to a level comparable to the reference level of the control system when the high voltage generator is connected to it. This output pulse is then connected to the control system where it effectively triggers the desired operation.

2.3.8 Chart Recorder

All breakdowns were recorded on a Minneapolis-Honeywell chart reconder manufactured by Brown Instrument Division, Model No 153 x 17-V-II-III-6, which was linear in response over the range of 0 - 10 mV at its input terminals. A resistive divider chain at the input to the recorder controlled the recorder's input sensitivity set according to the varying range of applied voltages which were used throughout the experiments for the different gap lengths. Calibrations for all settings of the resistive divider were made using a Philips D.C. Micrometer, model no. PM2436, with Philips High Voltage Probe GM 6071.

CHAPTER III

APPLICATION OF THE THEORY OF EXTREME VALUE DISTRIBUTION TO THE BREAKDOWN OF LIQUID DIELECTRICS

CHAPTER III

APPLICATION OF THE THEORY OF EXTREME VALUE DISTRIBUTION TO THE BREAKDOWN OF LIQUID DIELECTRICS

The breakdown voltage of a sample of liquid dielectric is determined by the breakdown voltage value of the weakest volume element. Therefore its distribution may be regarded as a distribution of minimal values.

Let $p(x)$ represent the probability density of a population with an arbitrary distribution, and of sample size n. The sample values are ordered so that:

$$x_1 \leq x_2 \leq \ldots\ldots\ldots \leq x_n \qquad (1)$$

Choose a certain m^{th} smallest observation .
The probability of a value less or equal to ξ is:

$$P(x \leq \xi) = \int_{-\infty}^{x_m} p(\lambda)\,d\lambda \qquad (2)$$
$$= P(x_m)$$

and the probability of a value equal or greater than ξ, called the probability of exceedance, is:

$$P(x \geq \xi) = \int_{x_m}^{\infty} p(\lambda)\,d\lambda \qquad (3)$$

On condition that the n values are independent of each other, the probability that k among n future trials will be less than the observation ξ is given by the Binomial formula:

$$F(x_k) = b\left[P(x),\, n,\, k\right]$$
$$\begin{Bmatrix} n \\ k \end{Bmatrix} \left[\int_{-\infty}^{x_m} p(\lambda)\,d\lambda\right]^{k} \left[\int_{x_m}^{\infty} p(\lambda)\,d\lambda\right]^{n-k} \quad (4)$$

By differntiation, we obtain the density:

$$f(x_k) = \frac{n!}{k!\,(n-k)!}\left[\int_{-\infty}^{x_k} p(\lambda)\,d\lambda\right]^{k-1}\left[\int_{x_k}^{\infty} p(\lambda)\,d\lambda\right] k p(x_k)$$
$$= \frac{n!}{(k-1)!\ \ (n-k)!}\left[\int_{-\infty}^{x_k} p(\lambda)\,d\lambda\right]^{k-1}\left[\int_{x_k}^{\infty} p(\lambda)\,d\lambda\right] p(x_k) \quad (5)$$

If k=1 in the above equation, then the probability distribution of the smallest value x_1 is:

$$f(x_1) = n\left(\int_{x_1}^{\infty} p(\lambda)\,d\lambda\right)^{n-1} p(x_1) \quad (6)$$

Now let the cumulative distribution functions of p(x) and f(x) be represented by P(x), F(x). If F(x) is the probability that the minimal value x among n independent observations is not greater than x,

$$f(x) = n(1 - F(x))^{n-1}\, p(x) \quad (7)$$

and hence

$$\text{Prob}\ (X \leq x) = 1 - \left\{1 - P(x)\right\}^{n} \quad (8)$$

Equation (7) shows the distribution of the minimal values, whilst (8) shows the distribution function of X.

The exponential distribution is basic to many physical phenomena. To obtain the asymptotic distribution of the smallest values for the exponential type, we expand the initial probability function $1-e^{-ax}$, about the m^{th} smallest characteristic value u_m. Since the probability of a value equal to or larger than x is $1 - F(x)$, we expect $n\left[1 - F(x)\right]$ values in a sample of size n to be equal or larger than x and then define the characteristic smallest value $u_n(1) = u_1$ by

$$F(u_1) = 1/n \tag{9}$$

Thus, with the initial probaility function represented by p_m, the Taylor series expansion of it about u_m is:

$$P(x) = P(u_m) + \frac{x-u}{1!} p_m + \frac{(x-u)^2}{2!} p_m' + \cdots + \frac{(x-u_m)^{\nu}}{\nu!} p_m^{\nu-1} + \cdots \tag{10}$$

Where $P(u_m) = m/n;\ p_m = p(u_m);\ u=u_m$ (11)

$$P(x) = \frac{m}{n} + \frac{x-u}{1!} p_m + \frac{(x-u)^2}{2!} p_m' + \cdots + \frac{(x-u)^{\nu}}{\nu!} p_m^{\nu-1} + \tag{12}$$

Multiplication and division by (m/n) leads to:

$$P(x) = \frac{m}{n} + \frac{m}{n}\frac{(x-u)}{1!}\cdot\frac{n}{m} p_m + \frac{m}{n}\frac{(x-u)^2}{2!}\cdot\frac{n}{m} p_m' + \cdots + \frac{m}{n}\frac{(x-u)^{\nu}}{\nu!}\frac{n}{m} p^{\nu-1} + \cdots$$

$$= \frac{m}{n}\left[1 + \sum_{\nu=1}^{\infty} \frac{(x-u)}{\nu!} \frac{n}{m} p_m^{\nu-1}\right] \tag{13}$$

For large positive (negative) values of the variate, the probability density p(x) and the probability $1 - P(x)$ (and P(x)) are small. The derivatives $p'(x)$ are also samll and negative (positive) and the quotients p/(1-P) and p/P become indeterminate for large and small values of the variate respectively. If this holds, it is proper to apply L'Hôpital's Rule (54).

$$\lim_{x \to \infty} \frac{p(x)}{1 - P(x)} = \lim_{x \to \infty} - \frac{p'(x)}{p(x)} \qquad (14)$$

$$\lim_{x \to -\infty} \frac{p(x)}{P(x)} = \lim_{x \to -\infty} \frac{p'(t)}{p(x)} \qquad (15)$$

We can apply this to obtain successive derivatives of p_m. Thus, from equation (11), we have

$$\frac{p'_m}{p_m} = \frac{p_m}{P_m} = \frac{n}{m} p_m \qquad (16)$$

We write $\frac{n}{m} p_m = \alpha_m$ (17)

Thus equation (16) may be written from (17) as:

$$p'_m = \alpha_m p_m \qquad (18)$$

From (17) we obtain the first derivative in the expansion of (13):

$$\frac{n}{m} p'_m = \alpha_m^2 \qquad (19)$$

In the same way we obtain higher derivatives. From (16) we see that:

$$p_m' = \frac{p_m^2}{p_m} \qquad (20)$$

with the same approximation as previously used, further differentiation gives:

$$p_m'' = \frac{2p_m p_m'}{p_m} - \frac{p_m^2}{p_m^2} p_m \qquad (21)$$

Dividing through by p_m gives:

$$\frac{p_m''}{p_m} = \frac{2p_m p_m'}{p_m p_m} - \frac{p_m^2 \; p_m}{p_m^2 p_m}$$

$$= \frac{2\alpha_m p_m}{p_m} - \alpha_m^2$$

$$= 2\alpha_m^2 - \alpha_m^2$$

$$= \alpha_m^2$$

Therefore $\quad p_m'' = \frac{m}{n}\alpha_m^3 \qquad (22)$

In general, it can be shown (see appendix II) that

$$\frac{n}{m} p_m^{\nu} = \alpha_m^{\nu+1} \qquad (23)$$

By writing $(\nu-1)$ instead of $(\nu+1)$ equation (13) can be modified to read as:

$$P(x) = \frac{m}{n}\left[1 + \sum^{\infty} \frac{(x-u)}{\nu!}\alpha_m^{\nu}\right] \quad (24)$$

We introduce the reduced m^{th} smallest value y_m defined by:

$$y_m = \alpha_m(x - u_m) \quad (25)$$

as the difference of the m^{th} smallest value from the characteristic m^{th} smallest value multiplied by a factor which has the dimension x^{-1}. This transformation of equation (25) reduces the largest value in size and changes the scale so that y_m has no dimension. The probability function in equation (24) becomes:

$$P(x) = \frac{m}{n}\left[1 + e^{y_m} - 1\right]$$

$$= \frac{m}{n} e^{y_m} \quad (26)$$

This approximation holds for any initial probability function of the exponential type and for large x. The distribution function becomes under the same conditions:

$$p(x) = \frac{m}{n}\alpha_m e^{y_m} \quad (27)$$

The initial probability P(x) and the initial distribution p(x) in the neighborhood of the characteristic smallest value tend for m = 1 to

$$P(x) = \frac{e^y}{n}; \qquad p(x) = \frac{\alpha_1 e^y}{n}; \qquad y = \alpha_1 (x-u_1) \qquad (28a,b)$$

Substitution of this expression into equation (8) leads to the first asymptotic probability function:

$$\lim_{n\to\infty} \Phi(x) = \lim_{n\to\infty} \left\{ 1 - \left[1 - \frac{e^y}{n} \right]^n \right\} \qquad (29)$$

Applying the Binomial Theorum with $t = e^y$

$$\Phi(x) = 1 - \left[1 - \frac{nt}{n} + \frac{n(n-1)}{2!}\frac{t^2}{n^2} - \frac{n(n-1)(n-2)}{3!}\frac{t^3}{n^3} + \ldots \right]$$

As $n \to \infty$

$$= 1 - \left[1 - t + \frac{t^2}{2!} - \frac{t^3}{3!} + \right]$$

$$\Phi(x) = 1 - \exp(-e^y) \qquad (30)$$

and,

$$\phi(x) = \exp(-y - e^{-y}) \; ; \quad y = \alpha_1 (x-u_1) \quad (31a,b)$$

The probability and distribution functions of the reduced extremes are parameter free. Equation (30) is called the first asymptotic distribution or the first asymptote. It is also called the second double exponential distribution.

Moments can in general be used to describe the shape of a distribution. For example, the first moment tells us the average value of the random value;

the second moment about the mean tells us something about the spread or dispersion of a distribution, i.e. how close one can expect the random variable to be near the mean. The third moment about the mean is used to describe the symmetry or lack thereof (skewness) of a probability distribution.

Thus, to estimate the parameters of this distribution, the moment generating function is determined.

$$G_n(t) = \int_{-\infty}^{\infty} e^{ty} e^{(-y-e^{ty})} dy = \int_{-\infty}^{\infty} e^{ty} e^{-e^{y}} e^{-y} dy$$

By the transformation $e^{-y} = z$, this becomes

$$= \int_{0}^{\infty} z^{t} e^{-z} \frac{zdz}{z}$$

$$= \Gamma(1 + t) \qquad (32)$$

Instead of the usual standardization of variates, the following linear transformation is employed:

$$y = \alpha (x - \beta) \qquad (33)$$

Where β is an average of the same dimension as x and $1/\alpha$ is of the dimension of x. Consequently y has no dimension; y is called the reduced variate, whereas x is called the initial variate.

Any function may, by appropriate substitutions, be made linear. An advantage of doing this is that the question of the acceptance or rejection of the probability function may be settled by mere inspection. After the observations have been plotted, a straight line may be drawn provided that the scatter of the observations is sufficiently small.

The method of least squares is applied to the linear reduction of

$$x = \beta + \frac{y}{\alpha} \quad ; \quad y = \alpha(x - \beta) \qquad (34a,b)$$

The criterion of least squares selects these values of α and β in a way which makes the square of the horizontal distances a minimum (47).

$$\sum_{i=1}^{n}\left[x_i - (b_1 + \frac{y_i}{a_1})\right]^2$$

The quantities a_1 and b_1 are the least squares estimates of α and β. Differentiating partially with respect to b_1 and $1/a_1$, we obtain:

$$\sum_{i=1}^{n} -2\left[x_i - (b_1 + \frac{y_i}{a_1})\right] = 0 \qquad (35)$$

and

$$\sum_{i=1}^{n} -2y_i\left[x_i - (b_1 + \frac{y_i}{a_1})\right] = 0 \qquad (36)$$

Consequently from (35)

$$\sum_{i=1}^{n} x_i - \sum_{i=1}^{n} (b_1 + \frac{y_i}{a_1}) = 0 .$$

$$\sum_{i=1}^{n} x_i - nb_1 - \sum_{i=1}^{n} \frac{y_i}{a_1} = 0$$

After dividing by n:

$$x_o = b_1 + \frac{\bar{y}_n}{a_1} \quad (37)$$

Similarly from (36) we obtain:

$$\sum_{i=1}^{n} y_i x_i = b_1 \sum_{i=1}^{n} y_i + \frac{1}{a_1} \sum_{i=1}^{n} y_i^2 \quad (38)$$

The solutions to equations (37) and 38) are:

$$\frac{1}{a_1} = \frac{\overline{(xy)}_n - x_o}{\sigma_n^2} \quad (39)$$

$$x_o - b_1 = \bar{y}_n / a_1 \quad (40)$$

Where

$$\bar{x}_o = \frac{1}{n} \sum_{i=1}^{n} x_i ; \quad \overline{x_o^2} = \frac{1}{n} \sum_{i=1}^{n} x_i^2 ; \quad s_x^2 = \frac{n(\overline{x_o^2} - \bar{x}_o^2)}{n-1}$$

$$\bar{y}_n = \frac{1}{n} \sum_{i=1}^{n} y_i ; \quad \overline{y_n^2} = \frac{1}{n} \sum_{i=1}^{n} y_i^2 ; \quad \sigma_n^2 = \overline{y_n^2} - \bar{y}_n^2$$

$$\overline{(xy)}_n = \frac{1}{n} \sum_{i=1}^{n} x_i y_i \quad (41)$$

The foregoing minimized the horizontal distances. A second set of equations, can be written minimizing the vertical distances, i.e. in this case we seek to minimize

$$\sum^{n} \left[y_i - a_2(x_i - b_2) \right]^2$$

where a_2 and b_2 are the least squares estimates of α and β in the relation $y = \alpha(x-\beta)$. Following the same procedure as before we partially differentiate with respect to a_2 and b_2 the equations:

$$\bar{y}_n = a_2\bar{x}_o - a_2b_2 \qquad (42)$$

$$\overline{(xy)}_n = \overline{a_2x_o^2} - a_2b_2\bar{x}_o \qquad (43)$$

the solutions of which are:

$$\frac{1}{a_2} = \frac{s_x^2}{\overline{(xy)}_n - \bar{x}_o\bar{y}_n} \qquad (44)$$

$$\bar{x}_o - b_2 = \bar{y}_n/a_2 \qquad (45)$$

Each solution requires the knowledge of four averages. The mean $\bar{x}_o$ and the standard deviation s_x of the observations have to be calculated from experimental data. The averages $\bar{y}_n$ and σ_n of the reduced variate depend only upon the number of observations and can be calculated for all conditions. However, the cross product$(xy)_n$ which occurs in both solutions depends on both the experimental observations and the number of observations and would have to be calculated anew for each series of observations. To eliminate the calculation of the cross-product, define new variables a, and b by:

$$1/a = \sqrt{1/(a_1 a_2)} \tag{46}$$

$$\bar{x}_o - b = \sqrt{(\bar{x}_o - b_1)(\bar{x}_o - b_2)} \tag{47}$$

Thus, when equations (39) and (44) are multiplied together,

$$1/a = s_x/\sigma_n \tag{48}$$

Similarly, when (40) and (45) are multiplied together the result is:

$$b = \bar{x}_o - (\bar{y}_n/ a) \tag{49}$$

These estimates in (48) and (49) require only the knowledge of the sample mean and standard deviation and the population mean $\bar{y}_n$ and standard deviation σ_n of that population.

The mean of the reduced extremes is found by taking the first derivative of $\Gamma(1+t)$ for $t = 0$. Taking advantage of the derivation given for $\Gamma^1(1)$ on page 39 of reference (43) :

$$\Gamma^1(1) = -\gamma \tag{50}$$

where γ is Euler's constant (0.57721....). This is the first central moment of the reduced variate. The second moment is given by

$$\Gamma''(1) = \gamma^2 + (\pi^2/6) \qquad (51)$$

Therefore, the standard deviation of the reduced variate is:

$$\sigma_n = \sqrt{\overline{y_n^2} - \bar{y}_n^2}$$

$$= \sqrt{\gamma^2 + \pi^2/6 - \gamma^2}$$

$$= \pi/\sqrt{6} \qquad (52)$$

Substituting these results into (48) and (49), we have:

$$1/a = \sqrt{6}\ s_x/\pi \quad ; \quad b = \bar{x}_o - (\gamma/a) \qquad (53)$$

Applying this to the reduced variate defined in (25), with m =1 we have as a practical result:

$$\alpha_1 = \pi/\sqrt{6}\ s_x \text{ and } u_1 = \bar{x}_o - (\sqrt{6}\ s_x\gamma/\pi) \qquad (54a,b)$$

The expressions for the second and third asymptotic distributions of reduced smallest values may be obtained by logarithmic transformations of the expression for the first asymptote.

The second asymptotic distribution is obtained in the case where the initial distribution is of the Cauchy type (55). Following substitution in equation (30):

$$\alpha_1(x - u_1) = c(-\log_e z + \log_e v_1) \qquad (55)$$

where z is the variate for the second asymptotic distribution and c and v_1 are constants. So that the expression for the second asymptote of reduced smallest values is:

$${}_2\Phi(z) = 1 - \exp(-e^{\log_e (v_1/z)^c})$$

$$= 1 - \exp \left[-(v_1 / z)^c\right] \qquad (56)$$

$$v_1 < 0 \qquad z \leq 0 \qquad c > 0$$

and the density is obtained by differentiation:

$${}_2\phi(z) = -(c/v_1)(v_1/z)^{c+1}\exp\left[-(v_1/z)^c\right] \quad (57)$$

The expression in (55) means that the logarithms of a logarithmic extreme value distribution are extreme value distributed (76). The parameters which are calculated for the first type of extreme value distribution can be used in the second type. From equation (55) we have:

$$\alpha_1(x - u_1) = -c(\log_e z - \log v_1)$$

Thus,

$$\alpha_1 = -c; \quad u_1 = \log v_1 \text{ or } e^{u_1} = v_1 \qquad (58a,b)$$

For both the initial distributions of the first and second asymptotic distribution, the variate is unlimited. However the initial distribution for the third type of asymptotic distribution given by $1 - (x - \epsilon)^k$ where ϵ is a lower limit to the left in that $x \geq \epsilon$. To obtain an expression for the third asymptote, which is also known as the Weibull distribution, we make the following substitution in equation (30) Ref. (55) :

$$\alpha_1(x - u_1) = k \log_e\left[\frac{x - \epsilon}{v' - \epsilon}\right] \qquad (59)$$

The parameter ϵ represents the lower limit on the value that x can have and is called the location parameter whereas $v' - \epsilon$ or simply v' is called the scale parameter. Each is so named because of the effect they have on the distribution. We have then,

$$\begin{aligned} {}_3\Phi(x) &= 1 - \exp\left[-\exp^{\log_e \left(\frac{x - \epsilon}{v' - \epsilon}\right)^k}\right] \\ &= 1 - \exp - \left[\frac{x - \epsilon}{v' - \epsilon}\right]^k \end{aligned} \qquad (60)$$

with conditions $x \geq \epsilon$; $v' > \epsilon$; $k > 0$

Parameter k is known as the shape parameter and can be estimated from the symmetry or skewness of the sample values.

The density of this distribution is

$$ {}_3\phi(x) = \frac{k}{v'-\epsilon} \cdot \left(\frac{x-\epsilon}{v'-\epsilon}\right)^{k-1} \exp\left[-\left[\frac{x-\epsilon}{v'-\epsilon}\right]^{k} \right] \quad (61) $$

The sample moments are used to estimate the unknown parameters of a distribution. For non-negative variates, the calculation of the population moments about the origin and of integral order q is given by

$$ x^{q} = \int_0^{\infty} x^{q} f(x)dx \quad (62) $$

where f(x) is density of the distribution of the random variable x. Applying this, the reduced moments of order q are:

$$ \left(\frac{x-\epsilon}{v'-\epsilon}\right)^{q} = \int_0^{\infty} \left(\frac{x-\epsilon}{v'-\epsilon}\right)^{q} \left(\frac{k}{v'-\epsilon}\right)\left(\frac{x-\epsilon}{v'-\epsilon}\right)^{k-1} \exp\left[-\left(\frac{x-\epsilon}{v'-\epsilon}\right)^{k}\right]dx \quad (63) $$

Let $\frac{x-\epsilon}{v'-\epsilon} = \theta$ so that $dx = (v'-\epsilon)d\theta$. Consequently, the right hand side of (63) becomes

$$ k\int_0^{\infty} \theta^{k+q-1} \exp(-\theta^{k})d\theta \quad (64) $$

Let $\theta^{k} = \zeta$. Therefore

$$ \begin{aligned} d\theta &= d\zeta / (k\,\zeta^{k-1}) \\ &= d\zeta / k(\zeta/\theta) \end{aligned} $$

so that

$$ d\theta/\theta = d\zeta/(k\,\zeta) $$

As a result of this transformation, equation (64) becomes

$$\int_0^{\infty} \zeta^{(q/k)+1} \exp(-\zeta) \frac{d\zeta}{\zeta} = \int_0^{\infty} \zeta^{(q/k)} \exp(-\zeta) d\zeta$$

$$= \Gamma(1 + q/k) \qquad (65)$$

Whence,

$$(x - \epsilon)^q = (v - \epsilon)^q \; \Gamma(1 + q/k) \qquad (66)$$

For q = 1, the mean is:

$$\bar{x} = \epsilon + (v' - \epsilon) \; \Gamma(1 + 1/k) \qquad (67)$$

The variance is

$$\sigma^2 = (v'-\epsilon)^2 \; \Gamma(1 + 2/k) - \left[(v'-\epsilon) \; \Gamma(1 + 1/k)\right]^2$$

$$= (v'-\epsilon)^2 \left\{\Gamma(1+ 2/k) - \Gamma^2 (1 + 1/k)\right\} \qquad (68)$$

The estimation of the parameter k is done by calculating the skewness of the sample. Skewness is defined as (48):

$$\rho = \mu_3/\sigma^3 \qquad (69)$$

where μ_3 is the third central moment and σ is the standard deviation. The expression for the third central moment is determined by the use of the relation

$$\mu_3 = E(\bar{\xi} - \mu)^3$$

$$= \mu_3' - 3\mu\mu_2' + 2\mu^3 \qquad (70)$$

where E denotes the mathematical expectation of the random variable $(\bar{\xi} - \mu)$; μ denotes the average and μ_r' denotes the r^{th} moment about the origin. Thus from (66) we have

(71)

$$\mu_3' = (v'-\epsilon)^3 \Gamma(1+3/k) - 3(v'-\epsilon)^3 \Gamma(1+1/k) \; \Gamma(1+2/k) +$$

$$2(v'-\epsilon)^3 \Gamma^3(1+1/k)$$

Hence, the skewness as defined in (69) is:

$$\frac{\mu_3}{\sigma^3} = \frac{\Gamma(1+3/k) - 3\,\Gamma(1+1/k)\,\Gamma(1+2/k) + 2\,\Gamma^3(1+1/k)}{\left[\Gamma(1+2/k - \Gamma^2(1+1/k)\right]^{3/2}} \tag{72}$$

Once the skewness of the sample of breakdown voltages has been determined, it is possible to solve for the root, (1/k), of this nonlinear equation by means of Aitken's Δ^2 method. This method consists of the algorithm (128)

$$r \simeq x_n + 2 - \frac{(x_{n+2} - x_{n+1})^2}{x_{n+2} - 2x_n} \tag{73}$$

where r is the exact root. To make use of this iterative method, the nonlinear equation (72) has to be brought into the form of:

$$x = g(x) \tag{74}$$

For this purpose use is made of the identity

$$a\,\Gamma(a) = \Gamma(a+1) \tag{75}$$

Thus,

$$\frac{1}{k} = \frac{\Gamma(1+3/k) - 3\,\Gamma(1+1/k)\,\Gamma(1+2/k) + 2\,\Gamma^3(1+1/k)}{\rho\,(1/k)^2\left[2k\,\Gamma(2/k) - \Gamma^2(1/k)\right]} \tag{76}$$

with 1/k representing x in (74)

After employing an initial starting value of $1/k$, successive interations of the recursive formula of (73) converges to a root. An initial estimate of $1/k$ by using the table on page 282 of (53) speeds convergence and helps avoid instability problems which arise in the computer calculations when skewness is small and negative.

Once $1/k$ has been determined, the scale and location parameters, namely v' and ϵ respectively, can be estimated.

$$v' - \bar{x} = v' - \epsilon - (v' - \epsilon)\,\Gamma(1 + 1/k)$$
$$= (v' - \epsilon)\left[1 - \Gamma(1 + 1/k)\right] \qquad (78)$$

From (68)

$$\sigma = (v' - \epsilon)\left[\Gamma(1 + 2/k) - \Gamma^2(1 + 1/k)\right]^{1/2} \qquad (79)$$

Dividing (78) by (79) yields

$$\frac{v' - \bar{x}}{\sigma} = \frac{1 - \Gamma(1 + 1/k)}{\left(\Gamma(1 + 2/k) - \Gamma^2(1 + 1/k)\right)^{1/2}} \qquad (81)$$

So, the scale parameter v, can be estimated as

$$v' = \bar{x} + \sigma\left\{\frac{1 - \Gamma(1 + 1/k)}{\left[\Gamma(1 + 2/k) - \Gamma^2(1 + 1/k)\right]^{1/2}}\right\}. \qquad (81)$$

Where σ here represents the standard deviation determined from the sample values and k is the shape parameter.

The lower limit or location parameter ϵ is estimated from (67) by employing the estimate of v'just determined in (81). Thus,

$$\bar{x} = \epsilon + v'\Gamma(1 + 1/k) - \epsilon\,\Gamma(1 + 1/k)$$
$$= \epsilon\left[1 - \Gamma(1 + 1/k)\right] + v'\,\Gamma(1 + 1/k)$$

Hence

$$\epsilon = \frac{\bar{x} - v'\Gamma(1 + 1/k)}{1 - \Gamma(1 + 1/k)} \qquad (82)$$

In this chapter has been derived the distribution of smallest values of N samples, each of size n taken from a parent population which has an exponential distribution. Then by appropriate logarathmic transformations of this expression there were obtained expressions for the second and third asymptotes which have the Cauchy and the "limited" distribution as their initial distributions respectively (56).

We are interested in the distribution of the smallest values of a sample size n, which in our case, corresponds to the results of one experimental run at a certain electrode gap length. According to the extreme value probability theory (the stability postulate), where an asymptote exists, a sample size n taken from the parent population, will also have the same asymptotic distribution as the Nn observations that could otherwise have been carried out. The practical advantage of this is that results obtained on a scaled-downed model, say of a transformer , can be transferred to the corresponding arrangement in the actual transformer which is N times larger.

If the voltage breakdown distribution obeyed the normal law, such would not be the case (152).

Of the three extreme value distributions of smallest value considered, the third type which is also called the Weibull distribution should be expected to yield the most fruitful results in breakdown measurements beause its variate has a lower limit. Physically this is analogous to a minimum voltage below which there are no breakdown voltages.

CHAPTER IV

RESULTS AND DISCUSSION OF RESULTS

4.1 GRAPHICAL COMPUTER PLOTS

If the actual probability of occurence of a particular value of a random variable could be determined, then the cumulative distribution of this observed distribution could be constructed. If there is a theoretical distribution which is thought to adequately describe the observed distribution, then their cumulative distributions may be compared by plotting one against the other. If the two distributions coincide, the plotted line will lie on a diagonal between (0,0) and (1,1). The degree to which there exists a lack of this coincidence will be characterized by a skewness in the plotted line. Thus, a graphical plot will give a visual indication of how adequately the chosen distribution describes the actual distribution of the random variable.

The only way of experimentally determining the actual probability distribution of the breakdown voltages is to examine a sample drawn at random from the population (155). Such a sample yields a somewhat diffuse image of the parent population. The sharpness of this image depends entirely on the size of the sample (155). In order to do this, a set of breakdown voltages from an experiment is considered as a random sample drawn from a larger population whose values have not been obtained. The probability associated with each breakdown voltage value is found by ordering the breakdown values from smallest to largest, as was done in equation 1 of Ch.3 so that:

$$x_1 \leq x_2 \quad \ldots\ldots\ldots\ldots \leq x_u \ldots \leq x_n \qquad (1)$$

where u represents the rank number and n is the sample size. The ratio of u/n is the relative order number of a one dimensional random variable of x. The probability of having a breakdown at a value equal to or less than x_u is equal to this ratio: i.e.

$$\text{Prob}\ (x \leq u) = u/n \qquad (2)$$

This formula would be precise if the sample size drawn were infinitely large. In such a case, equation (1) would say that the last value in the ordered set would always occur:

$$\text{Prob}\ (x_n) = 1$$

However, the sample size in reality is finite and there exists the finite probability that breakdown will not occur. This is accounted for by writing

$$F(x_i) = i/(n+1)$$

where i is the rank number of the breakdown voltage, and n is the total number of breakdowns. (NOTE: In accordance with the procedure followed by Gumbel and Goldstein (59), breakdown values that were identical for all practical purposes were given equal rank numbers.)

The quantity $P(x_i)$ is called the plotting position (156) because the observed values of x are plotted against it. The error introduced by this procedure diminishes as the sample size increases.

The distribution functions which were chosen were the three types of extreme value distributions discussed in Chapter III (see equations 30,56, and 60 in Chapter III) and the log-normal. Choice of this latter distribution was included because it has found application in describing the distribution of the life time of rubber tires (76). Usually, there is no explicit reason indicating why a particular distribution should be used (67), the best thing to do is simply to try it.

In order to carry out the graphical evaluation described, equations 30, 56, and 60 of Chapter III were transformed for the purposes of plotting by the following method which is demonstrated for the first asymptotic distribution function of smallest values (equation 30 of Chapter III):

$$_1\Phi(x) = 1 - \exp\left(-e^{\alpha_1(x-u_1)}\right)$$

$$1 - {_1\Phi(x)} = \exp\left(-e^{\alpha_1(x-u_1)}\right)$$

$$\log_e\left[1 - {_1\Phi(x)}\right] = -\exp(\alpha_1(x-u_1))$$

$$\log_e\left[\frac{1}{1 - {_1\Phi(x)}}\right] = \exp \alpha_1(x-u_1)$$

$$\ln \ln \frac{1}{1 - {}_1\Phi} = \alpha_1 (x - u_1) \qquad (5)$$

If we follow this same mehtod for the second asymptotic distribution of smallest values (equation 56, Chapter III), and also the distribution function for the third asymptotic distribution better known as the Weibull distribution (equation 60, Chapter III) we have, respectively:

$$\ln \ln \frac{1}{1 - {}_2\Phi} = c \ln \left(\frac{v_1}{x} \right) \qquad (6)$$

$$\ln \ln \frac{1}{1 - {}_3\Phi} = k \ln \left[\frac{x - \epsilon}{v' - \epsilon} \right] \qquad (7)$$

where x represents the breakdown voltage and the constants c, v_1, v', ϵ and k are the same constants as determined by the method in Chapter III.

The suitability of the log-normal distribution for the purpose of representing breakdown values was also examined. This distribution function is given by:

$$P(x) = \frac{1}{\sqrt{2\pi}} \int_{-\infty}^{h(u)} e^{-1/2\, u^2} \, du \qquad (8)$$

where $h(u) = \dfrac{\log x - u_e}{\sigma_e}$

x = the breakdown voltage values

u_e = the mean value of the logarithms of breakdown voltages

σ_e = the standard deviation of the logarithms of breakdown voltages (77).

In order to calculate P(x) on the computer, advantage is taken of the fact that the error function is part of the Scientific Subroutine Package available on the IBM computer system at McGill. The error function is defined as:

$$\mathrm{erf}(\lambda) = 2/\sqrt{\pi} \int_0^{\lambda} e^{-\lambda^2} d\lambda \tag{10}$$

Consequently, P(x) can be expressed as:

$$P(x) = 1/\sqrt{2\pi}\int_{-\infty}^{0} e^{-1/2\ u^2} du + 1/\sqrt{2\ \pi}\int_{0}^{h(u)} e^{-1/2\ u^2} du \tag{11}$$

$$= 1/2 + 1/2\mathrm{erf}(u/\sqrt{2}) \tag{12}$$

The $1/\sqrt{2}$ factor appearing in (11) and not appearing in the expression defining the error function (10) is accounted for by observing that the substitution of $\lambda = u/\sqrt{2}$ into (10) produces a factor of $1/\sqrt{2}$ in the resultant new differential that is substituted for 'du' into (10). To be able to plot the log-normal distribution on the same set of axes as the previous three distributions, for purposes of comparision, the distribution must be expressed in the form of lnln(1/1-P(x)) as before. Consequently (12) is simply transformed by writing

$$\ln\ln\left[\frac{1}{1 - P(x)}\right] = \ln\ln\left[\left\{1/2 - 1/2\mathrm{erf}(u/\sqrt{2})\right\}^{-1}\right] \tag{13}$$

From all this there result four sets of points produced from assumed distributions all to be plotted against a fifth set of points produced from actual observations. This is set out in the following Table.

TABLE 4-1

RELATIONS PLOTTED

	vs		
$\ln\ln \dfrac{1}{1 - F(x_i)}$		$\ln\ln \dfrac{1}{1 - {}_1\Phi(x)}$	Type I extreme value
$\ln\ln \dfrac{1}{1 - F(x_i)}$		$\ln\ln \dfrac{1}{1 - {}_2\Phi(x)}$	Type II extreme value
$\ln\ln \dfrac{1}{1 - F(x_i)}$		$\ln\ln \dfrac{1}{1 - {}_3\Phi(x)}$	Type III (Weibull)
$\ln\ln \dfrac{1}{1 - F(x_i)}$		$\ln\ln \dfrac{1}{1 - P(x)}$	Log-normal

where $F(x_i)$ rpresents the actual distribution of breakdown voltages.

An example of the resulting plot for experiment no. 25 is shown in Figure 4-1. The computer printout along the ordinate axis shows $\ln\ln 1/(1 - F(x))$, where $F(x)$ signifies the actual observed probability distribution. An auxillary scale alongside the ordinate axis indicates $F(x)$. Similarly a computer printout along the abscissa displays $\ln\ln 1/1 - P(x)$ where $P(x)$ is the theoretical distribution. An auxillary scale alongside the abscissa shows $P(x)$. The value of this type of plot lies in the fact that it has magnified the ends of the distribution. Often it is only by examination of the tail of a distribution that it can be accurately determined which theoretical distribution provided the best fit of the

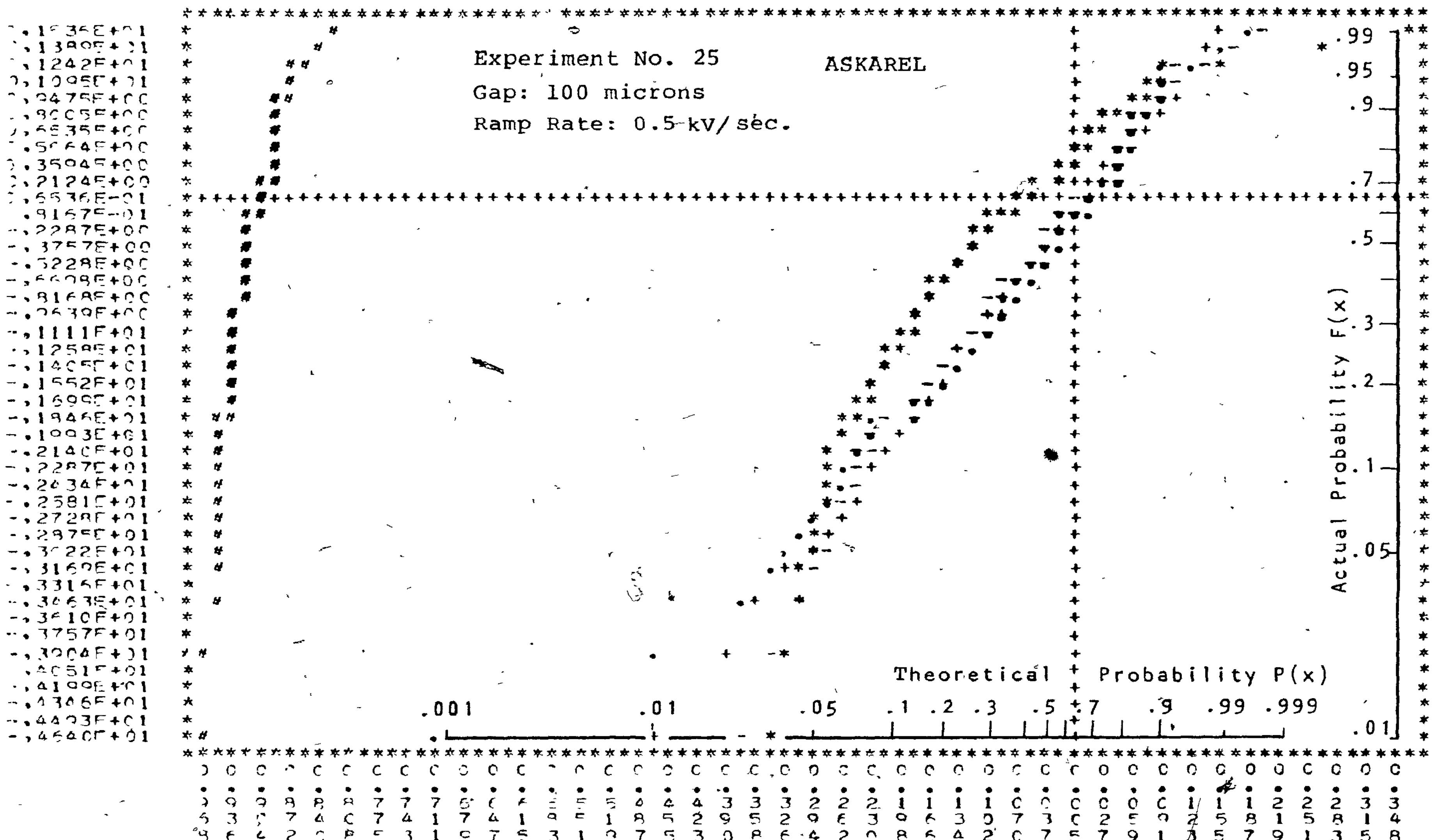

X AXIS (HORIZONTAL-AXIS) EXPONENT 1

FIGURE 4-1

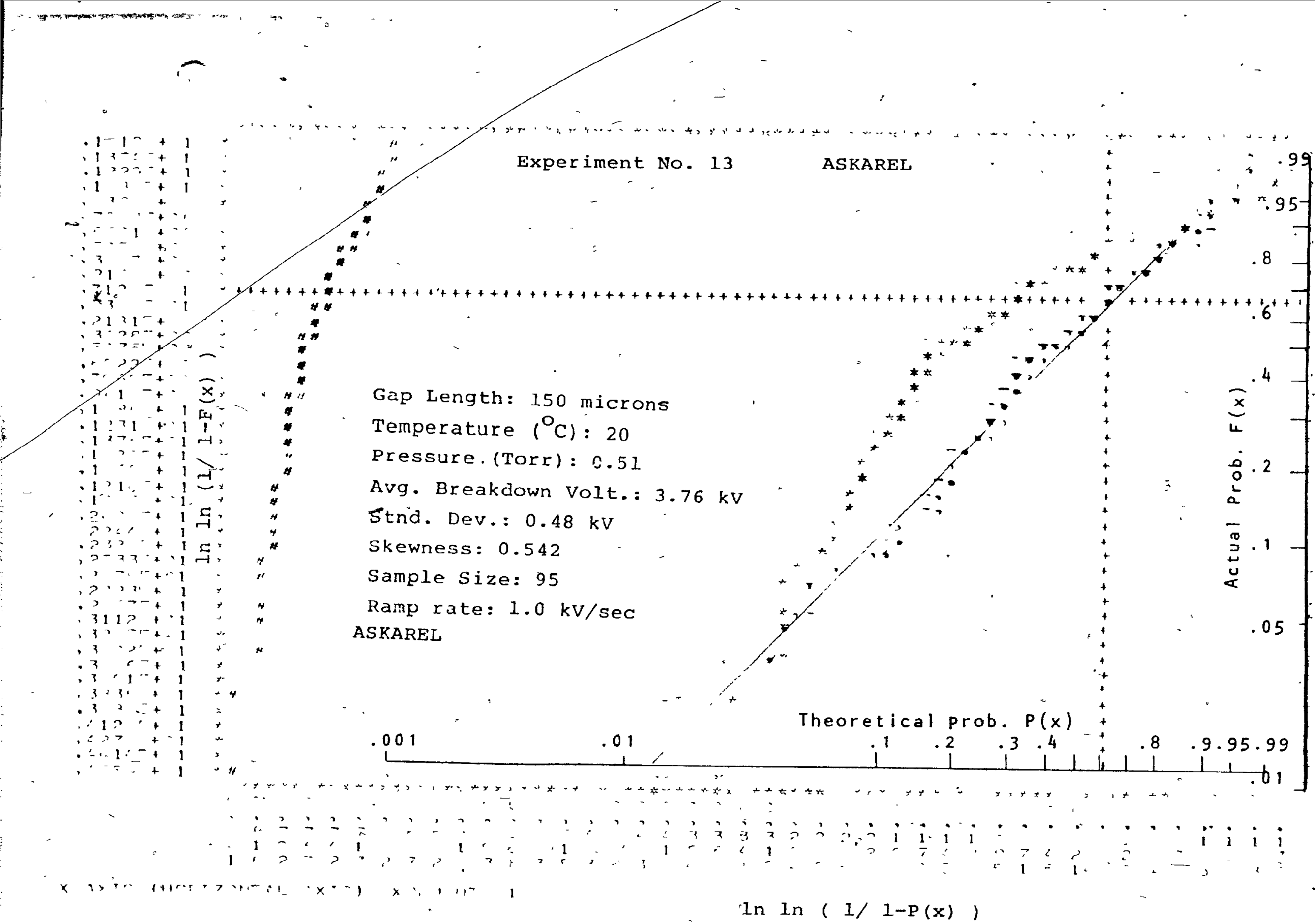
Experiment No. 13
ASKAREL
Gap Length: 150 microns
Temperature (°C): 20
Pressure (Torr): 0.51
Avg. Breakdown Volt.: 3.76 kV
Stnd. Dev.: 0.48 kV
Skewness: 0.542
Sample Size: 95
Ramp rate: 1.0 kV/sec
ASKAREL
ln ln (1/ 1-F(x))
Actual Prob. F(x)
.99
.95
.8
.6
.4
.2
.1
.05
.01
Theoretical prob. P(x)
.001
.01
.1
.2
.3
.4
.8
.9
.95
.99
ln ln (1/ 1-P(x))

FIGURE 4-2

data. A similar plot is shown in Figure 4-2 for a typical experiment but without the '+' symbols showing the position of the line corresponding to the actual distribution. These have been omitted to prevent "cluttering" of the plot. Instead, a line was drawn to represent the line that would have been drawn with the '+' symbols by the computer.

From both these graphs it can be seen that the chosen distributions which best represent the breakdown values observed are the log-normal and the Type III extreme value distribution. The first asymptotic distribution (represented by '*') is noticably skewed. The second asymptotic distribution despite its similarity of form (Type II) (represented by '#') does not fit the observed distribution function at all, but instead lies far to the right of the graph, off the diagonal. These results were observed consistently for all plots made.

4.2 GOODNESS-OF-FIT TEST

A more precise answer to the question of how well the various assumed distribution functions correspond to the actual distribution is obtained by application of the Kolmogorov-Smirnov Goodness-of-Fit test. The statistic used for this significance test is the maximum absolute deviation of the assumed null distribution function $F_o(x)$ (which in our case is ${}_1\Phi(x)$, ${}_2\Phi(x)$,

$_3\Phi(x)$ or $P_{LN}(x)$) from the sample distribution function $F(x)$:

$$D = \max_{-\infty < x < \infty} \left| F(x) - F_o(x) \right| \qquad (14)$$

This can be represented graphically by obtaining the value $Y_i = F_o(x_i)$ for breakdown voltage x_i of the sample and then ordering the Y_i from smallest to largest. A "staircase" can then be plotted of the points $(Y_i, i/n)$ where i/n represents the probability of Y_i according to the reasoning in eq. 2, (91). A diagonal is then plotted consisting of the points (Y_i, Y_i). The maximum absolute deviation between this diagonal and the "staircase" for some value of x_i furnishes the statistic of eq. (14). For each size of deviation there is a corresponding probability that the particular observed distribution could have arisen as a set of N independent samples from the assumed distribution. The details of the calculation required to determine this probability is set out in Appendix IV.

If the resulting probability for a particular maximum deviation D is 0.05, then it means that the conclusion that a particular breakdown voltage value does not come from the population that it is assumed to belong to, has a probability of at least 0.95 of being right, and a probability not exceeding 0.05 of being wrong. The probability of being wrong about such a conclusion is referred to as the test significance level (27). The

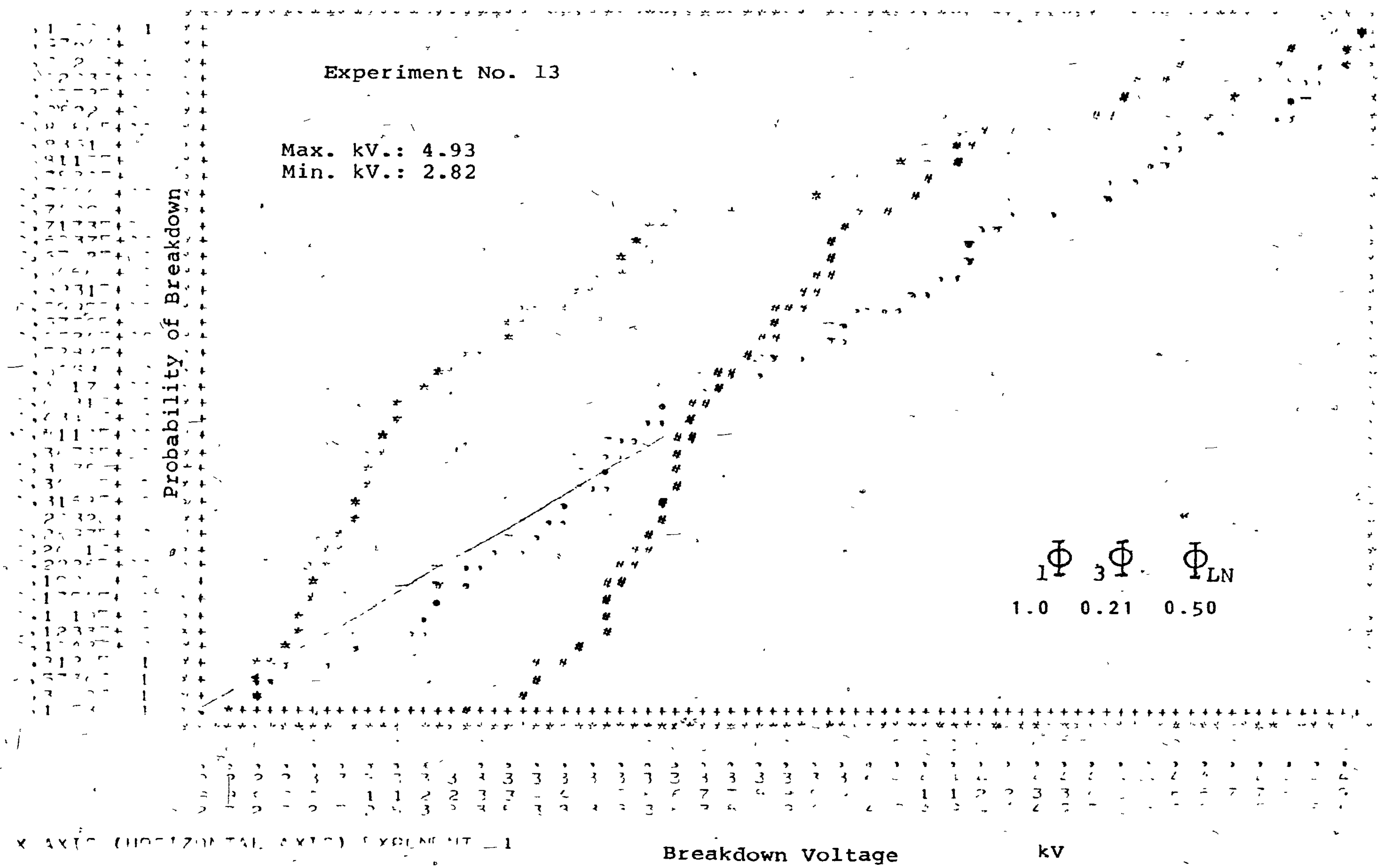
Experiment No. 13
Max. kV.: 4.93
Min. kV.: 2.82
Probability of Breakdown
$_1\Phi$ $_3\Phi$ Φ_{LN}
1.0 0.21 0.50
Breakdown Voltage kV

FIGURE 4-3

decreasing significance levels mean that the breakdown values are being better fitted by the particular distribution function chosen.

A sample computer plot showing the diagonal or "staircase" associated with this goodness-of-fit test for experiment no. 13 is shown in Figure 4-3. The large number of minute steps that would compose the "staircase" of a perfectly fitting distribution are represented by a straight line drawn as a diagonal. The goodness-of-fit test results for this experiment are shown on the graph.

4.3. THE CUMULATIVE HAZARD RATE

If we wish to know the probability of failure of items that have survived up to point x, for some additional increment $x + \Delta x$, this is obtained by use of the hazard function which is defined by (78).

$$h(x) = f(x) / 1 - F(x) \tag{15}$$

where $h(x)$ = the hazard function

$f(x)$ = the probability density function

$1 - F(x)$ = the survival function

The hazard function in the present context refers to a probability of occurrence of breakdown stress, after some past history of applied stress. This function is also known as:

1. The instantaneous failure rate of a distribution

2. The conditional failure rate
3. The intensity function
4. The force of mortality

The quantity $\Delta x \cdot h(x)$ is the probability that a voltage value known to be equal to or larger than x will be situated between x and $x + \Delta x$. This is known as the hazard rate (58). The sample cumulative hazard function, based on the sum of conditional probabilities is approximated by the theoretical cumulative hazard function, which is the integral of the instantaneous fairlure rate. Consequently the cumulative hazard rate is (79):

$$H(x) = \int_0^x \frac{f(x)}{1 - F(x)} dx = \int_0^x h(x)\,dx = -\log_e (1 - F(x)) \quad (16)$$

Thus, the relationship between the cumulative distribution and the cumulative hazard function for a distribution is:

$$F(x) = 1 - e^{-H(x)} \quad (17)$$

The sample cumulative hazard function is used because it smooths the data better than the instantaneous failure rate.

The advantages of using hazard plotting compared to a probability plot are (80):

(1) The capability of readily handling arbitrarily censored data. In the experiments which were conducted, the voltage was raised until breakdown occurred. Suppose this voltage was allowed to rise only to a certain pre-set maximum. If no breakdown occurred in that interval, it would only be known that the breakdown voltage for that particular instance was beyond the maximum possible voltage. In such a situation, that voltage level would be referred to as "censored". This would be useful if for example a "conditioning" procedure used involved prestressing the liquid dielectric by a train of ramp voltages which were gradually increased in magnitude over a period of time. In such a case a breakdown would not occur with every voltage application.

(2) The ability to obtain standard probability statements directly from an auxilary probability scale which can be readily computed.

(3) Determination of the instantaneous failure rate which can be found by drawing a tangent to the cumulative hazard curve.

The empirical cumulative hazard values and plot can be obtained by considering any two consecutive breakdown voltages x_i and x_{i+1} with $x_{i+1} > x_i$. The corresponding probabilities of breakdown F(x) are:

$$F(x_i) = \frac{i}{N+1} \quad ; \qquad F(x_{i+1}) = \frac{i+1}{N+1} \qquad (18)$$

Consequently $h(x_i) \cdot \Delta x = F(x_{i+1}) - F(x_i)$

$$\doteq 1/(N+1)$$

The denominator in equation (16), $1 - F(x)$, is given for the purposes of computation as:

$$1 - F(x_i) = 1 - (i/N+1) = \frac{N + 1 - i}{N + 1} \qquad (19)$$

Consequently the computational form of eq (16) which can be obtained for the discrete voltage distribution obtained experimentally is

$$H(x_i) = \sum_{i=1}^{n} \frac{h(x_i)}{1 - F(x_i)}$$

$$= \sum_{i=1}^{n} \frac{1}{N - i + 1} \qquad (20)$$

The quantity $1/(N - i + 1)$ where N = sample size, i = rank number of the random variable (breakdown voltage) (see Section 4.1) is called the hazard value.

The cumulative hazard rates of the various assumed probability distributions under investigation can be obtained by applying equation (17) to equations

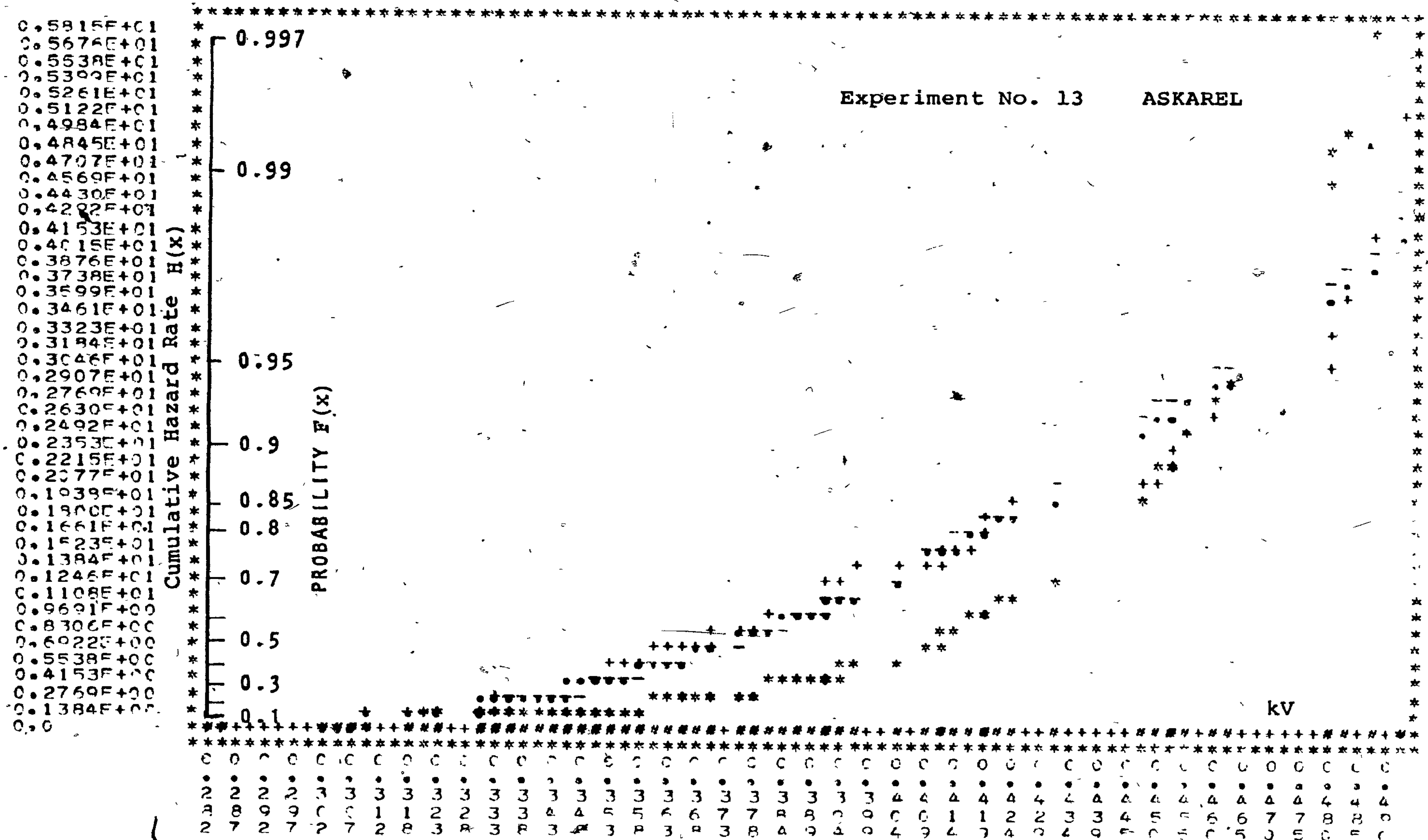

X-AXIS (HORIZONTAL-AXIS) EXPONENT 1

Y MAXIMUM C.58145E+C1
Y MINIMUM C.
X MAXIMUM 0.49283E+C1
X MINIMUM C.28194E+C1

FIGURE 4-4

CUMULATIVE HAZARD PLOT

30, 56, and 60 of Chapter III. Thus expression of the cumulative hazard rate for the first, second, and third asymtotic distributions:

$$_1H(x) = \alpha_1(x - u_1) \qquad (21)$$

$$_2H(x) = \log_e(v_1/x)^c \qquad (22)$$

$$_3H(x) = -\log_e((x-\epsilon)/(v'-\epsilon))^k \qquad (23)$$

where the constants α_1, u_1 v_1, k, v' and ϵ are the same as those determined in Chapter III; x is the breakdown voltage. An expression of the cumulative hazard rate for the log-normal distribution is directly obtained by application of equation (21) and the log-normal distribution (given by eqs.(8) and (9))

$$H_{LN}(x) = -\ln \left[1 - P(h(u))\right] \qquad (24)$$

where h(u) has been defined in equation (9).

A typical plot of the cumulative hazard rate against breakdown voltages for the probability distributions is illustrated in Figure 4-4. This is from experiment no. 13 whose graph of $\ln\ln\left[(1-F)^{-1}\right]$ was shown in Figure 4-2. The actual cumulative hazard rate calculated for an experiment is represented by '+' How far the other curves lie from the curve of actual values again indicates the lack of suitability of the paricular distribution function as furnishing a statistical description of the breakdowns.

An estimate of the instantaneous failure rate can be obtained for any breakdown value shown on the abscissa by drawing a tangent to the curve represented by '+'. In all cases it could be seen that the failure rate increased with increasing voltage.

4.4 'FREQUENCY OF BREAKDOWN VOLTAGE' PLOTS

4.4.1 The "Pile of Sand" Technique

The method by which density plots show the relative frequency of breakdown voltages were obtained, can be understood by picturing a straight line with points representing breakdown voltages randomly distributed on the line. If a small pile of sand were deposited on each point, then the individual piles would quickly form a mound where the points are more densely clustered along the line. This method of plotting density is realized by the use of the Fortran function 'AMAXI' which functions in the same manner as our figurative "pile of sand", because a plot of it has a triangular shape. To make sure that the density plot would be an analytically useful tool, care was taken to scale the "pile of sand" so that their sum over the entire range of breakdown voltages is unity, thus satisfying the requirement

$$\sum_{i=1}^{\infty} f(x_i) = 1$$

These summations were carried out in double precision. By varying the scale parameter, the "spikiness" of the "pile of sand" and therefore the sensitivity or coarseness of the plot could be controlled. This scale parameter is chosen by experiment according to which value yields the best result.

4.4.2 The Pearson System

The density functions of many continuous distributions satisfy a differential equation of the form

$$f'(x) = \frac{x - t}{c_2x^2 + c_1x + c_o} f(x) \qquad (25)$$

where t and the c's are constants. It can be shown that the constants of the equation can be expressed in terms of the first four moments of the density function, if these are finite (38). The solutions are classified according to the nature of the roots of the equation $c_o + c_1x + c_2x^2 = 0$ and in this way a great variety of possible types of density curves are obtained. The details of the "Pearson System" are set out in Appendix V.

A program suggested by Prof. Marsaglia was applied to the breakdown data (See Appendix V, subroutine PRSPLT). The results for experiment no. 25 and 49 are shown in Figures 4-5(a) and 4-6(a). These

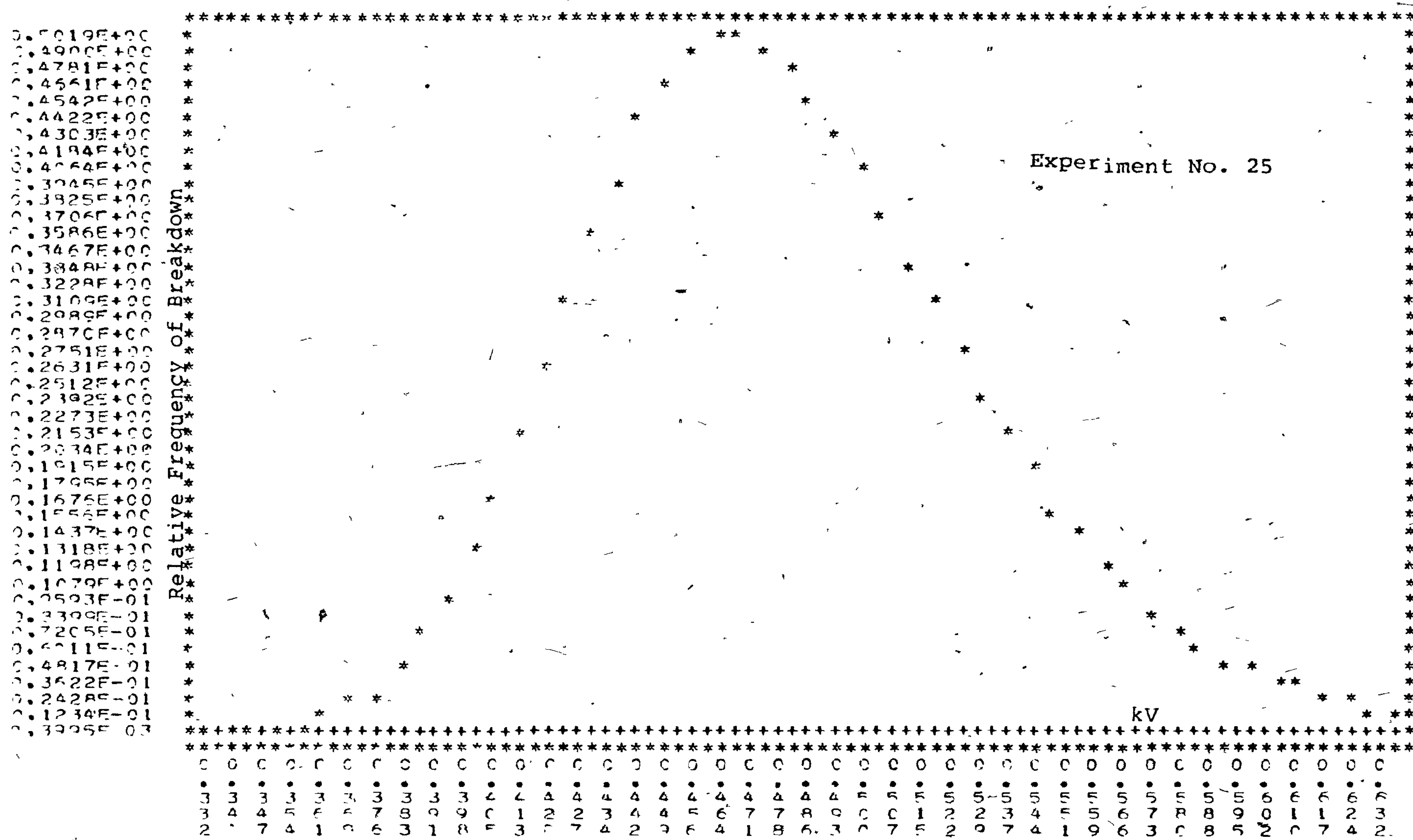

X-AXIS (HORIZONTAL AXIS) EXPONENT 1 0 REAL ROOTS, MEAN= 4.91 MODE= 4.67 SIG= .515

Y MAXIMUM 0.50195E+00
Y MINIMUM 0.39954E-03
X MAXIMUM 0.63526E+01
X MINIMUM 0.33224E+01

FIGURE 4-5 -a

Pearson System Applied to Plotting Breakdown Frequency as Applied to Experiment No. 25

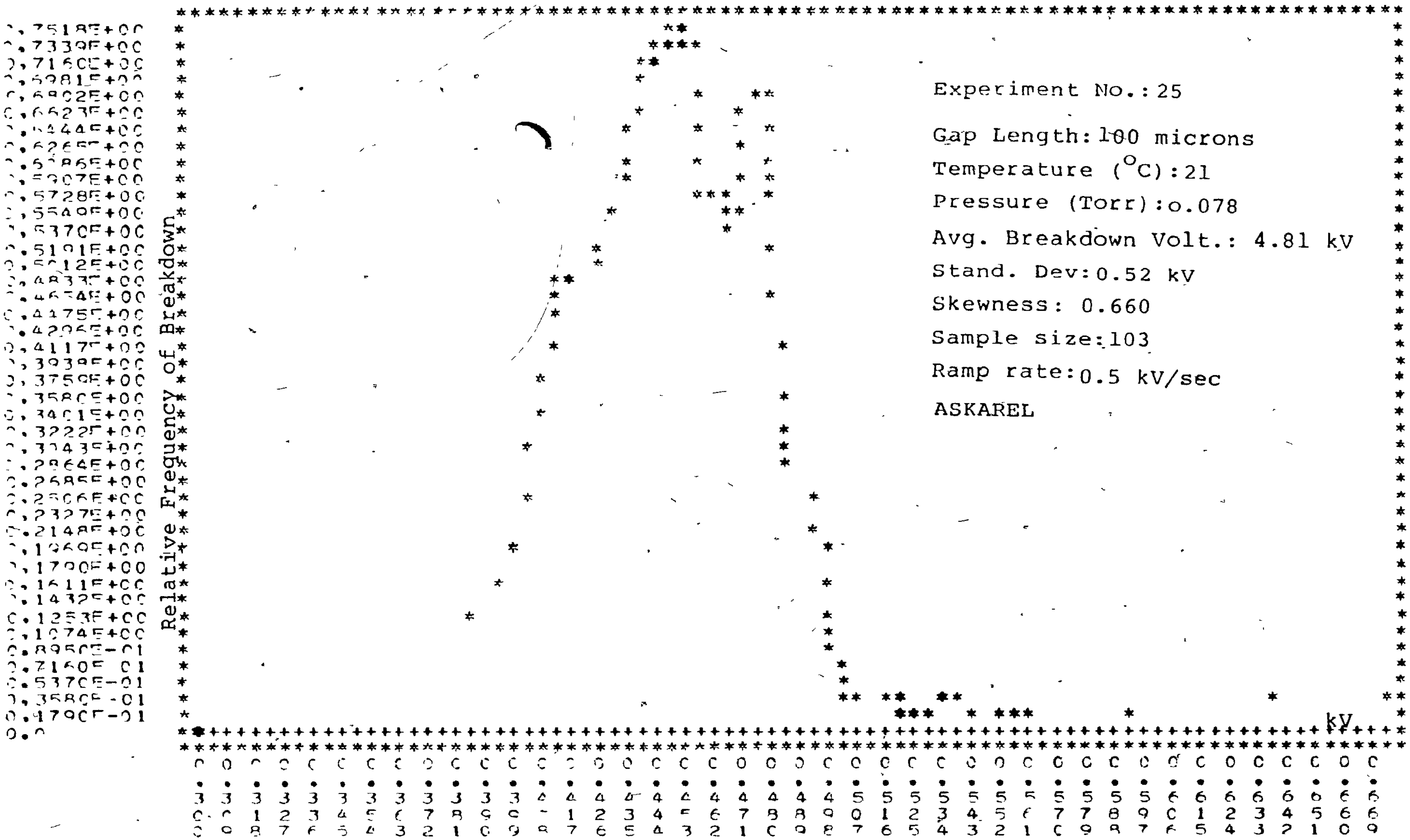

X-AXIS (HORIZONTAL-AXIS) EXPONENT 1

Y MAXIMUM 0.75178E+00
Y MINIMUM 0.0
X MAXIMUM 0.67300E+01
X MINIMUM 0.30000E+01

FIGURE 4-5-b

Pile of Sand Method to Determine the Breakdown Density as Applied to Experiment No. 25

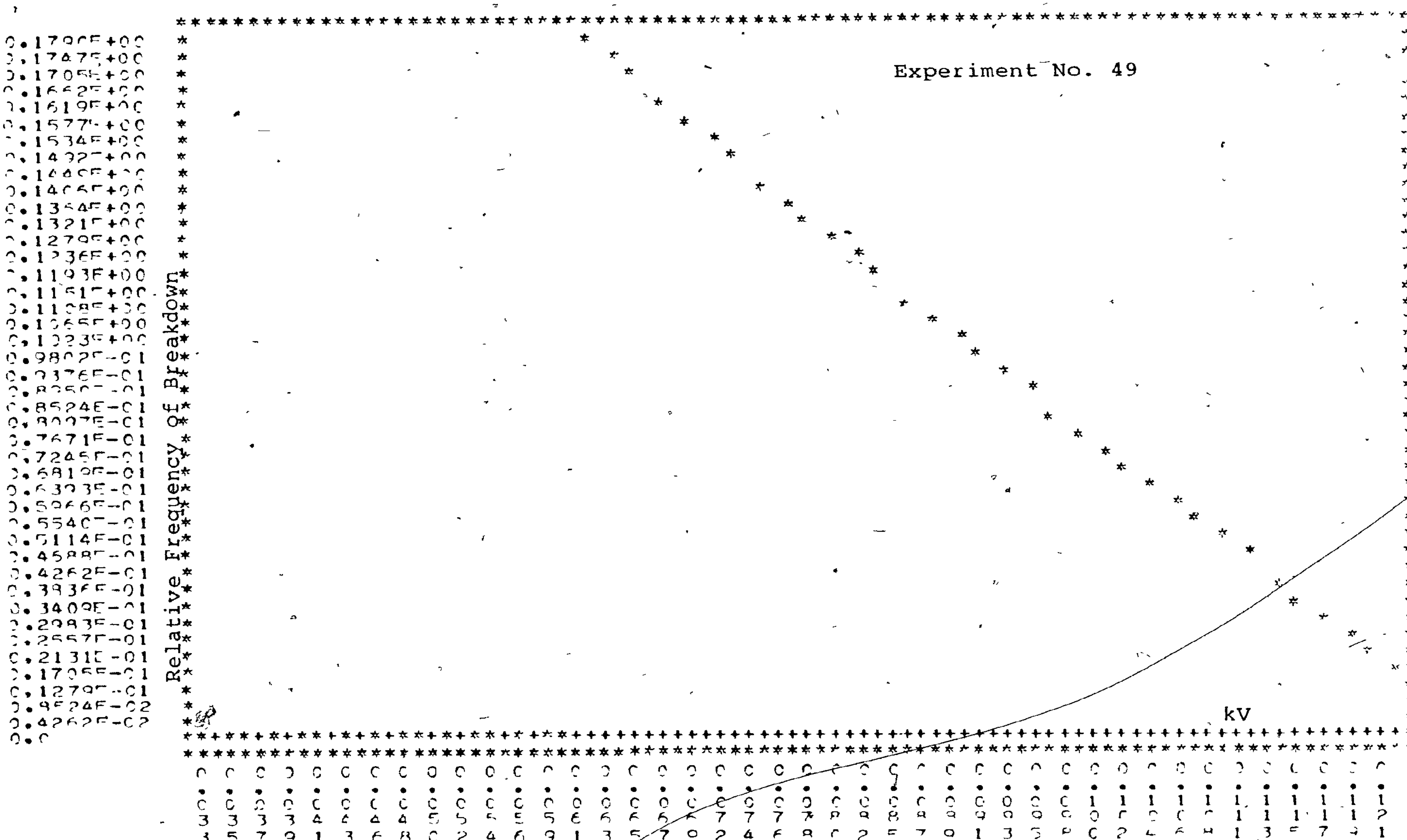

X-AXIS (HORIZONTAL-AXIS) EXPONENT 2

FIGURE 4-6-a

Y MAXIMUM 0.17899E+00
Y MINIMUM 0.0
X MAXIMUM 0.12250E+02
X MINIMUM 0.32673E+01

DOTS= 6.10 13.2 MEAN= 7.68 MODE= 2.30 SIG= 1.33

Pearson System Applied to Plotting Breakdown Frequency as Applied to Experiment No. 49

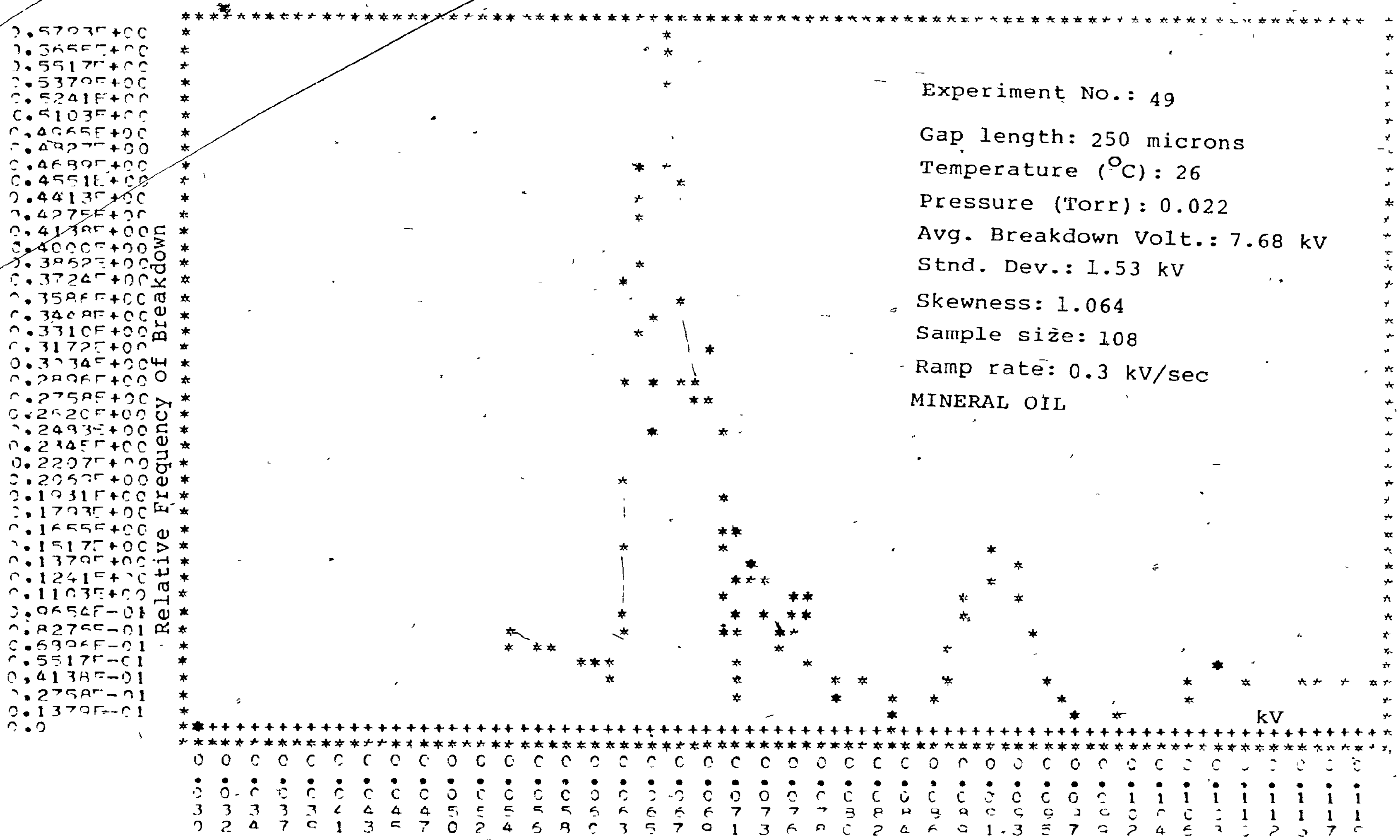

X-AXIS (HORIZONTAL-AXIS) EXPONENT 2

Y MAXIMUM C.57926E+00
Y MINIMUM 0.0
X MAXIMUM 0.12000E+02
X MINIMUM 0.30000E+01

FIGURE 4-6-b

Pile of Sand Method to Determine the Breakdown Density as Applied to Experiment No.49

may be compared with the corresponding density plots obtained by the "pile of sand" technique which are shown in Figures 4-5(b) and 4-6(b). In both cases, the curve obtained by the Pearson System describes an 'envelope' about the more precise "pile-of-sand" method. The Pearson System also yields the constants of equation (25) thereby permitting mathematical expression of the envelope.

4.5 Conditioning

The basic difference distinguishing the method by which results were obtained for experiments nos. 1 through 24 from those obtained for experiments 25 to 50, lies in the method of "conditioning"(Section 1.3.3). For the first series of experiments (nos. 1 to 24) the method of Bulke (25) was followed whereby the gap was initially set to about 1000 microns and then stressed by about 3 kV. The gap was then gradually set to the desired length over a period of about one-half hour. It generally took about an hour more before no further breakdowns would occur with the voltage across the gap at 3 kV. This procedure was changed for the second series of experiments (nos. 25-50) by commencing the experiment immediately i.e. applying ramp voltages and recording breakdowns, immediately after the gap had been set to the desired length. In this way, the effect of conditioning would be included in the observations.

The effect of conditioning is demonstrated for experiments nos. 35 and 42 in figures 4-7(a) and 4-7(b) respectively which graphically portray the data shown in Table 4-2. Each of these experiments has been divided into three segments, each segment containing about a third of the breakdown values for the entire experiment. An average breakdown value was calculated for each segment. This result is represented by the broken line on the graphs of figures 4-7(a) and 4-7(b). This calculation was repeated for the same experiments but with the first few breakdowns ignored: 8 initial breakdowns in the case of experiment no. 35 and 10 for experiment no. 42. An average breakdown value was calculated again for each segment, and the results are shown by the solid lines on the two figures. These results show an increase in the initial breakdown strength upon the occurrence of an initial few breakdowns.

TABLE 4-2

EFFECT OF CONDITIONING ON BREAKDOWN STRENGTH

Exp. no.	B.D.no.	avg. B.D. vol. (kV)	B.D. no.	Avg. B.D. vol. (kV)
35	1 - 33	10.51	9 - 38	10.96
	34 - 36	10.99	39 - 68	11.06
	67 - 99	9.89	69 - 99	9.84
42	1 - 29	5.17	11 - 35	5.25
	30 - 58	4.99	36 - 60	4.89
	59 - 87	5.18	61 - 87	5.25

B.D. = breakdown Vol. = voltage

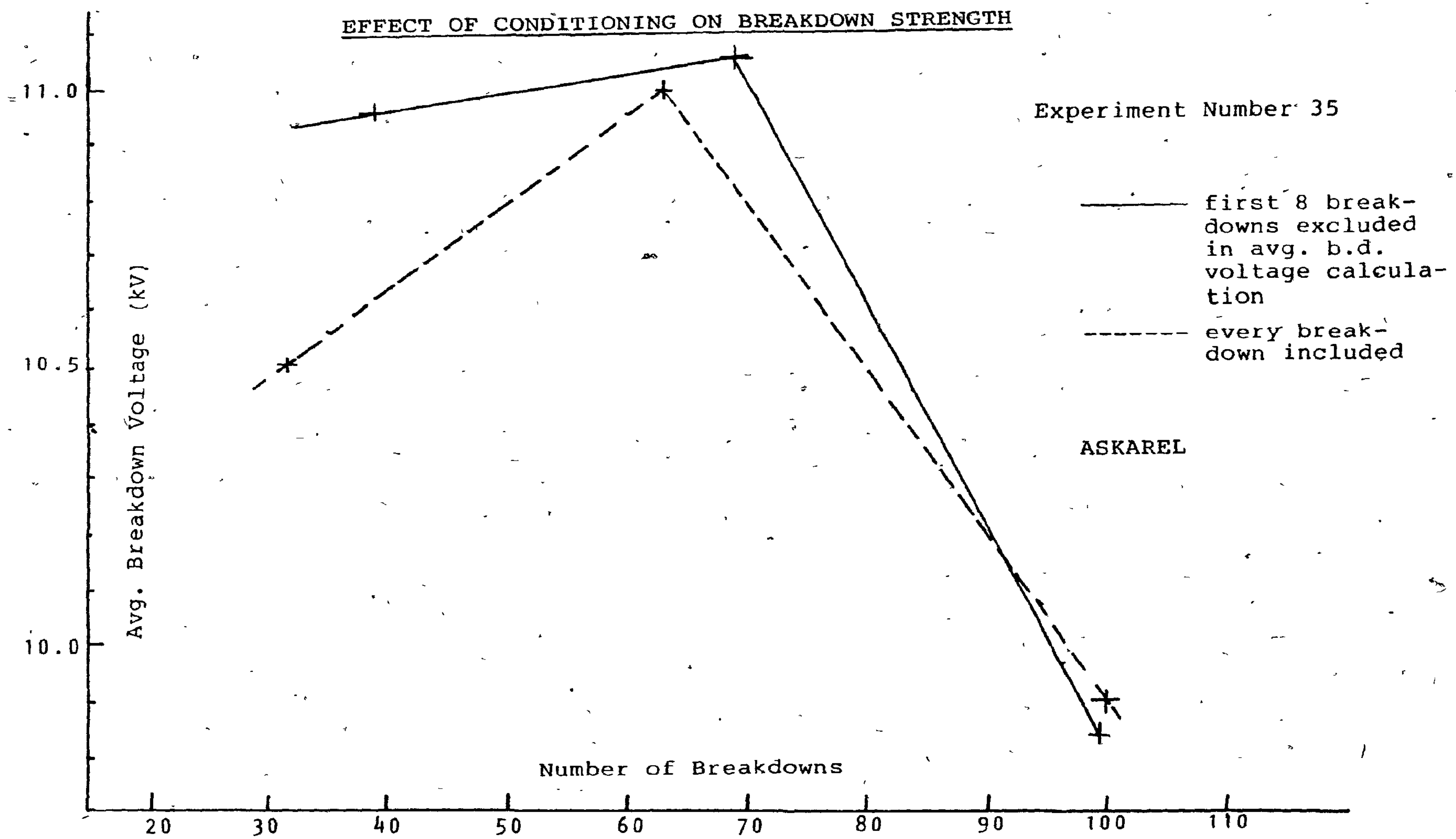

EFFECT OF CONDITIONING ON BREAKDOWN STRENGTH
Experiment Number 35
first 8 breakdowns excluded in avg. b.d. voltage calculation
every breakdown included
ASKAREL
Avg. Breakdown Voltage (kV)
11.0
10.5
10.0
Number of Breakdowns
20
30
40
50
60
70
80
90
100
110

FIGURE 4-7a

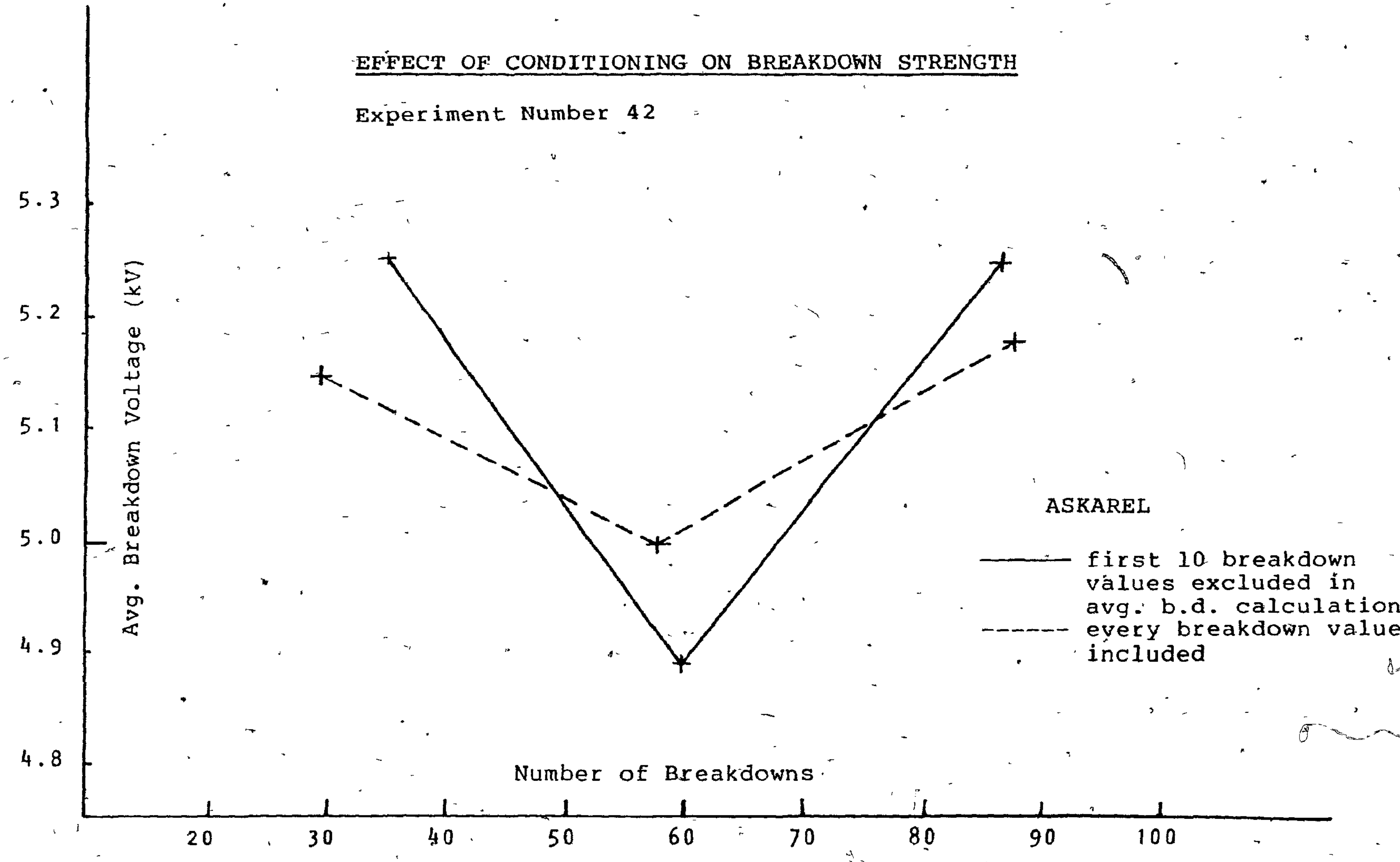
EFFECT OF CONDITIONING ON BREAKDOWN STRENGTH
Experiment Number 42
5.3
5.2
5.1
5.0
4.9
4.8
Avg. Breakdown Voltage (kV)
Number of Breakdowns
20
30
40
50
60
70
80
90
100
ASKAREL
first 10 breakdown values excluded in avg. b.d. calculation
every breakdown value included

FIGURE 4-7b

TABLE 4-3

AVERAGE BREAKDOWN STRENGTH PER ONE THIRD SEGMENT OF EXPT. (kV)

exp. no.	Gap microns	Ramp Rate kV/sec.	1st third	2nd third	3rd third
		ASKAREL			
16	100	1.0	3.76	4.10	3.84
20	100	3.0	3.67	3.56	3.22
21	100	3.0	4.04	3.80	4.21
25	100	0.5	4.69	4.88	4.86
26	125	3.0	6.69	6.55	6.62
28	125	1.0	5.46	5.84	6.35
29	125	0.3	5.51	6.60	6.16
33	250	1.0	11.31	10.66	10.88
35	250	0.75	10.96	11.06	9.84
36	250	1.5	9.29	9.71	10.06
38	250	3.0	9.02	9.74	9.58
39	250	0.3	10.30	10.67	10.37
42	125	0.75	5.25	4.84	5.25
		MINERAL OIL			
46	125	1.0	6.25	6.12	6.29
47	125	3.0	8.30	8.17	7.11
48	250	1.0	11.09	7.45	6.95
49	250	0.3	6.67	6.73	6.97
50	250	3.0	12.27	8.70	7.86

Due to uncertainty as to when the conditioning period could be considered as completed and a desire to account for it and still have breakdown data with relatively fresh electrodes, the first 8 breakdown voltages were ignored before the breakdown values of an experiment were divided into three equal portions and each sequence examined separately. The experiments generally consisted of 80 to 100 breakdowns. Therefore it was thought reasonable that the experiment should be divided into three portions, leaving, therefore, at least 20 breakdown values per segment after the first 8 had been ignored. Dividing the experiments into smaller segments raises the question of whether the number of breakdown voltages per segment is large enough to use accurately the method of parameter estimation given in Chapter II. Results of this operation showing average breakdown strength per one third segment of experiment are presented in Table 4-3 on page 125.

4.6 IDENTICAL CONDITION EXPERIMENTS FOR ASKAREL AND MINERAL OIL

Experiments which were carried out both in askarel and mineral oil having the same electrode configuration, gap distance and ramp rates are set out in Table 4-4, page 127.

The most important results of these and all other experiments are set out in Appendix III Various selected graphs associated with these experiments are shown in Figures 4-8 to 4-17.

TABLE 4-4

DIRECT COMPARISON EXPERIMENTS

Mineral Oil Experiment no.	Gap microns	Rate kV/sec	Askarel Experiment no.
46	125	1	28
47	125	3	26
48	250	1	33
49	250	3	39
50	250	3	38

* * * * * * * * * *

4.7 RATE EFFECT DETECTION

An attempt was made to ascertain whether the the rate of rise of voltage had a discernable effect on the distribution of breakdown voltages. Experiements no.'s 1 to 12 consisted of about 24 breakdowns each, which had occurred with askarel as the dielectric medium. Each of these experiments was designed to contain at least twice, breakdown values obtained at all voltage ramp rates obtainable with the automatic controller described in Chapter II. Some results for these experiments including the significance tests are shown in Table 4-5 page 128. Other experiments were conducted, both with askarel and mineral oil, at a single voltage ramp rate throughout

TABLE 4-5

Exp. no.	Gap Length (Microns)	Ramp Rate	Sample Size	Avg. Breakdown Voltage (kV)	Standard Deviation	Skew	Significance Φ_1	Φ_3	Φ_{LN}*
1	150	Mixed	24	5.48	1.39	1.110	0.58	0.06	0.13
2	176	"	23	6.23	1.10	0.661	0.60	0.03	0.03
3	150	"	24	4.30	0.37	0.646	1.00	0.26	0.46
4	150	"	26	5.48	1.48	0.779	0.52	0.03	0.07
5	150	"	23	5.60	1.12	0.597	0.10	0.02	0.16
6	150	"	24	4.21	0.61	-0.131	0.95	0.10	0.15
7	150	"	24	4.30	0.64	0.593	0.97	0.03	0.13
8	150	"	24	4.00	0.70	0.244	0.91	0.24	0.30
9	150	"	25	4.31	0.93	0.566	0.98	0.36	0.50
10	150	"	23	3.71	0.46	0.037	0.99	0.04	0.17
11	150	"	23	3.85	0.67	0.537	0.92	0.23	0.29
12	150	"	24	3.39	0.38	1.520	1.00	0.26	0.17

Combined Experiments

Exp. no.	Gap Length (Microns)	Ramp Rate	Sample Size	Avg. Breakdown Voltage (kV)	Standard Deviation	Skew	Significance Φ_1	Φ_3	Φ_{LN}*
A	150	Mixed	121	5.02	1.24	1.234	1.00	1.00	0.83
B	"	"	120	3.97	.76	0.793	1.00	0.25	0.67
C	"	"	96	4.79	1.28	1.049	0.99	0.21	0.56

A = expt. 1,3,4,5,6 B = expt. 7,8,10,11,12 C= expt. 4,5,7,10 *LN=Log-Normal an experiment. The existence of a rate-of -voltage rise effect could be inferred if the significance test showed a better result for experiments conducted at a single ramp rate than for the case of a mixture of ramp rates in the same experiment. Even if the breakdown values at the different ramp rates followed the same distribution law, presumably each rate would possess its own distribution parameters and the result would be a mixed distribution.

Breakdown values of the mixed ramp rate experiments (nos. 1 to 12) were combined to form several single large samples of breakdown voltages. The sample size of these combined experiments were made comparable to those conducted at a single ramp rate. Thus, two groups of experiments labelled A and B were formed by grouping of the individual experiments (nos. 1 to 12). A third group labelled C was formed by choosing only from among these experiments conducted with mixed ramp rates for which the significance test for the Weibull distribution was less or equal to 0.05. The significance test results for these combined experiments, presented in Table 4-5 on page 128, show that the goodness-of-fit was equal or inferior to those of the worst fitting individual experiments which composed part of the set of of breakdown values. The significance test results for these individual experiments form the upper portion of the Table (experiments no. 1-12). This deterioration in the goodness-of-fit when mixed ramp rates are considered, is especially demonstrated by combined experiment group C which was composed of 4 individual experiments for which the goodness-of-fit test of each for the Weibull distribution was less or equal to 0.05. Nevertheless, the goodness-of-fit test result for the combination experiments was 0.21 Such a discrepency is attributed to the mixture of ramp rates which has its own effect on the distribution of breakdown voltages. Pressure and temperature conditions were not significantly different for any of the experiments. The graphs associated with these three groups of breakdown voltages are shown in Figures 4-18 to 4-20 respectively.

In a similar manner, the possibility of discerning a rate effect was also investigated by combining the results of a pair of experiments, each having been done at a different ramp rate, but with the same gap distance. The combination of experiments made are set out in Table 4- 6, page 131.

TABLE 4-6

HYBRID TWO-RATE EXPERIMENT

Experiment no.	Gap microns	Ramp* kV/sec	Dielectric	Hybrid Exp. no.
39 & 40	250	0.3/6.0	askarel	D
21 & 24	100	3.0/0.75	askarel	E
46 & 47	125	1.0/3.0	mineral oil	F
49 & 50	250	0.3/3.0	mineral oil	G

*Combination of Ramp Rates (kV/sec.)

The results of these groupings including the goodness-of-fitness test results appear in Table 4-7 page 132. The graphs associated with these results appear in Figures 4-21 to 4-24 respectively.

Another method of attempting observation of the rate effect was by noting the change of probability of occurrence of a particular breakdown voltage common to all experiments even though the experiments were conducted at different rates of rise of voltage.

TABLE 4-7

HYBRID TWO-RATE EXPERIMENTS

Exp. no.	Gap (microns)	Ramp Rate kV/sec.	Sample Size	Avg. B.D. Voltage kV	Stnd. Dev. kV	Skewness kV	Goodness-of-Fit		
							$_1\Phi$	$_3\Phi$	Φ_{LN}
D	250	.3/.6	126	9.76	2.10	0.213	0.99	0.21	0.56
E	100	3./.75	121	3.98	0.48	0.583	1.00	0.45	0.37
F	125	1./3.	130	7.25	1.50	0.430	0.99	0.46	0.67
G	250	.3/3.	129	9.13	2.35	0.795	0.98	0.33	0.27

Experiments D and E were performed with askarel.
Experiments F and G were performed with mineral oil.

4.8 Rate Effect

If the rate of rise of the voltage (ramp rate) stressing the dielectric fluid in the gap has an effect on the form of the distribution, then its influence may be observed if the following graphical procedure is visualized as shown below:

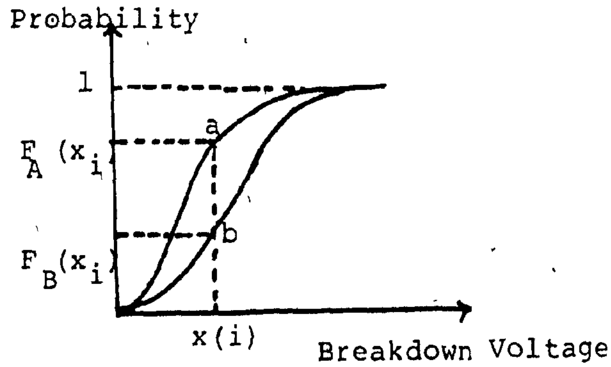

FIGURE 4-25

where $F_A(x)$ and $F_B(x)$ are the distribution of breakdown voltages for the ramp rates A and B respectively; 'a' and 'b' represent two different cumulative distribution functions associated with ramp rates A and B respectively.

From the diagram it can be seen that for the same breakdown voltage values, the corresponding probability of breakdown may be higher or lower, depending on the rate at which the voltage rises. It was with this concept that the experimentally observed probability values of a particular breakdown voltage common to all experiments having the same gap length were given in

Table 4-8 page 136. This table is divided into several parts labelled A to F. The experiments contained in a particular part of the table identified by a letter have a breakdown voltage value common to all observations in that part. Determination of the probability of breakdown for this voltage is obtained by application of the theory of order statistics. Thus, the table was prepared by examining the ordered set of breakdown values of an experiment, locating the particular breakdown voltage which has been determined to be common to that particular group of experiments, determining the rank number of the breakdown value, and then applying:

$$F(x) = i/n$$

where n is the sample size, as is done in the Kolmogorov-Smirnov test (90). If there are several breakdown values which for practical purposes are identical, each is assigned the same rank number; n then reprents not sample size , but rather the number of different breakdown values.

The probability of breakdown in chlorobiphenyls increases with increasing rate of voltage rise. This conclusion rests mainly on the evidence of Figure 4-26. This graph represents the average of the results of 9 experiments presented in Table 4-8, part D. Examination of other parts of this table will show variations, but in each set so examined it can be seen that the lowest probability of breakdown corresponds to the lowest rate of voltage rise (i.e. ramp rate), whereas the highest probability of breakdown corresponds to the highest ramp rate.

Before attempting to explain this observation, it should be observed that chlorobiphenyls of commercial purity can be expected to contain a small amount of water and dissolved gas despite the experimental degassing procedure followed (34).

Pure chlorobiphenyls exhibit no space charge phenomena (34). Consequently, the presence of such phenomena in chlorobiphenyls of commercial purity is attributed to the dissociation of the H_2O molecule (34) resulting in H^+ ions. This accumulation of positive space charge near the cathode sets up an intense local field between the electrodes, thereby inducing breakdown. During an experiment, even in the interval between applications of the ramp voltage to the electrodes, there is at all times a voltage applied to the electrodes(sec. 4.5) The field causes a constant circulation of the liquid in the vicinity of the electrodes (sec. 1.2.6). If upon application of a ramp voltage to the electrodes the field is made to rise rapidly, the inertia and viscosity of the liquid will necessitate a delay before this convective- type flow can adjust itself to new conditions. The rapid increase in the field causes a local increase of temperature in a volume element between the electrodes. There is an increase in the concentration of dissociation products, creating a space charge which sharply increases

TABLE 4- 8

VARIATION OF BREAKDOWN PROBABILITY FOR A PARTICULAR VOLATAGE

	Experiment no.	Gap (microns)	Ramp kV/sec.	Voltage kV	Probability
Askarel A	31	100	0.30	4.60	0.30
	25	100	0.50	4.60	0.40
	32	100	6.00	4.60	0.46
Askarel B	29	125	0.30	5.88	0.47
	41	125	0.50	5.88	0.65
	42	125	0.75	5.88	0.85
	43	125	0.75	5.88	0.62
	28	125	1.00	5.88	0.56
	27	125	1.50	5.88	0.83
	26	125	3.00	5.88	0.21
	30	125	6.00	5.88	0.65
Askarel C	39	250	0.30	11.52	0.66
	37	250	0.50	11.52	0.61
	35	250	0.75	11.52	0.66
	33	250	1.00	11.52	0.57
	34	250	1.50	11.52	0.93
	36	250	1.50	11.52	0.85
	38	250	3.00	11.52	0.87
	40	250	6.00	11.52	0.75
Askarel D	23	100	0.75	4.07	0.44
	24	100	0.75	4.07	0.53
	15	100	1.00	4.07	0.59
	15	100	1.00	4.07	0.62
	17	100	1.00	4.07	0.85
	25	100	1.00	4.07	0.39
	18	100	3.00	4.07	0.95
	20	100	3.00	4.07	0.88
	21	100	3.00	4.07	0.52
Mineral Oil E	46	125	1.00	6.91	0.77
	47	125	3.00	6.91	0.26
Mineral Oil F	49	250	0.30	8.83	0.79
	48	250	1.00	8.83	0.67
	50	250	3.00	8.83	0.45

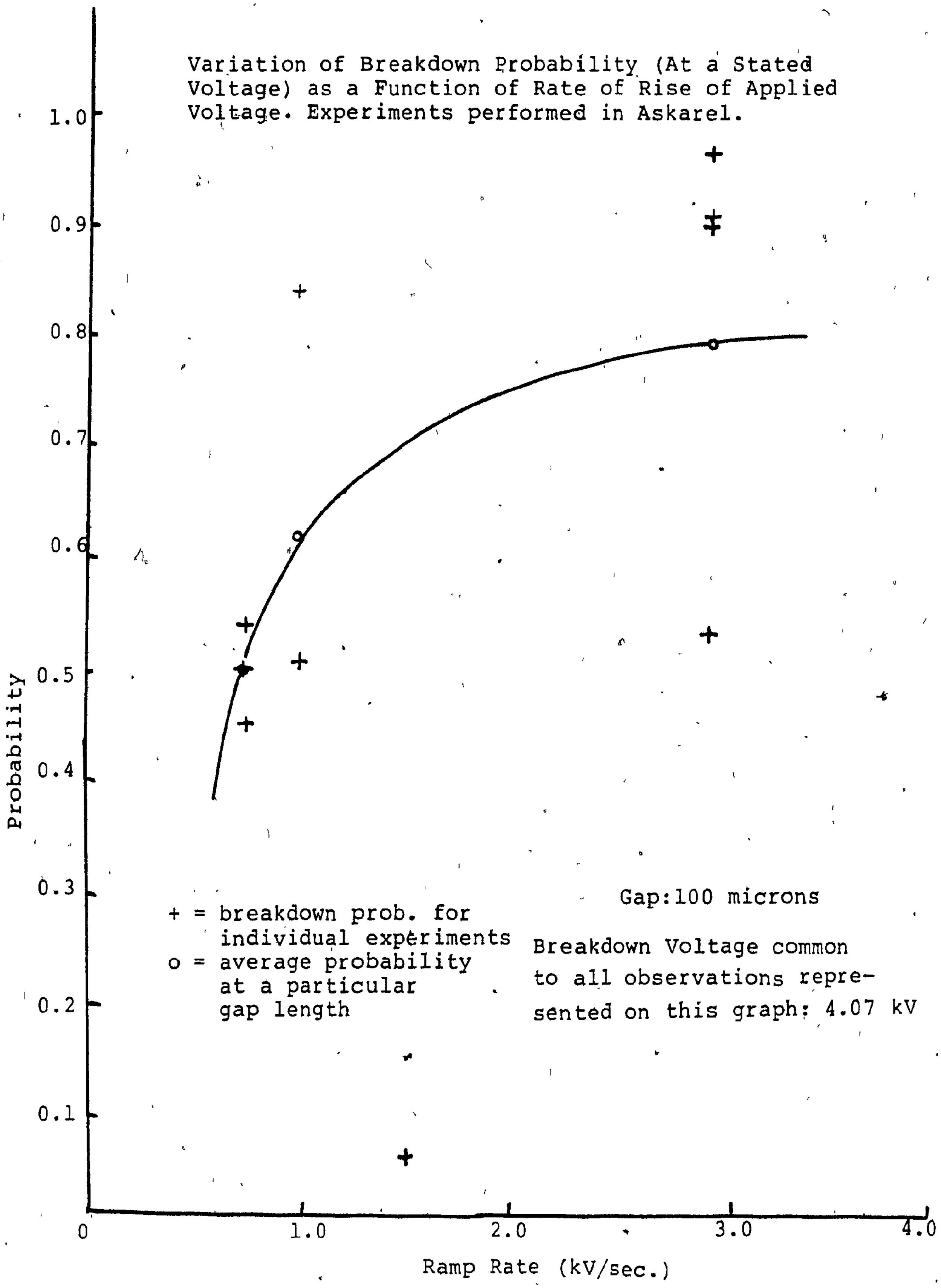
Variation of Breakdown Probability (At a Stated Voltage) as a Function of Rate of Rise of Applied Voltage. Experiments performed in Askarel.
Probability
1.0
0.9
0.8
0.7
0.6
0.5
0.4
0.3
0.2
0.1
0
1.0
2.0
3.0
4.0
Ramp Rate (kV/sec.)
+ = breakdown prob. for individual experiments
o = average probability at a particular gap length
Gap:100 microns
Breakdown Voltage common to all observations represented on this graph: 4.07 kV

FIGURE 4-26

the local field. It may therefore be expected that this local increase in both temperature and local field due to space charges coupled with the relatively slow movement of a volume element between the electrodes leads to a higher probability of breakdown as has been observed.

4.9 Change of Form of Distribution with Time

By considering the experiments in segments, it was expected to observe to some extent the influence of time on the shape of the distribution of breakdown voltages. Such dependence would probably be due to contamination of the dielectric fluid by products formed by the electrical discharges and deterioration of the electrodes. For example, both in the case of askarel and mineral oil, it was found that there would be a dark waxy deposit on the electrodes when they were disassembled at the end of an experiment. Microscopic examination revealed numerous craters scattered over the electrode face as shown in Figure 4-27.

Experiments performed in mineral oil and the corresponding experiments performed in askarel, as set out in Table 4-4 were segmented and examined in this way. The results per segment of these experiments appear in Table 4-9, page 140.

FIGURE 4-27

Typical View of Electrode Cleansed After Experiment

(Magnified Approximately 50x)

The continuous change in the form of the distribution of breakdown voltages is well illustrated by Figures 4-28 a, b, c, which are the frequency of breakdown voltage plots of the three sequential portions of experiment number 36. The frequency curve for the entire experiment when all the breakdown voltages are taken together, is produced in Figure 4-28 d. The results of the significance test for each of these distributions is presented on page 140 in Table 4-9.

In this case two peaks developed in the progression of density plots. However, the hint of such a development existed in the first third of the experiment (See Figure 4-28a). The subsequent appearance of

TABLE 4-9 **

SIGNIFICANCE TEST RESULTS ASSOCIATED WITH FIG. 4-28

Exp. no.	Breakdowns	AvgB.D* (kV)	Goodness-of-Fit Test Φ_1	Φ_3	Log-Normal	Fig. No.
36	1 - 95	9.69	0.58	0.24	0.66	4-28-d
36	1 - 31	9.29	0.21	0.03	0.39	4-28-a
36	32 - 62	9.71	0.07	0.03	0.24	4-28-b
36	63 -95	10.06	0.39	0.37	0.68	4-28-c

*AvgB.D. = average breakdown voltage
**askarel,gap = 25 microns, ramp rate = 1.5 kV/sec.

another peak in the plot of breakdown frequency at a lower voltage suggests that deterioration of the purity of the liquid dielectric and increasing surface asperities introduced another breakdown mechanism at a lower breakdown voltage.

The appearance of double peaks in the voltage breakdown density plots was a frequent observation, and in some cases multiple peaks were recorded. Experiments in which a double peak could be clearly distinguished in the density plots are given on page 142 in Table 4-10 along with the voltage at which the peaks occurred.

The ratio of the voltage at which the first peak occurs to that at which the second peak occurs is also given in Table 4-10. For a particular gap distance, these ratios cluster about a single value. Such a degree of consistency in a field of research where it is difficult to get uniform results suggests that a theoretical explanation would describe this ratio as a constant. Since a peak in a density curve can be

TABLE 4-10

EXPERIMENTS WITH DOUBLE PEAKS IN DENSITY PLOTS

Expt. no.	Gap(microns)	Ramp rate kV/sec	1st peak kV	2nd peak kV	voltage ratio
		ASKAREL			
14	100	3.0	4.09	4.37	1.07
25	100	0.5	4.53	4.8	1.06
26	125	3.0	6.61	7.8	1.18
27	125	1.5	4.7	5.17	1.10
41	125	0.5	4.37	5.17	1.18
33	250	1.0	9.7	11.6	1.20
35	250	0.75	9.9	11.5	1.16
36	250	1.5	9.1	10.4	1.14
38	250	3.0	9.4	11.2	1.19
39	250	0.3	9.0	11.5	1.28
		MINERAL OIL			
46	125	1.0	5.44	6.36	1.17
47	125	3.0	7.7	8.7	1.13
49	250	0.3	6.6	9.1	1.38

associated with a particular breakdown mechanism, the appearance of a second peak at a determinable point indicates that the other breakdown mechanism that develops in the course of an experiment is always the same, and quite probably due to the same accumulation of impurities.

4.10 Choice of Distribution Function

The Gaussian normal distribution and log normal distributions are inexpedient for the purpose of describing the result of destructive tests because they would indicate a finite probability of failure even without stressing the specimen, which clearly contradicts physical reality (44). Furthermore the normal law is not a good approximation to the distribution of values which are weak link in character.

Suppose that there are a large number of types of failure, which cause breakdown at electrical stresses of E_i' to E_m' i.e. E_i is the notional breakdown voltage which would be observed if all types of failure except the i^{th} were suppressed. The actual breakdown stresses are then the minimum of $E_1' \ldots\ldots E_m'$ and are denoted by E_m. If it is assumed that the E_i' are mutually independent and identically distributed (sec. 1.5.1) random variables with the cumulative distribution function F(x), then, since(44)

$$E_m \geq x \qquad (27)$$

if and only if $E_i' \geq x$ $(i = 1,m)$ where x represents breakdown stress, it follows that:

$$\text{Prob } (E_m \geq x) = \text{prob}\left\{E_i' \geq x \quad i = (1,\ldots m)\right\} \qquad (28)$$

$$= (1 - F(x))^n \qquad (29)$$

For sufficiently large n and small x, equation (29) becomes $\simeq \exp(-nF(x))$

Therefore, the probability of breakdown occurring is given by

$$\text{Prob } \left[E_m \leq x\right] = 1 - \exp(-nF(x)) \qquad (30)$$

This corresponds to equation (12) of Chapter II. Depending on the form of F(x), any one of the extreme value distributions can be obtained. If for example F(x) is the of the form ax^b where a and b are constants, a form of Weibull distribution is obtained.

The distributions which were examined, namely the log normal, Type I and III extreme value distributions, have all been applied elsewhere in the life testing of various materials. To use a statistical model to characterize a physical phenomenon, such as a distribution of breakdown voltages, whose failure mechanism is not entirely known, is at best, an approximation. Although there is little theoretical justification for choosing the Weibull distribution as the failure model, there is much experimental evidence to indicate that the Weibull distribution provides the best fit of the break-

TABLE 4-11 GOODNESS-OF-FIT PER SEGMENT OF EXPERIMENT

EXPERI-MENT NO.	GAP microns	RAMP kV/Sec	SEG-MENT	NUMBER OF BREAKDOWNS	AVG.B.D.* (kV)	STND. DEV.	SKEWNESS	GOODNESS-OF-FIT Φ_1	Φ_3	Φ_{LN}*
					ASKAREL					
16	100	1.0	1	24	3.76	0.58	-0.085	0.92	0.12	0.28
			2	24	4.10	0.55	0.151	0.94	0.00	0.04
			3	25	3.84	0.52	1.054	0.99	0.16	0.42
20	"	3.0	1	18	3.57	0.42	0.001	0.96	0.22	0.45
			2	18	3.56	0.42	1.039	1.00	0.01	0.21
			3	18	3.22	0.30	-0.145	1.00	0.13	0.42
21	"	"	1	23	4.04	0.43	-0.093	0.95	0.04	0.21
			2	23	3.80	0.64	-1.302	0.89	0.64	0.87
			3	25	4.21	0.53	-0.141	0.80	0.57	0.68
25	"	0.5	1	34	4.69	0.45	-0.209	0.96	0.14	0.57
			2	34	4.88	0.53	0.616	1.00	0.01	0.01
			3	35	4.86	0.56	0.938	1.00	0.33	0.80
26	125	3.0	1	30	6.69	0.73	0.067	0.72	0.00	0.02
			2	31	6.55	0.75	0.645	0.87	0.24	0.07
			3	32	6.62	1.06	0.163	0.58	0.04	0.13
28	"	1.0	1	30	5.46	0.91	0.609	0.66	0.40	0.65
			2	31	5.84	1.06	-0.028	0.24	0.30	0.67
			3	30	6.35	1.08	-0.738	0.05	0.13	0.93
29	"	0.3	1	30	5.51	1.26	0.085	0.17	0.00	0.25
			2	30	6.62	1.19	-0.410	0.25	0.20	0.87
			3	32	6.16	1.11	-0.130	0.16	0.07	0.52

*B.D.=Breakdown

*LN= Log-Normal

TABLE 4-11 (Continued)

EXPERI-MENT NO.	GAP microns	RAMP kV/sec	SEG-MENT	NUMBER OF BREAKDOWNS	AVG.B.D. (kV)	STND. DEV.	SKEWNESS	GOODNESS-OF-FIT Φ_1	Φ_3	Φ_{LN}
33	250	1.0	1	30	11.31	2.30	-0.422	0.87	0.31	0.85
			2	30	10.66	2.01	-0.720	0.80	0.16	0.90
			3	31	10.88	1.75	-0.510	0.77	0.56	0.88
35	"	0.75	1	30	10.96	1.78	-0.488	0.40	0.17	0.70
			2	30	11.06	1.95	-0.321	0.86	0.61	0.94
			3	31	9.94	1.57	-0.351	0.44	0.22	0.57
36	"	1.5	1	29	9.20	1.49	-0.181	0.21	0.03	0.39
			2	29	9.71	1.46	-0.453	0.07	0.03	0.24
			3	37	10.06	1.65	0.097	0.39	0.37	0.68
38	"	3.0	1	30	9.02	1.48	0.701	0.16	0.15	0.03
			2	30	9.74	1.40	0.101	0.28	0.11	0.38
			3	31	9.58	1.98	0.313	0.76	0.21	0.28
39	"	0.3	1	30	10.30	1.98	-0.293	0.84	0.41	0.86
			2	30	10.67	2.00	-0.042	0.39	0.05	0.36
			3	32	10.37	1.60	-0.198	0.56	0.16	0.56
42	125	0.75	1	25	5.25	0.68	0.495	0.96	0.02	0.01
			2	25	4.84	0.83	0.957	0.91	0.00	0.93
			3	27	5.25	0.87	0.200	0.52	0.14	0.37

MINERAL OIL

EXPERI-MENT NO.	GAP microns	RAMP kV/sec	SEG-MENT	NUMBER OF BREAKDOWNS	AVG.B.D. (kV)	STND. DEV.	SKEWNESS	GOODNESS-OF-FIT Φ_1	Φ_3	Φ_{LN}
46	125	1.0	1	30	6.25	0.77	-0.035	0.83	0.45	0.72
			2	30	6.12	0.79	0.000	0.77	0.20	0.20
			3	31	6.29	0.66	-0.035	0.92	0.04	0.12

TABLE 4-11 (Concluded)

EXPERI-MENT NO.	GAP microns	RAMP kV/sec	SEG-MENT	NUMBER OF BREAKDOWNS	AVG.B.D. (kV)	STND. DEV.	SKEWNESS	GOODNESS-OF-FIT Φ_1	Φ_3	Φ_{LN}
				MINERAL OIL						
47	125	3.0	1	30	8.30	1.45	0.000	0.39	0.07	0.67
			2	30	8.17	1.42	-0.255	0.46	0.33	0.78
			3	30	7.11	0.97	-0.285	0.02	0.03	0.48
48	250	1.0	1	31	11.09	2.17	0.000	0.96	0.85	0.92
			2	31	7.45	0.75	0.224	0.88	0.11	0.14
			3	32	6.95	0.60	-0.459	0.96	0.18	0.67
49	"	0.3	1	33	6.67	1.50	0.090	0.54	0.09	0.14
			2	33	6.73	0.75	0.410	0.96	0.09	0.22
			3	34	6.97	0.46	0.188	1.00	0.02	0.05
50	"	3.0	1	22	12.27	2.43	-0.555	0.67	0.10	0.82
			2	22	8.70	0.84	0.139	0.65	0.41	0.50
			3	22	7.86	1.13	-0.495	0.06	0.08	0.62

TABLE 4-12

GOODNESS-OF-FIT RESULTS FOR TYPE III EXTREME VALUE DISTRIBUTION (WEIBULL) AS PER SEGMENT OF EXPERIMENT COMPARED WITH GOODNESS-OF-FIT FOR ENTIRE EXPERIMENT

ASKAREL

EXPERIMENT NUMBER	GAP microns	RAMP kV/sec	FIRST SEGMENT	SECOND SEGMENT	THIRD SEGMENT	ENTIRE EXPERIMENT
16	100	1.0	0.12	0.00	0.16	0.09
20	"	3.0	0.22	0.01	0.13	0.21
21	"	3.0	0.04	0.64	0.57	0.32
25	"	0.5	0.14	0.01	0.33	0.22
26	125	3.0	0.00	0.24	0.04	0.11
28	"	1.0	0.40	0.30	0.13	0.25
29	"	0.3	0.00	0.20	0.07	0.15
33	250	1.0	0.31	0.16	0.66	0.52
35	"	0.75	0.17	0.61	0.22	0.11
36	"	1.5	0.03	0.03	0.37	0.24
38	"	3.0	0.15	0.11	0.21	0.17
39	"	0.3	0.41	0.05	0.16	0.44
42	125	0.75	0.02	0.00	0.14	0.01

MINERAL OIL

EXPERIMENT NUMBER	GAP microns	RAMP kV/sec	FIRST SEGMENT	SECOND SEGMENT	THIRD SEGMENT	ENTIRE EXPERIMENT
46	125	0.30	0.45	0.20	0.04	0.05
47	"	3.0	0.07	0.33	0.03	0.21
48	250	1.0	0.85	0.11	0.18	0.91
49	"	0.3	0.09	0.09	0.02	0.59
50	"	3.0	0.10	0.41	0.08	0.72

down voltage data. For example if the breakdown voltages of an entire experiment are fitted to a Type I, a Type III Extreme value distribution and to a Log Normal distribution, the resulting significance statistic for each of these distributions, as listed in columns o,p, and q respectively in Appenix III, Table A, shows that the Weibull Distribution consistently provides the closest fit. The superiority of this distribution is emphasized if the results of an experiment are analysed in segments, each segment consisting of about 1/3 of the breakdown values of an experiment. Table 4-11 on page 145 presents this per segment analysis giving the goodness-of-fit test results for each segment in the order of their occurence in time. Here it can further be observed that there was in most cases a goodness-of-fit test result per segment occurring which was superior to the significance test result for the entire experiment which is listed in Table 4-12 on page 148. For example, the overall significance test result for the Weibull distribution in its entirety is given in Table 4-12 as 0.22 whereas the results of the significance test for each one third of the same experiment are 0.14, 0.01 and 0.33 respectively. Table 4-12 highlights the per segment goodness-of-fit test results associated with the Weibull distribution.

The variation from segment to segment is influenced by both conditioning and change in condition of both liquid and electrodes. It is only for a portion of an experiment that the paramenters of a theoretical distribution function will not significantly change. This progressive change in the physical attributes if considered with the results of the per segment study leads to the conclusion that although no one distribution function can fully describe the breakdown data, the Weibull function is the most satisfactory.

The Weibull function, which can be expressed as :

$$F(x) = 1 - \exp\left[-\left(\frac{x - \gamma'}{\alpha'}\right)^{\beta'}\right] \qquad (31)$$

where α' = scale parameter

β' = the shape parameter

γ' = the location parameter

x = the breakdown voltage

(see also Chapter III eq 60)

Equation (31) is attractive because it is easy to handle and coincides with the derived equation of the expected breakdown probability (Section 1.5.2 Chapter I). The effect of the various known factors which affect breakdown values, such as gap distance and rate of rise of voltage can be related to the scale, shape or location parameter. For example, if a certain type of behavior leading to breakdown were to manifest itself only after a certain voltage level, then this could be expressed by a location parameter. Figure 4-29 presents a graph based on Table 4-13 showing the Weibull shape parameter as a function of gap length. The influence of the ramp rate has been ignored because its effect did not seem significant in comparison to

THE WEIBULL SHAPE PARAMETER AS A FUNCTION OF GAP LENGTH

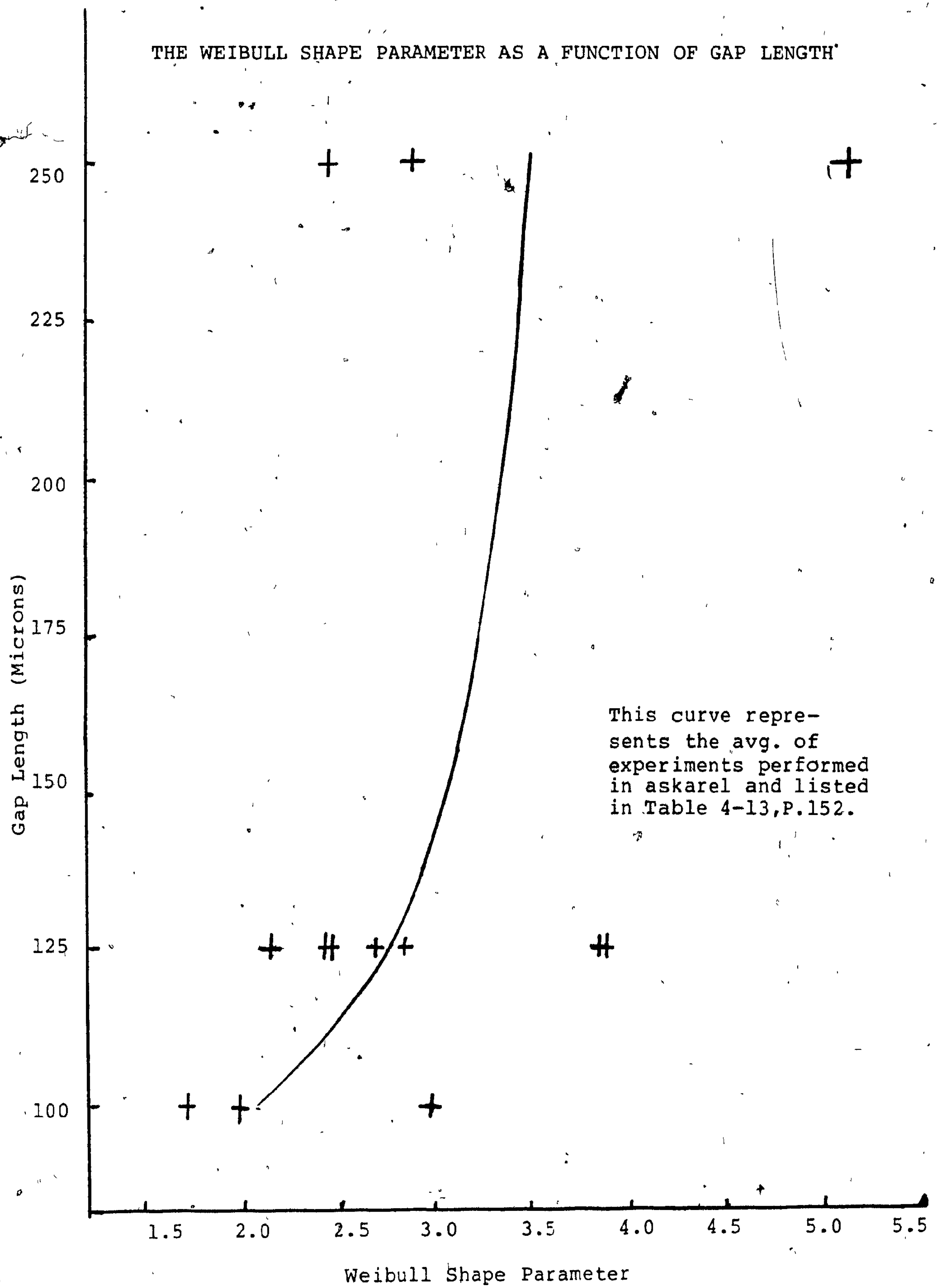

FIGURE 4-29

TABLE 4-13

RELATION OF WEIBULL SHAPE PARAMETER TO GAP LENGTH *

Experiment No.	Gap (microns)	Shape Parameter
25	100	1.96
31	100	1.73
32	100	2.96
27	125	2.47
26	125	2.88
29	125	3.85
30	125	3.80
41	125	2.42
42	125	2.14
43	125	2.11
35	250	5.16
38	250	2.45
40	250	2.93

*Plotted in Figure 4-29

that of gap length. The data for this graph was drawn from experiments 25 to 50 in which the same method of conditioning was used. Except for three observations at 100 microns gap length for which there was no other choice of data, experiments were chosen in which the goodness-of-fit test for the Weibull distribution was 0.2 or less. The results show that the shape parameter increases with increasing gap length.

It has been observed that a Type I extreme value distribution may be regarded as an approximation of a Type III (Weibull) distribution with a large value of shape parameter (68). Endicott and Weber (152) reported good agreement of their breakdown value results with a Type I extreme value distribution. Their tests were conducted using 60 Hz alternating voltages, rising at a rate of 3.0 kV/sec. with a gap length of 75 mil (approximately 1905 microns). The gap was uniformly stressed by circular flat electrodes of 2 and 3 inches in diameter. Thus it may be that breakdown experiments of any gap length follow a Weibull distribution provided that the gap is uniformly stressed, except that for relatively large gaps, the Type I extreme value distribution may be applied. In any event, an objection to insisting on the application of the Type I extreme value distribution is that the negative values of breakdown voltage have a finite probability of occurrence even though a positive voltage is being applied (7). Therefore this distribution should not be the theoretical distribution of electric strength.

4.11 Composite Distribution Functions

It was observed that not in all cases did the Weibull function provide what would normally be called an acceptable fit. In view of the foregoing, whatever be the mechanisms of breakdown producing a skewed distribution, it may be possible to describe them by a combination of extreme value distributions, either additively or multiplicatively mixed. Since the Weibull distribution gave a very good fit when the experiments were analysed in smaller segments, it is natural to assume that a combination of Weibull functions would best serve this purpose.

Because one of the assumptions of the weak link theory is that flaws act independently of each other (see 1.5.1), we can describe the breakdown event B' as a result of several mutually independent events B_i' (44):

$$B' = B_1' + B_2' + \cdots\cdots \qquad (32)$$

where $B_i'B_j' = 0 \qquad i \neq j$

The probability distribution of B_i' which represents a distribution of breakdown voltages, can be represented by a linear combination of the various independent flaw activities. Thus, with $P(B_i')$ representing the probability of the occurrence of event B_i' due to a particular type of flaw existing in the dielectric, and c_i representing a weighing factor, we obtain:

$$P(B') = \sum_{i}^{n} c_i P(B_i') \qquad (33)$$

$$\text{with} \qquad \sum_{1}^{n} c_i = 0$$

The distribution given in Eq.33 therefore takes the following form for an additively mixed distribution of n components:

$$F(x) = \sum_{i=1}^{n} c_i F(x_i)$$

$$= 1 - \sum_{i=1}^{n} c_i e^{-\left(\frac{x - \gamma_i'}{\alpha_i'}\right)^{\beta_i'}} \qquad (34)$$

Impulse voltage breakdown studies made on butyl rubber cable and crosslinked polyethylene cable have been fitted by such a compound Weibull function (129).

An expression for the multiplicatively mixed Weibull function is obtained by considering the complement B_i' i.e. that there has been no breakdown. This complementary event can be expressed by (44):

$$\overline{B}' = \overline{B}_1' \cdot \overline{B}_2' \cdot \overline{B}_3' \ldots\ldots \qquad (35)$$

where the $\overline{B}_i'$ represent mutually independent events. There is no similar restriction such as $B_i'B_j' = 0$. Thus, the probability of the nonoccurrence of a breakdown event is:

$$P(\overline{B}') = \prod_{i=1}^{n} P(\overline{B}_i') \qquad (36)$$

Consequently, the probability of breakdown is:

$$1 - P(\overline{B}') = 1 - \prod_{i=1}^{n} P(B_i')$$

This result was obtained through consideration of the complementary event $\overline{B}'$ because an event B_i' renders the observation of further events B_j' in the same sample impossible whereas $\overline{B}_i'$ (flaw activity not leading to breakdown) can be present without causing damage to the sample. Hence the multiplicatively mixed Weibull distribution is:

$$F(x) = 1 - \prod_{i=1}^{n} \exp\left[-\left(\frac{x-\gamma_i'}{\alpha_i'}\right)^{\beta_i'}\right]$$

$$= 1 - \exp - \sum_{i=1}^{n}\left(\frac{x-\gamma_i'}{\alpha_i'}\right)^{\beta_i'}$$

A plot of a multiplicatively mixed Weibull function appears to be similarly skewed as the additively mixed one, except that the former always has a concave curvature towards the ordinate (probability) axis (45).

In the experiments it would be reasonable to assume that if the distributions are due to a mixture of Weibull distributions, they would be multiplicatively mixed. Additively mixed distributions are to be expected when the specimens constituting a random sample can be distinguished with regard to their pre-breakdown behavior due to for instance, differences in prior history, method of production and material (46). This is not so where experiments are conducted with a stainless steel vessel filled with a uniform liquid dielectric. The additively mixed distribution was derived on the assumption that

$$B_i'B_j' = 0 \quad (i \neq j)$$

i.e. that when one flaw is actively engaged in causing breakdown the others were not. While this might serve as a model where a cable is involved, it is submitted that breakdowns occurring in the homogeneous surroundings described above, would be due to the combined activity of all the flaws. Therefore a multiplicatively mixed model would be more suitable.

4.12 Conclusions

1. Of the four distributions examined, the Type III extreme value distribution (Weibull distribution) best describes the distribution of breakdown voltages in liquid dielectrics examined, namely chlorobiphenyls and mineral oil.

2. The equations representing the probability of breakdown of askarel under uniform field conditions at room temperature in gap lengths of 100, 125, and 250 microns during which a minimum of 3kV was applied to the electrodes at all times, are respectively:

$$P(v)_{100} = 1 - \exp\left(-\left[\frac{v - 3.0}{2.1}\right]^{2.2}\right)$$

$$P(v)_{125} = 1 - \exp\left(-\left[\frac{v - 3.0}{3.2}\right]^{2.9}\right)$$

$$P(v)_{250} = 1 - \exp\left(-\left[\frac{v - 3.0}{7.4}\right]^{3.5}\right)$$

3. If a dielectric liquid is stressed by a uniform field, increasing the rate of rise of voltage which is applied to the electrodes will cause an increase in the probability of breakdown for any particular voltage value considered.

4. The Weibull shape parameter used to describe a distribution of breakdown voltages in a uniform field, increases with increasing gap length.

5. A compound or multiplicatively mixed Weibull function should be employed when the simple Weibull distribution does not appear to provide adequate results. Such composite distributions may be either multiplicatively or additively mixed.

6. Different breakdown mechanisms in liquid dielectrics can be detected by plotting the relative frequency of breakdown against breakdown voltage to obtain a plot of the density of breakdown voltages. When experiments are performed under similar conditions, density plots in which two peaks can be observed will be positioned apart from each other at approximately the same ratio of breakdown voltages of the peaks.

7. The Pearson system of obtaining relative frequency or density plots, provides the means of obtaining a mathematical expression of the density curve. This curve describes the major features of the density curve which is more accurately represented by the "pile of sand" method. The Pearson system may therefore be applied when further mathematical manipulation of the density curve is desired.

8. An advantage in using the Weibull distribution or any extreme value distribution , is that test results which are obtained on a smaller experimental model can be transferred to a larger unit. Often only a small number of tests are required to gain an accurate estimate of the parameters of the distribution so that it is economically sound, where the breaking strength of material is concerned, to carry out such systematic tests. In this way the financial consequences of a single major failure may be avoided.

4.13 Suggestions for Future Work

Because of the important role played by particles in the electrical breakdown of liquid dielectrics, the following investigation involving colloidal chemistry is suggested. Expressions can be developed for the probability of the formation of bridges in an electric field. An example of such an expression has been given in this thesis (section 1.3.4). A computer simulation of electrical breakdown can then be carried out by generating random numbers representing the distribution of particle sizes found in insulating liquids (147). To these are applied the mathematical expressions for bridge formation. As the calculations are repeated for each particle encountered during the simulation, summation of the particle sizes establishes the length of the bridge at any point in time. A criterion for the determination of the occurence of breakdown might be the calculated electric field strength when the summation of particle sizes forming the bridge, equals the gap length, or is some fraction of it. For long periods of service, simulations involving transformer oil would have to include the effects of oxidation and thermal degradation.

It should also be profitable to isolate the various distributions that comprise the observed distribution function which bears a strong resemblance to the Weibull distribution, as has been demonstrated in this thesis. For this purpose, the effects on the breakdown distribution of various known phenomena and of materials during breakdown should be studied. For example, a liquid dielectric which has been aged through numerous electrical breakdowns contains metal from the electrodes and this affects breakdown in a host of ways not fully understood. The extent to which this contamination, or perhaps simply the asperities remaining on the electrodes, contribute to the complication of the breakdown distribution might be demonstrated if the dielectric were aged by using a laser beam focussed to a point within the dielectric. The oil would then have been aged through electrical breakdowns and it would contain chemical and particulate contaminants similar to those formed during conventional electrical breakdown, but without any metal.

Further study would reveal the effect on the parameters of the Weibull distribution exerted by other factors, such as dissolved gases. The method of plotting frequency of breakdown used in this thesis is sensitive and would indicate by means of multiple peaks, the presence of a mixed distribution. Similarly, expressions obtained for the envelope of these curves by means of the Pearson method (Appendix V, Section 4.4.2) would reflect changes which could be analysed further by mathematical manipulation. This method yields parameters which are in a form suitable for direct analysis by a computer.

EXPLANTION OF FIGURES 4-8 to 4-24

Figures 4-8 to 4-24 are each composed of three different graphs identified by the letter 'a', 'b', or 'c' in the figure number. Of these figures, those containing 'a' in their number, identify the frequency of breakdown or density curves. The plotting symbol is simply a '*'. Those figures identified by 'b' in their figure number present a linearised plot of the actual observed probability distribution of breakdown voltages, against the probability of breakdown these same breakdown voltages are expected to have when it is assumed they belong to a particular theoretical probability distribution. Perfect correspondence of the theoretical and observed distributions would result in a plot lying on the straight line drawn at a slant across the figure. Four plots appear on the figure plotted against the same axes because four different theoretical distributions are examined. Each distribution is identified by a plotting symbol the key to which is given below on this page. The figure numbers containing 'c' present a graphical visulization of the goodness-of-fit of each of the four theoretical distributions applied. The plotting symbol (the key to which is also given below) identifies the theoretical distribution to which the plot refers. The straight line representing the diagonal is where the plots would lie if the theoretical distribution were the observed distribution.

KEY TO PLOTTING SYMBOLS

* : Φ_1 # : Φ_2 . : Φ_3 - : Lognormal Distr.

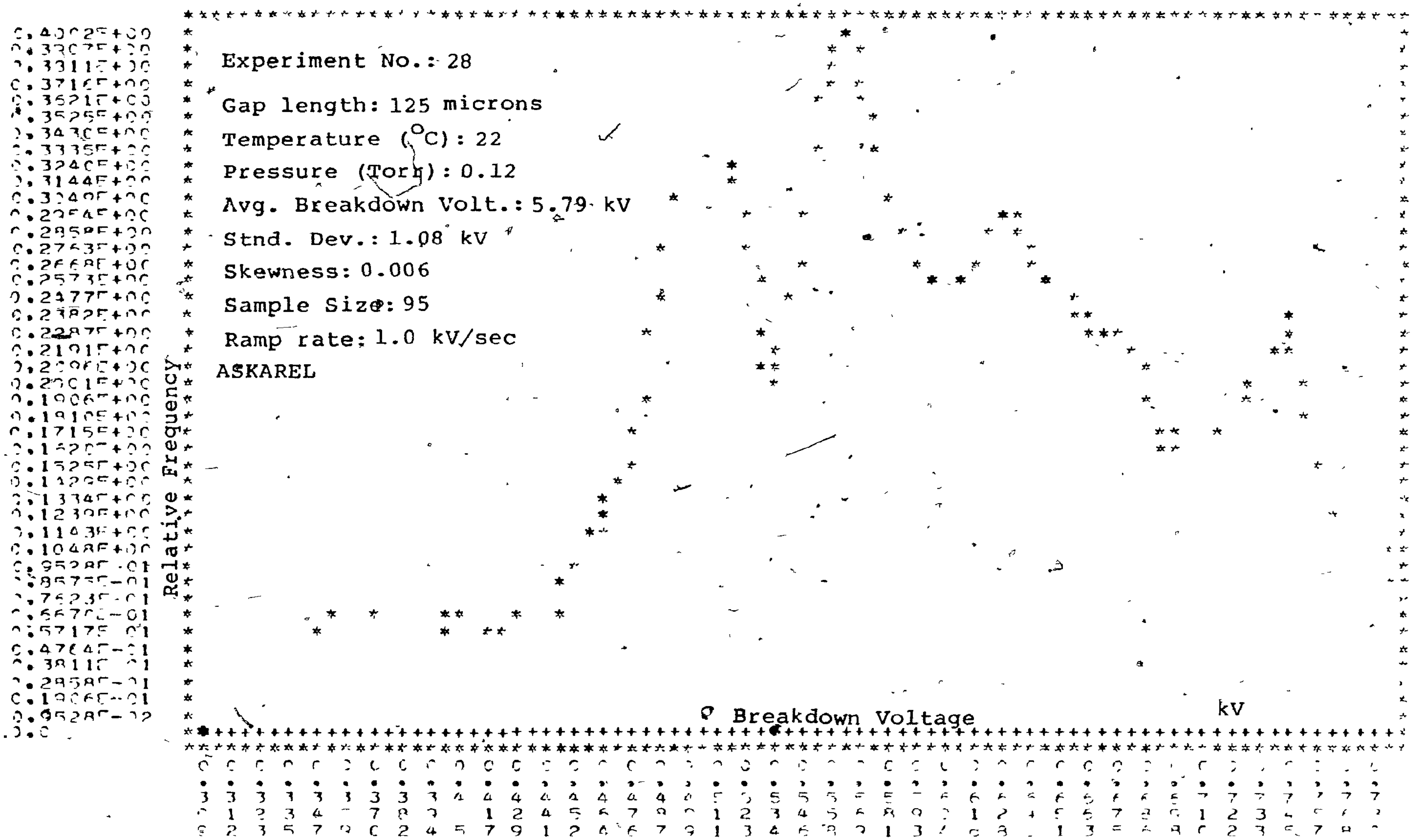

X-AXIS (HORIZONTAL-AXIS) EXPONENT 1

Y MAXIMUM 0.4019E+00
Y MINIMUM 0.0
X MAXIMUM 0.7960E+01
X MINIMUM 0.3000E+01

FIGURE 4-8-a

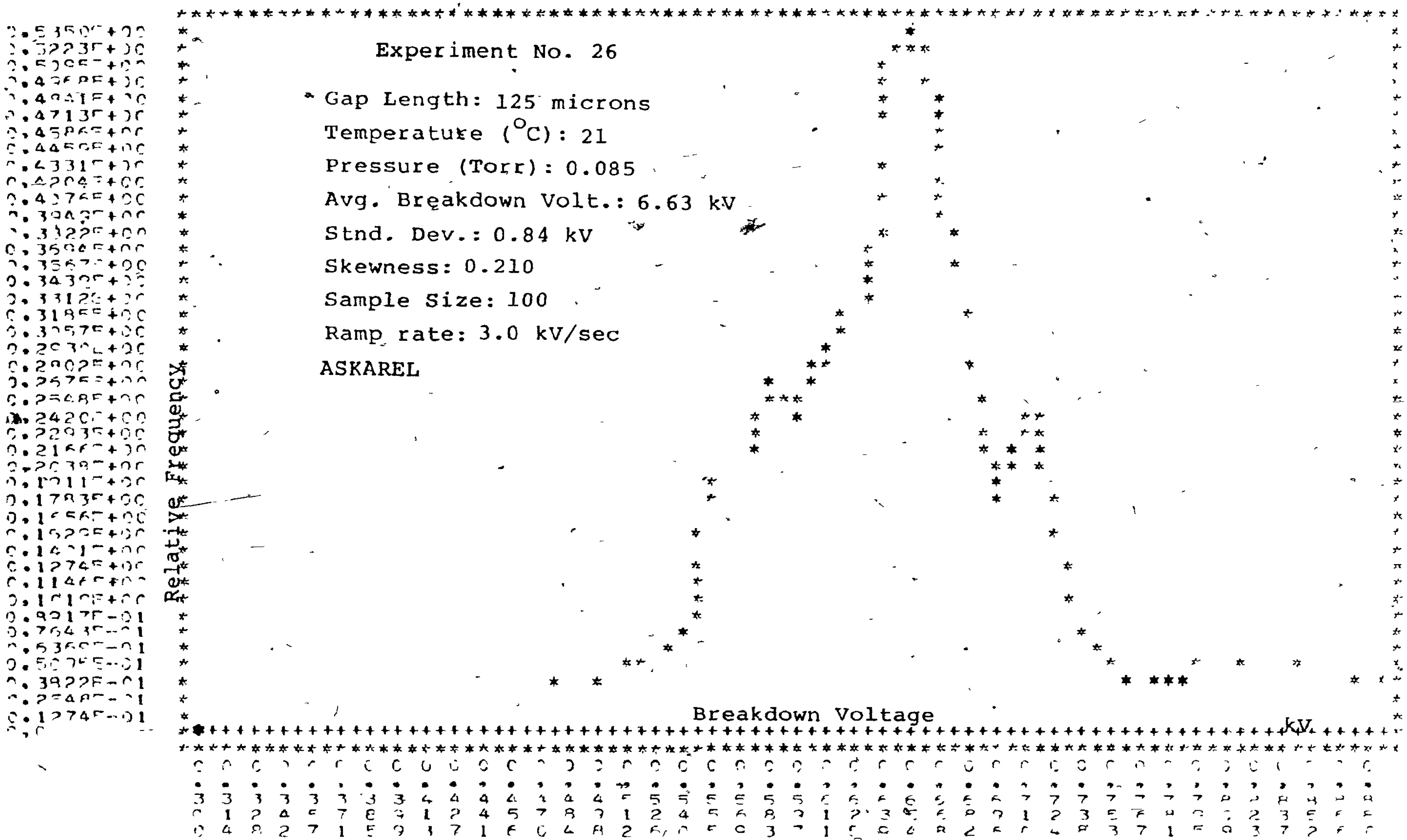

X-AXIS (HORIZONTAL-AXIS) EXPONENT 1

Y MAXIMUM 0.53502E+00
Y MINIMUM 0.0
X MAXIMUM 0.88700E+01
X MINIMUM 0.30000E+01

FIGURE 4-9-a

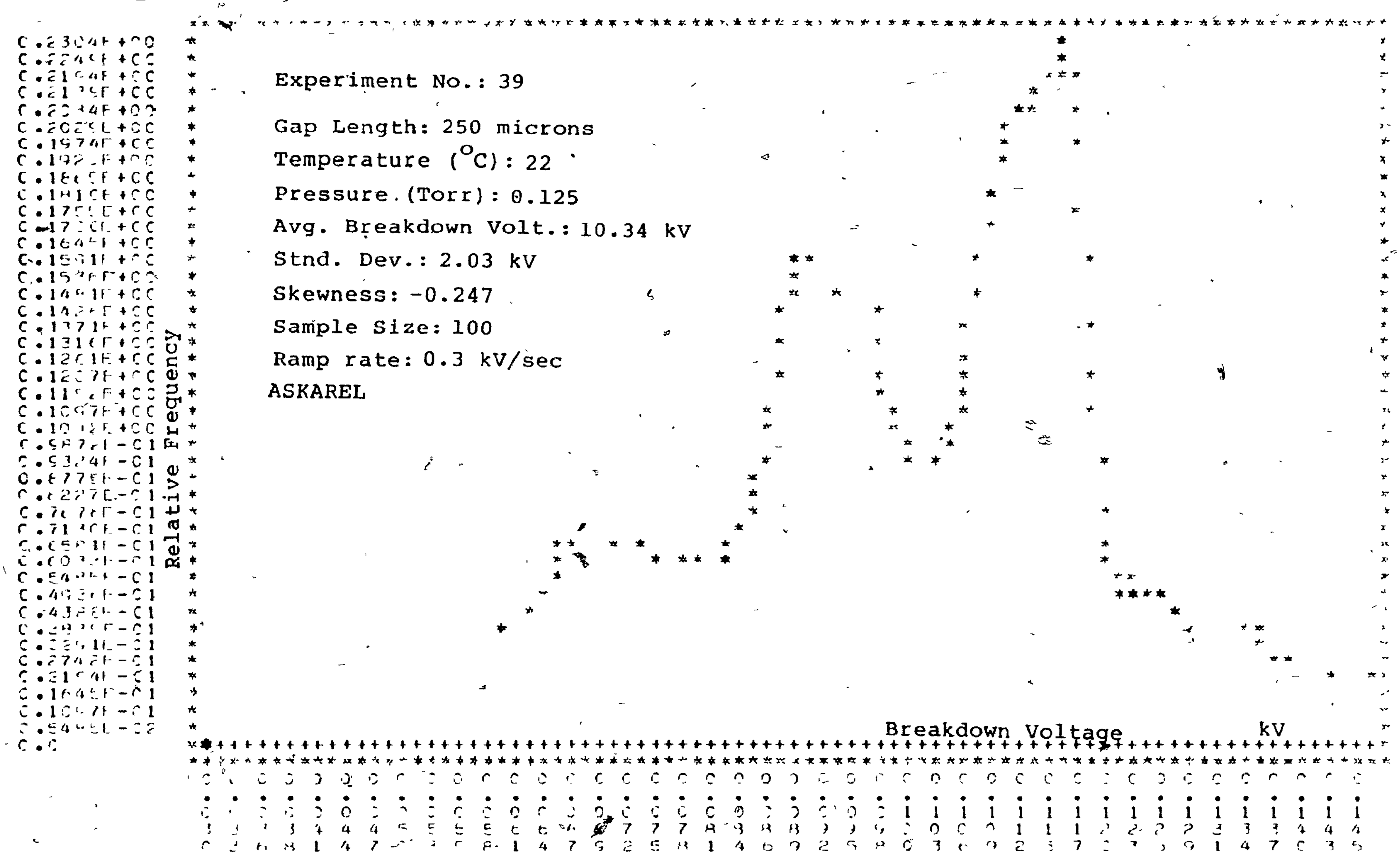

X-AXIS (HORIZONTAL-AXIS) EXPONENT 2

Y MAXIMUM [illegible]
Y MINIMUM [illegible]
X MAXIMUM [illegible]
X MINIMUM [illegible]

FIGURE 4-10-a

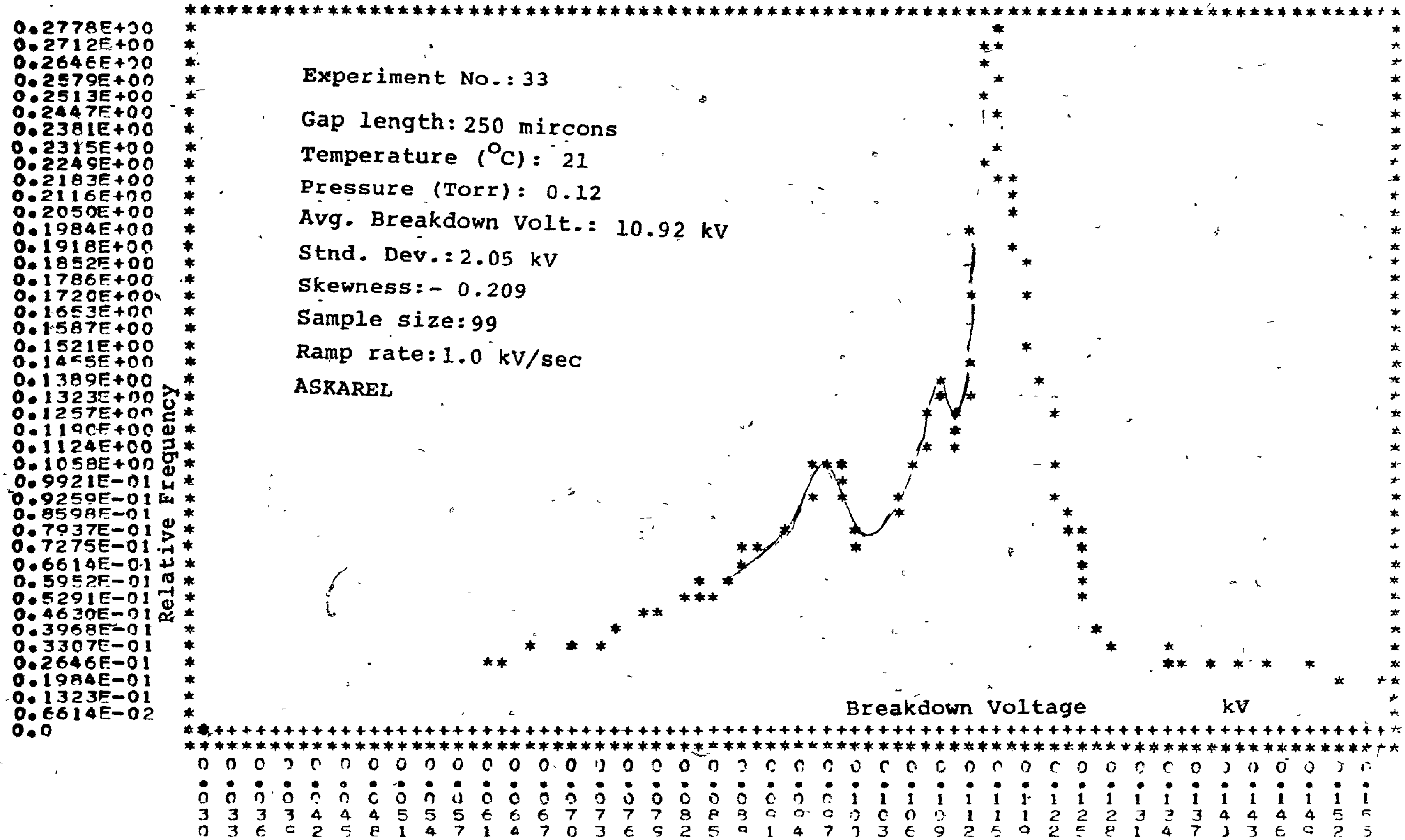

X-AXIS (HORIZONTAL-AXIS) EXPONENT 2

Y MAXIMUM 0.27778E+00
Y MINIMUM 0.0
X MAXIMUM 0.15680E+02
X MINIMUM 0.30000E+01

FIGURE 4-11-a

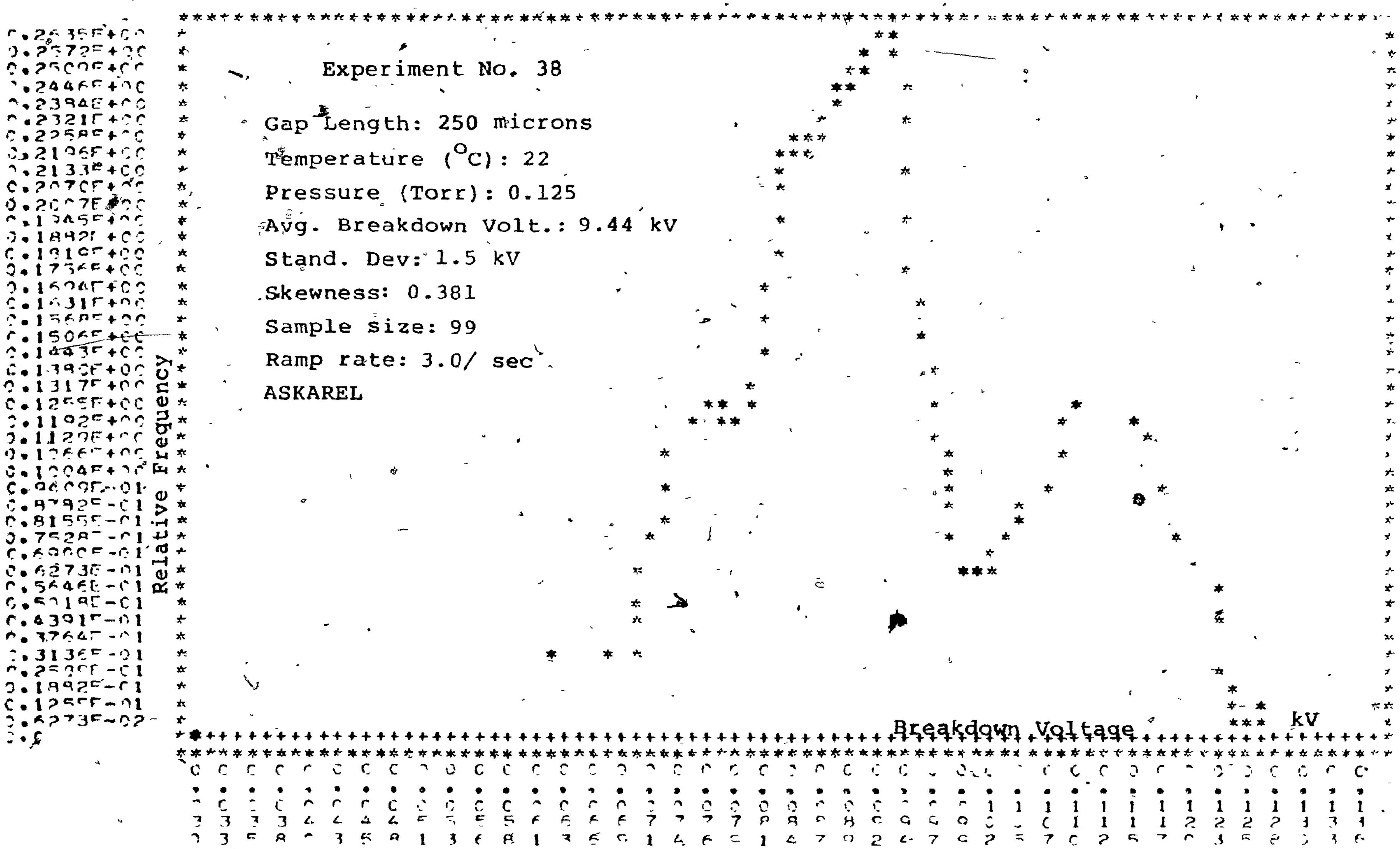

X-AXIS (HORIZONTAL-AXIS) EXPONENT 2

Y MAXIMUM 0.26346E+00
Y MINIMUM 0.0
X MAXIMUM 0.13690E+02
X MINIMUM 0.300E+01

FIGURE 4-12-a

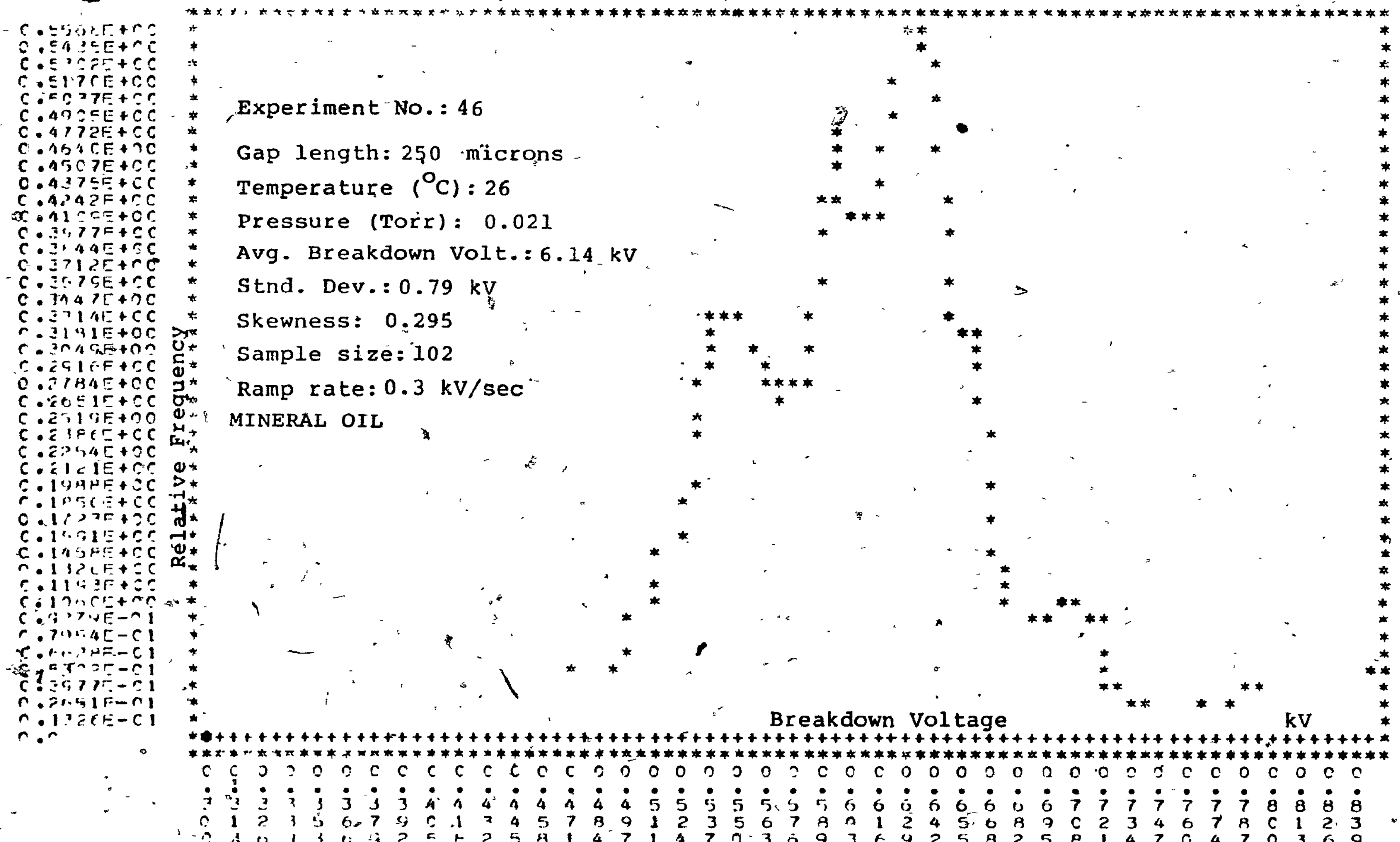

X-AXIS (HORIZONTAL-AXIS) EXPONENT 1

Y MAXIMUM 0.5567GE+00
Y MINIMUM 0.0
X MAXIMUM 0.840000E+01
X MINIMUM 0.300000E+01

FIGURE 4-13-a

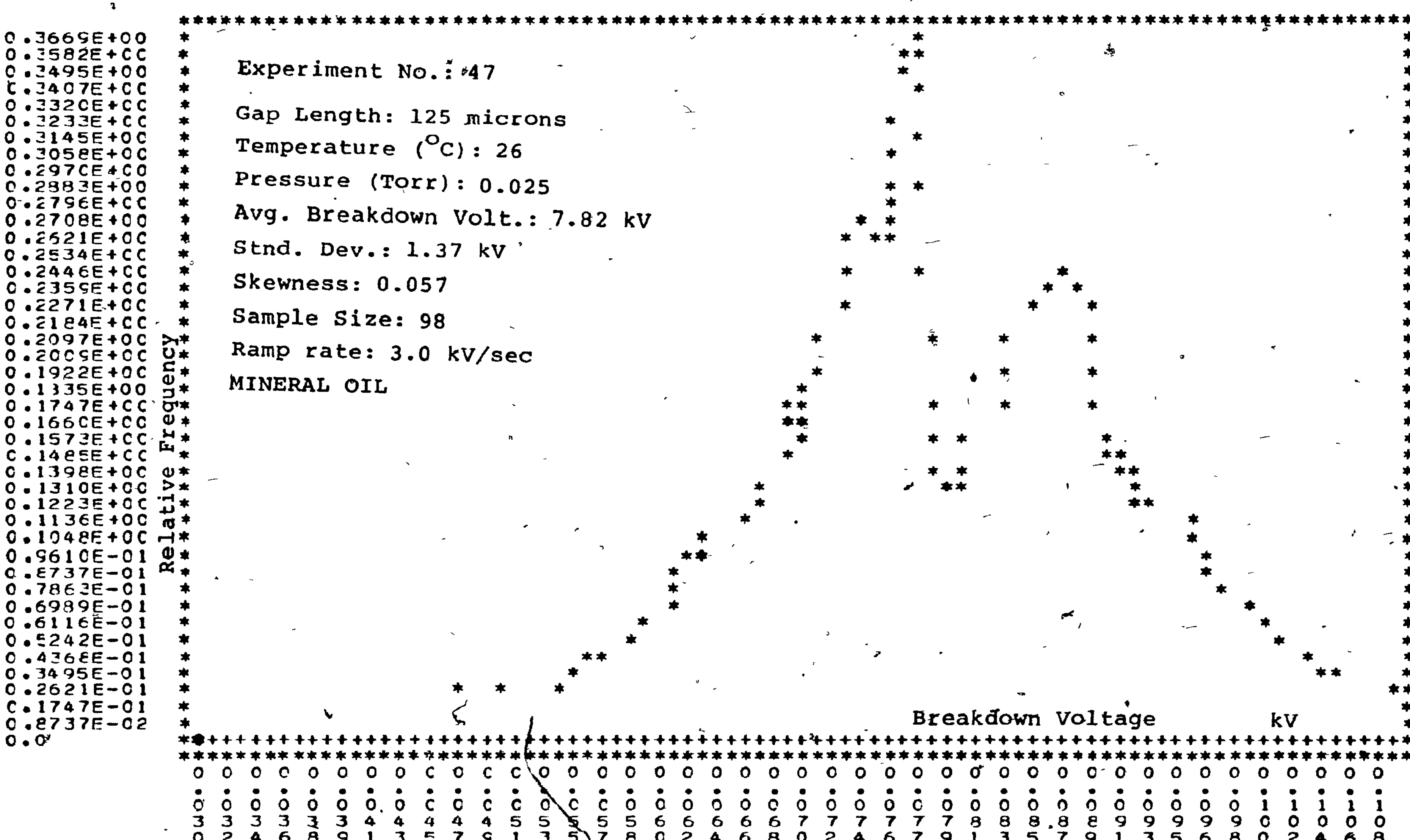

X-AXIS (HORIZONTAL-AXIS) EXPONENT 2

Y MAXIMUM 0.36693E+00
Y MINIMUM 0.0
X MAXIMUM 0.10880E+02
X MINIMUM 0.30000E+01

FIGURE 4-14-a

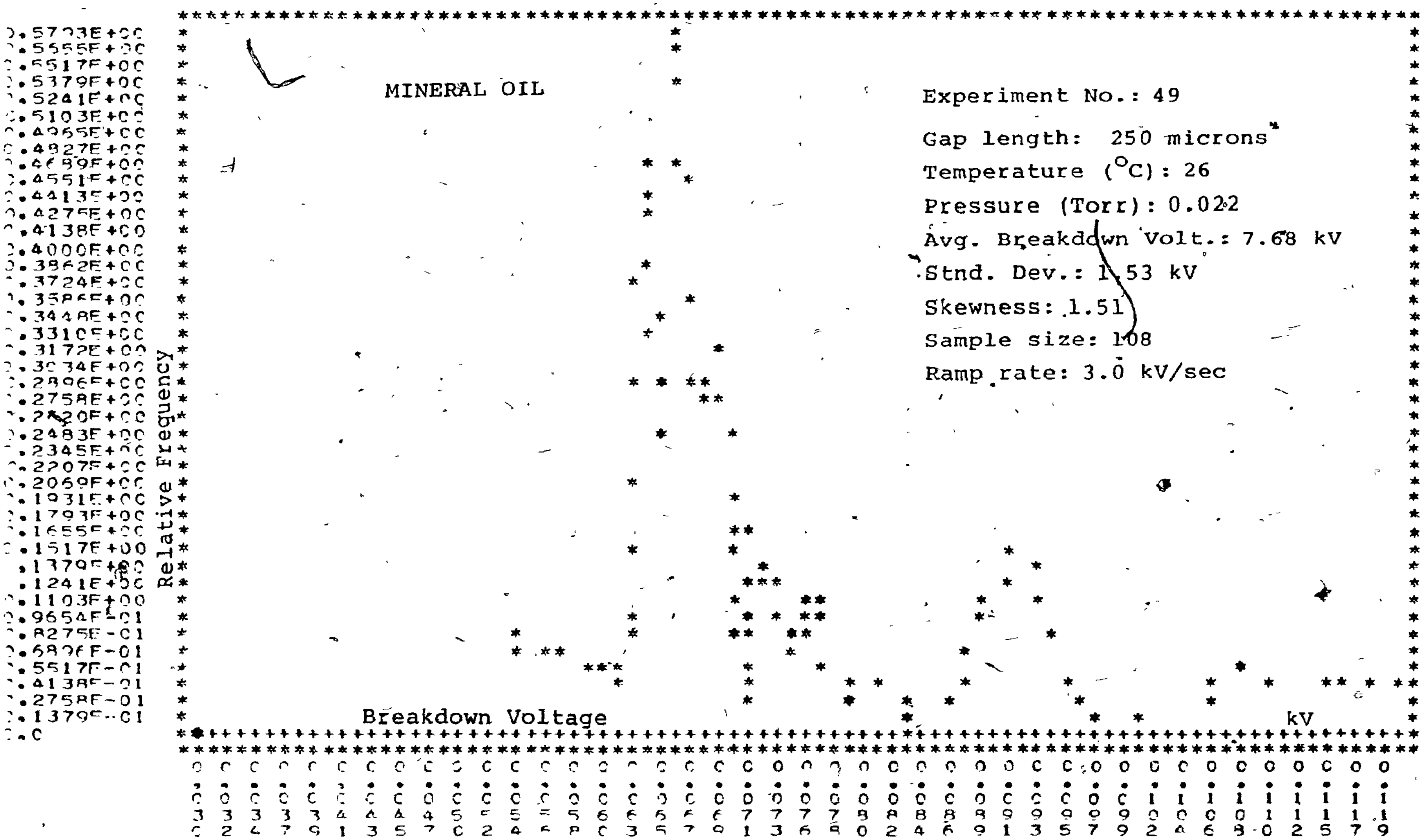

X-AXIS (HORIZONTAL-AXIS) EXPONENT 2

Y MAXIMUM 0.57926E+00
Y MINIMUM 0.0
X MAXIMUM 0.12000E+02
X MINIMUM 0.30000E+01

FIGURE 4-15-a

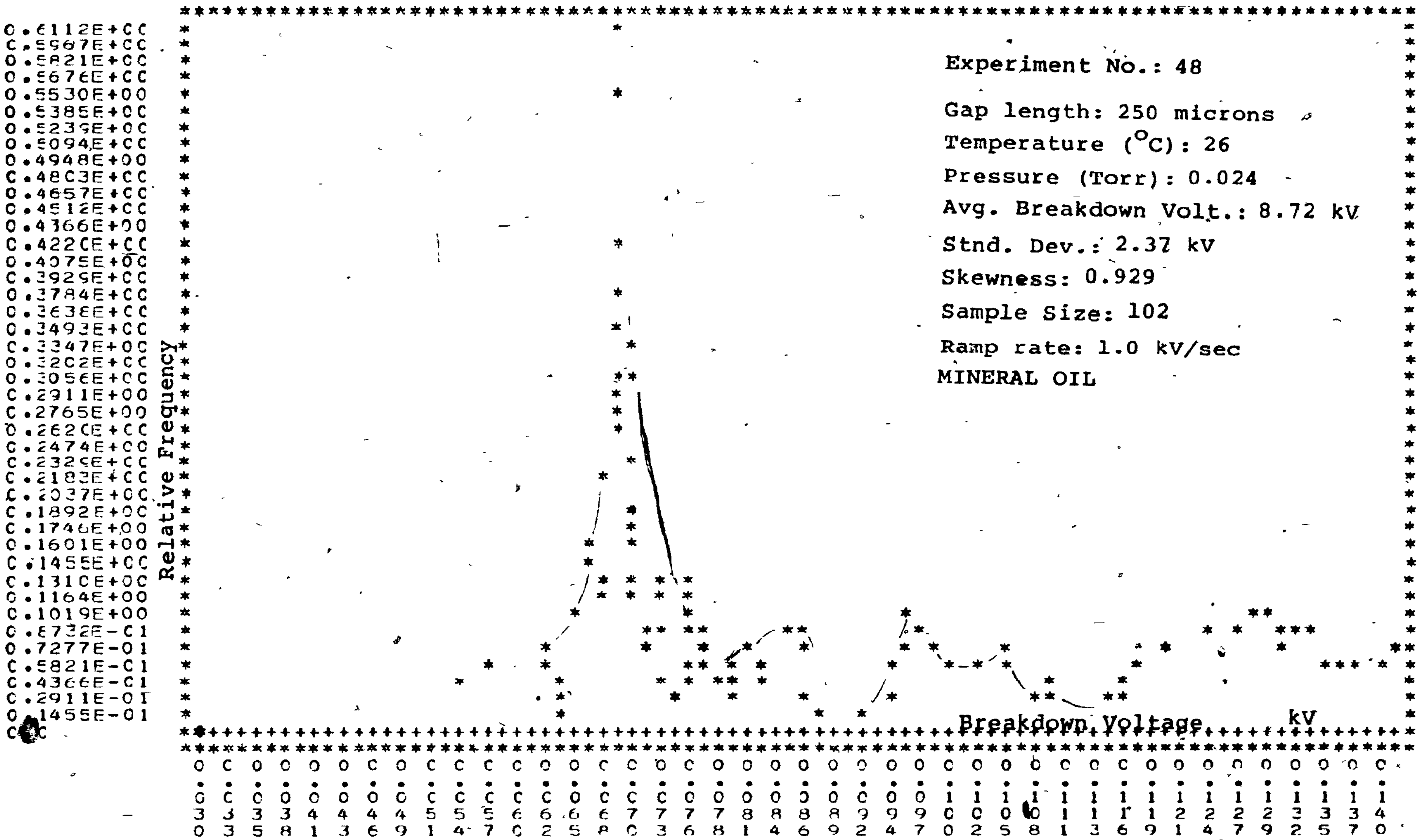

X-AXIS (HORIZONTAL-AXIS) EXPONENT 2

Y MAXIMUM 0.61124E+00
Y MINIMUM 0.0
X MAXIMUM 0.14140E+02
X MINIMUM 0.30000E+01

FIGURE 4-16-a

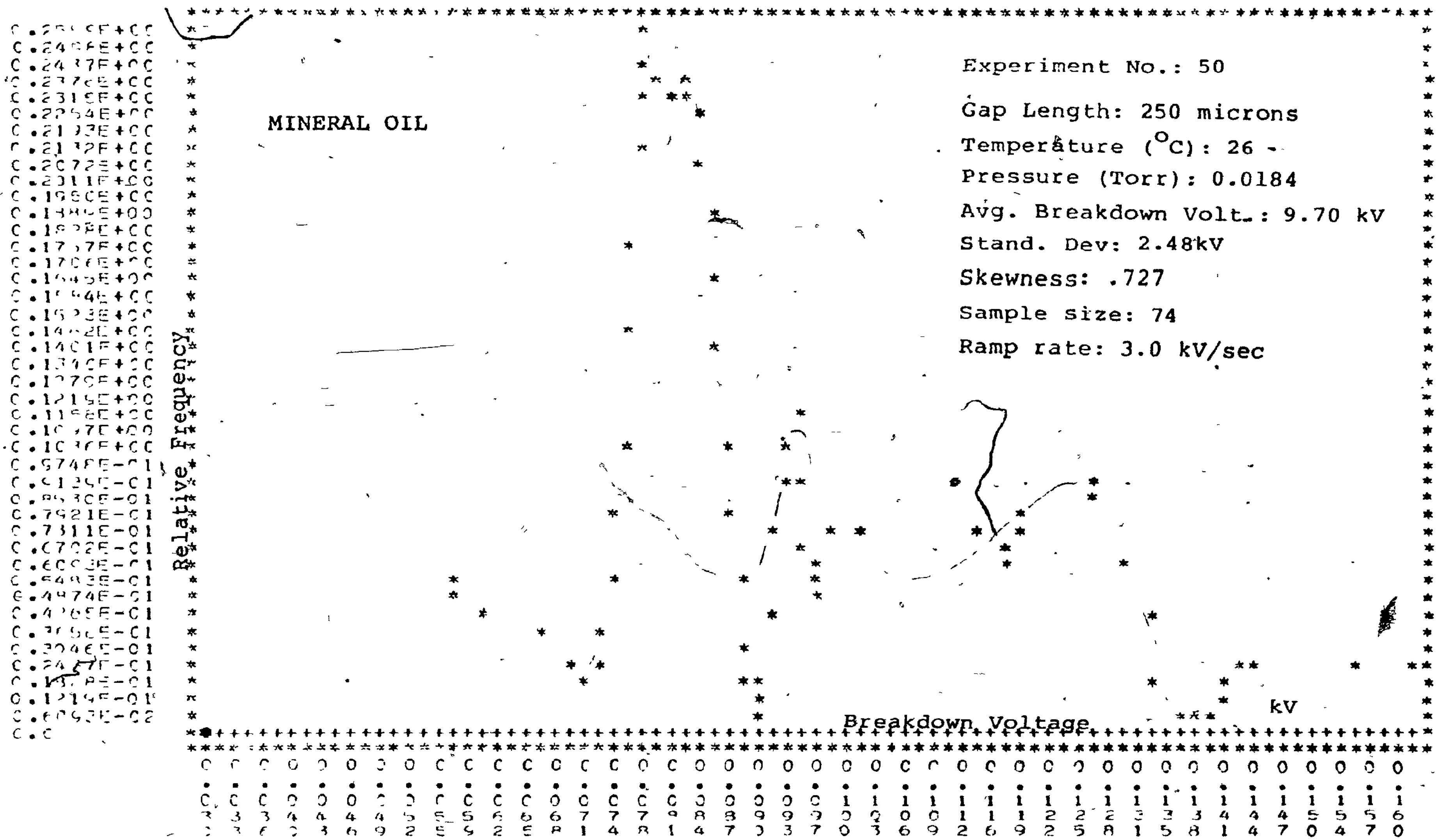

X-AXIS (HORIZONTAL-AXIS) EXPONENT 2

Y MAXIMUM 0.2539E+00
Y MINIMUM 0.0
X MAXIMUM 0.1605E+02
X MINIMUM 0.3000 +01

FIGURE 4-17-a

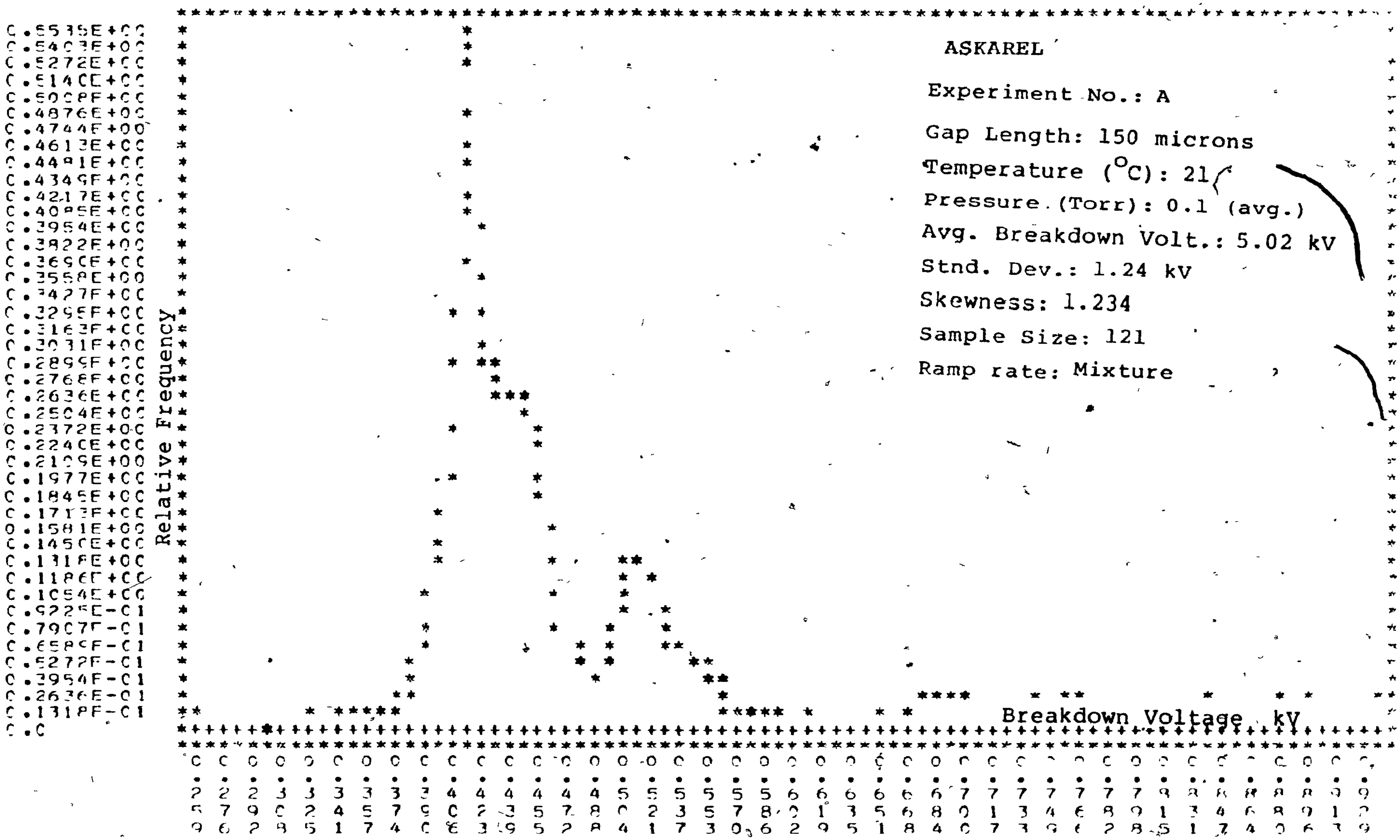

X-AXIS (HORIZONTAL-AXIS) EXPONENT 1

Y MAXIMUM 0.55351E+00
Y MINIMUM 0.0
X MAXIMUM 0.93726E+01
X MINIMUM 0.25927E+01

FIGURE 4-18-a

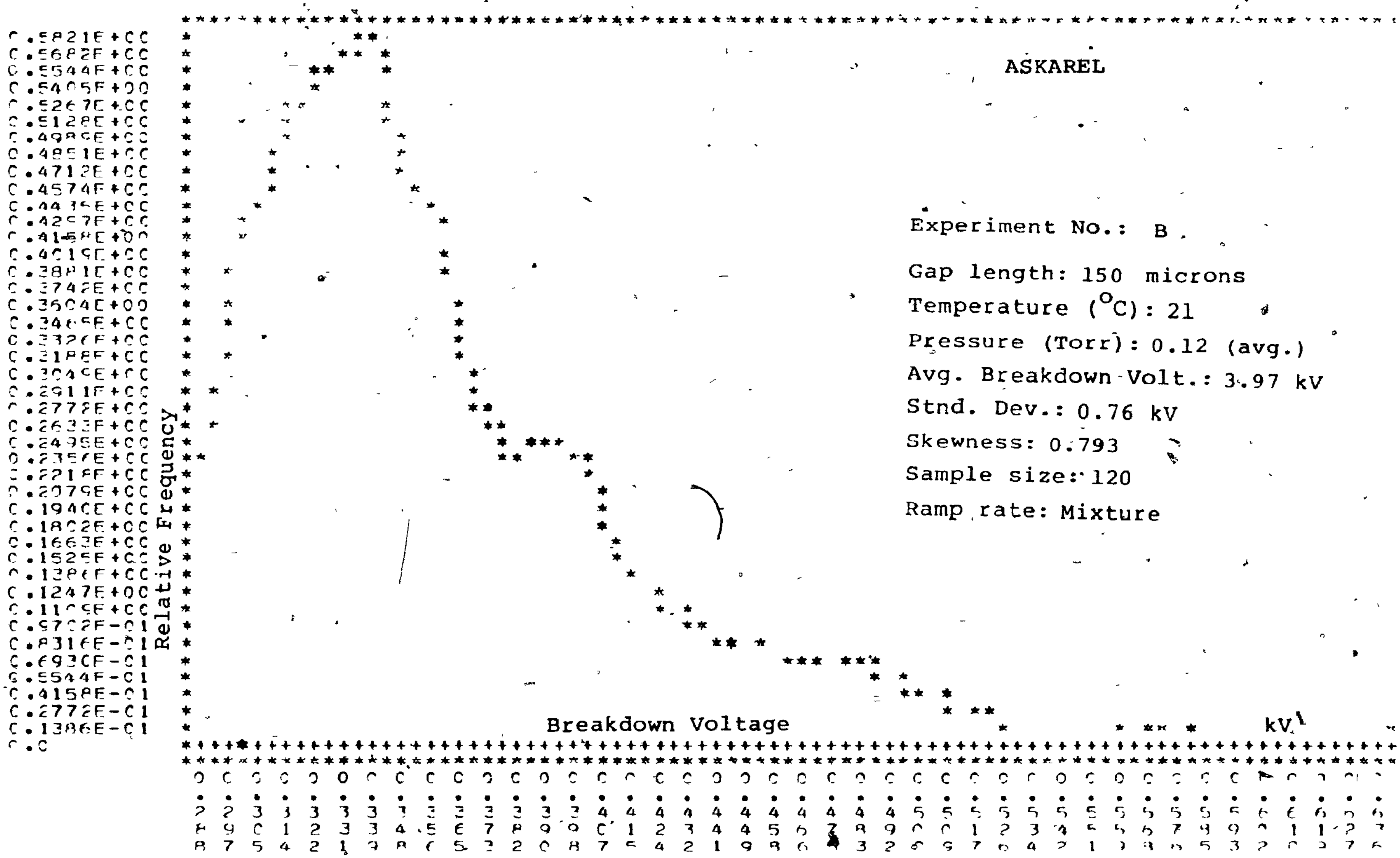

X-AXIS (HORIZONTAL-AXIS) EXPONENT 1

Y MAXIMUM C.58211E+00
Y MINIMUM C.0
X MAXIMUM 0.63938E+01
X MINIMUM C.28833E+01

FIGURE 4-19-a

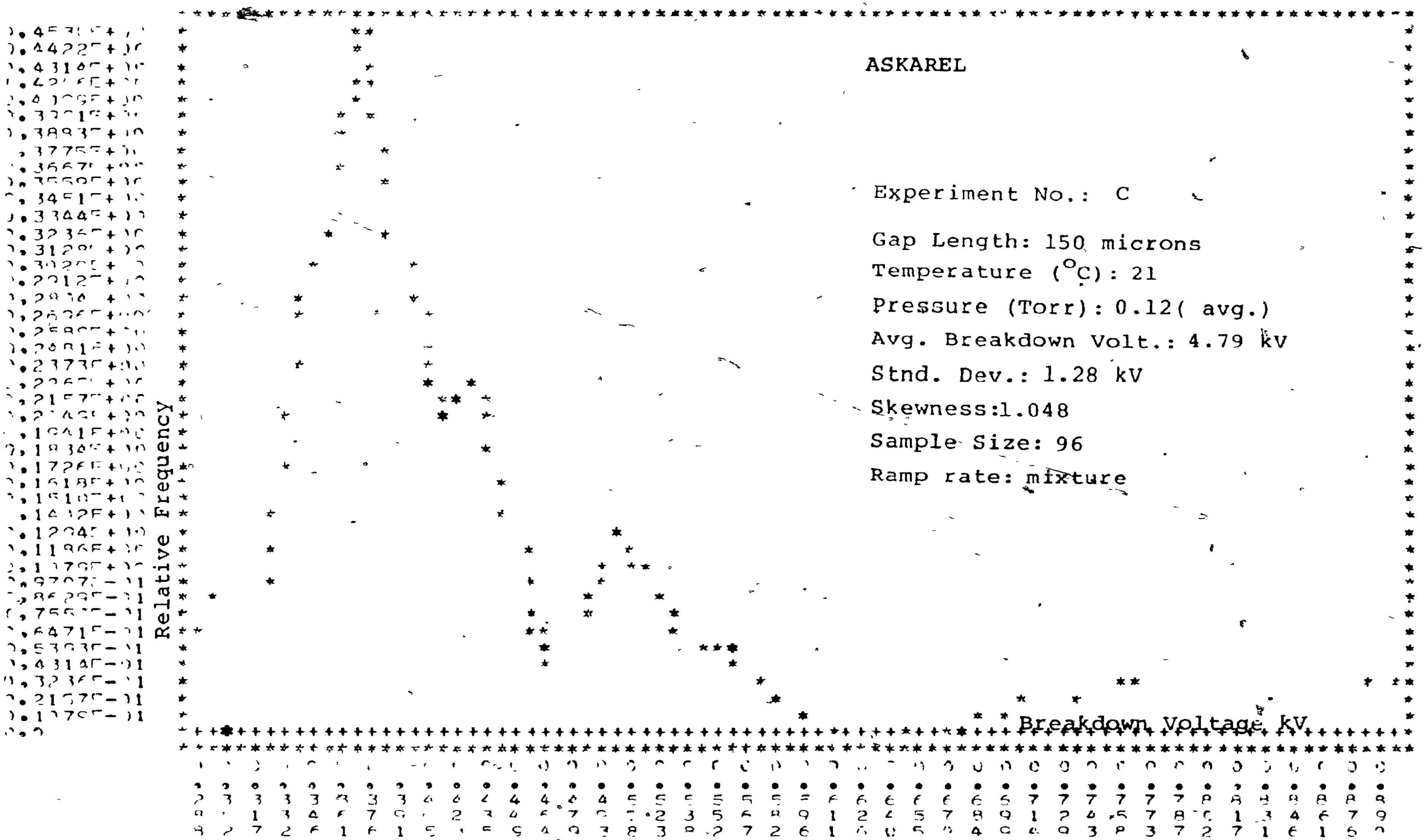

X-AXIS (HORIZONTAL-AXIS) EXPONENT 1

Y MAXIMUM [illegible]
Y MINIMUM [illegible]
X MAXIMUM [illegible]
X MINIMUM [illegible]

FIGURE 4-20-a

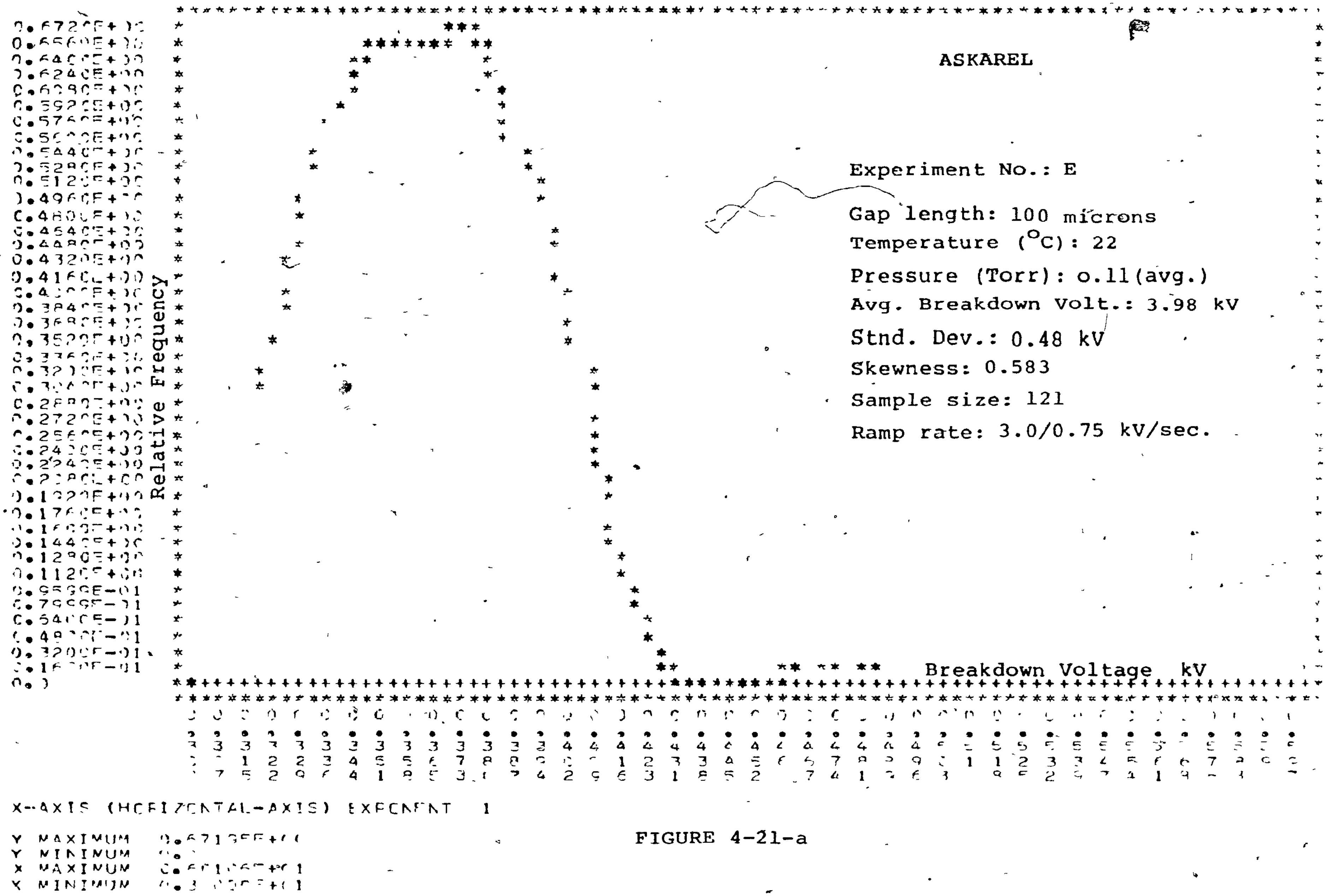
ASKAREL
Experiment No.: E
Gap length: 100 microns
Temperature (°C): 22
Pressure (Torr): 0.11(avg.)
Avg. Breakdown Volt.: 3.98 kV
Stnd. Dev.: 0.48 kV
Skewness: 0.583
Sample size: 121
Ramp rate: 3.0/0.75 kV/sec.
Relative Frequency
Breakdown Voltage kV
X-AXIS (HORIZONTAL-AXIS) EXPONENT 1
Y MAXIMUM
Y MINIMUM
X MAXIMUM
X MINIMUM

FIGURE 4-21-a

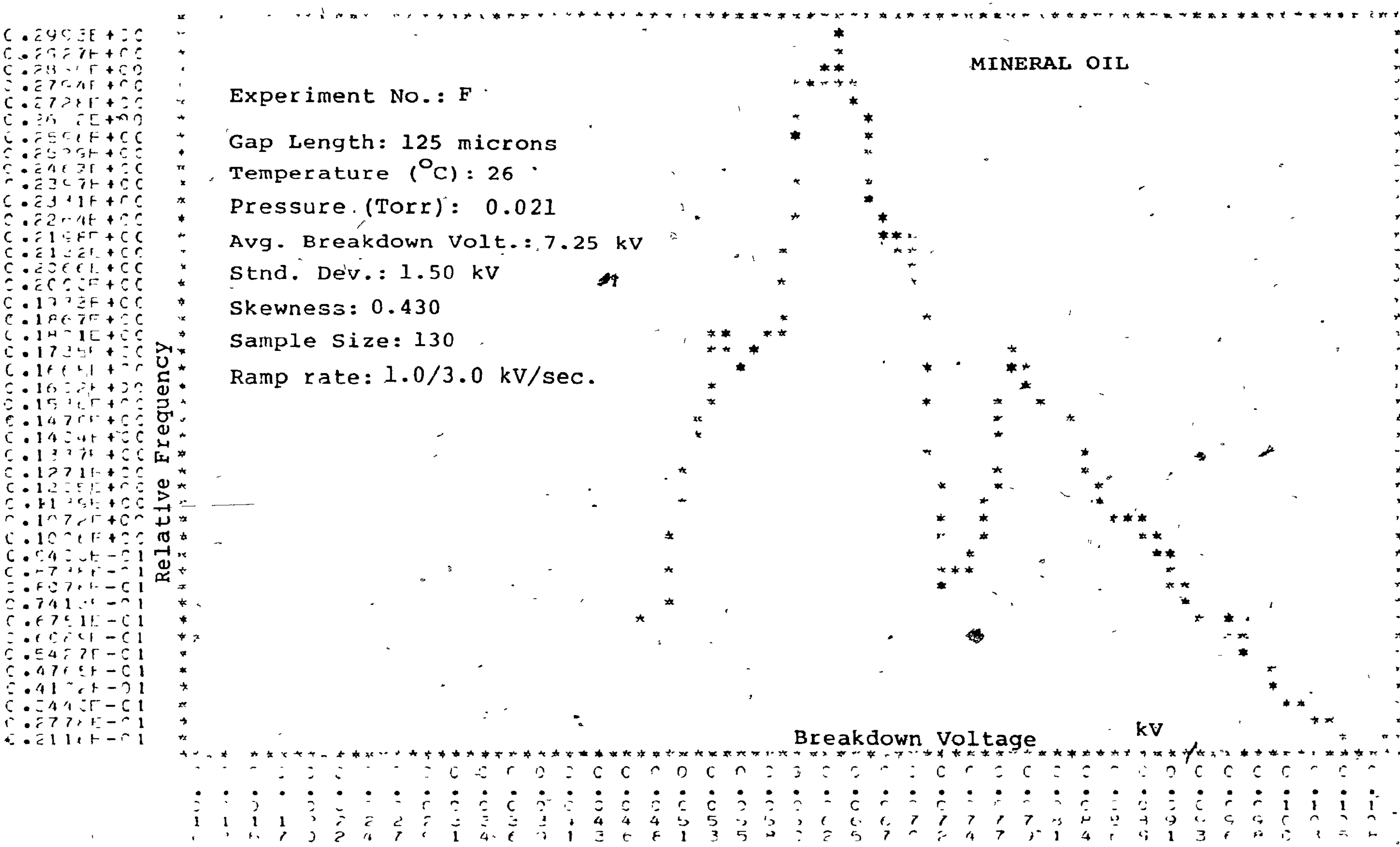

X-AXIS (HORIZONTAL-AXIS) EXPONENT [illegible]

Y MAXIMUM [illegible]E+00
Y MINIMUM 0.211 [illegible]E-01
X MAXIMUM [illegible]
X MINIMUM 0.10 [illegible] +01

FIGURE 4-22-a

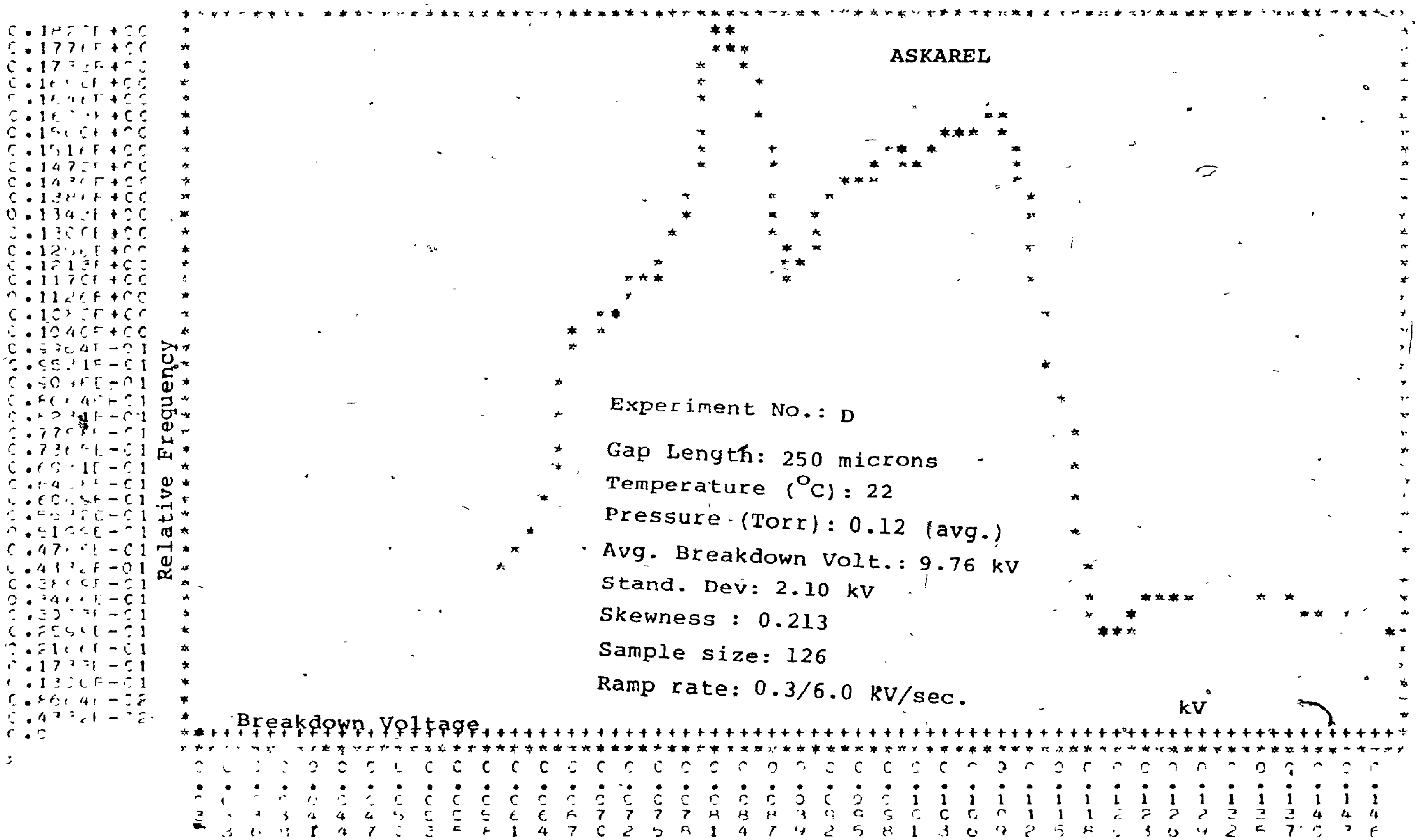

X-AXIS (HORIZONTAL-AXIS) EXPONENT 2

Y MAXIMUM
Y MINIMUM
X MAXIMUM
X MINIMUM

FIGURE 4-23-a

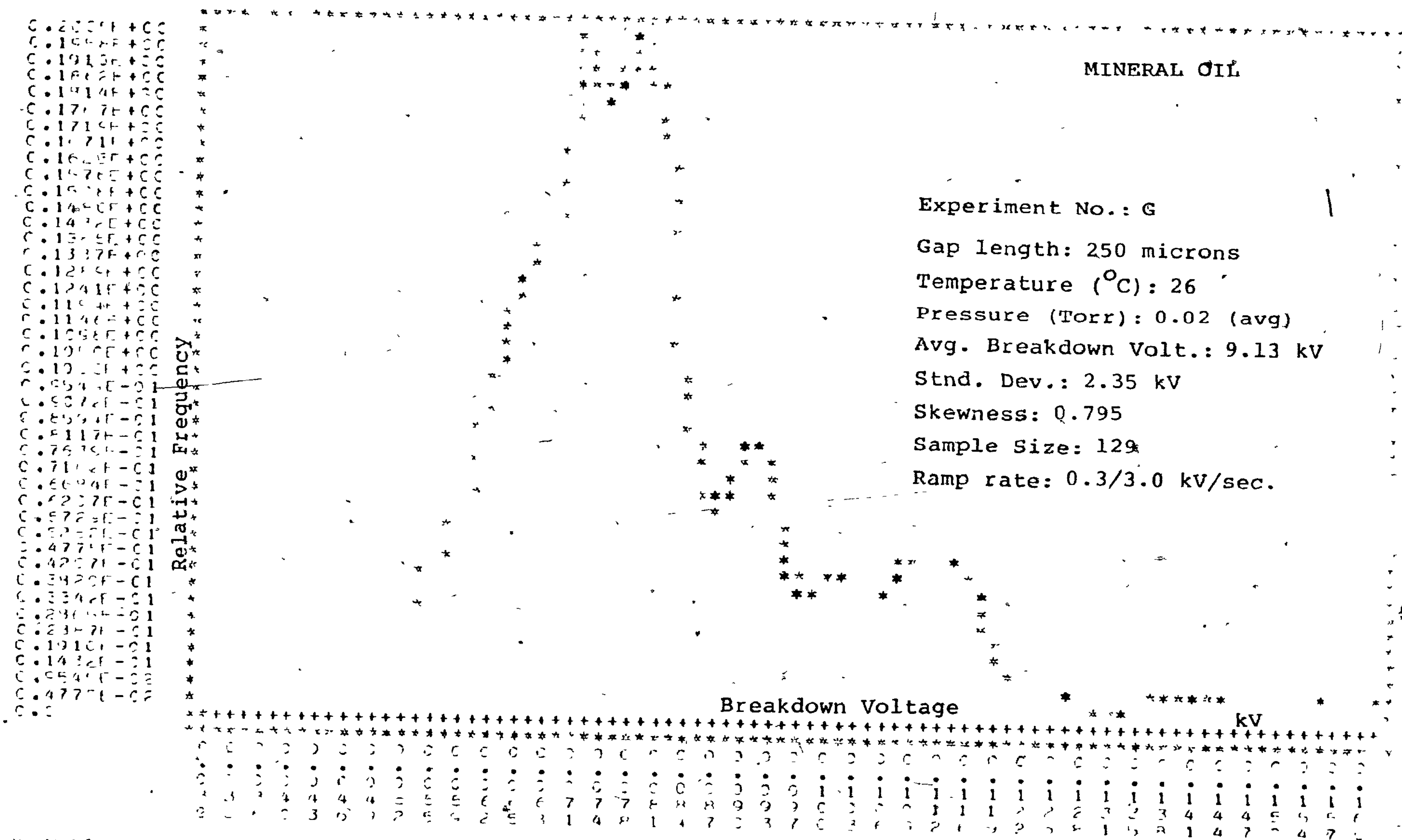

X-AXIS (HORIZONTAL-AXIS) EXPONENT

Y MAXIMUM

Y MINIMUM

X MAXIMUM

X MINIMUM

FIGURE 4-24-a

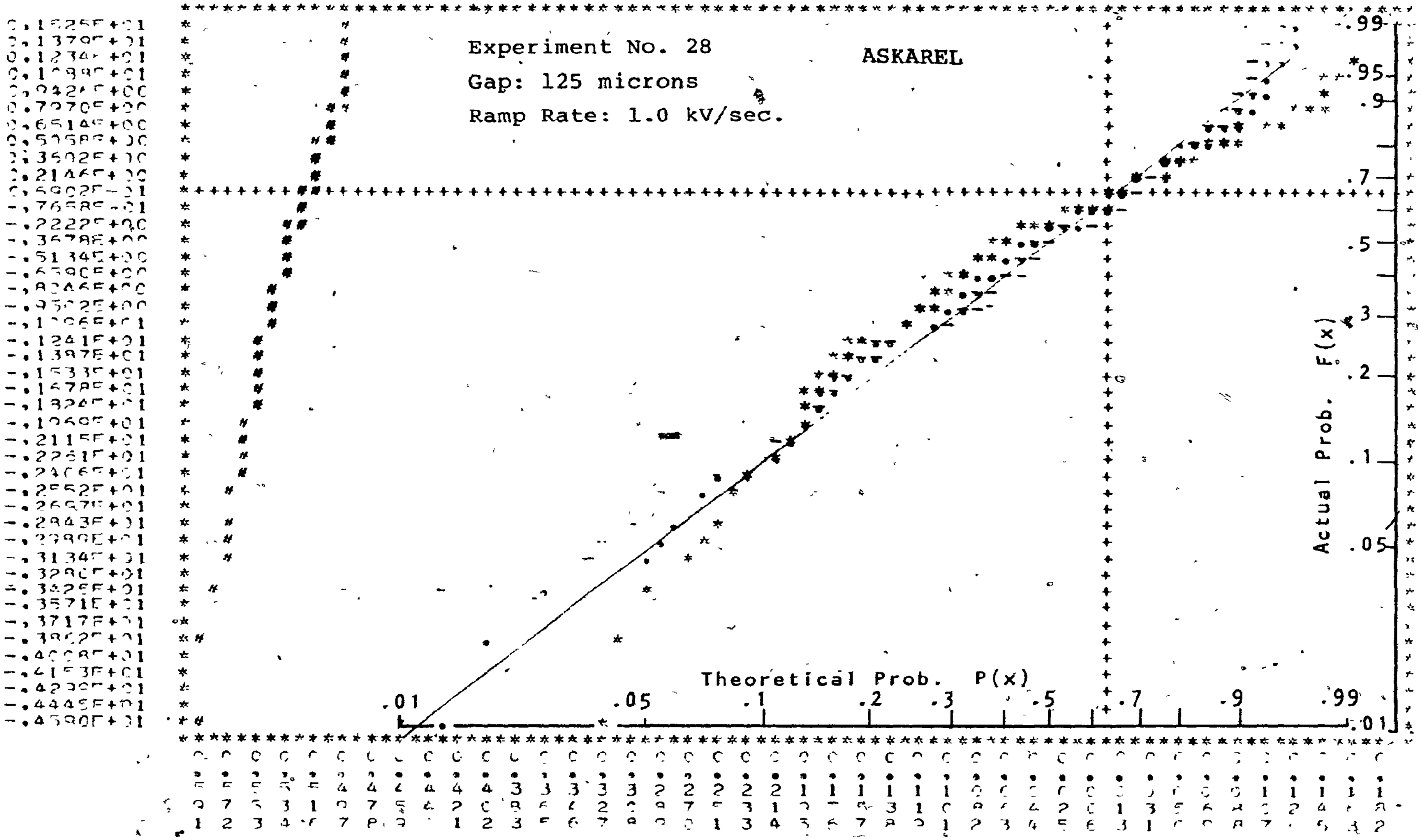

X-AXIS (HORIZONTAL AXIS) EXPONENT 1

Y MAXIMUM 0.15250E+01
Y MINIMUM -0.45901E+01
X MAXIMUM 0.19178E+01
X MINIMUM -0.[illegible]E+01

FIGURE 4-8-b

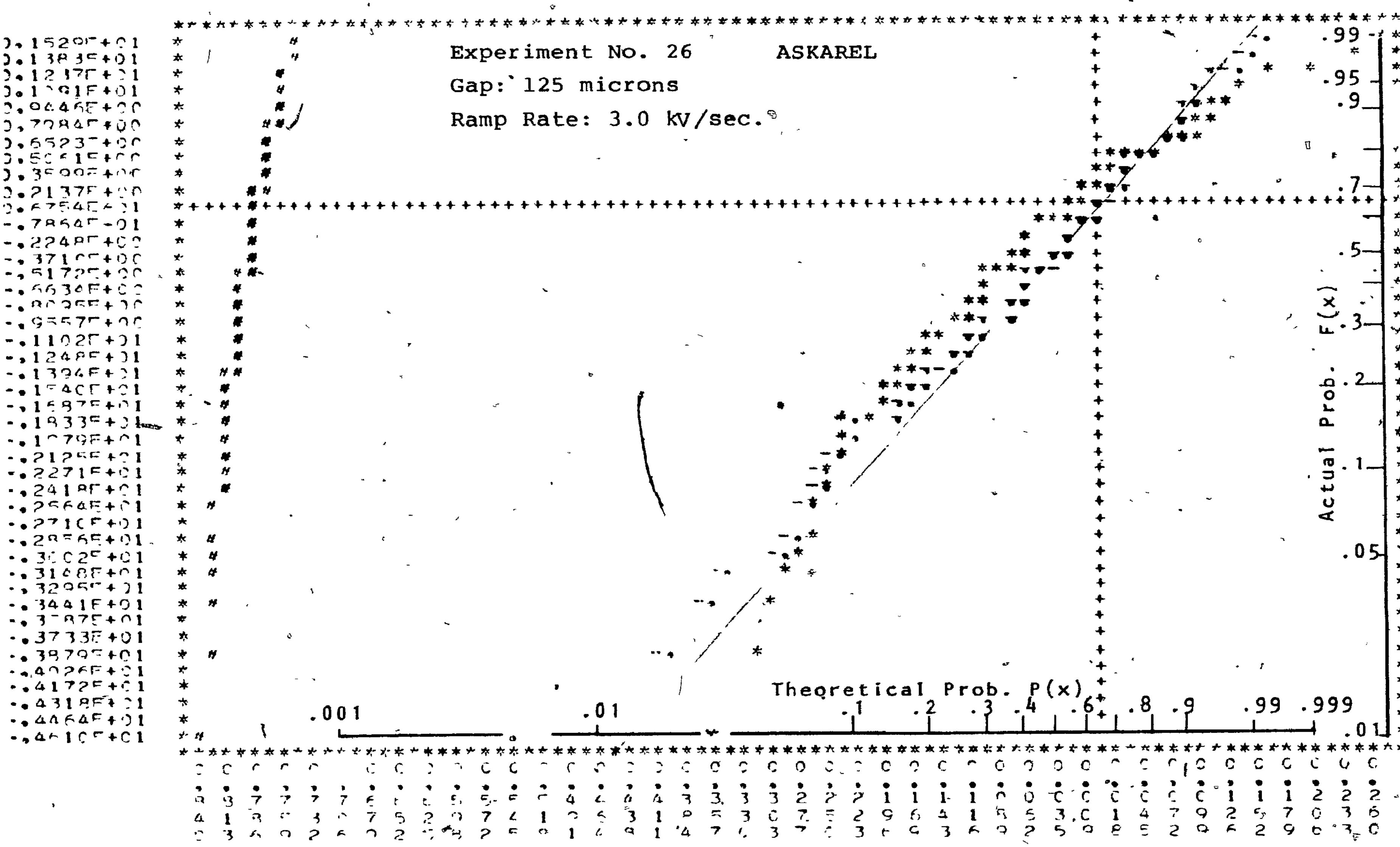

X-AXIS (HORIZONTAL-AXIS) XPONENT 1

Y MAXIMUM 0.15293E+01
Y MINIMUM -0.46102E+01
X MAXIMUM 0.27303E+01
X MINIMUM -0.33070E+01

FIGURE 4-9-b

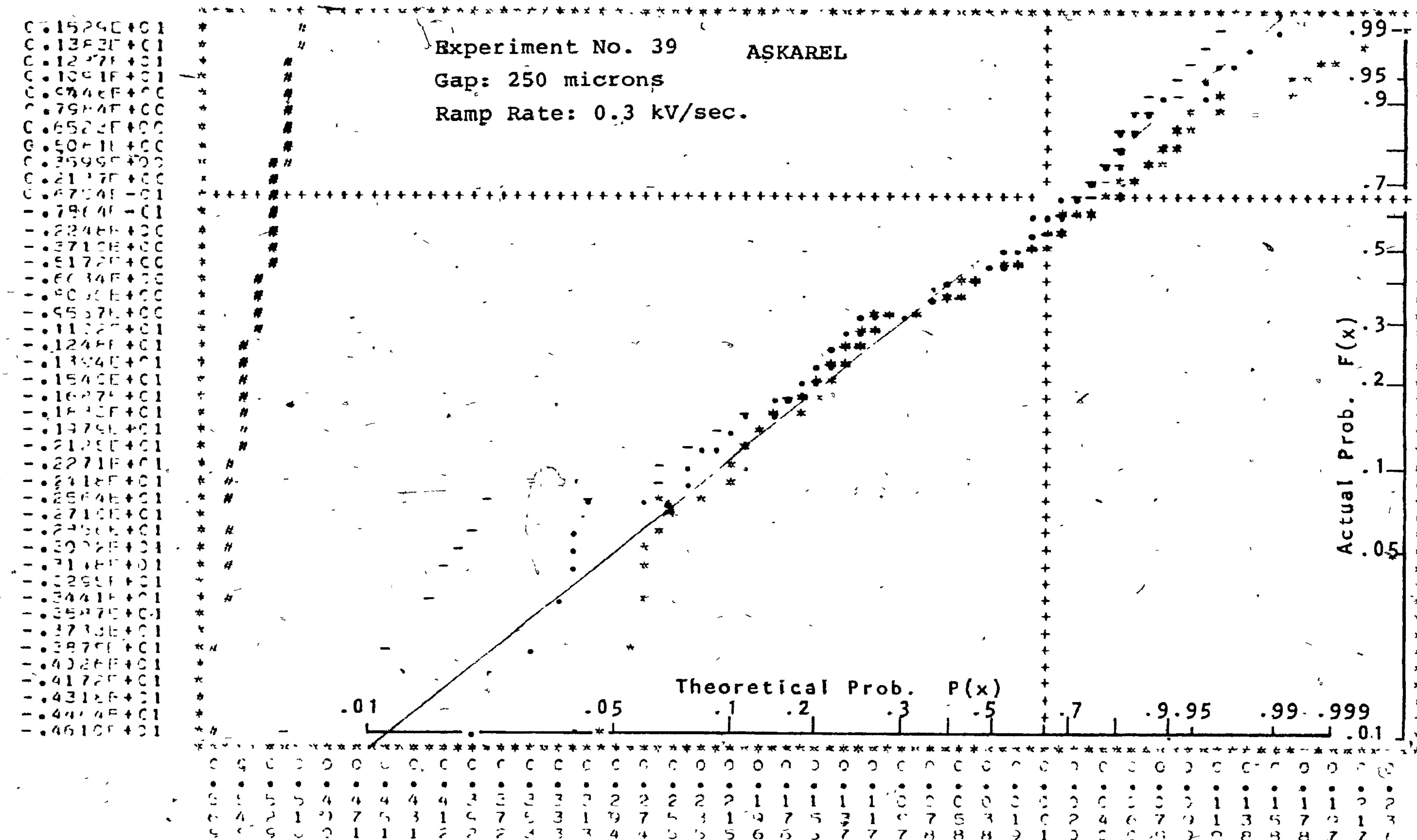

X-AXIS (HORIZONTAL-AXIS) EXPONENT 1

Y MAXIMUM 0.15[illegible]E+01
Y MINIMUM -0.461[illegible]E+01
X MAXIMUM 0.24[illegible]E+01
X MINIMUM -0.[illegible]E+01

FIGURE 4-10-b

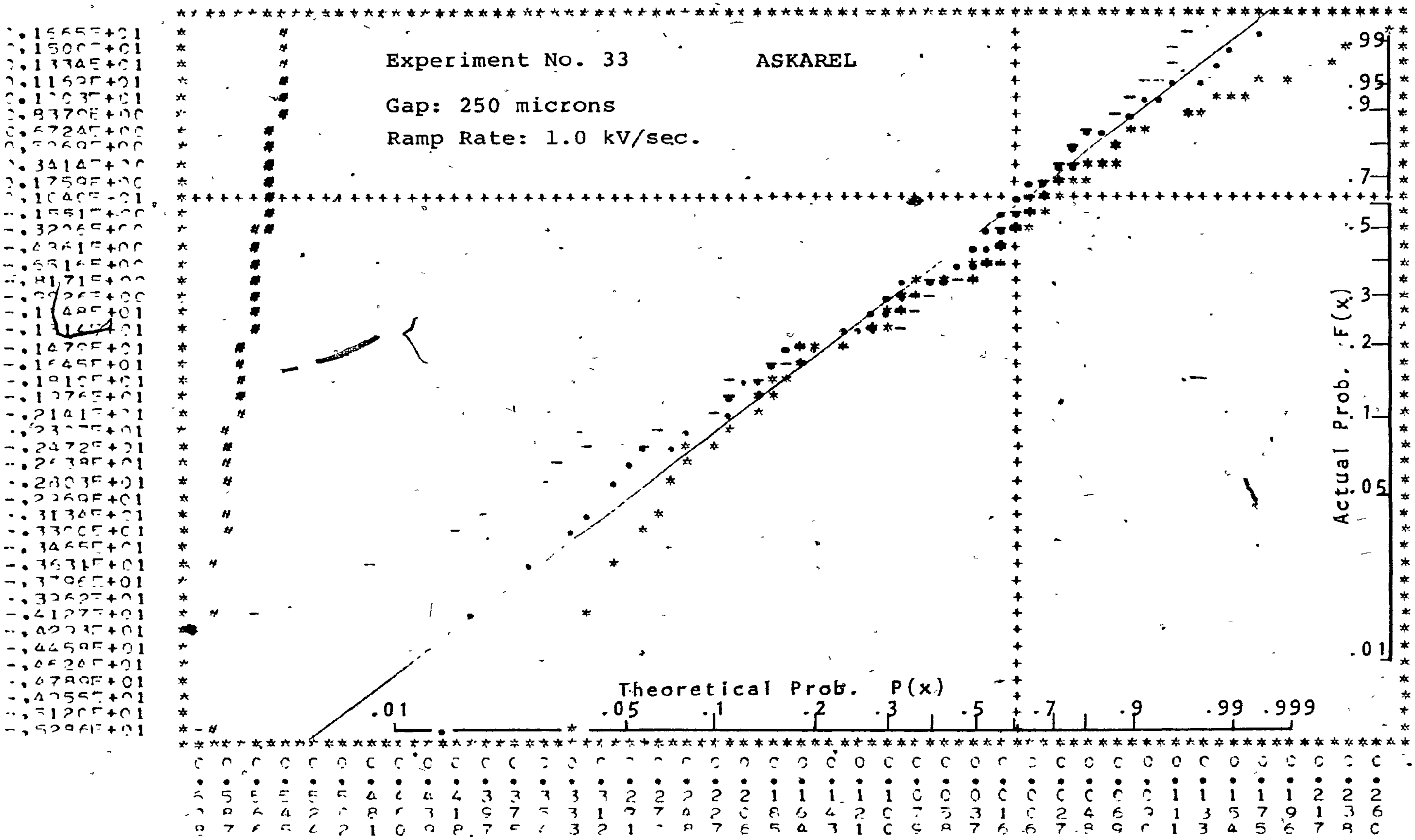

X-AXIS (HORIZONTAL-AXIS) EXPONENT 1

Y MAXIMUM 0.16655E+01
Y MINIMUM -0.52859E+01
X MAXIMUM 0.27025E+01
X MINIMUM -0.66820E+01

FIGURE 4-11-b

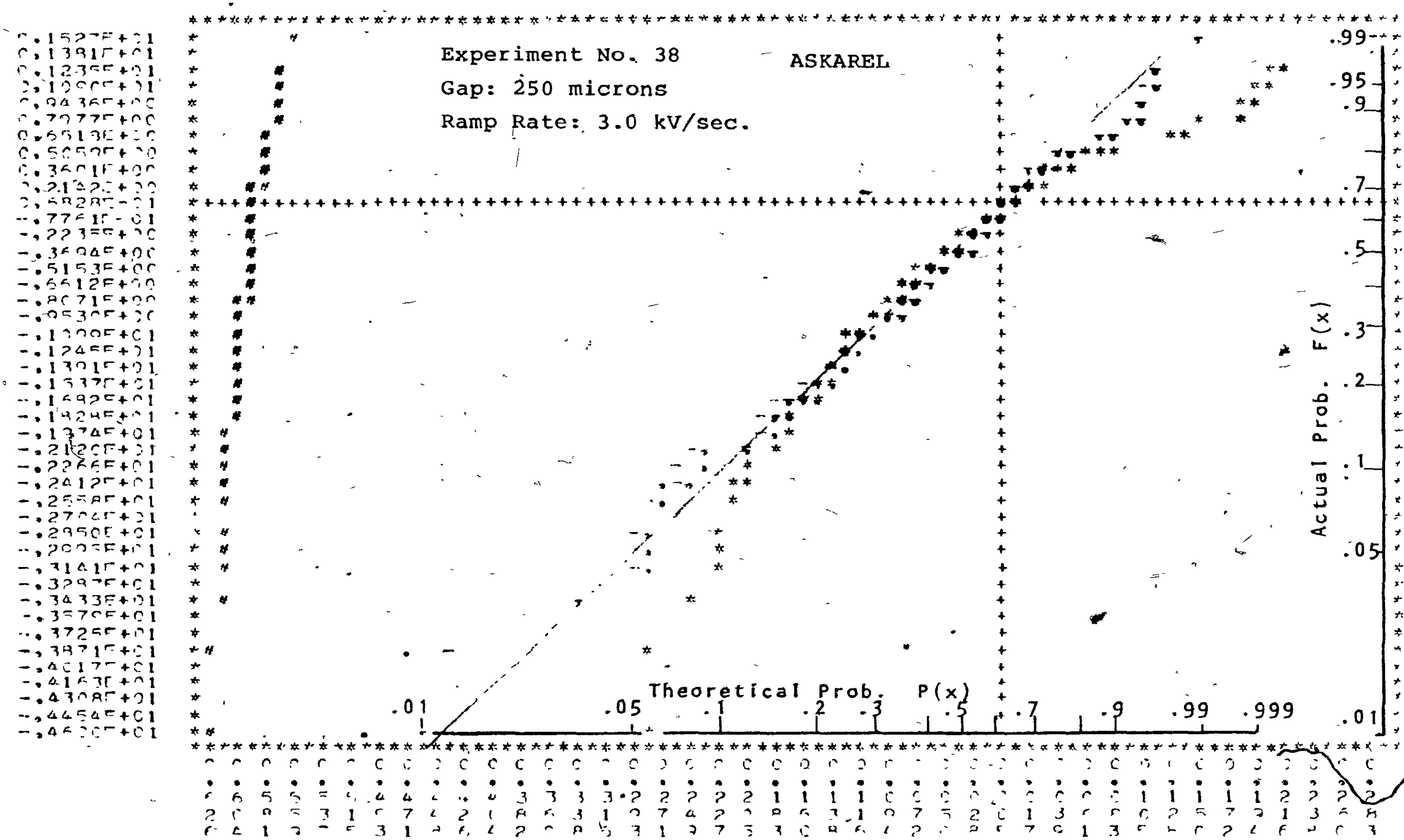

X-AXIS (HORIZONTAL-AXIS) EXPONENT 1

Y MAXIMUM 0.15272E+01
Y MINIMUM -0.460[illegible]2E+01
X MAXIMUM 0.22370 +01
X MINIMUM -0.62571E+01

FIGURE 4-12-b

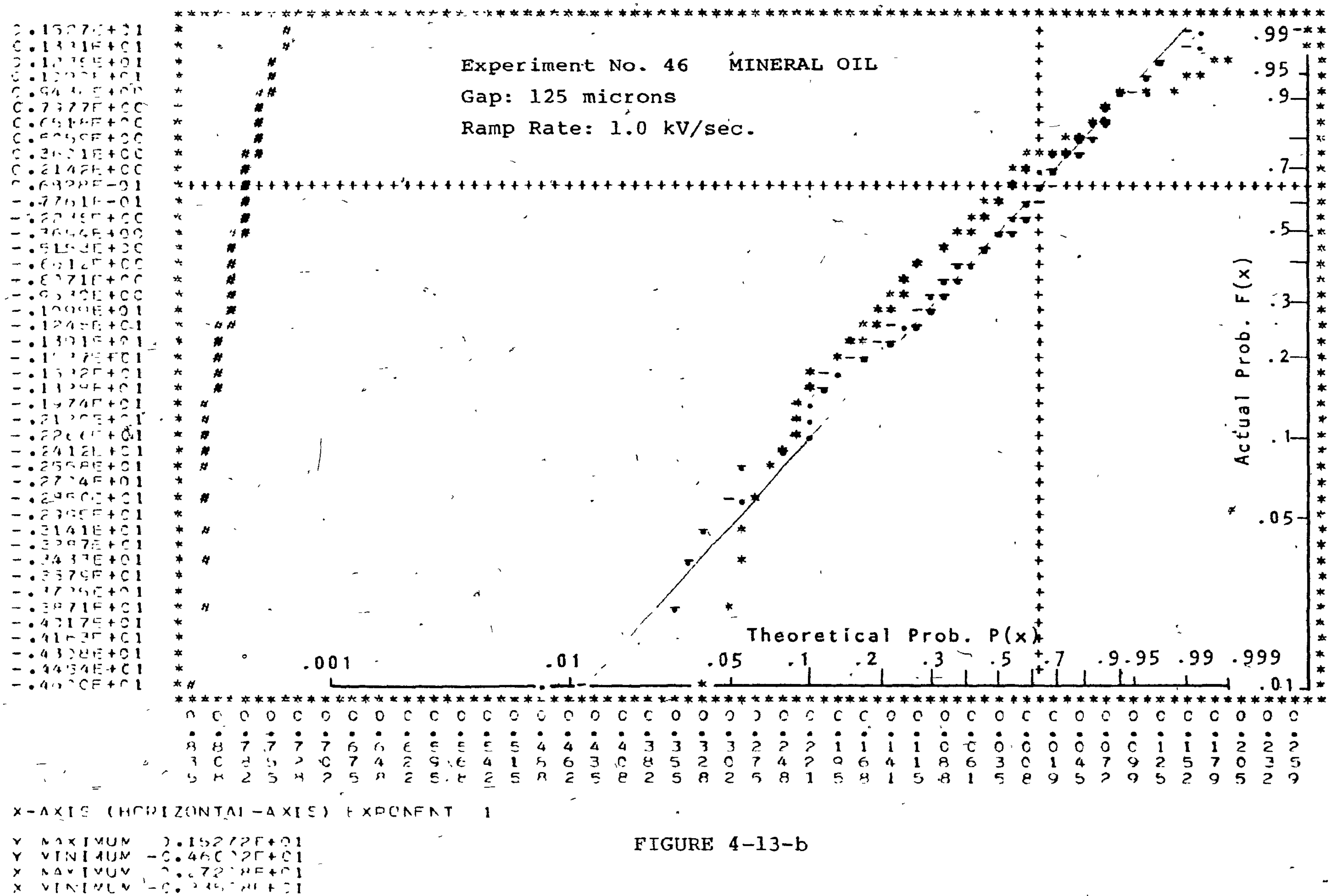
Experiment No. 46 MINERAL OIL
Gap: 125 microns
Ramp Rate: 1.0 kV/sec.
Actual Prob. F(x)
Theoretical Prob. P(x)
.001
.01
.05
.1
.2
.3
.5
.7
.9
.95
.99
.999
.01
.05
.1
.2
.3
.5
.7
.9
.95
.99
X-AXIS (HORIZONTAL-AXIS) EXPONENT 1
Y MAXIMUM 0.15272E+01
Y MINIMUM -0.460[illegible]E+01
X MAXIMUM [illegible]
X MINIMUM [illegible]

FIGURE 4-13-b

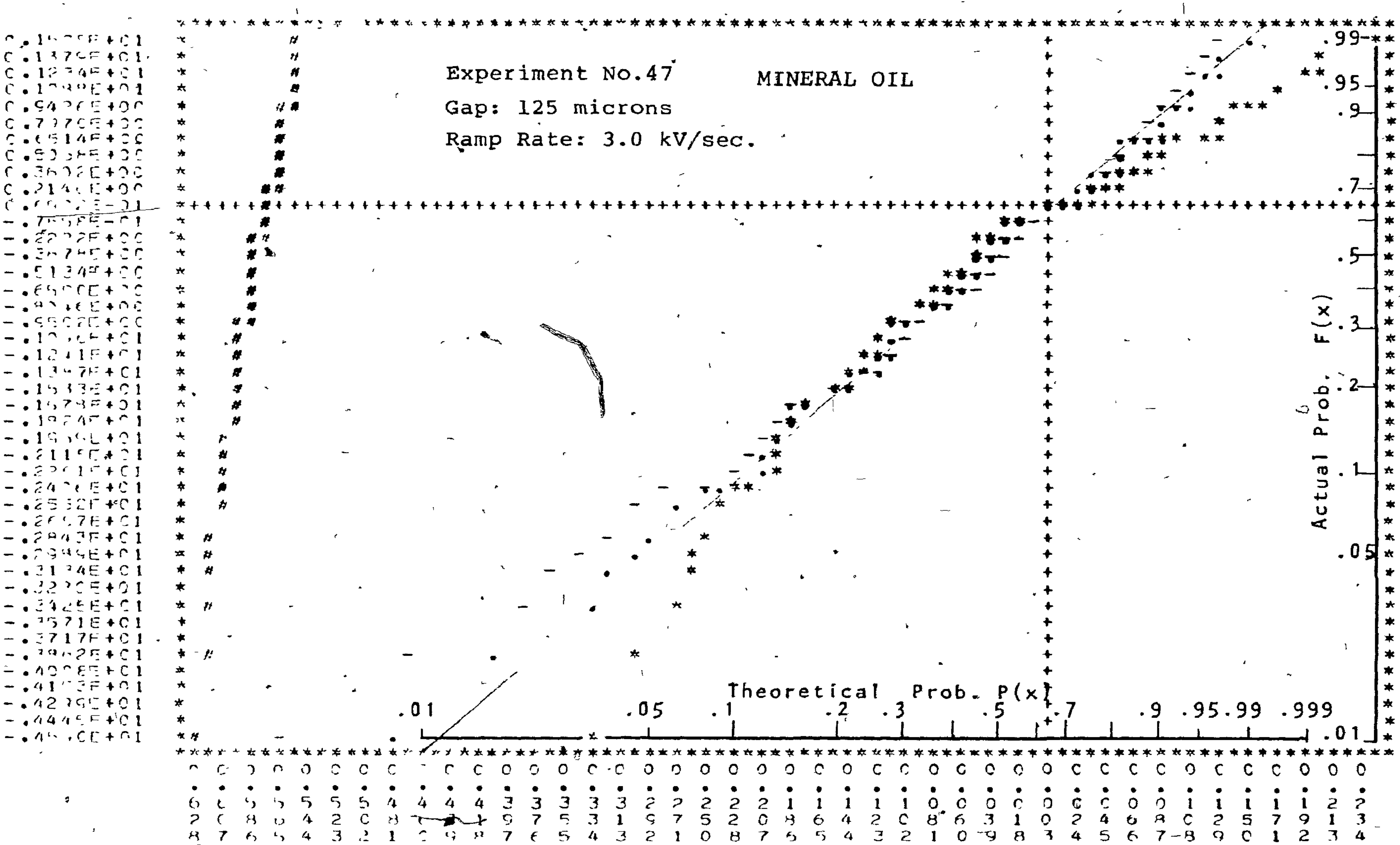

X-AXIS (HORIZONTAL-AXIS) EXPONENT 1

Y MAXIMUM 0.15250E+01
Y MINIMUM -0.45901E+01
X MAXIMUM 0.24431E+01
X MINIMUM -0.62775E+01

FIGURE 4-14-b

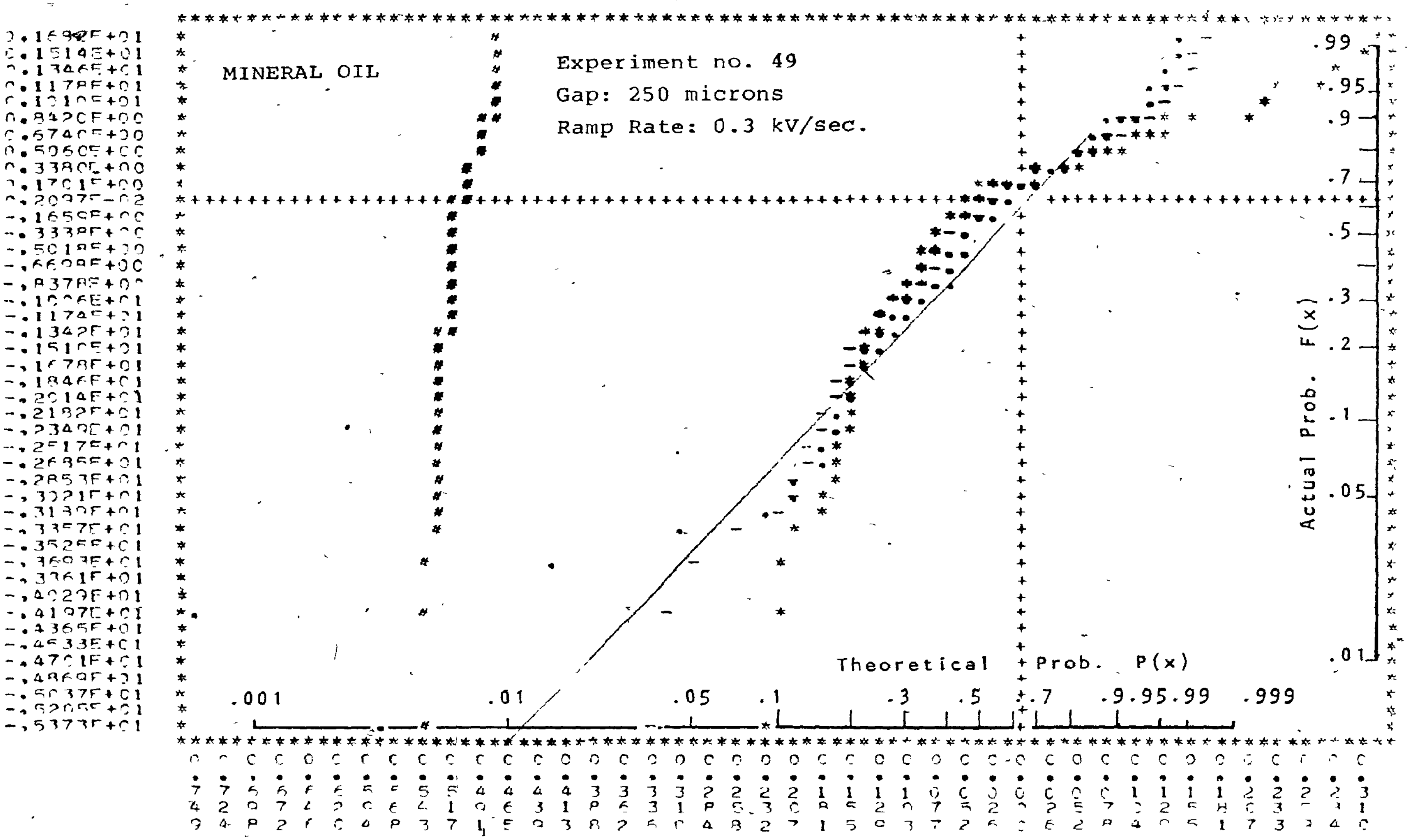

X-AXIS (HORIZONTAL-AXIS) EXPONENT 1

Y MAXIMUM 0.16918E+01
Y MINIMUM -0.53730E+01
X MAXIMUM 0.32319E+01
X MINIMUM -0.74942E+01

FIGURE 4-15-b

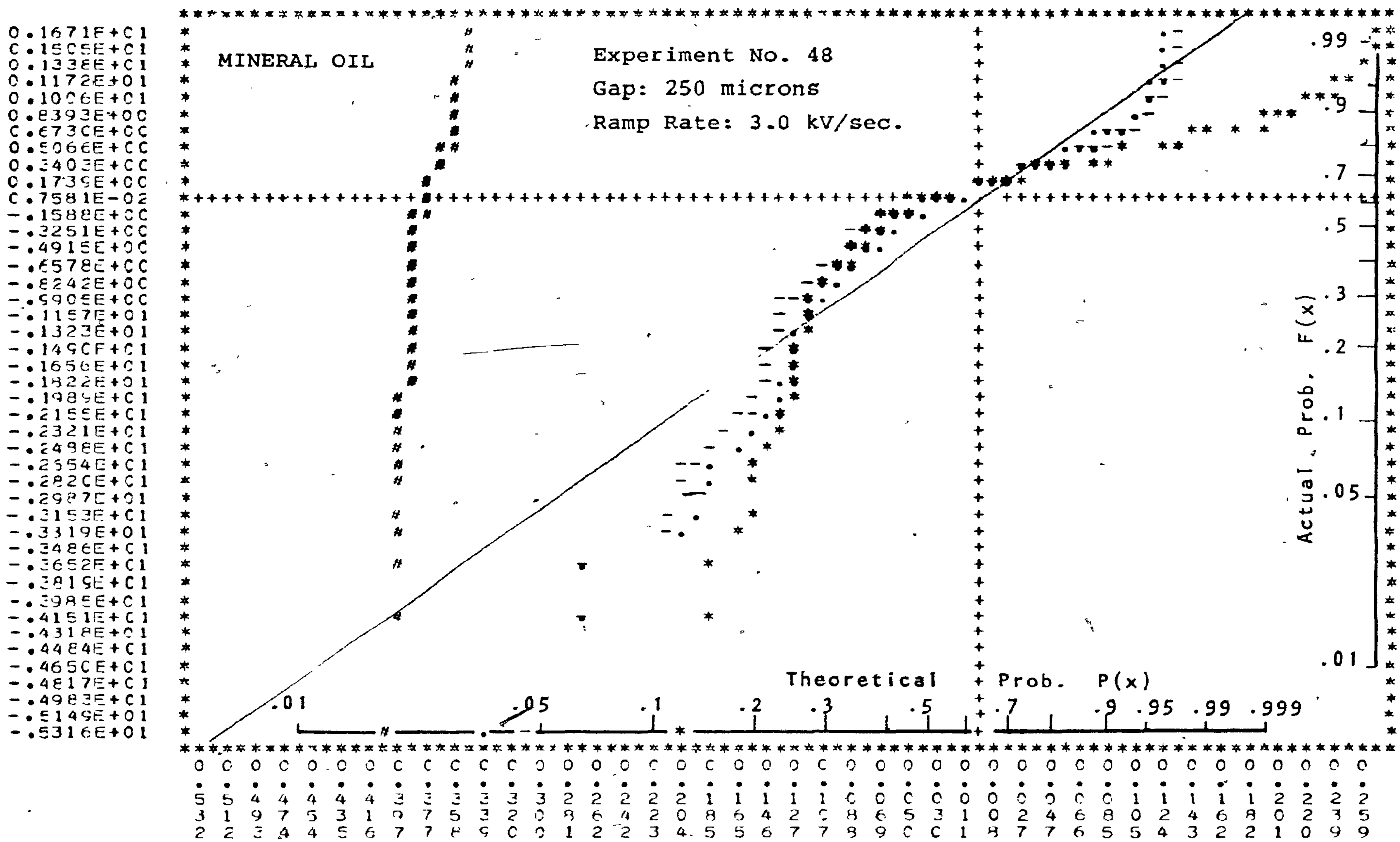

X-AXIS (HORIZONTAL-AXIS) EXPONENT 1

Y MAXIMUM 0.16711E+01
Y MINIMUM -0.53157E+01
X MAXIMUM 0.26840E+01
X MINIMUM -0.53157E+01

FIGURE 4-16-b

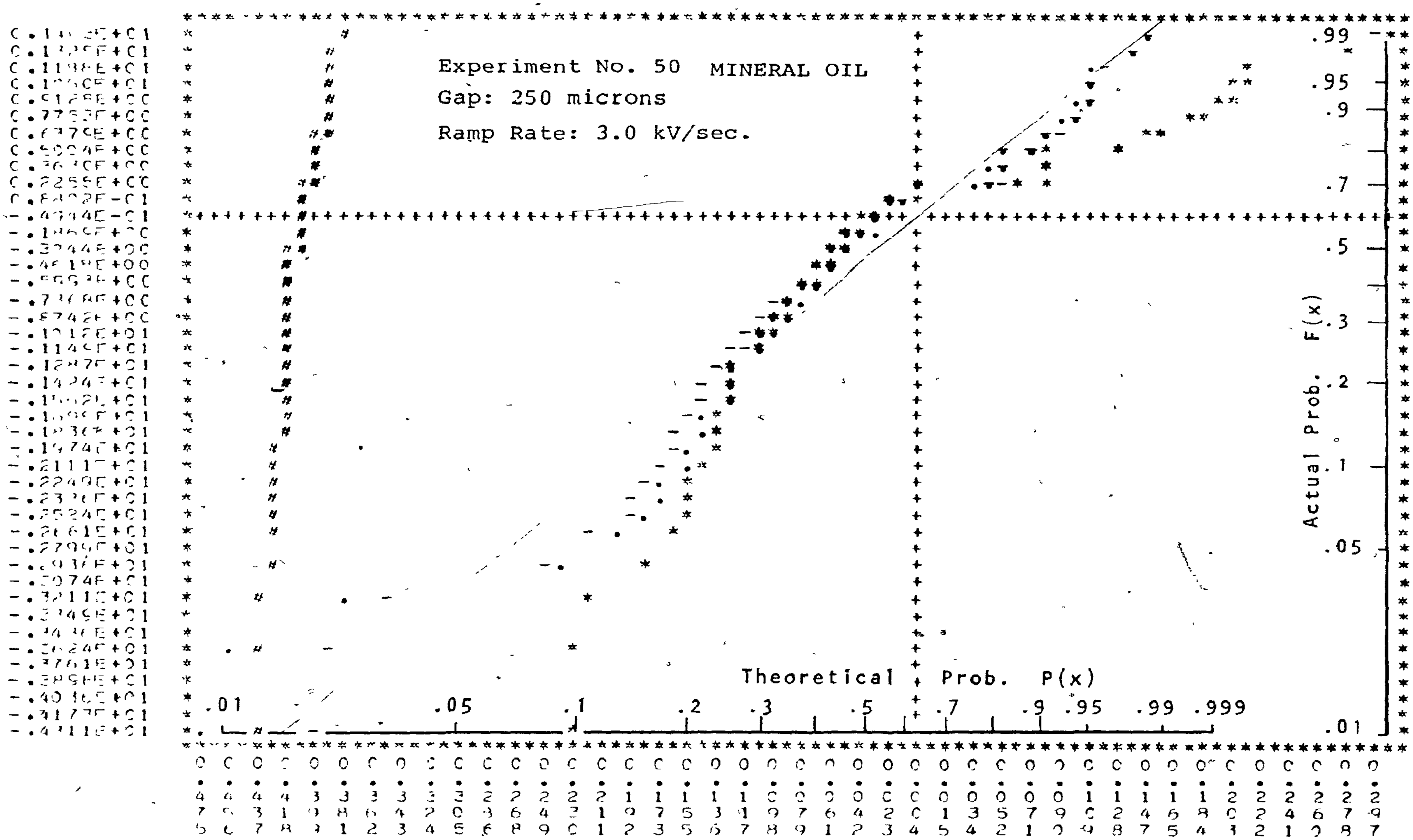

X-AXIS (HORIZONTAL-AXIS) EXPONENT 1

Y MAXIMUM 0.14627E+01
Y MINIMUM -0.43110E+01
X MAXIMUM 0.27657E+01
X MINIMUM -0.47466E+01

FIGURE 4-17-b

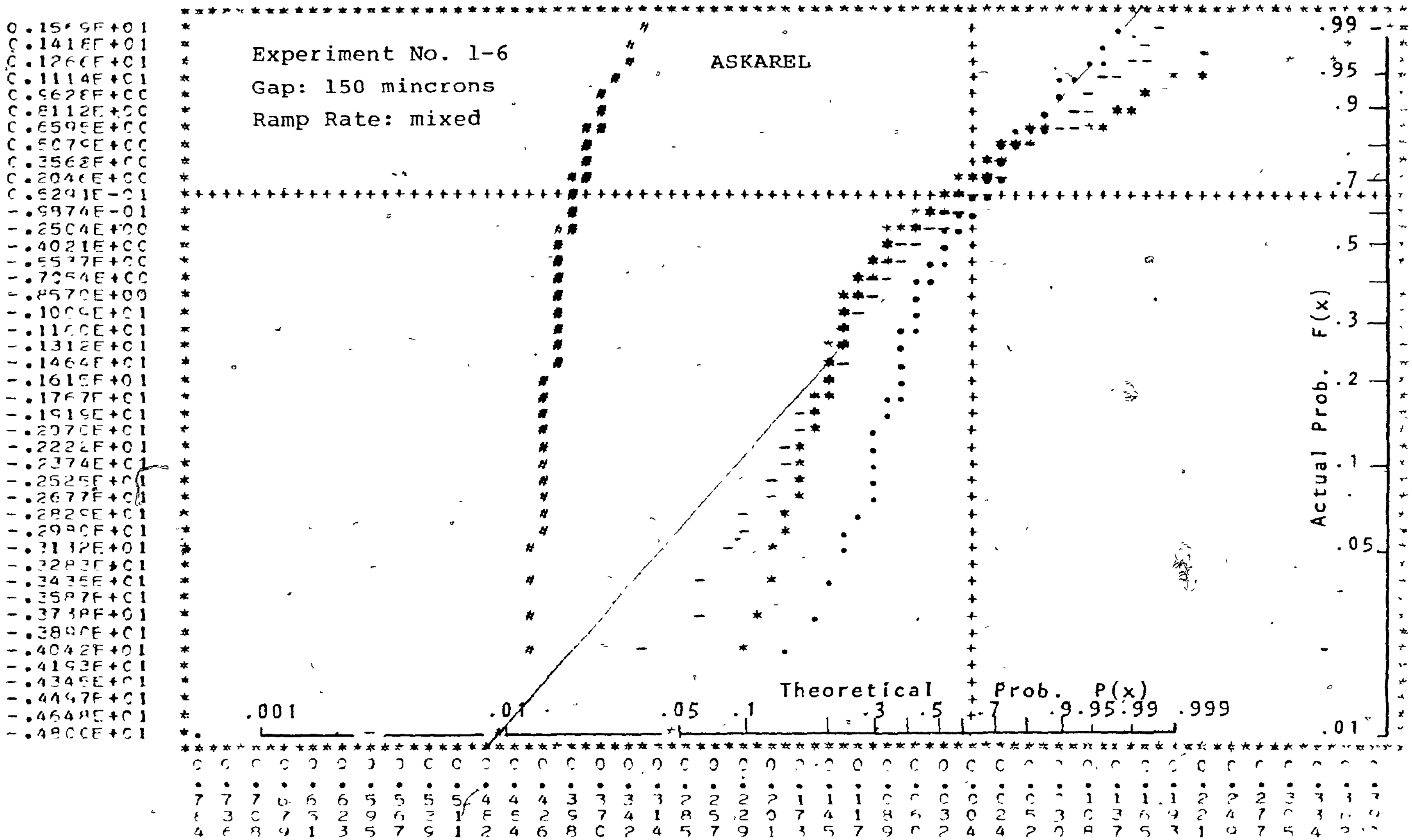

X-AXIS (HORIZONTAL-AXIS) EXPONENT 1.

Y MAXIMUM 0.15695E+01
Y MINIMUM -0.48000E+01
X MAXIMUM 0.40386E+01
X MINIMUM -0.76382E+01

FIGURE 4-18-b

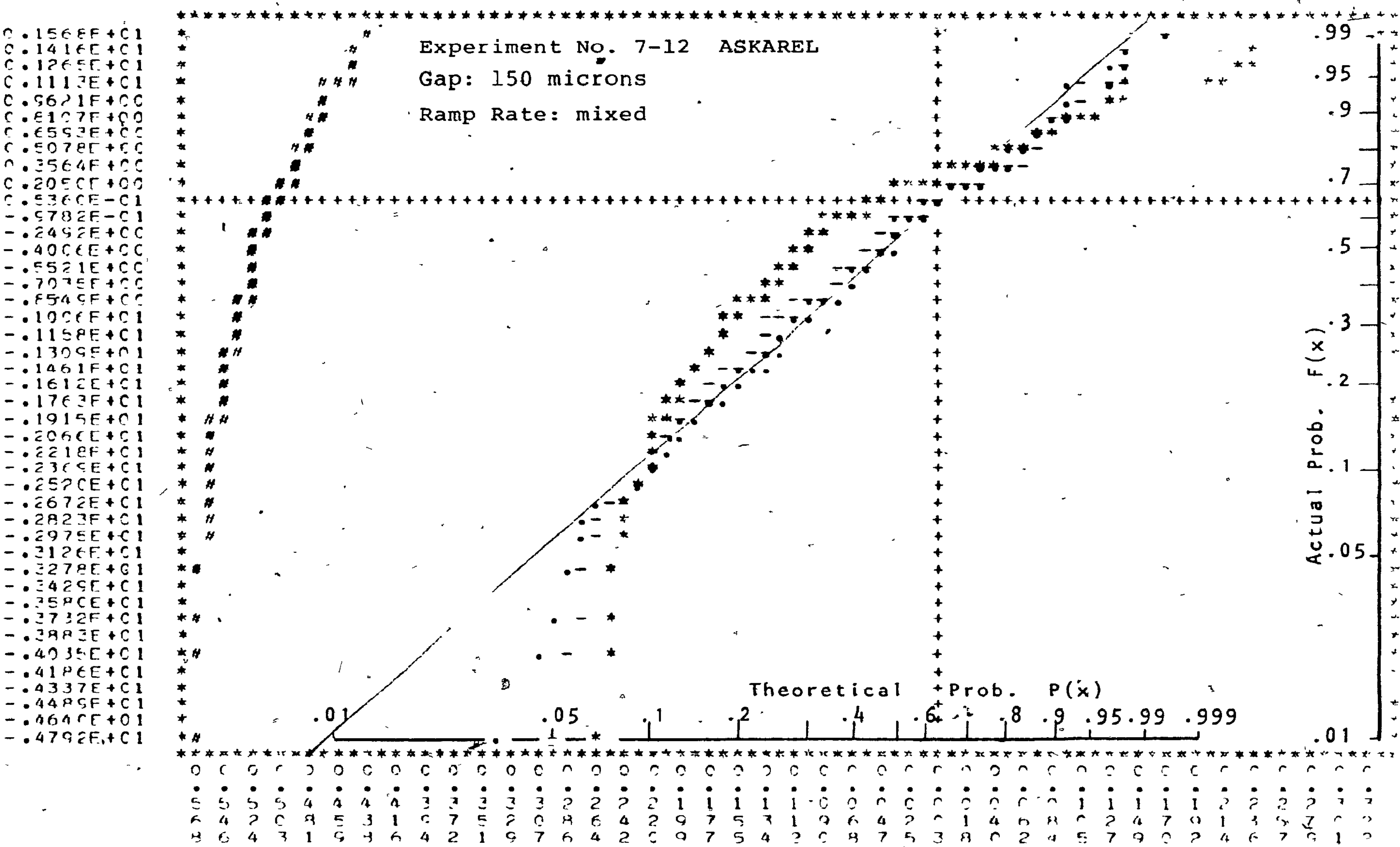

X-AXIS (HORIZONTAL-AXIS) EXPONENT 1

Y MAXIMUM 0.15677E+01
Y MINIMUM -0.47917E+01
X MAXIMUM 0.33323E+01
X MINIMUM -0.56702E+01

FIGURE 4-19-b

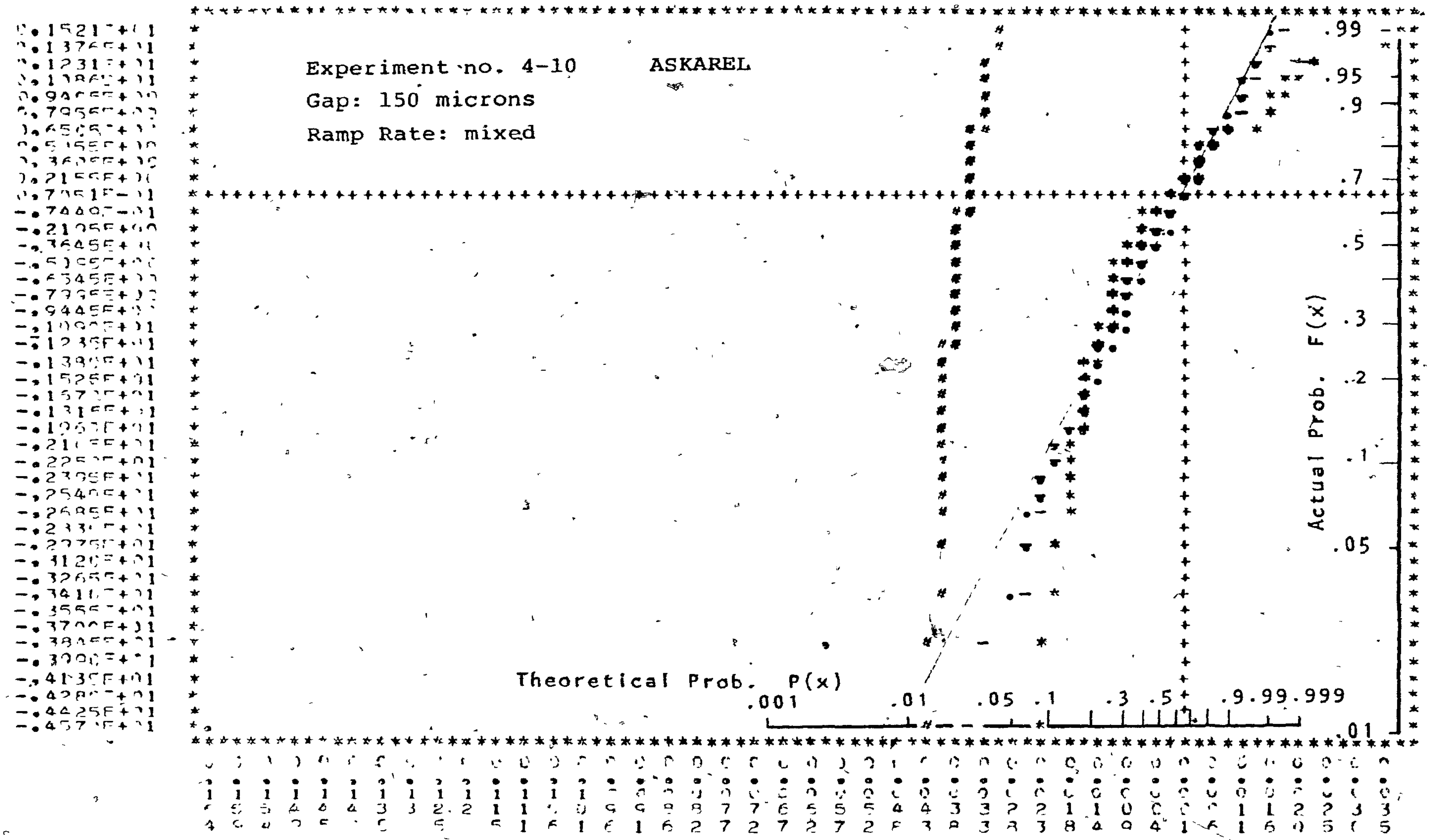

X-AXIS (HORIZONTAL-AXIS) EXPONENT 2

Y MAXIMUM 0.15205E+ 1
Y MINIMUM -0.4[illegible]E+01
X MAXIMUM [illegible]0.37351[illegible]E+01
X MINIMUM -0.164[illegible]E+02

FIGURE 4-20-b

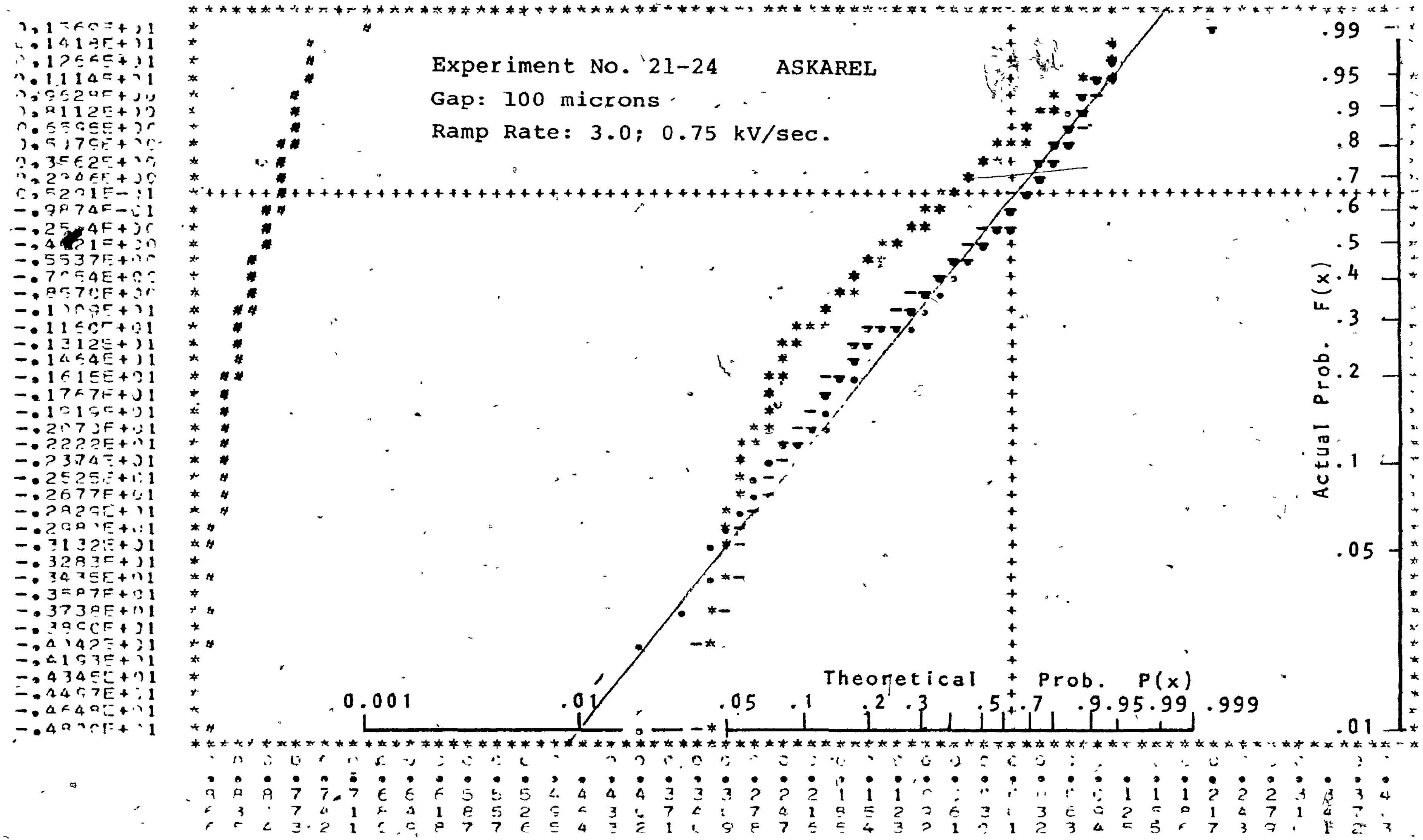

X-AXIS (HORIZONTAL-AXIS) EXPONENT 1

Y MAXIMUM 0.15695E+01
Y MINIMUM -0.4880CE+01
X MAXIMUM 0.41863E+01
X MINIMUM -0.88611E+01

FIGURE 4-21-b

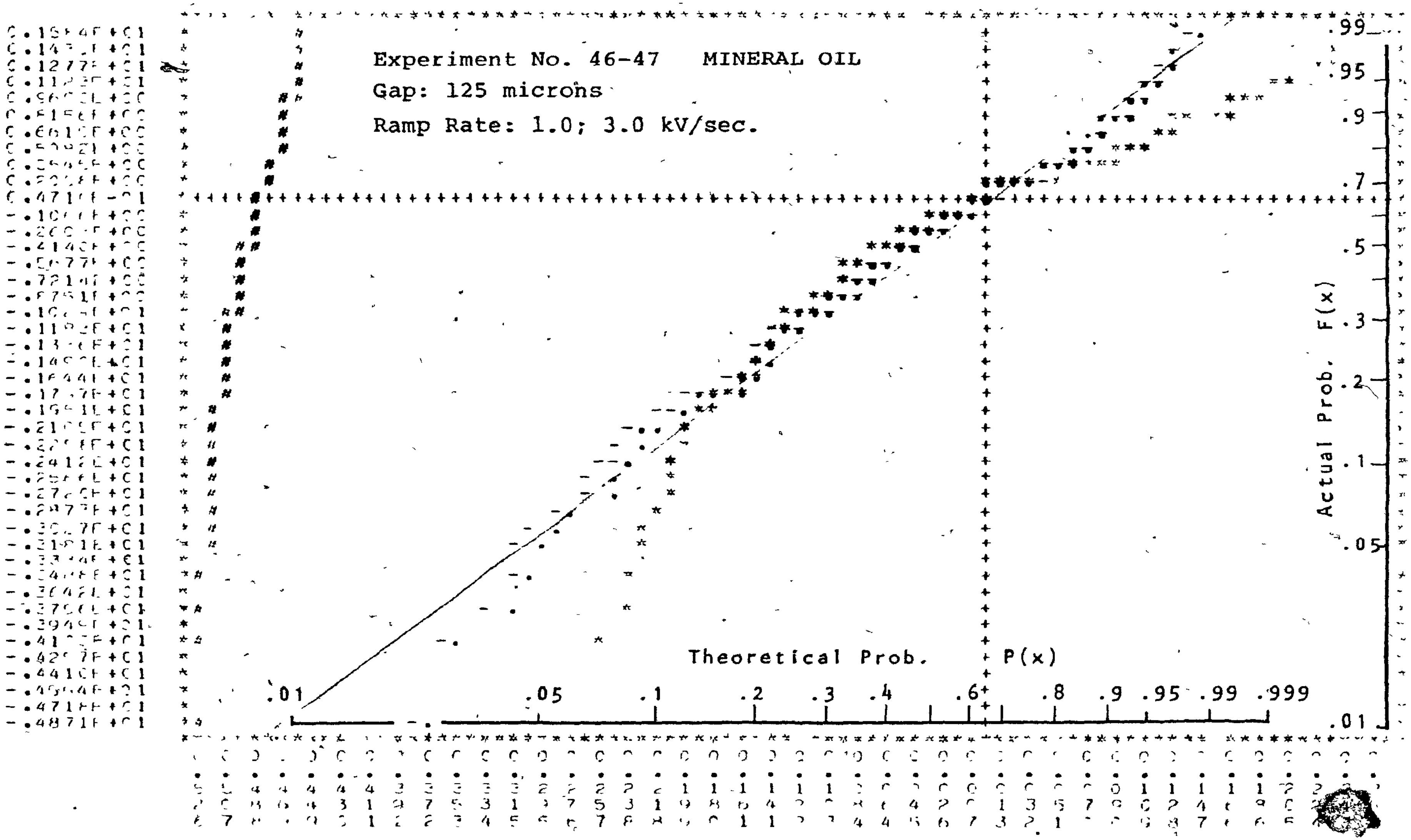

X-AXIS (HORIZONTAL-AXIS) EXPONENT 1

Y MAXIMUM [illegible]
Y MINIMUM [illegible]
X MAXIMUM [illegible]
X MINIMUM [illegible]

FIGURE 4-22-b

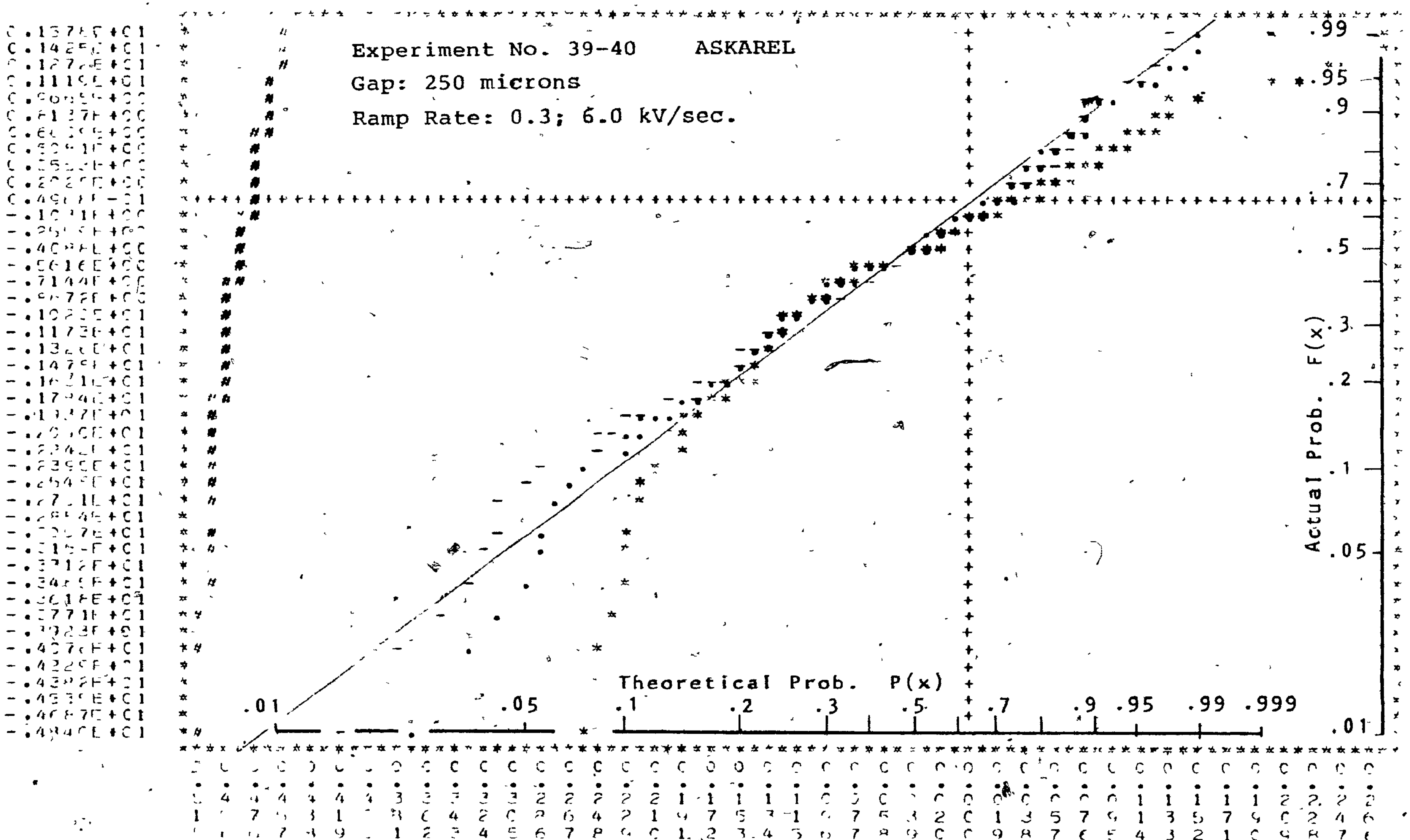

X-AXIS [illegible] EXPONENT 1

Y MAXIMUM [illegible]
Y MINIMUM [illegible]
X MAXIMUM [illegible]
X MINIMUM [illegible]

FIGURE 4-23-b

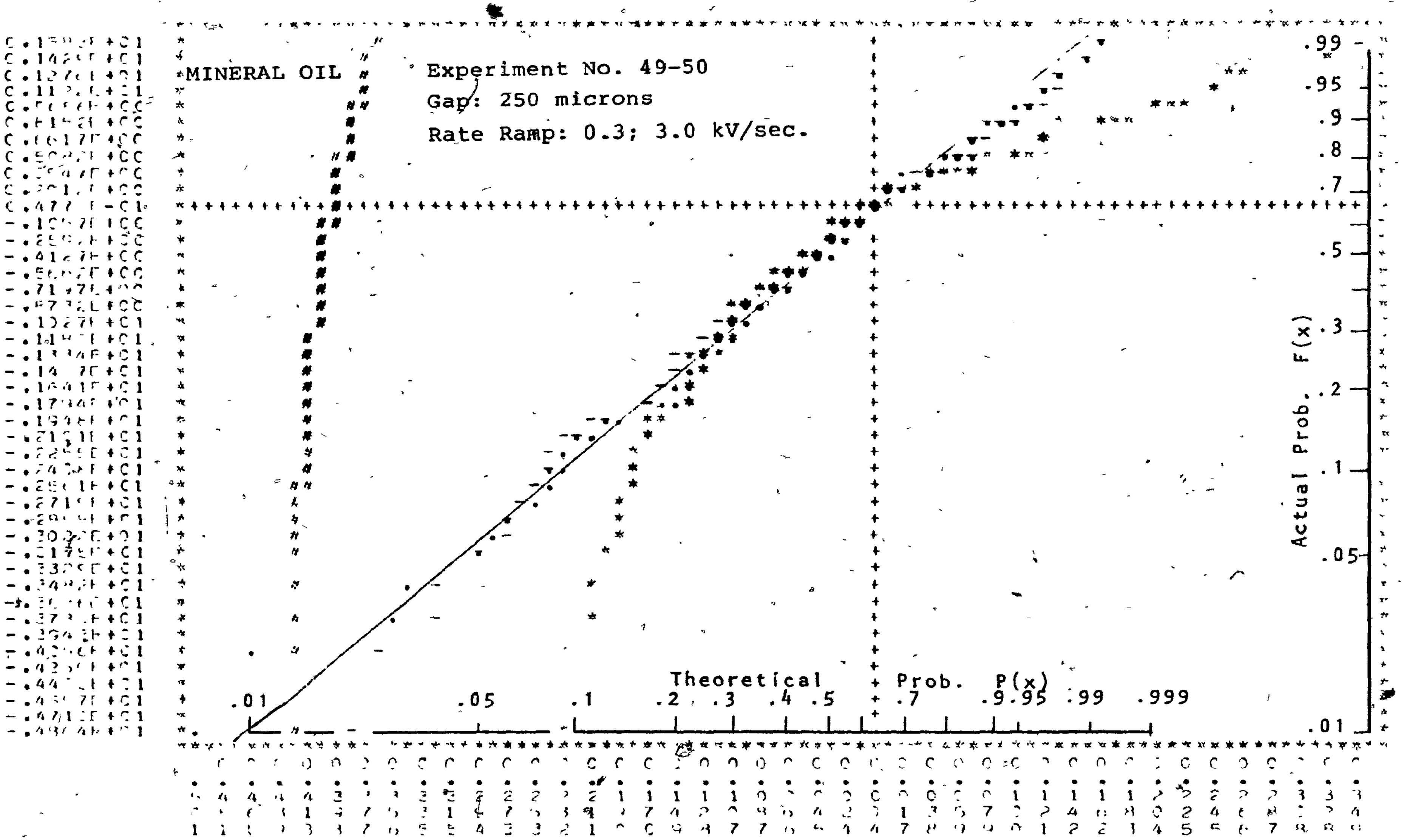

MINERAL OIL
Experiment No. 49-50
Gap: 250 microns
Rate Ramp: 0.3; 3.0 kV/sec.
Theoretical Prob. P(x)
.01
.05
.1
.2
.3
.4
.5
.7
.9
.95
.99
.999
Actual Prob. F(x)
.99
.95
.9
.8
.7
.5
.3
.2
.1
.05
.01

FIGURE 4-24-b

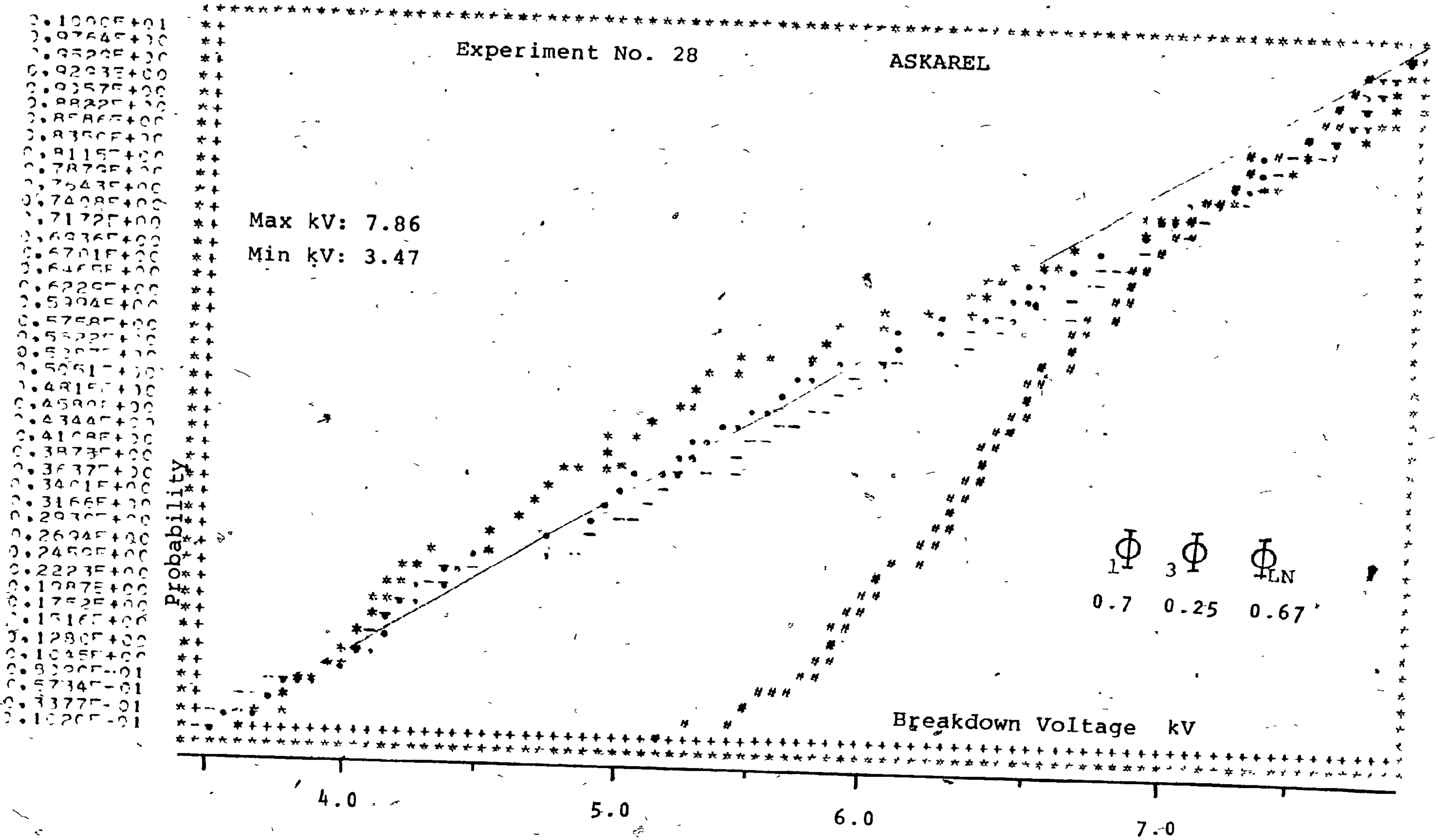
Experiment No. 28
ASKAREL
Max kV: 7.86
Min kV: 3.47
Probability
Breakdown Voltage kV
4.0
5.0
6.0
7.0
$_1\Phi$ $_3\Phi$ Φ_{LN}
0.7 0.25 0.67

FIGURE 4-8-c

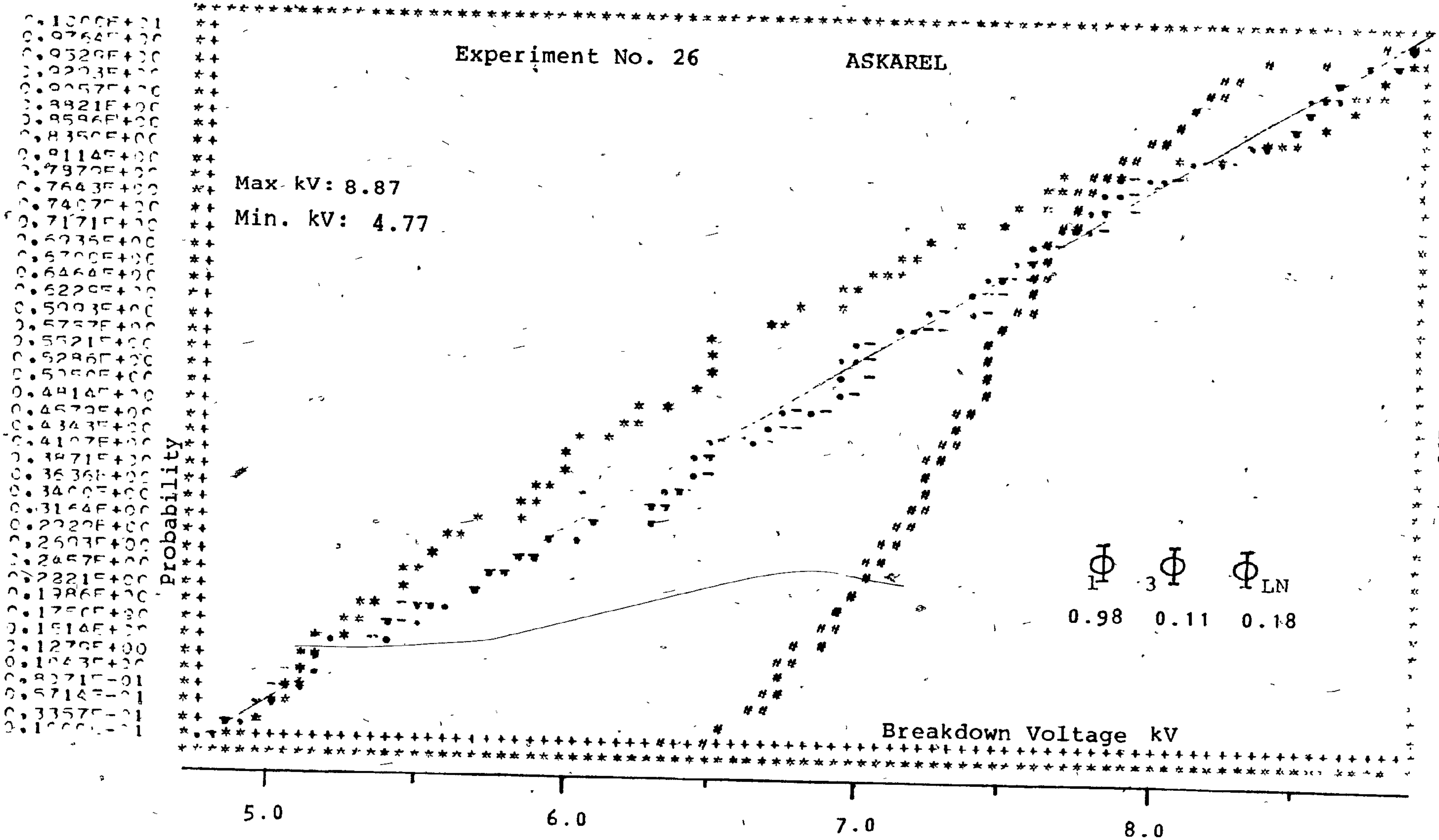
Experiment No. 26
ASKAREL
Max kV: 8.87
Min. kV: 4.77
Probability
Breakdown Voltage kV
5.0
6.0
7.0
8.0
$_1\Phi$ $_3\Phi$ Φ_{LN}
0.98 0.11 0.18

FIGURE 4-9-c

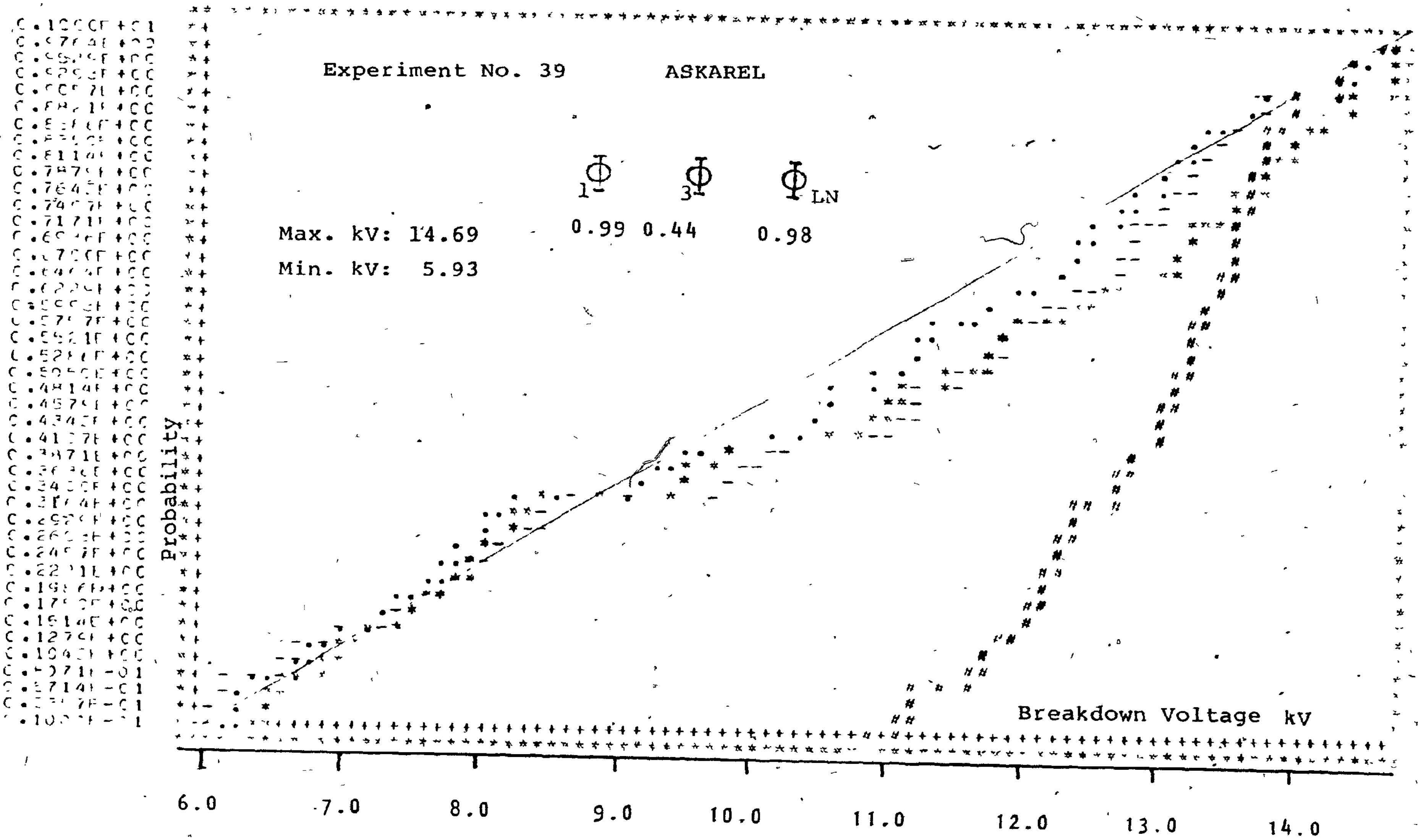

Experiment No. 39
ASKAREL
$_1\Phi$ $_3\Phi$ Φ_{LN}
0.99 0.44 0.98
Max. kV: 14.69
Min. kV: 5.93
Probability
Breakdown Voltage kV
6.0
7.0
8.0
9.0
10.0
11.0
12.0
13.0
14.0

FIGURE 4-10-c

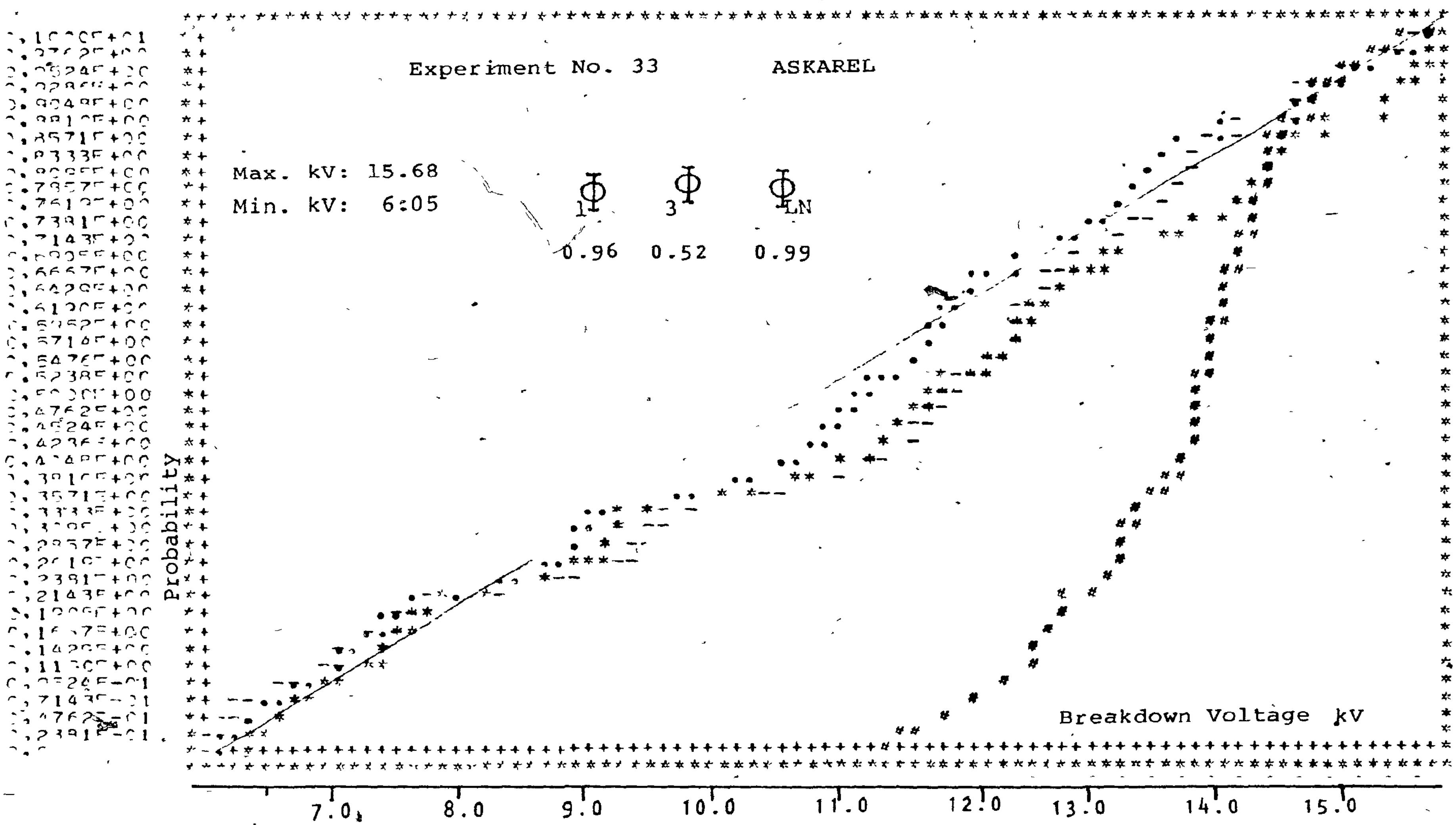
Experiment No. 33
ASKAREL
Max. kV: 15.68
Min. kV: 6:05
Φ_1 0.96
Φ_3 0.52
Φ_{LN} 0.99
Probability
Breakdown Voltage kV
7.0
8.0
9.0
10.0
11.0
12.0
13.0
14.0
15.0

FIGURE 4-11-c

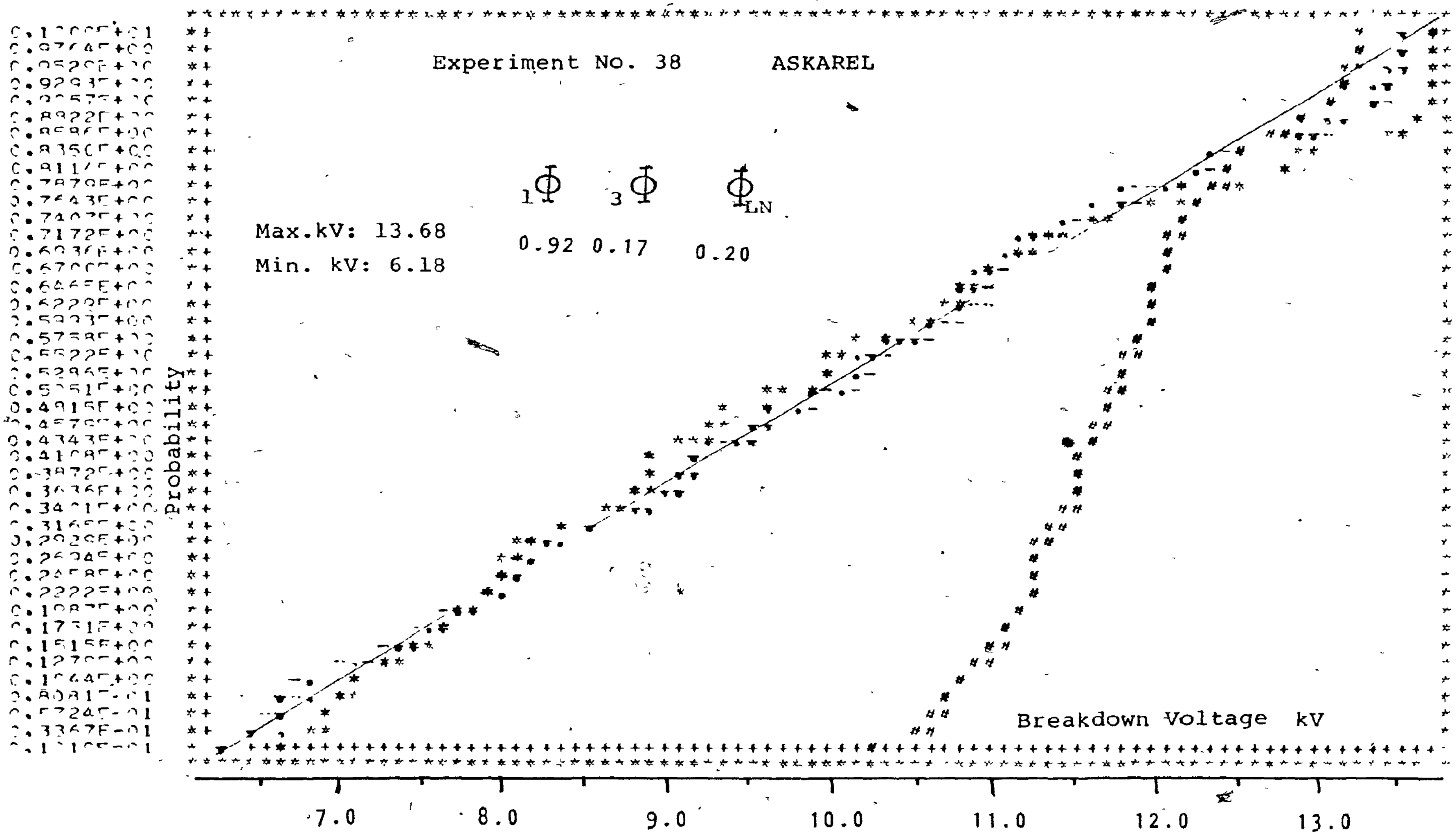
Experiment No. 38
ASKAREL
Max.kV: 13.68
Min. kV: 6.18
$_1\Phi$ $_3\Phi$ Φ_{LN}
0.92 0.17 0.20
Probability
Breakdown Voltage kV
7.0
8.0
9.0
10.0
11.0
12.0
13.0

FIGURE 4-12-c

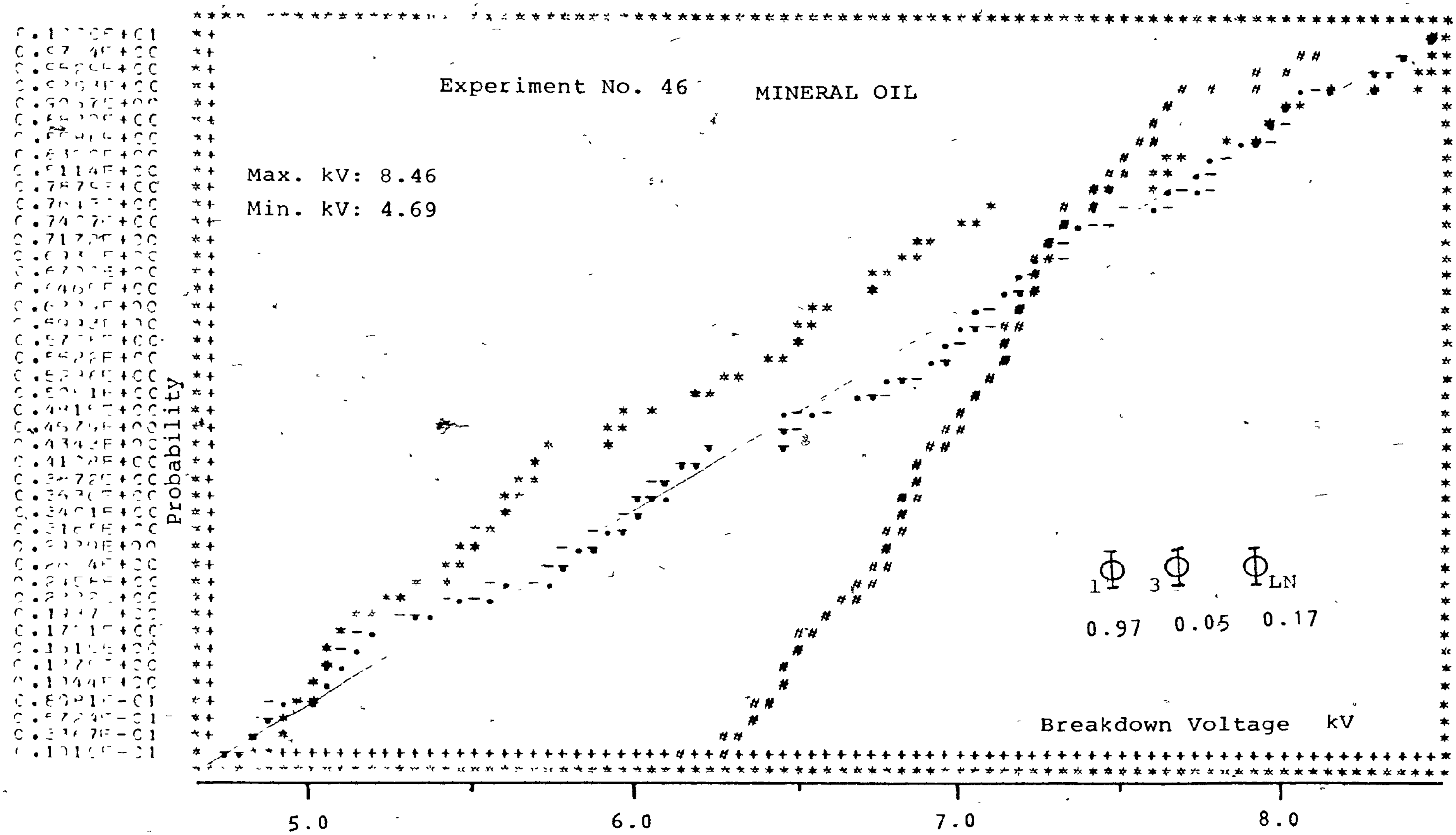
Experiment No. 46
MINERAL OIL
Max. kV: 8.46
Min. kV: 4.69
Probability
$_1\Phi$ $_3\Phi$ Φ_{LN}
0.97 0.05 0.17
Breakdown Voltage kV
5.0
6.0
7.0
8.0

FIGURE 4-13-c

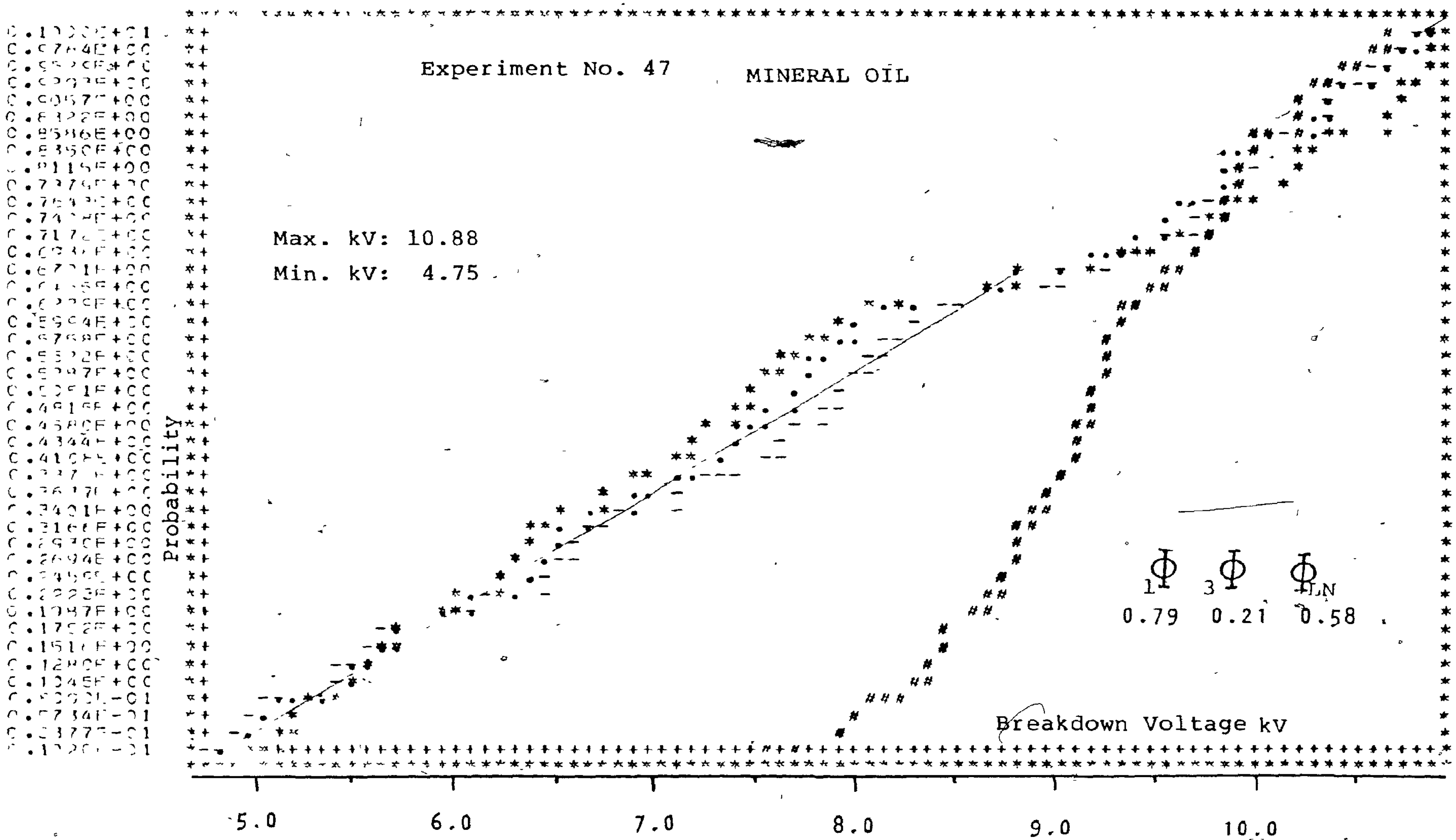
Experiment No. 47
MINERAL OIL
Max. kV: 10.88
Min. kV: 4.75
Probability
Φ1 Φ3 ΦLN
0.79 0.21 0.58
Breakdown Voltage kV
5.0
6.0
7.0
8.0
9.0
10.0

FIGURE 4-14-c

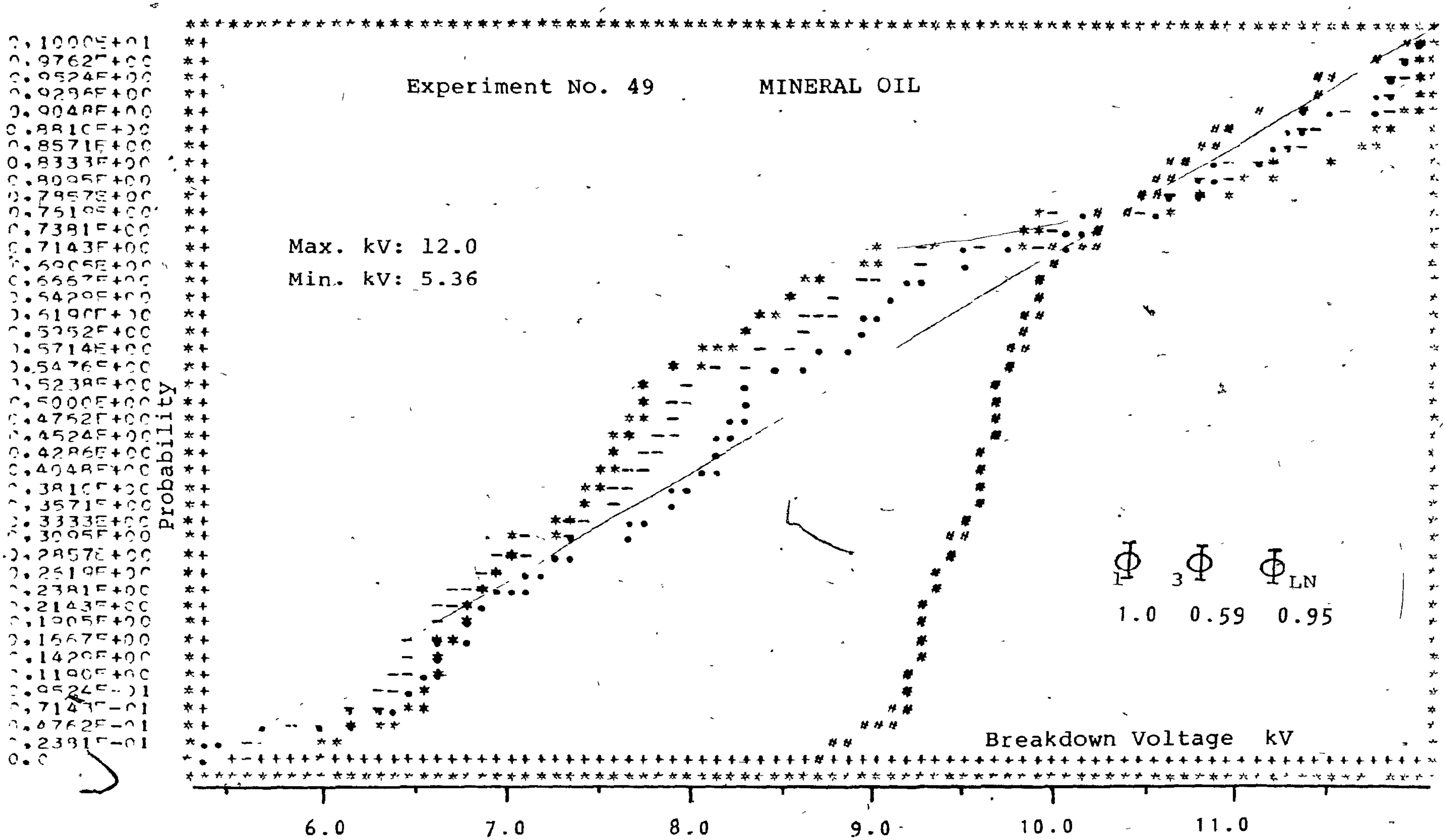
Experiment No. 49
MINERAL OIL
Max. kV: 12.0
Min. kV: 5.36
Probability
Breakdown Voltage kV
Φ_1 $_3\Phi$ Φ_{LN}
1.0 0.59 0.95
6.0
7.0
8.0
9.0
10.0
11.0

FIGURE 4-15-c

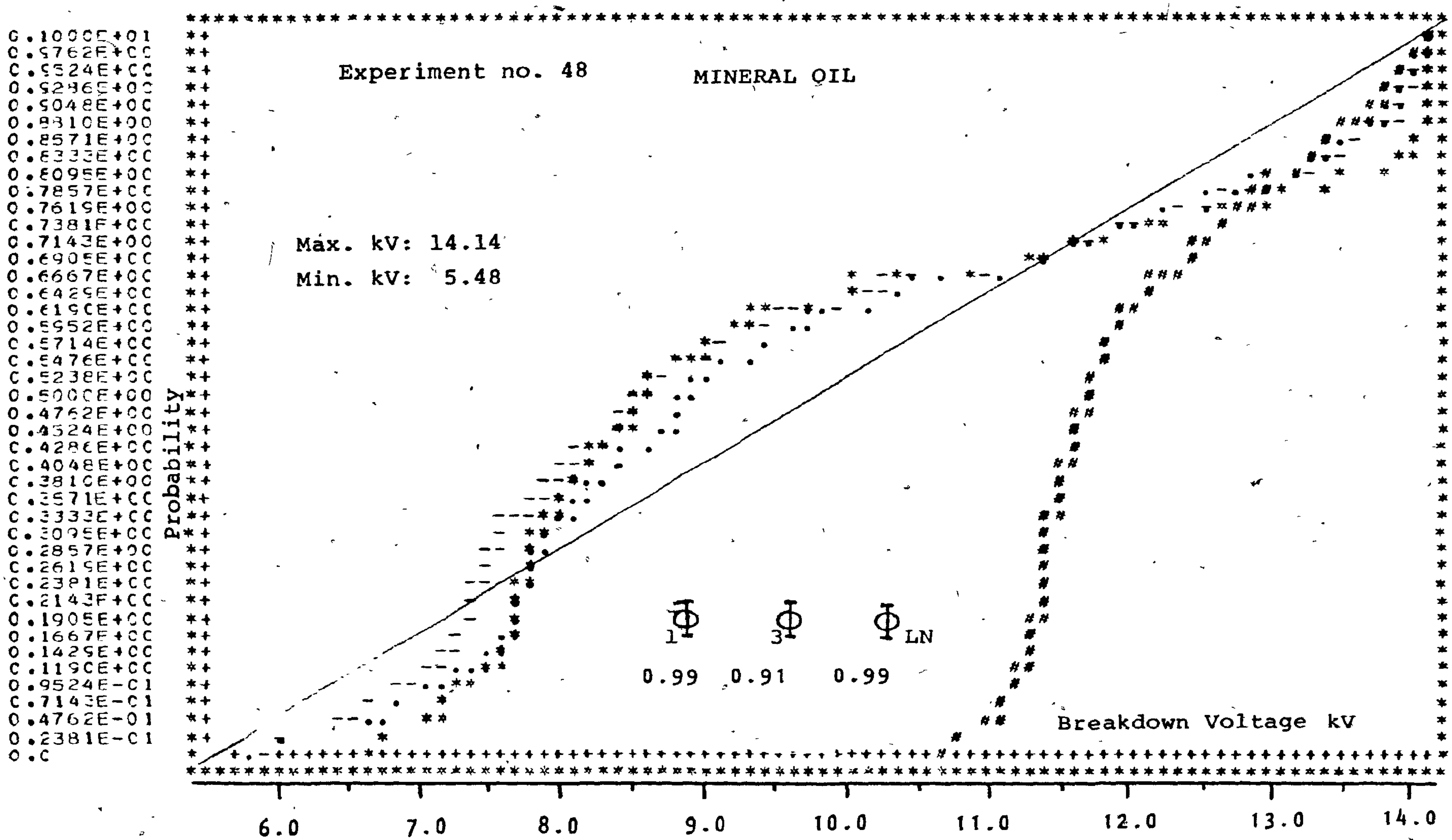

Experiment no. 48
MINERAL OIL
Max. kV: 14.14
Min. kV: 5.48
0.1000E+01
0.9762E+00
0.9524E+00
0.9286E+00
0.9048E+00
0.8810E+00
0.8571E+00
0.8333E+00
0.8095E+00
0.7857E+00
0.7619E+00
0.7381E+00
0.7143E+00
0.6905E+00
0.6667E+00
0.6429E+00
0.6190E+00
0.5952E+00
0.5714E+00
0.5476E+00
0.5238E+00
0.5000E+00
0.4762E+00
0.4524E+00
0.4286E+00
0.4048E+00
0.3810E+00
0.3571E+00
0.3333E+00
0.3095E+00
0.2857E+00
0.2619E+00
0.2381E+00
0.2143E+00
0.1905E+00
0.1667E+00
0.1429E+00
0.1190E+00
0.9524E-01
0.7143E-01
0.4762E-01
0.2381E-01
0.0
Probability
Φ_1 Φ_3 Φ_{LN}
0.99 0.91 0.99
Breakdown Voltage kV
6.0
7.0
8.0
9.0
10.0
11.0
12.0
13.0
14.0

FIGURE 4-16-c

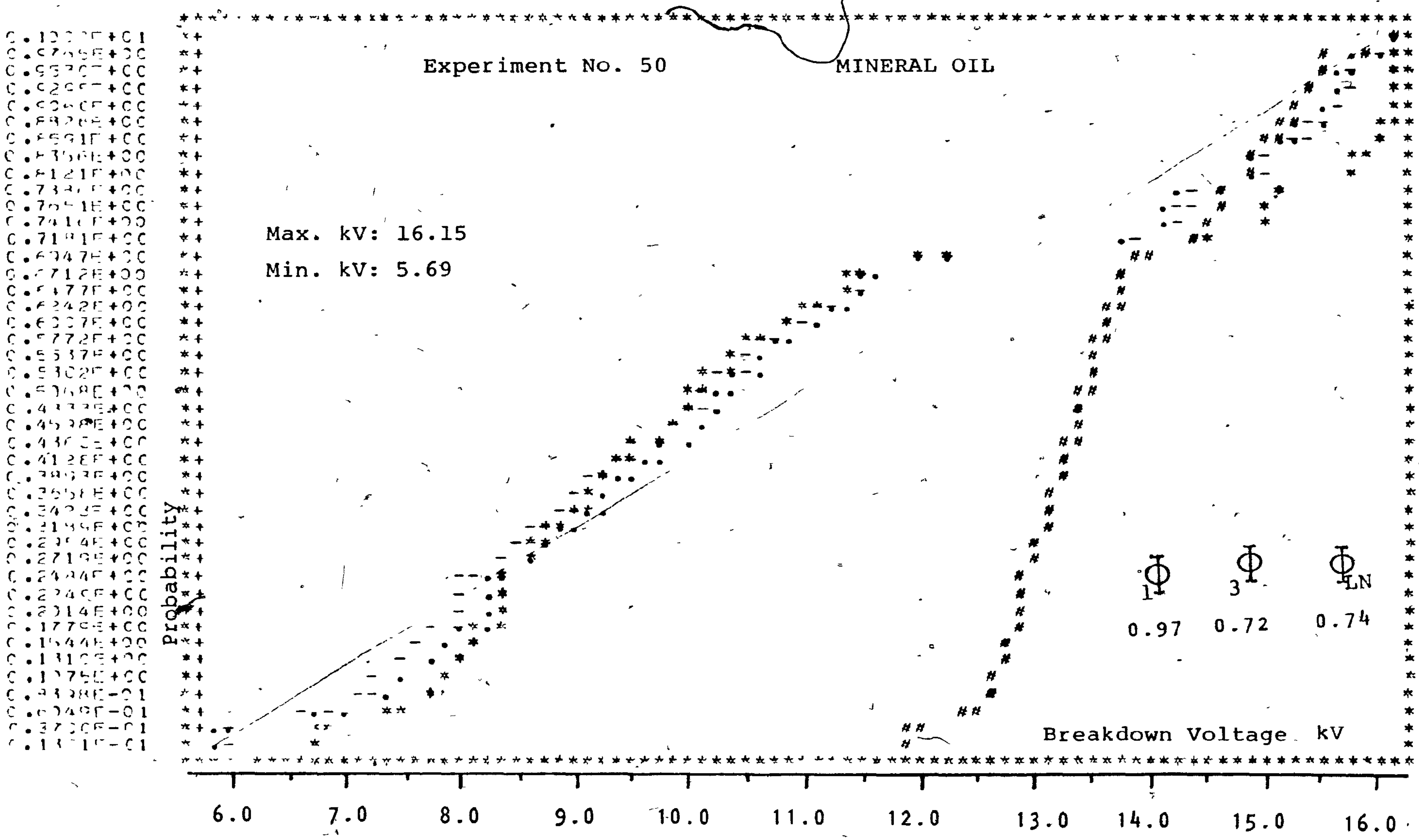
Experiment No. 50
MINERAL OIL
Max. kV: 16.15
Min. kV: 5.69
Probability
Breakdown Voltage kV
6.0
7.0
8.0
9.0
10.0
11.0
12.0
13.0
14.0
15.0
16.0
Φ_1
Φ_3
Φ_{LN}
0.97
0.72
0.74

FIGURE 4-17-c

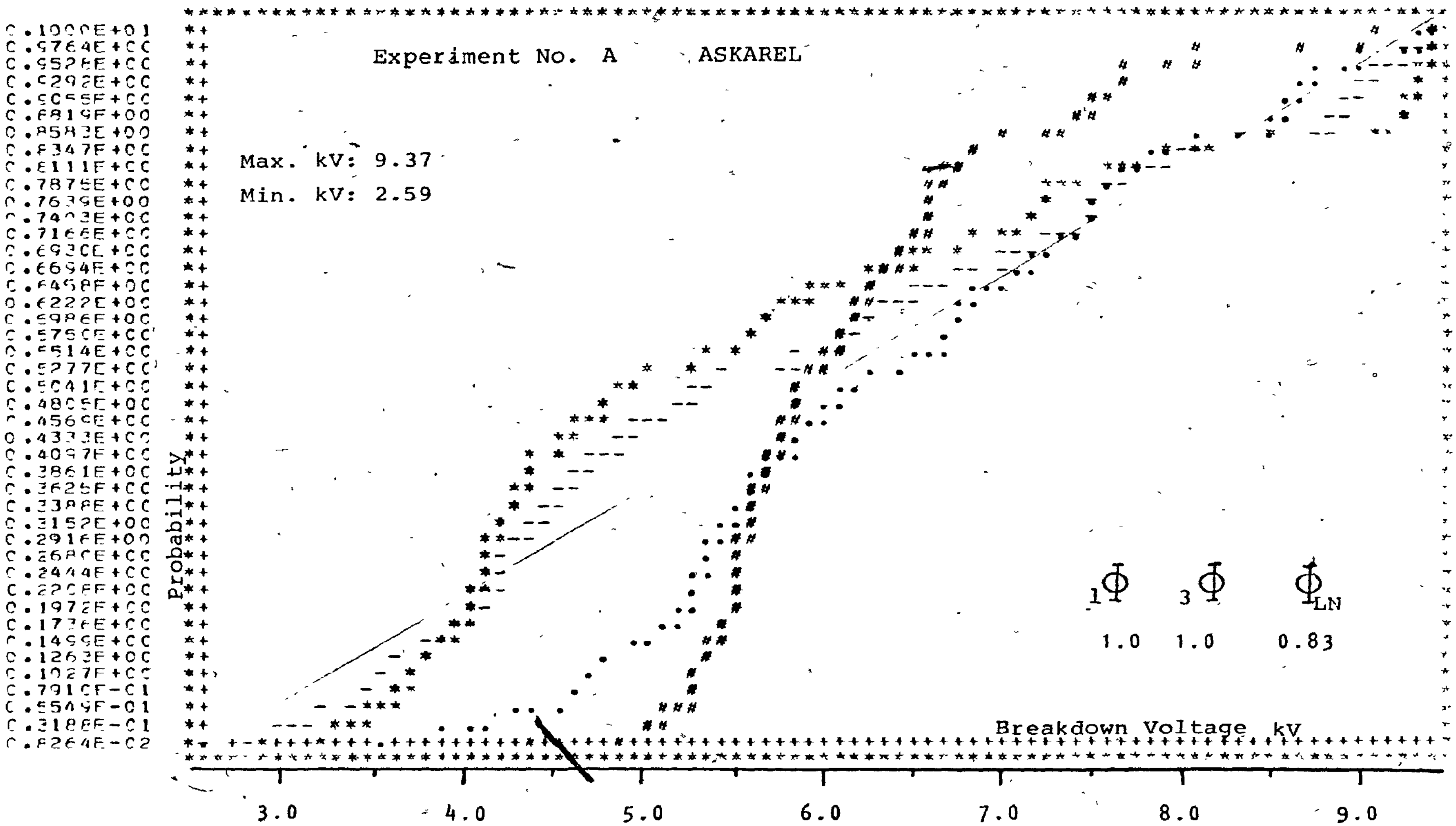
Experiment No. A ASKAREL
Max. kV: 9.37
Min. kV: 2.59
Probability
Breakdown Voltage kV
$_1\Phi$ $_3\Phi$ Φ_{LN}
1.0 1.0 0.83
3.0
4.0
5.0
6.0
7.0
8.0
9.0

FIGURE 4-18-c

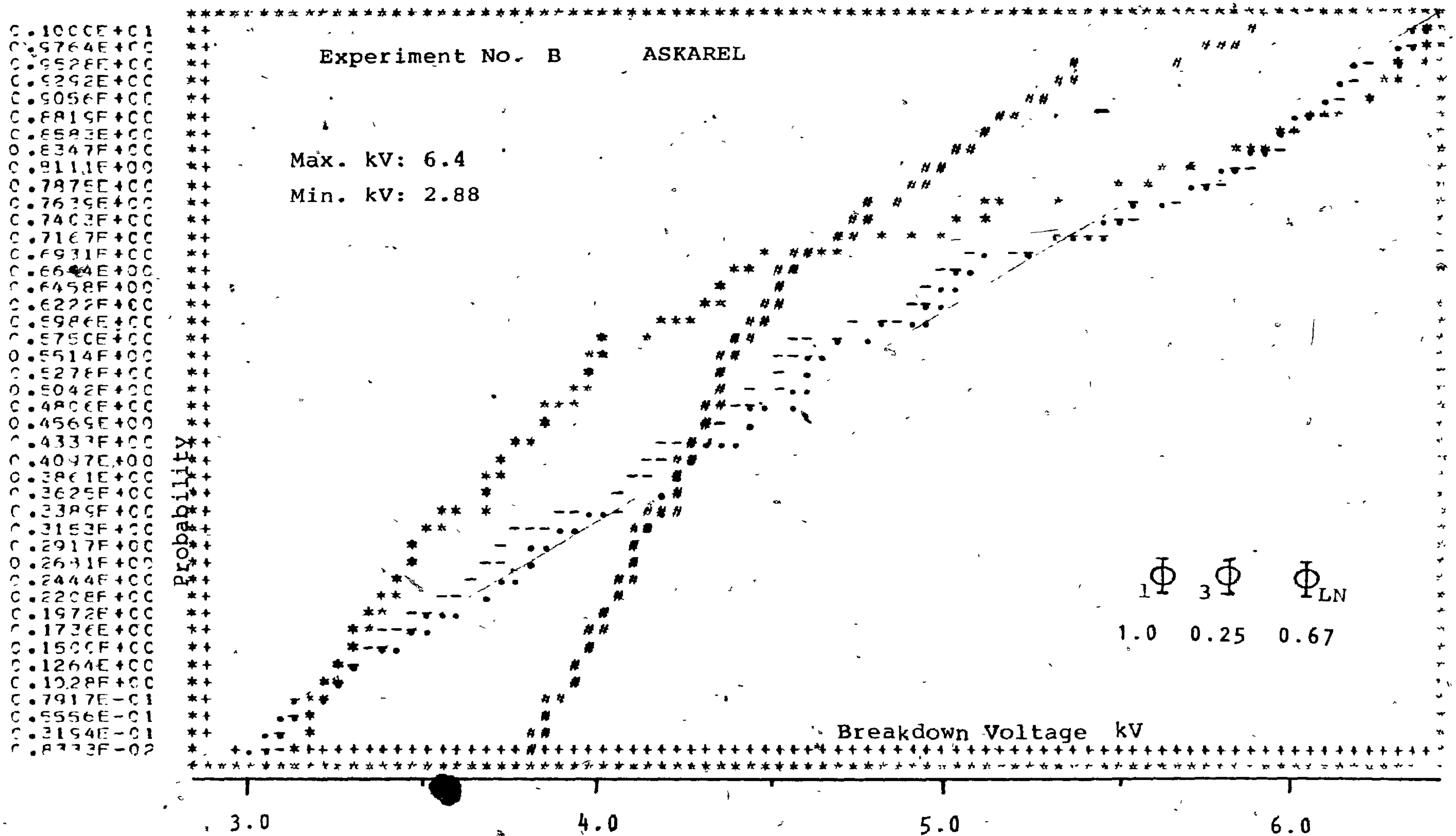
Experiment No. B
ASKAREL
Max. kV: 6.4
Min. kV: 2.88
Probability
Breakdown Voltage kV
3.0
4.0
5.0
6.0
$_1\Phi$ $_3\Phi$ Φ_{LN}
1.0 0.25 0.67

FIGURE 4-19-c

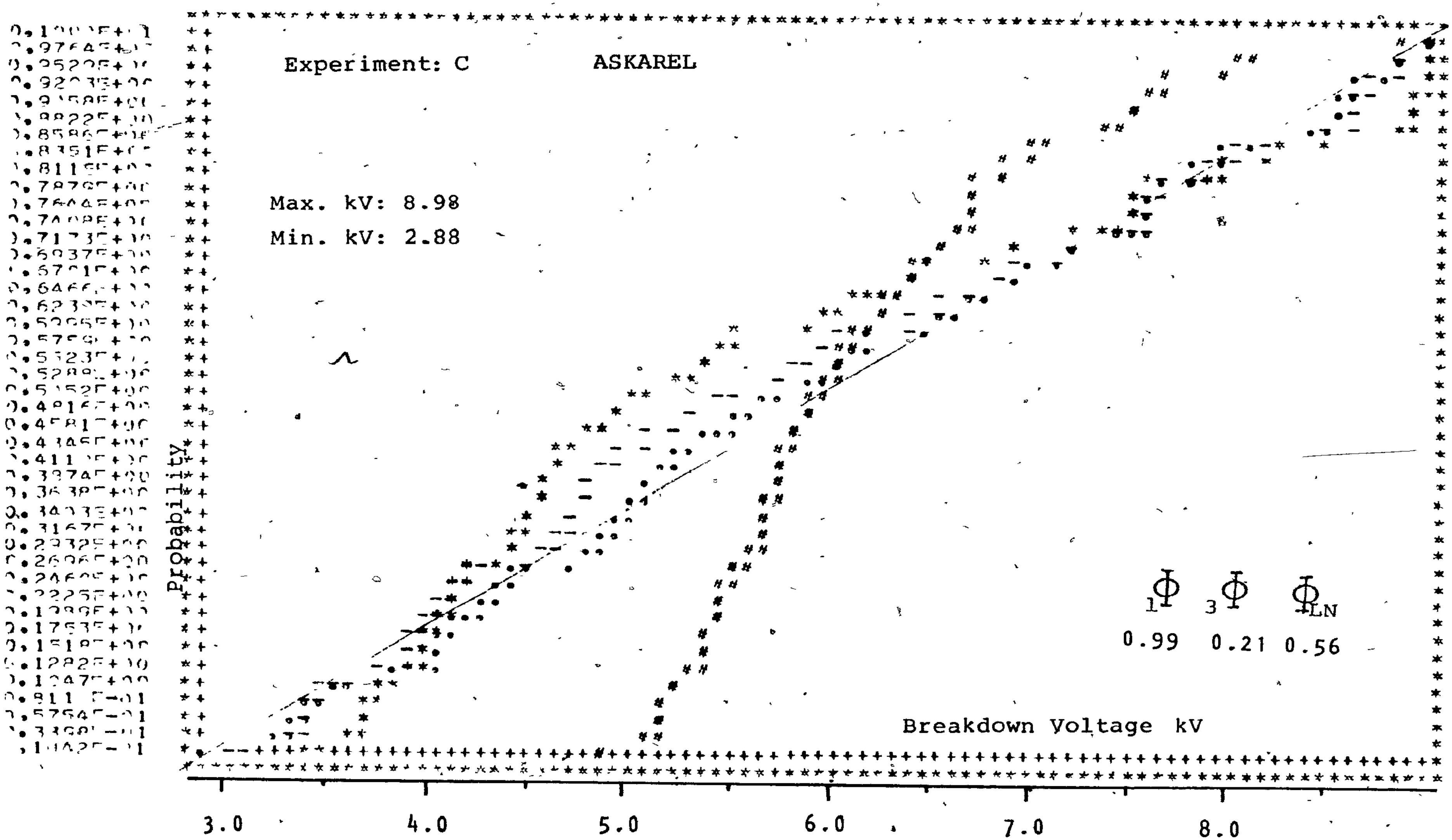
Experiment: C
ASKAREL
Max. kV: 8.98
Min. kV: 2.88
Probability
$_1\Phi$ $_3\Phi$ Φ_{LN}
0.99 0.21 0.56
Breakdown Voltage kV
3.0
4.0
5.0
6.0
7.0
8.0

FIGURE 4-20-c

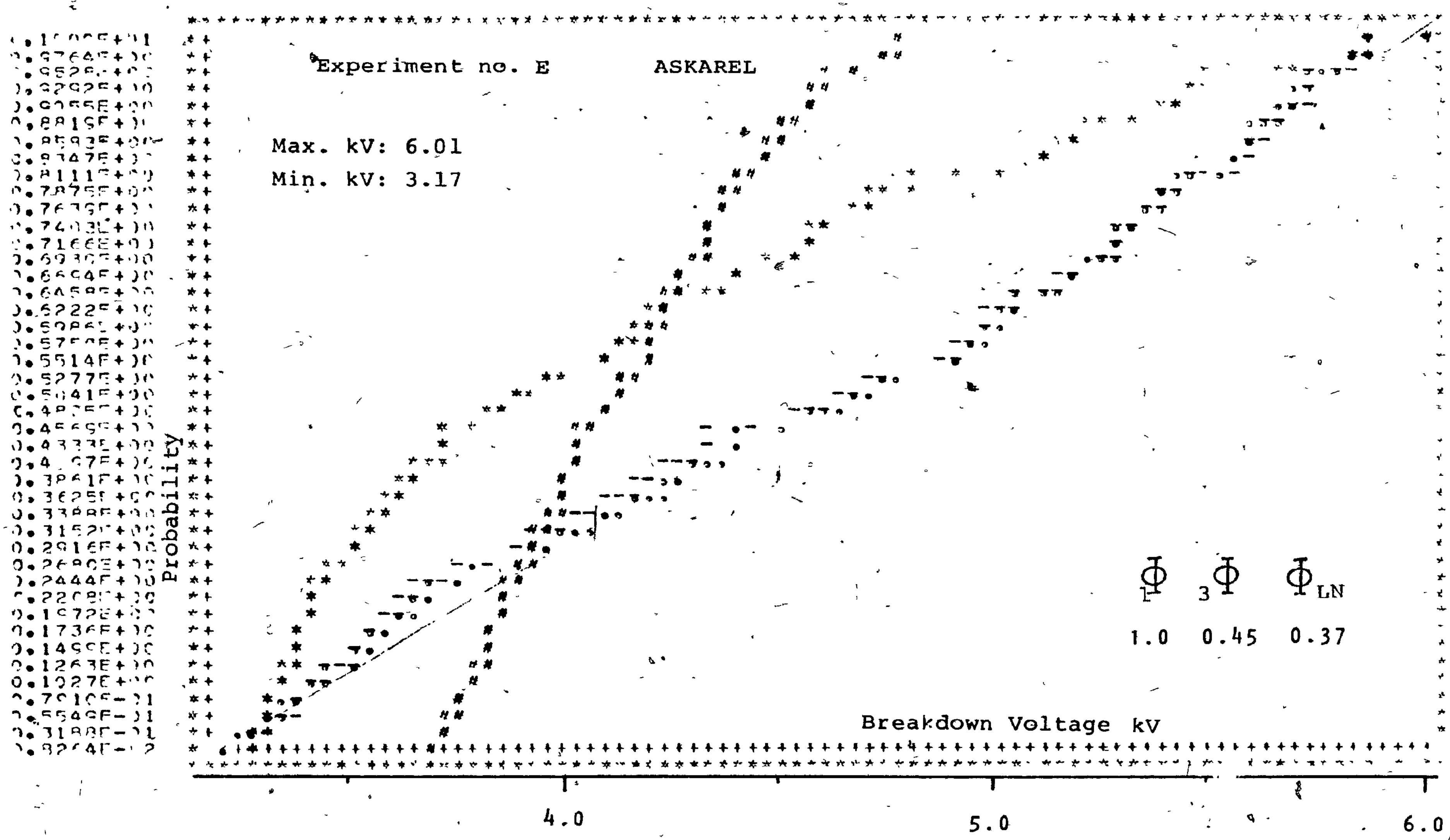
Experiment no. E
ASKAREL
Max. kV: 6.01
Min. kV: 3.17
Probability
Breakdown Voltage kV
4.0
5.0
6.0
Φ_1 $_3\Phi$ Φ_{LN}
1.0 0.45 0.37

FIGURE 4-21-c

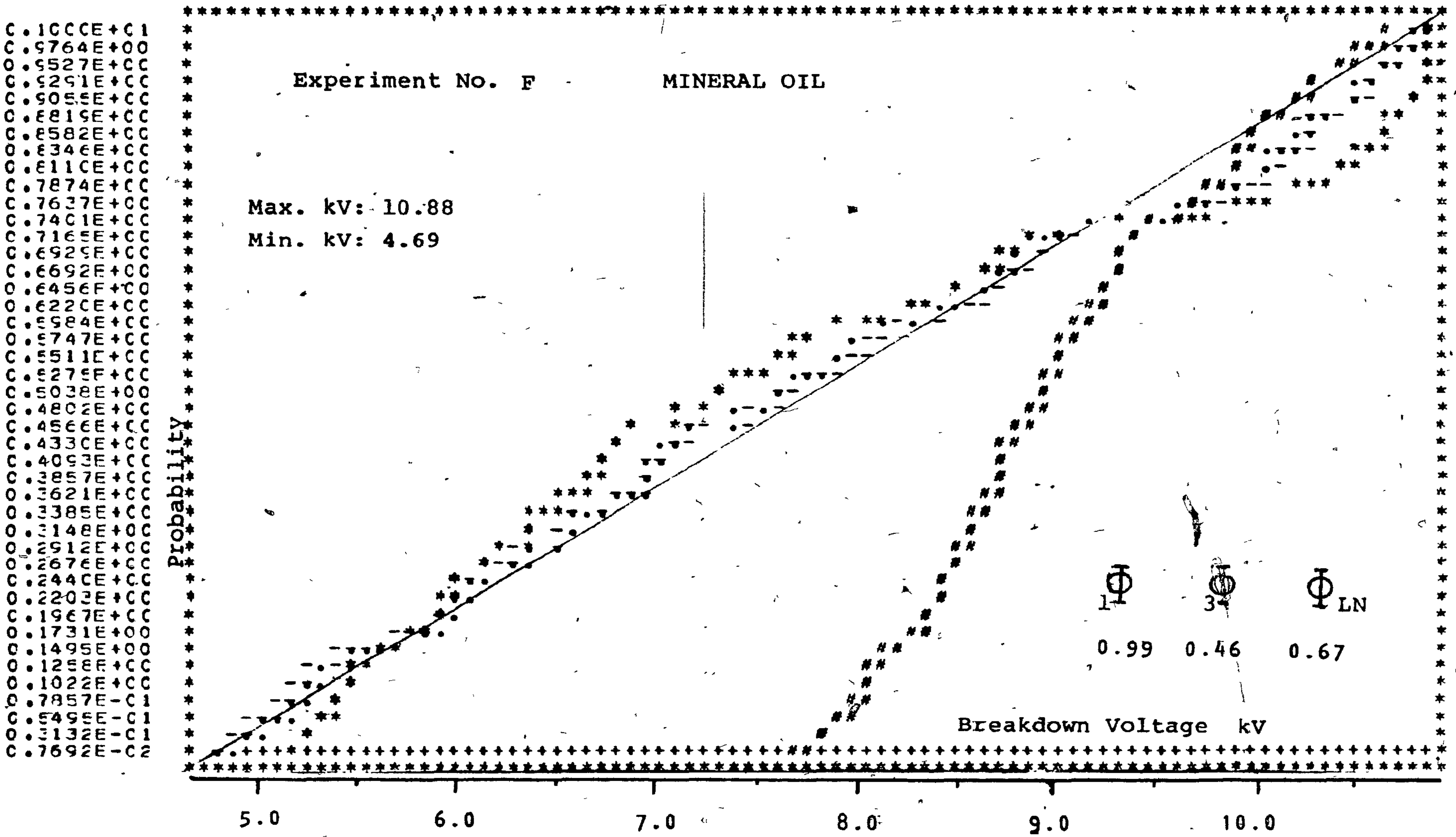

Experiment No. F
MINERAL OIL
Max. kV: 10.88
Min. kV: 4.69
Probability
0.1000E+01
0.9764E+00
0.9527E+00
0.9291E+00
0.9055E+00
0.8819E+00
0.8582E+00
0.8346E+00
0.8110E+00
0.7874E+00
0.7637E+00
0.7401E+00
0.7165E+00
0.6929E+00
0.6692E+00
0.6456E+00
0.6220E+00
0.5984E+00
0.5747E+00
0.5511E+00
0.5275E+00
0.5038E+00
0.4802E+00
0.4566E+00
0.4330E+00
0.4093E+00
0.3857E+00
0.3621E+00
0.3385E+00
0.3148E+00
0.2912E+00
0.2676E+00
0.2440E+00
0.2203E+00
0.1967E+00
0.1731E+00
0.1495E+00
0.1258E+00
0.1022E+00
0.7857E-01
0.5495E-01
0.3132E-01
0.7692E-02
Φ1 Φ3 ΦLN
0.99 0.46 0.67
Breakdown Voltage kV
5.0
6.0
7.0
8.0
9.0
10.0

FIGURE 4-22-c

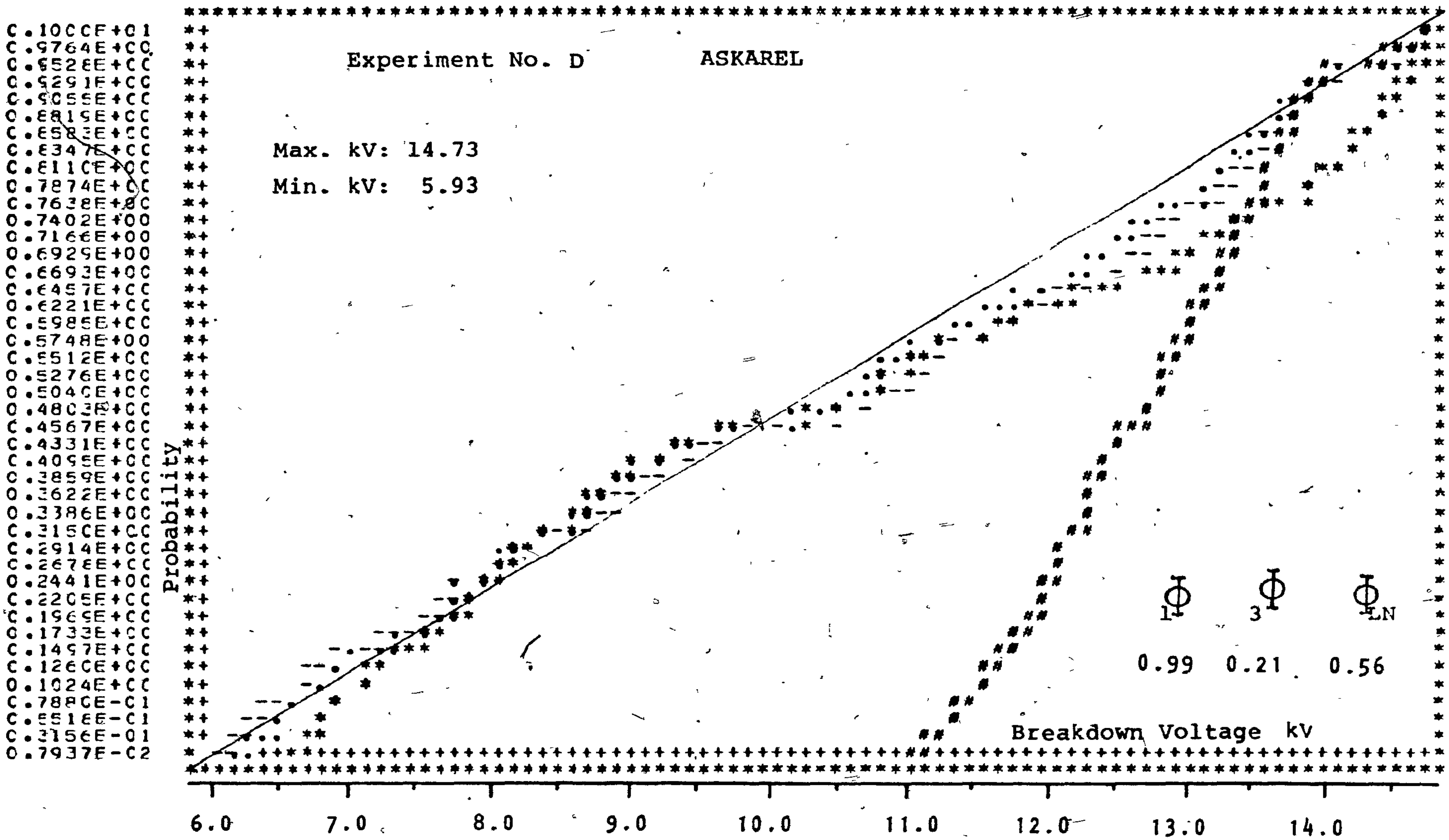
Experiment No. D
ASKAREL
Max. kV: 14.73
Min. kV: 5.93
0.1000E+01
0.9764E+00
0.9528E+00
0.9291E+00
0.9055E+00
0.8819E+00
0.8583E+00
0.8347E+00
0.8110E+00
0.7874E+00
0.7638E+00
0.7402E+00
0.7166E+00
0.6929E+00
0.6693E+00
0.6457E+00
0.6221E+00
0.5985E+00
0.5748E+00
0.5512E+00
0.5276E+00
0.5040E+00
0.4803E+00
0.4567E+00
0.4331E+00
0.4095E+00
0.3859E+00
0.3622E+00
0.3386E+00
0.3150E+00
0.2914E+00
0.2678E+00
0.2441E+00
0.2205E+00
0.1969E+00
0.1733E+00
0.1497E+00
0.1260E+00
0.1024E+00
0.7880E-01
0.5516E-01
0.3156E-01
0.7937E-02
Probability
Φ_1 Φ_3 Φ_{LN}
0.99 0.21 0.56
Breakdown Voltage kV
6.0
7.0
8.0
9.0
10.0
11.0
12.0
13.0
14.0

FIGURE 4-23-c

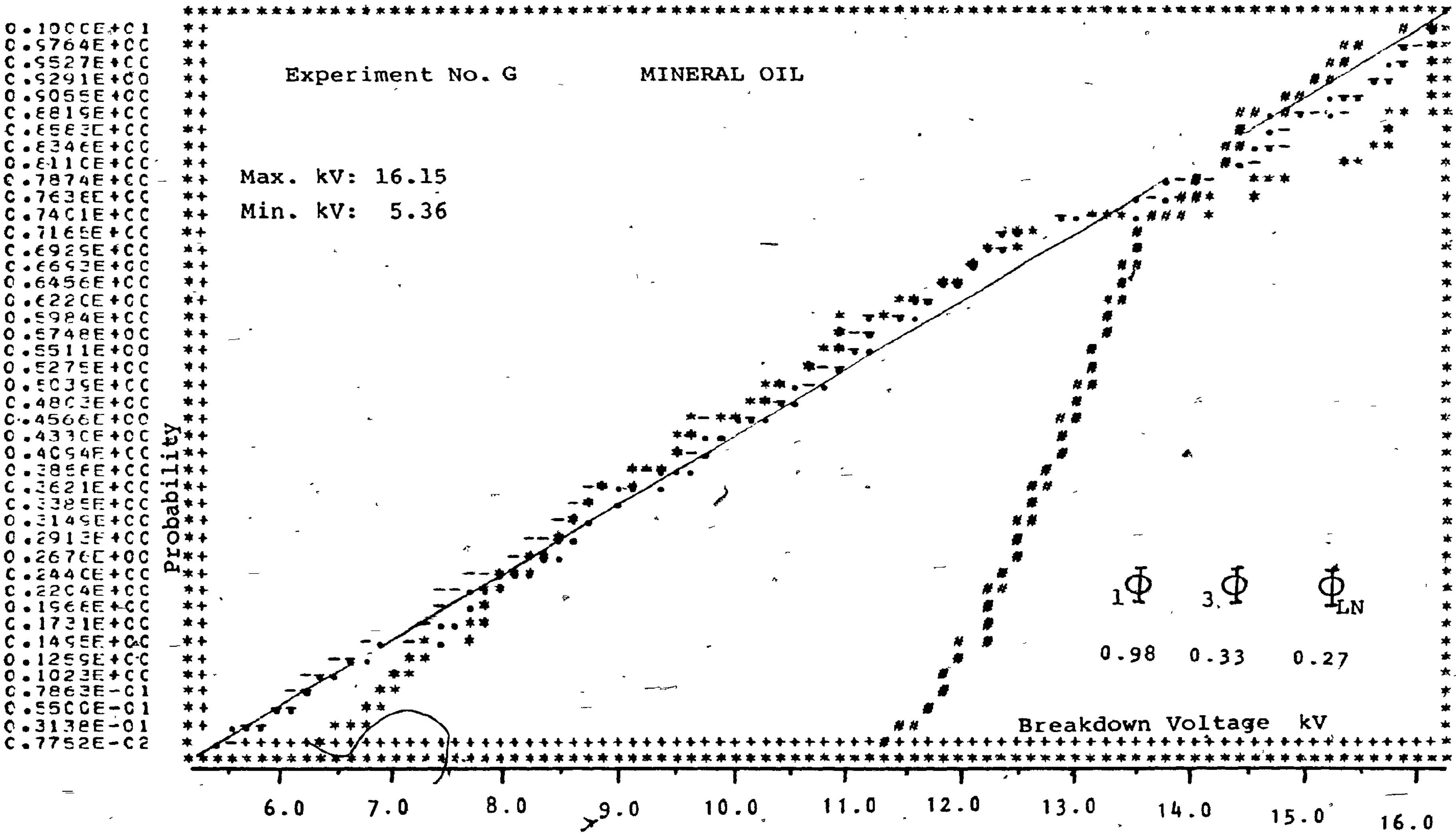
Experiment No. G
MINERAL OIL
Max. kV: 16.15
Min. kV: 5.36
Probability
0.1000E+01
0.9764E+00
0.9527E+00
0.9291E+00
0.9055E+00
0.8819E+00
0.8583E+00
0.8346E+00
0.8110E+00
0.7874E+00
0.7638E+00
0.7401E+00
0.7165E+00
0.6929E+00
0.6693E+00
0.6456E+00
0.6220E+00
0.5984E+00
0.5748E+00
0.5511E+00
0.5275E+00
0.5039E+00
0.4803E+00
0.4566E+00
0.4330E+00
0.4094E+00
0.3858E+00
0.3621E+00
0.3385E+00
0.3149E+00
0.2913E+00
0.2676E+00
0.2440E+00
0.2204E+00
0.1968E+00
0.1731E+00
0.1495E+00
0.1259E+00
0.1023E+00
0.7863E-01
0.5500E-01
0.3138E-01
0.7752E-02
$_1\Phi$ $_3\Phi$ Φ_{LN}
0.98 0.33 0.27
Breakdown Voltage kV
6.0
7.0
8.0
9.0
10.0
11.0
12.0
13.0
14.0
15.0
16.0

FIGURE 4-24-c

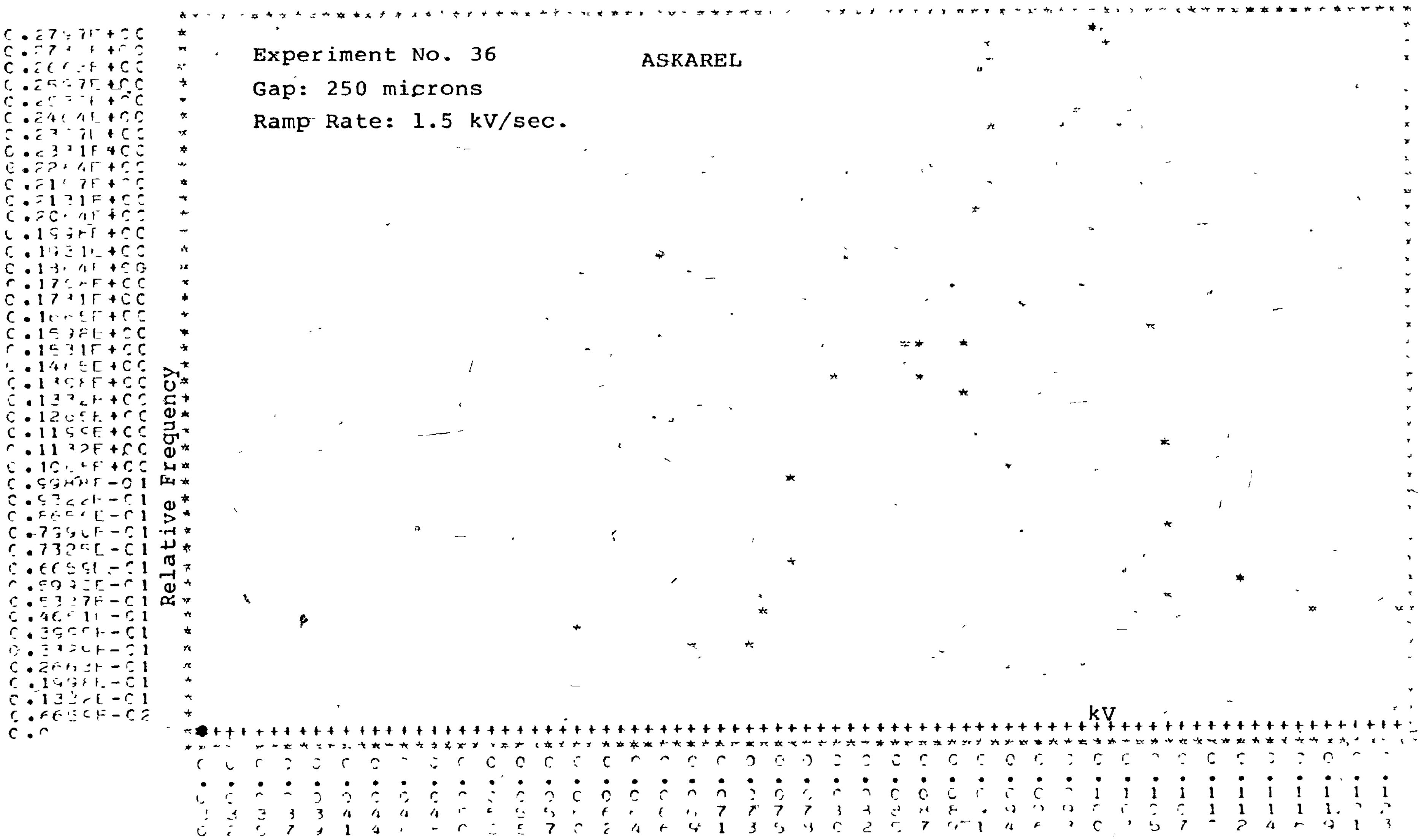

X-AXIS (HORIZONTAL-AXIS) EXPONENT

Y MAXIMUM 0.279[illegible]E+00
Y MINIMUM 0.0
X MAXIMUM 0.124[illegible]E+02
X MINIMUM 0.30[illegible]E+01

FIGURE 4-28-a

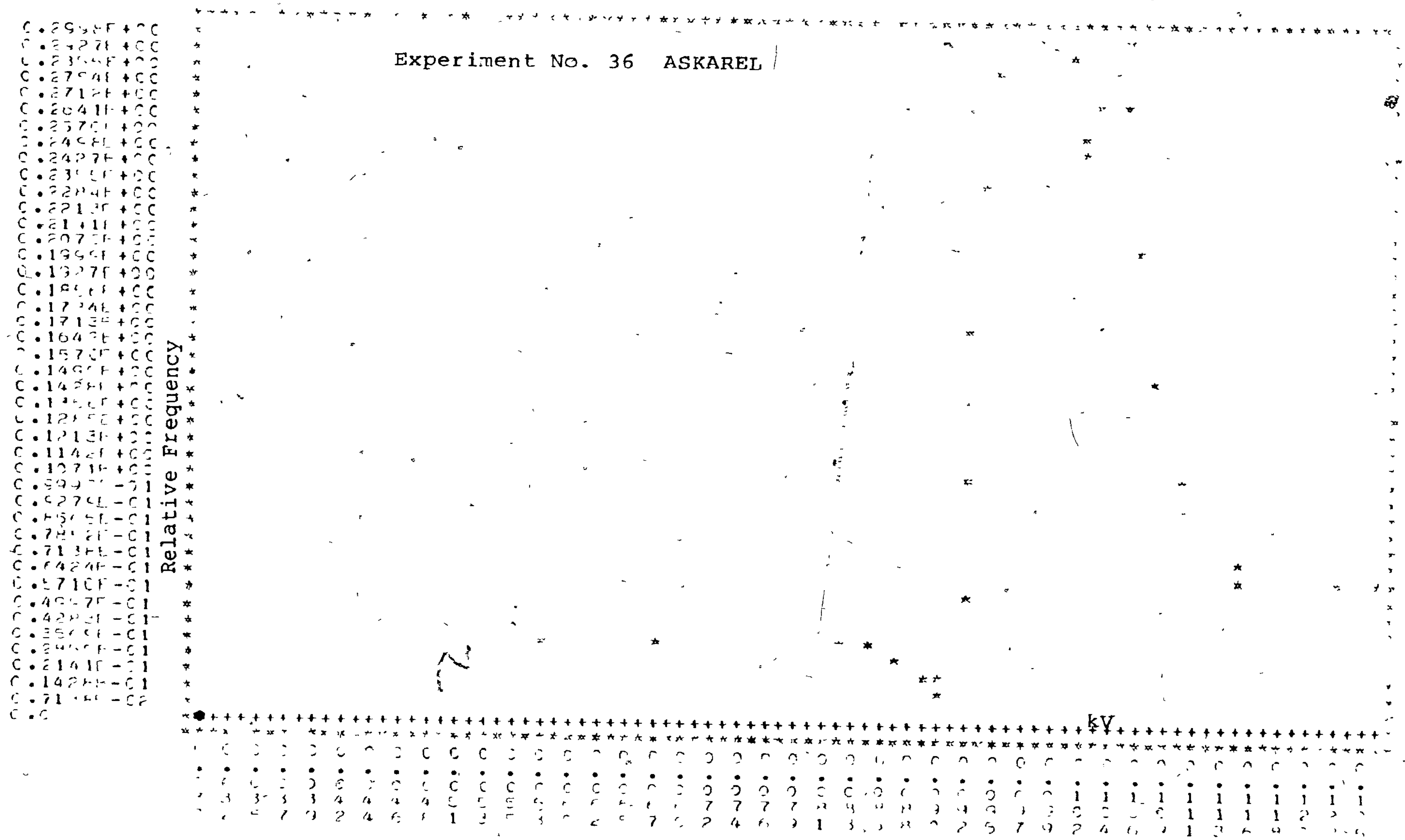

X-AXIS (HORIZONTAL-AXIS) EXPONENT [illegible]

Y MAXIMUM [illegible]
Y MINIMUM [illegible]
X MAXIMUM [illegible]
X MINIMUM [illegible]

FIGURE 4-28-b

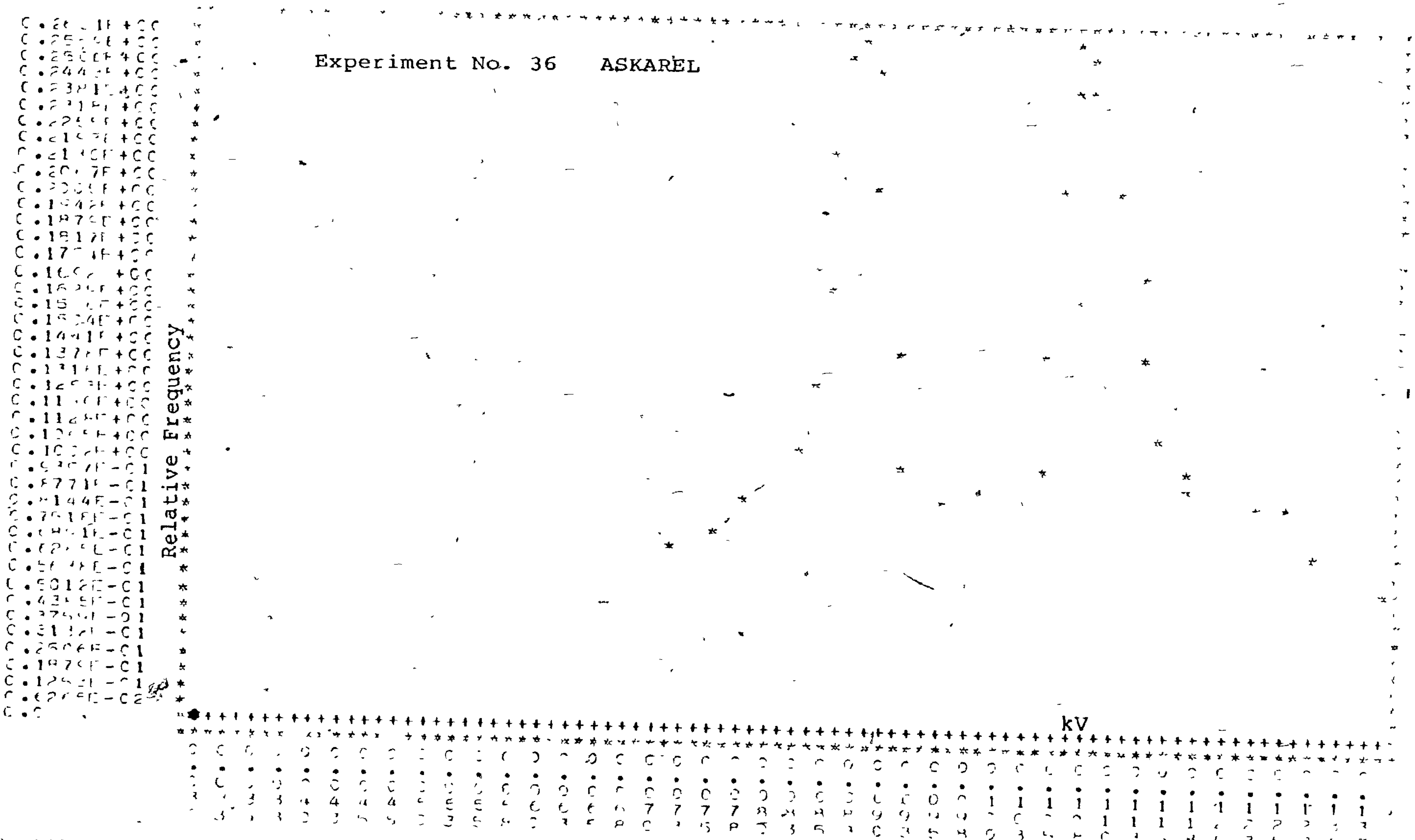

X-AXIS (HORIZONTAL-AXIS) EXPONENT 2

Y MAXIMUM
Y MINIMUM
X MAXIMUM
X MINIMUM

FIGURE 4-28-c

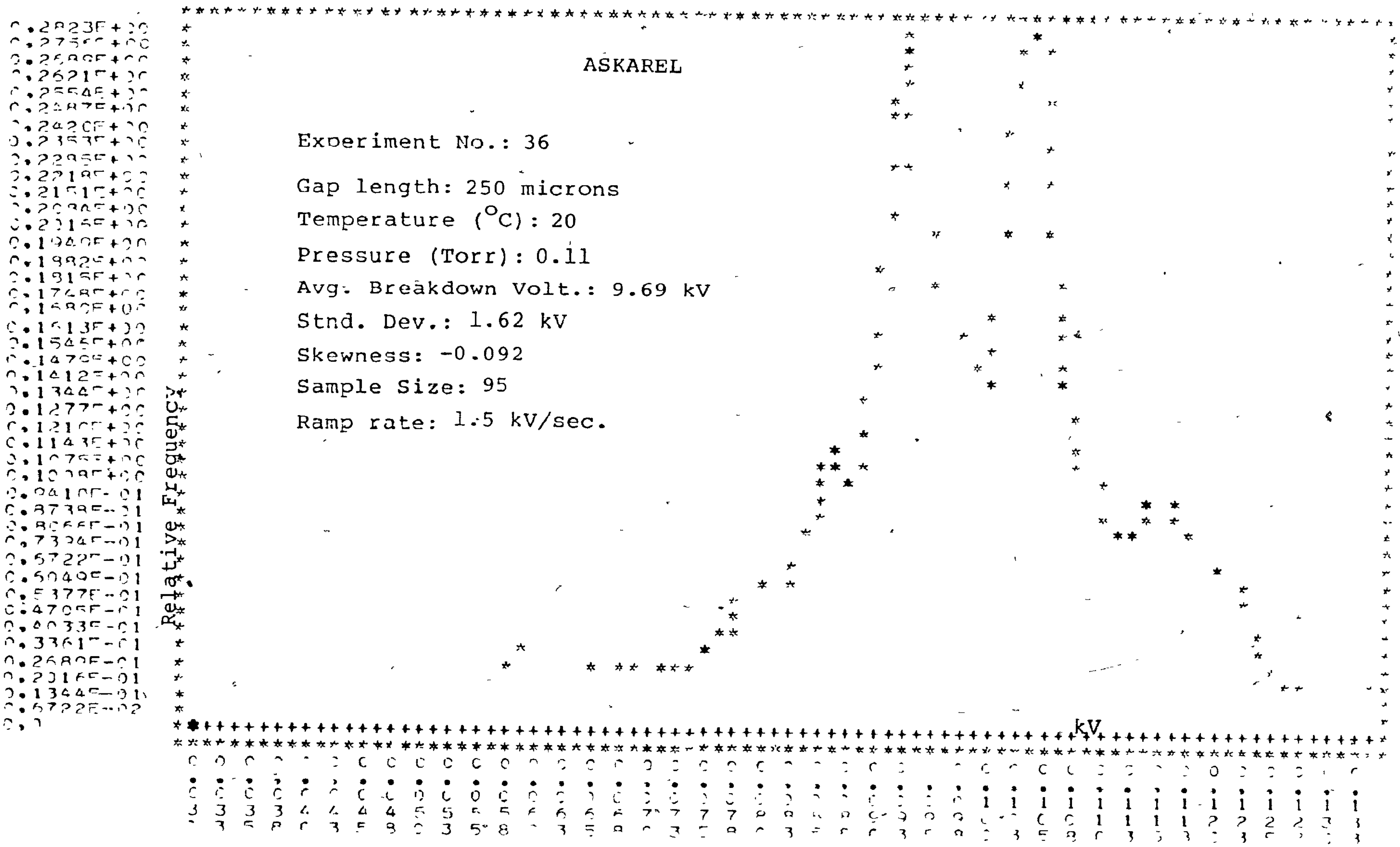

X-AXIS (HORIZONTAL-AXI.) EXPONENT 2

Y MAXIMUM 0.28231E+00
Y MINIMUM 0.0
X MAXIMUM 0.13320E+02
X MINIMUM 0.30200E+01

FIGURE 4-28-d

APPENDIX I

IDENTIFICATION OF PRINT CHARACTERS OF COMPUTER PLOTS

The following legend identifies the print characters used to represent the different probability distributions in the graphical plots displaying several different curves on the same axes.

* : Φ_1 First Asymptotic Distribution

: Φ_2 Second Asymptotic Distribution

. : Φ_3 Third Asymtotic Distribution (Weibull)

- : the Log-Normal Distribution

APPENDIX II

Derivation Concerning Chapter III, page 81.

It can be shown that in general

$$\frac{n}{m}\, p^{\nu} = \alpha_m^{\nu+1}$$

where the ν and $\nu+1$ represent the ν^{th} and $\nu+1^{th}$ order derivative.

Proof: Assume that:

$$\frac{n}{m}\, p_m^{\nu} = \alpha^{\nu+1}$$

holds for certain ν. It will now be shown that it holds for $\nu+1$.

$$p_m^{\nu} = \frac{m}{n}\,\alpha^{\nu+1}$$

$$= \left(\frac{m}{n}\right)\left(\frac{n}{m}\, p_m\right)^{\nu+1}$$

$$= p_m \frac{p_m^{\nu+1}}{p_m^{\nu+1}} = \frac{p_m^{\nu+1}}{p_m^{\nu}}$$

Differentiating with respect to p_m:

$$p_m^{\nu+1} = \frac{1}{p_m^{\nu}}\,(\nu+1)\, p_m^{\nu} p_m' - \frac{p_m^{\nu+1}}{p_m^{2\nu}}\,\nu\, p_m^{\nu-1} p_m$$

Dividing through with p_m:

$$\frac{p_m^{\nu+1}}{p_m} = \frac{(\nu+1)p_m^{\nu}\, p_m'}{p_m^{\nu} p_m} - \frac{p_m^{\nu+1}\,\nu\, p_m}{p_m^{\nu+1} p_m}$$

$$= (\nu+1)\alpha_m^{\nu+1} - \nu\alpha^{\nu+1}$$

$$= \alpha_m^{\nu+1}$$

Thus, $$p_m^{\nu+1} = \alpha^{\nu+1} p_m$$

$$= \frac{n}{m}\,\alpha_m^{\nu+2}$$

Hence $$\frac{m}{n}\, p_m^{\nu+1} = \alpha_m^{\nu+2}$$

which proves the proposition.

APPENDIX III

TABULATION OF STATISTICAL RESULTS OF THE EXPERIMENTS

Experiment nos. 1 to 44 done with Monsanto (7030) askarel.
Experiments nos. 45 to 50 done with mineral oil.

Identification of columns in Appendix III

a = experiment no.

b = gap length (microns)

c = ramp rate (kV sec.$^{-1}$)

d = number of breakdowns in the experiment

e = average breakdown voltage of experiment (kV)

f = standard deviation of breakdown voltages (kV)

g = average of logarithms of the breakdown voltages (see p.101)

h = standard deviation of the logarithms of the breakdown voltages (see p.101)

i = the smallest characteristic value of Type I Extreme Value Distrubtion, u_1 (see p. 79)

j = external intensity function, α_1 (p.80)

k = Weibull scale parameter, v' (p.91)

l = location parameter of Type III Extreme Value (Weibull) Distribution ϵ (p.91)

m = shape parameter of Weibull Distribution, k (p.91)

n = skewness ρ (p.93)

o = Kolmogorov-Smirnov Goodness-of-fit test for Type I Extreme Value Distribution ($_1\Phi$( ))

p = Kolmogorov-Smirnov Goodness-of-fit test for Type III Extreme Value Distribution ($_3\Phi$( ))

q = Kolmogorov-Smirnov Goodness-of-fit test for Log Normal Distribution (Φ_{LN})

Note that Table B (APPENDIX III) gives results per segment of experiments which have been divided into approximately three equal segments (see section 4.10, p.149). Each segment of an experiment is considered individually in the same way as the whole experiment was treated in Table A. Each segment is identified in column 'a' by the experiment number to which it belongs, and follow chronological order.

APPENDIX III (Continued)

TABLE A STATISTICAL RESULTS OF ENTIRE EXPERIMENT

a	b	c	d	e	f	g	h	i	j	k	l	m	n	o	p	q
1	150	mixed	24	5.48	1.39	1.673	0.235	5.93	0.93	5.69	3.48	1.47	1.110	0.58	0.06	0.13
2	176	mixed	23	6.23	1.10	1.185	0.172	6.68	1.16	6.50	4.16	4.16	0.661	0.60	0.03	0.03
3	150	mixed	24	4.30	0.37	1.455	0.084	4.75	3.47	4.39	3.60	2.00	0.646	1.00	0.26	0.46
4	150	mixed	26	5.48	1.48	1.668	0.258	5.93	0.88	5.80	2.91	1.80	0.779	0.52	0.03	0.07
5	150	mixed	23	5.60	1.12	1.703	0.206	6.05	1.14	6.00	2.29	3.23	0.097	0.10	0.02	0.16
6	150	mixed	24	4.21	0.61	1.428	0.153	4.66	2.09	4.44	1.91	4.23	-0.131	0.95	0.10	0.15
7	150	mixed	24	4.30	0.64	1.448	0.146	4.75	1.99	4.46	3.03	2.05	0.593	0.97	0.03	0.13
8	150	mixed	24	4.00	0.70	1.373	0.175	4.45	1.84	4.22	2.21	2.78	0.244	0.91	0.24	0.30
9	150	mixed	25	4.31	0.93	1.439	0.210	4.76	1.38	4.54	2.47	0.21	0.586	0.93	0.36	0.50
10	150	mixed	23	3.71	0.46	1.304	0.125	4.16	2.80	3.87	2.28	3.45	0.037	0.99	0.04	0.17
11	150	mixed	23	3.85	0.67	1.335	0.170	4.30	1.90	4.03	2.48	2.15	0.537	0.92	0.23	0.29
12	150	mixed	24	3.39	0.38	1.215	0.106	3.84	3.35	3.42	2.93	1.20	1.520	1.00	0.26	0.17
13	150	1.00	95	3.76	0.48	1.316	0.126	4.21	2.65	3.89	2.78	2.14	0.542	1.00	0.21	0.50
14	150	1.00	128	5.83	0.53	1.756	0.125	6.28	1.75	6.05	4.15	2.46	0.377	1.00	0.10	0.30
15	100	1.00	79	3.97	0.50	1.370	0.125	4.42	2.58	4.12	2.70	2.75	0.255	1.00	0.01	0.01
16	100	1.00	81	3.89	0.55	1.346	0.142	4.33	2.33	4.04	2.58	2.53	0.344	1.00	0.09	0.25
17	100	1.00	63	3.69	0.33	1.321	0.091	4.14	3.86	3.81	2.56	3.78	-0.042	1.00	0.71	0.80
18	100	3.00	70	3.49	0.34	1.245	0.096	3.39	3.82	3.58	2.75	2.35	0.431	1.00	0.33	0.18
19	100	1.00	75	4.20	0.60	1.425	0.149	4.64	2.12	4.43	1.90	4.29	-0.142	0.99	0.13	0.78
20	100	3.00	62	3.49	0.45	1.240	0.133	3.94	2.86	3.65	1.95	3.83	-0.051	1.00	0.21	0.50
21	100	3.00	79	4.00	0.55	1.375	0.155	4.45	2.34	4.23	-2.04	13.47	-0.752	1.00	0.32	0.77
22	100	1.50	57	5.66	1.08	1.716	0.195	6.11	1.18	6.02	2.78	2.89	0.204	0.72	0.21	0.48
23	100	0.75	70	4.19	0.63	1.422	0.149	4.64	2.03	4.37	2.86	2.24	0.487	0.99	0.06	0.03
24	100	0.75	60	4.00	0.53	1.380	0.129	4.45	2.42	4.13	3.06	1.87	0.722	1.00	0.63	0.52
25	100	0.50	103	4.81	0.52	1.565	0.106	5.26	2.48	4.94	3.84	1.96	0.660	1.00	0.22	0.23

TABLE A (Continued) STATISTICAL RESULTS OF ENTIRE EXPERIMENT (Continued)

a	b	c	d	e	f	g	h	i	j	k	l	m	n	o	p	q
26	125	3.00	100	6.63	0.84	1.883	0.128	7.08	1.52	6.90	4.40	2.88	0.210	0.98	0.11	0.18
27	125	1.50	72	5.00	0.88	1.593	0.176	5.45	1.45	5.26	2.95	2.47	0.372	0.98	0.07	0.13
28	125	1.00	95	5.79	1.08	1.738	0.193	6.24	1.18	6.17	2.30	3.58	0.006	0.70	0.25	0.67
29	125	0.30	100	5.97	1.27	1.764	0.224	6.42	1.01	6.44	1.59	3.85	-0.056	0.69	0.15	0.85
30	125	6.00	99	5.52	1.01	1.691	0.191	5.97	1.27	5.89	2.08	3.80	-0.044	0.70	0.07	0.60
31	100	0.30	100	5.11	0.93	1.616	0.176	5.56	1.38	5.30	3.55	1.73	0.837	0.98	0.50	0.02
32	100	6.00	98	4.73	0.76	1.541	0.162	5.18	1.68	4.98	2.66	2.98	0.182	1.00	0.31	0.66
33	250	1.00	99	10.92	2.05	2.371	0.201	11.37	0.63	11.72	1.54	5.27	-0.290	0.96	0.52	0.99
34	250	1.50	103	9.21	1.63	2.204	0.183	9.66	0.79	9.80	3.61	3.85	-0.055	0.95	0.34	0.72
35	250	0.75	101	10.45	1.92	2.328	0.197	10.90	0.67	11.20	1.83	5.16	-0.275	0.96	0.11	0.89
36	250	1.50	95	9.69	1.62	2.256	0.173	10.14	0.79	10.28	3.90	4.03	-0.092	0.58	0.24	0.66
37	250	0.50	104	10.91	2.38	2.364	0.230	11.36	0.54	11.77	2.79	3.81	-0.047	0.97	0.27	0.66
38	250	3.00	99	9.44	1.65	2.230	0.175	9.89	0.77	9.93	5.64	2.45	0.381	0.92	0.17	0.20
39	250	0.30	100	10.34	2.03	2.315	0.209	10.79	0.63	11.13	1.56	4.95	-0.247	0.99	0.44	0.98
40	250	6.00	99	10.01	1.99	2.284	0.202	10.46	0.64	10.66	4.66	2.93	0.193	0.91	0.06	0.36
41	125	0.50	103	5.56	0.93	1.701	0.167	6.01	1.37	5.83	3.44	2.42	0.396	0.94	0.20	0.39
42	125	0.75	87	5.11	0.76	1.621	0.147	5.56	1.68	5.31	3.56	2.14	0.546	1.00	0.01	0.04
43	125	0.75	95	5.65	0.96	1.719	0.166	6.10	1.33	5.90	3.73	2.11	0.564	0.93	0.02	0.08
44	250	0.50	104	8.79	2.09	2.146	0.233	9.24	0.62	9.30	4.79	2.01	0.627	0.89	0.02	0.14
45	250	0.30	102	6.14	0.79	1.806	0.125	6.59	1.63	6.29	4.83	1.71	0.854	1.00	1.00	0.91
46	250	0.30	102	6.14	0.79	1.806	0.125	6.59	1.63	6.56	4.34	2.65	0.295	0.97	0.05	0.17
47	125	3.00	98	7.82	1.37	2.041	0.180	8.27	0.94	8.29	3.63	3.38	0.057	0.79	0.21	0.58
48	250	1.00	102	8.72	2.37	2.133	0.252	9.17	0.54	9.16	4.94	1.63	0.929	0.99	0.91	0.99
49	250	0.30	108	7.68	1.53	2.021	0.186	8.13	0.84	7.93	5.41	1.51	1.064	1.00	0.59	0.95
50	250	3.00	74	9.76	2.48	2.248	0.244	10.21	0.52	10.32	5.30	1.87	0.727	0.97	0.72	0.74

APPENDIX III (Continued)

TABLE B STATISTICAL RESULTS PER ONE THIRD SEGMENT OF EXPERIMENT

a	b	c	d	e	f	g	h	i	j	k	l	m	n	o	p	q
16	100	1.00	24	3.76	0.58	1.312	0.158	4.21	2.22	3.97	1.71	3.99	-0.085	0.92	0.12	0.29
16	100	1.00	24	4.10	0.55	1.402	0.136	4.55	2.31	4.28	2.55	3.05	0.151	0.94	0.00	0.04
16	100	1.00	25	3.84	0.52	1.337	0.128	4.29	2.49	3.92	3.07	1.52	1.054	0.99	0.16	0.42
20	100	3.00	18	3.67	0.42	1.294	0.114	4.12	3.08	3.82	2.32	3.60	0.001	0.96	0.22	0.45
20	100	3.00	18	3.56	0.42	1.265	0.113	4.01	3.02	3.63	2.93	1.53	1.039	1.00	0.01	0.21
20	100	3.00	18	3.22	0.30	1.165	0.095	3.67	4.27	3.33	2.08	4.31	-0.145	1.00	0.13	0.42
21	100	3.00	23	4.04	0.43	1.391	0.108	4.49	2.97	4.20	2.49	4.03	-0.093	0.95	0.04	0.21
21	100	3.00	23	3.80	0.64	1.318	0.210	4.25	3.00	4.09	0.00	0.00	-1.392	0.89	0.64	0.87
21	100	3.00	25	4.21	0.53	1.430	0.129	4.66	2.42	4.41	2.20	4.28	-0.141	0.80	0.57	0.68
25	100	0.50	34	4.69	0.45	1.541	0.097	5.14	2.87	4.86	2.85	4.69	-0.209	0.96	0.14	0.57
25	100	0.50	34	4.88	0.53	1.580	0.056	5.33	2.43	5.01	3.86	2.02	0.616	1.00	0.01	0.01
25	100	0.50	35	4.86	0.56	1.575	0.112	5.31	2.28	4.97	3.97	1.62	0.938	1.00	0.33	0.80
26	125	3.00	30	6.69	0.73	1.894	0.110	7.14	1.75	6.94	4.47	3.34	0.067	0.72	0.00	0.02
26	125	3.00	30	6.55	0.75	1.874	0.112	7.00	1.17	6.73	5.13	1.98	0.645	0.87	0.24	0.07
26	125	3.00	32	6.62	1.06	1.877	0.161	7.07	1.21	6.97	3.69	3.02	0.163	0.58	0.04	0.13
28	125	1.00	30	5.46	0.91	1.684	0.174	5.91	1.40	5.78	2.70	3.33	0.609	0.66	0.40	0.65
28	125	1.00	30	5.84	1.06	1.748	0.186	6.29	1.21	6.22	2.30	3.72	-0.028	0.24	0.30	0.67
28	125	1.00	30	6.35	1.08	1.833	0.188	6.80	1.19	6.92	-5.09	12.95	-0.738	0.05	0.13	0.93
29	125	0.30	30	5.51	1.26	1.680	0.238	5.96	1.02	5.94	1.77	3.27	0.085	0.17	0.00	0.25
29	125	0.30	30	6.60	1.19	1.870	0.194	7.05	1.08	7.08	0.13	6.37	-0.410	0.25	0.20	0.87
29	125	0.30	32	6.16	1.11	1.801	0.188	6.61	1.15	6.58	2.00	4.22	-0.130	0.16	0.07	0.52
33	250	1.00	30	11.31	2.30	2.404	0.222	11.76	0.56	12.25	-1.47	6.51	-0.422	0.87	0.31	0.85
33	250	1.00	30	10.66	2.01	2.350	0.212	11.11	0.64	11.53	-9.69	12.31	-0.720	0.80	0.16	0.90
33	250	1.00	31	10.88	1.75	2.373	0.167	11.33	0.73	11.51	4.88	3.83	-0.510	0.77	0.66	0.89

<u>TABLE B</u> (Continued)   <u>STATISTICAL RESULTS PER ONE THIRD SEGMENT OF EXPERIMENT</u>

a	b	c	d	e	f	g	h	i	j	k	l	m	n	o	p	q
35	250	0.75	30	10.96	1.78	2.370	0.178	11.41	0.72	11.69	-0.09	7.32	-0.488	0.40	0.17	0.70
35	250	0.75	30	11.06	1.95	2.370	0.187	11.51	0.66	11.83	1.74	5.52	-0.321	0.86	0.61	0.94
35	250	0.75	31	9.84	1.57	2.270	0.170	10.29	0.82	10.46	2.00	5.79	-0.351	0.44	0.22	0.57
35	250	0.75	33	10.51	2.00	2.333	0.207	10.96	0.64	11.31	0.49	5.82	-0.354	0.78	0.09	0.64
35	250	0.75	33	10.99	2.06	2.377	0.205	11.44	0.62	11.84	-2.78	7.95	-0.530	0.72	0.17	0.90
35	250	0.75	33	9.89	1.58	2.278	0.170	10.34	0.81	10.52	1.99	5.81	-0.354	0.59	0.26	0.59
36	250	1.50	29	9.29	1.49	2.216	0.168	9.74	0.86	9.86	3.38	4.51	-0.181	0.21	0.03	0.39
36	250	1.50	29	9.71	1.46	2.262	0.162	10.16	0.88	10.31	1.18	6.88	-0.453	0.07	0.03	0.24
36	250	1.50	37	10.06	1.65	2.296	0.167	10.51	0.78	10.63	5.20	3.23	0.097	0.39	0.37	0.68
38	250	3.00	30	9.02	1.48	2.187	0.158	9.47	0.87	9.36	6.32	1.90	0.701	0.16	0.15	0.03
38	250	3.00	30	9.74	1.40	2.270	0.146	10.19	0.92	10.22	5.64	3.22	0.101	0.28	0.11	0.38
38	250	3.00	31	9.58	1.98	2.238	0.208	10.03	0.65	10.18	4.76	2.61	0.313	0.76	0.21	0.28
39	250	0.30	30	10.30	1.98	2.313	0.205	10.75	0.65	11.08	1.21	5.29	-0.293	0.84	0.41	0.86
39	250	0.30	30	10.67	2.00	2.350	0.195	11.12	0.64	11.40	3.91	3.78	-0.042	0.39	0.05	0.36
39	250	0.30	32	10.37	1.60	2.362	0.155	11.18	0.80	11.35	4.22	4.62	-0.198	0.56	0.16	0.56
42	125	0.75	25	5.25	0.68	1.652	0.127	5.70	1.90	5.43	3.82	2.23	0.495	0.96	0.02	0.01
42	125	0.75	25	4.84	0.80	1.575	0.156	5.34	1.60	5.34	3.63	1.61	0.957	0.91	0.00	0.03
42	125	0.75	27	5.25	0.87	1.645	0.166	5.70	1.48	5.53	2.93	2.90	0.200	0.52	0.14	0.37
42	125	0.75	29	5.17	0.63	1.636	0.119	5.62	2.04	5.33	3.95	2.04	0.602	0.98	0.46	0.05
42	125	0.75	29	4.99	0.77	1.597	0.146	5.44	1.67	5.13	3.78	1.62	0.940	0.97	0.04	0.15
42	125	0.75	29	5.18	0.89	1.630	0.172	5.63	1.45	5.46	2.85	2.84	0.222	0.61	0.13	0.36

TABLE B (Concluded) STATISTICAL RESULTS PER ONE THIRD SEGMENT OF EXPERIMENTS

a	b	c	d	e	f	g	h	i	j	k	l	m	n	o	p	q
45	250	0.30	31	6.82	0.89	1.912	0.128	7.27	1.44	7.06	4.98	2.18	0.518	0.83	0.15	0.14
45	250	0.30	31	5.86	0.37	1.160	0.065	6.31	3.46	6.01	3.40	7.87	-0.525	1.00	0.02	0.48
45	250	0.30	32	6.03	0.33	1.796	0.054	6.48	3.89	6.14	5.16	2.88	0.208	0.00	0.00	0.00
46	125	1.00	30	6.25	0.77	1.825	0.125	6.70	1.66	6.53	3.65	3.76	-0.035	0.83	0.45	0.72
46	125	1.00	30	6.12	0.79	1.804	0.128	6.57	1.63	6.36	4.23	2.57	0.327	0.77	0.20	0.20
46	125	1.00	31	6.29	0.66	1.834	0.100	6.74	1.96	6.53	4.09	3.75	-0.035	0.92	0.04	0.12
47	125	3.00	30	8.30	1.45	2.101	0.186	8.75	0.89	8.87	1.47	5.45	-0.312	0.39	0.07	0.67
47	125	3.00	30	8.17	1.42	2.085	0.183	8.62	0.90	8.72	1.96	5.01	-0.255	0.46	0.33	0.78
47	125	3.00	30	7.11	0.97	1.953	0.141	7.56	1.33	7.49	2.71	5.23	-0.285	0.02	0.03	0.48
48	250	1.00	31	11.09	2.17	2.386	0.205	11.54	0.59	11.91	2.71	4.36	-0.155	0.96	0.85	0.92
48	250	1.00	31	7.45	0.75	2.003	0.100	7.90	1.72	7.68	5.49	2.84	0.224	0.88	0.11	0.14
48	250	1.00	32	6.95	0.60	1.935	0.090	7.40	2.13	7.20	3.38	6.94	-0.459	0.96	0.18	0.67
49	250	0.30	33	6.67	1.50	2.145	0.177	9.12	0.85	9.19	4.22	3.26	0.090	0.54	0.09	0.14
49	250	0.30	33	6.73	0.75	1.900	0.110	7.18	1.71	6.94	5.04	2.39	0.410	0.96	0.09	0.22
49	250	0.30	34	6.97	0.46	1.939	0.066	7.42	2.79	7.12	5.73	2.94	0.188	1.00	0.02	0.05
50	250	3.00	22	12.27	2.43	2.485	0.219	12.72	0.53	13.28	-4.79	8.35	-0.555	0.67	0.10	0.82
50	250	3.00	22	8.70	0.84	2.159	0.097	9.15	1.52	8.99	6.32	3.09	0.139	0.65	0.41	0.50
50	250	3.00	22	7.86	1.13	2.051	0.152	8.31	1.14	8.33	0.77	7.42	-0.495	0.06	0.08	0.62

TABLE C STATISTICAL RESULTS OF MIXED RAMP RATE EXPTS. COMBINED (Sec. 4.7)

A	150	Mix'd	121	5.02	1.24	1.586	0.228	5.47	1.03	5.18	3.33	1.37	1.234	1.00	1.00	0.83
B	150	Mix'd	120	3.97	0.76	1.363	0.183	4.42	1.69	4.14	2.66	1.78	0.793	1.00	0.25	0.67
C	150	Mix'd	96	4.79	1.28	1.534	0.250	5.24	1.00	5.00	2.88	1.52	1.048	0.99	0.21	0.56

TABLE D STATISTICAL RESULTS OF HYBRID TWO RATE EXPTS. (P. 131)

G	250	0.3/3	129	9.13	2.35	2.180	0.247	9.58	0.55	9.63	5.09	1.78	0.795	0.98	0.33	0.27
E	100	3/.75	121	3.98	0.48	1.374	0.120	4.43	2.65	4.10	3.02	2.07	0.583	1.00	0.45	0.37
D	250	.3/6	126	9.76	2.10	2.250	0.219	10.21	0.61	10.44	4.21	2.87	0.213	0.99	0.21	0.56
F	125	1./3.	130	7.25	1.50	1.960	0.205	7.70	0.86	7.67	3.93	2.35	0.430	0.99	0.46	0.67

APPENDIX IV

SUMMARY OF KOLMOGOROV-SMIRNOV GOODNESS-OF-FIT TEST PROCEDURE

1. Generate a sample $T_1, T_2, \ldots, T_n$ whose distribution is supposed to be F.
2. Convert to uniform variates $F(T_1), F(T_2), \ldots, F(T_n)$.
3. Order these values to get $0 \leq X_1 \leq X_2 \leq \ldots \leq X_n \leq 1$
4. (Optional) Plot the staircase $(X_i, i/n)$, and the diagonal (X_i, X_i).
5. Compute:

$$D_+ = \max \left(i/n - X_i \right)$$

$$D_- = \max \left(X_i - (i-1)/n \right)$$

$$D = \max \left(D_+, D_- \right)$$

6. $$P1 = 1 - \exp\left(-2nD_+^2 \right)$$

$$P2 = 1 - \exp\left(-2nD_-^2 \right)$$

$$P3 = 1 + 2 \sum_{k=1}^{\infty} (-1)^k \exp\left(-2nD^2k^2\right), \text{ i.e.,}$$

$$P3 = 1 - 2t + 2t^4 - 2t^9 + 2t^{16} - 2t^{25} + 2t^{36} - \ldots$$

$$\text{with } t = \exp(-2nD^2)$$

Then, P1,P2,P3 are the probabilities associated with the observed deviations D_+, D_-, D. They may be taken as uniformly distributed on (0,1) provided that n is large, say $n \geq 50$. However, P1, P2, P3 are not independent.

APPENDIX V

THE PEARSON SYSTEM

If the density of X satisfies Pearson's differential equation

$$f'(x) = \frac{x - t}{c_2x^2 + c_1x + c_0} f(x)$$

then there are three types of solution—finite interval, half-infinite interval, and infinite interval. The finite interval solution is merely a translated and stretched beta density, which occurs when the roots r_1 and r_2 of the denominator span the mean, $r_1 < E(X) < r_2$. The half-infinite interval solution occurs when $r_1 < r_2 < E[X]$ or $E[X] < r_1 < r_2$ and the infinite interval solution occurs when the denominator has no real roots.

We will call these types P1, P2, and P3. The standard forms of these are as follows:

STANDARD TYPE P1. The beta density

$$g(y) = ky^{a-1}(1-y)^{b-1}, \qquad 0 < y < 1$$

Then

$$(1) \qquad g' = \frac{(a-1)}{y} g - \frac{b-1}{1-y} g = \frac{(2-a-b)y + (a-1)}{y(1-y)} g$$

STANDARD TYPE P2.

$$g(y) = k\frac{y^{b-1}}{(1+y)^{a+b}} = ky^{b-1}(1+y)^{-a-b}, \qquad 0 < y < \infty$$

$$(2) \qquad g' = \frac{b-1}{y} g - \frac{a+b}{1+y} g = \frac{-(a+1)y + (b-1)}{y(1+y)} g$$

This is sometimes called a beta type II density. Note that $\frac{1}{1+Y}$ has the beta density.

STANDARD TYPE P3.

$$g(y) = k(1+y^2)^a e^{-b \arctan(y)}, \qquad -\infty < y < \infty$$

$$(3) \qquad g' = \frac{2ay}{1+y^2} g - \frac{b}{1+y^2} g = \frac{2ay - b}{1+y^2} g$$

METHOD FOR DETERMINING TYPE:

If

$$f'(x) = \frac{x - t}{c_2x^2 + c_1x + c_0} f(x) = \frac{x - t}{c_2(x-r_1)(x-r_2)} f(x)$$

where $r_1 < r_2$ are the roots of the denominator then we get type P1 when $r_1 < E[X] < r_2$, type P2 when $r_1 < r_2 < E[X]$ or $E[X] < r_1 < r_2$ and type P3 when the roots are complex. Details are as follows:

Type P1. When $r_1 < E[X] < r_2$ then

$$Y = \frac{r_2 - X}{r_2 - r_1}$$

has the beta (a,b) density with

$$a = 1 + \frac{-t + r_2}{c_2(r_2-r_1)}$$

$$b = 2 - a + \frac{1}{c_2} .$$

Thus the density of X has this form

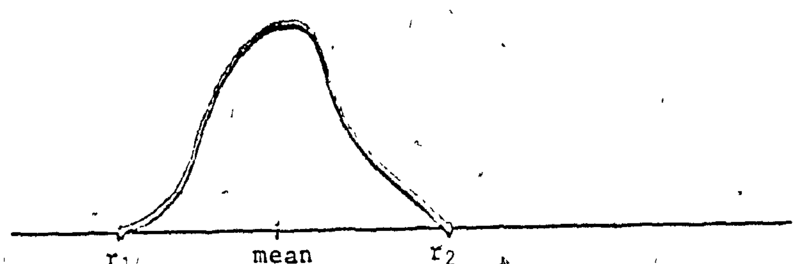

Type P2. When $r_1 < r_2 < E[X]$ then

$$Y = \frac{X - r_2}{r_2 - r_1}$$

has density $ky^{b-1}(1+y)^{-a-b}$, $0 < y < \infty$, and $(r_2-r_1)/(X-r_1)$ has the beta (a,b) density, where

$$a = -1 - 1/c_2$$

$$b = 1 + \frac{r_2 - t}{c_2(r_2-r_1)}$$

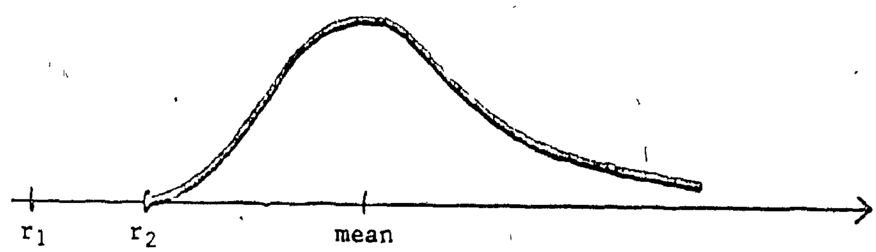

When $E[X] < r_1 < r_2$ then

$$Y = \frac{r_1 - X}{r_2 - r_1}$$

has density $ky^{b-1}(1+y)^{-a-b}$, $0 < y < \infty$, and $(r_2-r_1)/(r_2-X)$ has the beta (a,b) density, where

$$a = -1 - 1/c_2$$

$$b = 1 + \frac{t - r_1}{c_2(r_2-r_1)}$$

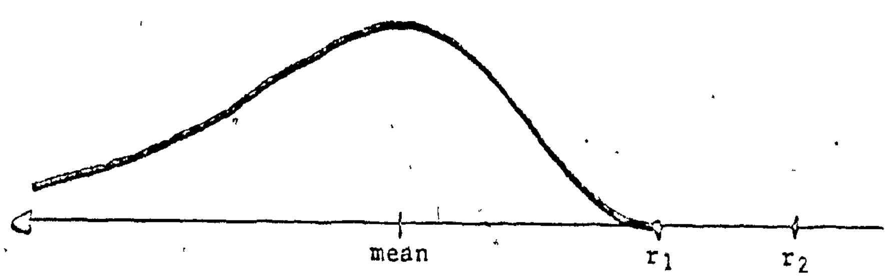

Type P3. When $c_2x^2 + c_1x + c_0$ has no real roots, that is, $Q = c_1^2 - 4c_0c_2 < 0$, then

$$Y = (X-s)/r$$

has density

$$k(1+y^2)^a e^{-b \arctan y}, \qquad -\infty < y < \infty$$

where

$$r = \sqrt{-Q}/(2c_2)$$
$$s = -c_1/(2c_2)$$
$$a = .5/c_2$$
$$b = (c_1+2c_2t)/(c_2\sqrt{-Q})$$

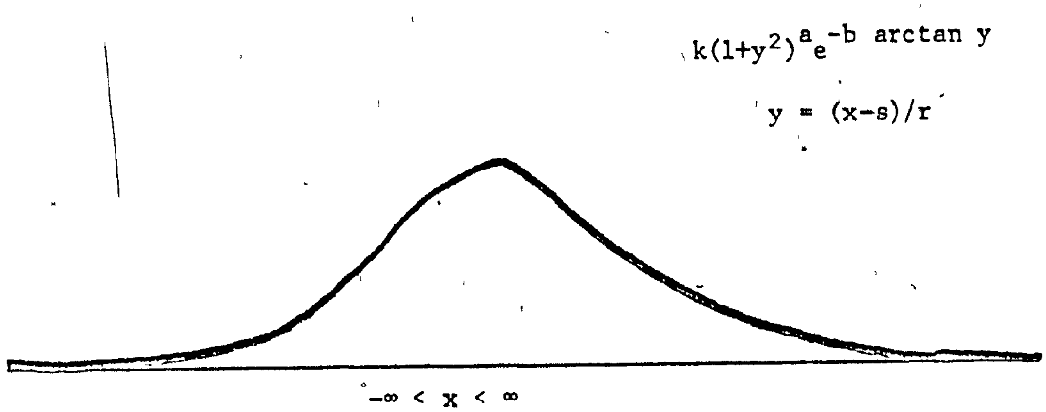

```
FORTRAN IV G1   RELEASE 2.0              PRSPLT          DATE = 77203          07/32/15

 0001                     SUBROUTINE PRSPLT  (S1, S2, S3, S4)
                   C
                   C      PLOTS DENSITY GIVEN FIST 4 MOMENTS
                   C      S1,S2,S3,S4 : THE FOUR MOMENTS USED
                   C
 0002                     DIMENSION WK1(50), WK2(50), WK3(50), IZ(50)
 0003                       REAL TITLE(12)/12*' '/
 0004                     INTEGER A/'*'/
                   C
                   C
 0005                     REAL*8 S1,S2,S3,S4,T,C0,C1,C2,E
 0006                     DIMENSION X(50),Y(50)
 0007                     FP2 (Z) = DEXP( .5* DLOG( 1.D0 + Z*Z) / C2 -B* ATAN(Z))
 0008                     FP1 (Z) = EXP( A* ALOG (ABS( Z R1)) + B* ALOG( ABS (Z-R2)))
 0009                     DO 5 I=1,50
 0010              5      IZ(I)= A
 0011                     SIG = DSQRT ( S2-S1**2)
 0012                     E = S3   S1*S2
 0013                     D = 2.* (5* S4 +4*S1*S3- 9*S2**2)*SIG**2 -12*E*E
 0014                     C1 = (*(3*S2**2-S4-2*S1*S3)-6*(S2*S3- S1*S4)*SIG**2)/D
 0015                     C2 =(3*E*E -2*( 2*S1*S3+ S4-3*S2**2)*SIG**2)/D
 0016                    T= C1 + S1*(1+2*C2)
 0017                     C0 = (T-2*C1)*S1  (1+3*C2)*S2
 0018                     Q= C1*C1 - 4.*C2*C0
 0019                     SQ= SQRT( ABS(Q))
 0020                     IF(Q.GT.0.)GO TO 3
 0021                     B=( C1+2.*C2*T)/(C2*SQ)
 0022                     PRINT 31,S1,T,SIG
 0023              31     FORMAT('NO REAL ROOTS, MEAN=',G10.3,'MODE=', G10.3,'SIG=',G10.3)
 0024                     GO TO 6
 0025              3      R1 = .5*(-C1/C2 - SQ/DABS( C2))
 0026                     R2 = .5*(-C1/C2 + SQ/DABS(C2) )
 0027                     PRINT 33, R1,R2,S1,T,SIG
 0028              33     FORMAT('ROOTS=',2G11.3, 'MEAN=',G10.3,'MODE=',G10.3,'SIG=',G10.3)
 0029                     A =(T- R1)/ (C2*(R2-R1))
 0030                     B = (T-R2)/(C2*(R1-R2))
 0031              6      SUM = 0.0
 0032                     DO 2 I=1,50
 0033                     X(I) = S1-(3.01 - .12*I)*SIG
 0034                     V= X(I)
 0035                     IF( Q.LT.0.) Y(I)=FP2(SNGL(2.*C2* V +C1)/SQ)
 0036                     IF( Q.LT.0.) GO TO 2
 0037                     Y(I) = 0.
 0038                    IF((R1-V)*(R1-S1).GT.0..AND.(R2-V)*(R2-S1).GT.0.) Y(I)=FP1(V)
 0039              2      SUM= SUM + Y(I)*.2 * SIG
 0040                     DO 8 I=1,50
 0041              8      Y(I) = Y(I)/SUM
 0042                     CALL MULPLT( TITLE, 50,Y,X,IZ,43,84,1,WK1,WK2,WK3)
 0043                     RETURN
 0044                     END

  *OPTIONS IN EFFECT*  NOTERM,ID,EBCDIC,SOURCE,NOLIST,NODECK,LOAD,NOMAP,NOTEST
  *OPTIONS IN EFFECT*  NAME = PRSPLT  , LINECNT =       56
  *STATISTICS*    SOURCE STATEMENTS =        44,PROGRAM SIZE =      3696
```

Implements Pearson System of Density Plotting

APPENDIX VI

This subroutine implements the "pile of sand" method to determine the frequency of breakdown graph.

```
FORTRAN IV G1   RELEASE 2.0           FSTIM                DATE = 77270            03/13/44
      SUBROUTINE FSTIM ( Z,M ,B)
C       PLOTS DENSITY BY 'PILE OF SAND' METHOD
      DIMENSION Z(M), X1(130), Y1(130), Z1(130)
      DIMENSION WK1(130),WK2(130), WK3(130), IZ(130)
      DOUBLE PRECISION T,XLIM,B,DEL,SUM,F,F1,F2,S1
        REAL TITLE(12)/12*' '/
      INTEGER A/'*'/
      DO 5 I=1,130
    5 IZ(I)= A
       DO 6 I=1,M
      Z1(I)= Z(I)
    6 CONTINUE
C
C     Z: MUST BE ORDERED: SMALLEST TO LARGEST.
      T = DBLE ( Z(1) )
      XLIM = DBLE ( Z(M) )
C
C
      DEL= (XLIM-T)/(M+0.)
C
      J= 1
    3 SUM = 0.D0
      DO 2 I= 1,M
      F= ( T- DBLE ( Z(I)) )/B
      F1 = 1.D0- DABS(F)
      F2= DMAX1( 0.D0, F1)
      SUM = SUM + F2
    2 CONTINUE
        S1= SUM/(M*B)
      X1(J)= SNGL( S1)
      T= T + DEL
      Y1(J)=FLOAT(J)/FLOAT(M)
     IF( T.GT. XLIM) GO TO 4
      J = J+1
     GO TO 3
C
    4 J= J-1
        PRINT101,J
  101 FORMAT('0',I5)
      J1= J+1
      DO 7  I=J1,130
      Z1(I)= 0.0
    7 CONTINUE
      DO 8 I=J1,130
      X1(I)=0.0
    8 CONTINUE
      CALL MULPLT(TITLE, 130,X1,Z1,IZ,43,84,1,WK1,WK2,WK3)
      RETURN
      END
 *OPTIONS IN EFFECT*  NOTERM,ID,EBCDIC,SOURCE,NOLIST,NODECK,LOAD,NOMAP,NOTEST
 *OPTIONS IN EFFECT*  NAME = FSTIM    , LINECNT =       56
 *STATISTICS*     SOURCE STATEMENTS =       42,PROGRAM SIZE =      4990
 *STATISTICS*  NO DIAGNOSTICS GENERATED
```

BIBLIOGRAPHY

1. Adamczewski, I. "Ionization, Conductivity, and Breakdown in Dielectric Liquids", Taylor and Francis Ltd. (1969)

2. ibid. p. 356

3. ibid. p. 368

4. ibid. p. 363

5. Alston, L.L., "High Voltage Technology", Oxford University Press p. 7 (1968)

6. ibid. p. 6

7. Artbauer, J., Griac J., "Some Factors Preventing Attainment of Intrinsic Electric Strength in Polymeric Insulation", IEEE Trans. on El. Insul. Vol. El-5 no. 4 p.104-105 (1970).

8. Bain, L.J.; Antle, C.E.; "Estimation of Parameters in the Weibull Distribution Technometrics" Vol. 9 no. 4 p. 621 (1967).

9. Birks, J.B., "Modern Dielectric Materials", Heywood & Co. p. 77 (London) (1960).

10. ibid. p. 68

11. ibid. p. 49

12. ibid. p. 76

13. Birks, J.B.; Hart, J., "Progress in Dielectrics" Vol. 4, Heywood & Co. Ltd. p. 231 (London) (1962).

14. Birks, J.B.; Hart, J., "Progress in Dielectrics" Vol. 6, Academic Press Inc. (New York) (1965).

15. Birlasekaran, S.; Darveniza, M. "Microdischarges from Particles in Transformer Oil", IEEE Trans. on Electrical Insulation, Vol EI - 11 no. 4, p 102 (1970).

16. ibid. p. 163

17. Bloomquist, W.C., "What is the Future for Askarel?" Power, Vol. 120 no. 2 p. 68 (1976).

18. ibid. p.69

19. Brignell, J.E.,"Statistical Nature of Breakdown Sequences in a Liquid Insulant", Proc. IEE Vol. 113 no. 10, p. 1683 (Oct.) (1966)

20. ibid. p.1684

21. ibid p.1688

22. ibid. p. 1687

23. ibid. p. 1689

24. ibid, p. 1690

25. Bulke, J., "Breakdown of Liquid Dielectrics", McGill University Master's Thesis p. 4 (1972).

26. Cantril, J.M.; Pohl, H.A., "Insulator Induced Conduction", J. Electrochem. Soc: Electrochemical Science Vol. 115, no. 7, p. 700 (1968).

27. Caulcott, E., "Significance Tests", Routledge & Kegan p. 65 (London) (1973).

28. Chadband W.G.; Calderwood, J.H., "Prebreakdown Events in Dielectric Liquids", Proc. of the Inst. of Elect. Engrs. , Vol. 119, no. 11 p. 1661 (1972).

29. ibid. p. 1664

30. ibid. p. 1665

31. ibid. p. 1662

32. ibid. p.1663

33. Chan, L.K.; Mead, E.R., "Linear Estimation of the Extreme Value Distribution Based on Suitably Chosen Order Statistics", IEEE Trans. on Reliability, Vol. R-20, no. 2 p. 74 (May) (1971).

34. Cherney, E.A.; Gross, J.D., "Space Charge Effects in Chlorobiphenyls", IEEE Trans. on Electrical Insulation Vol. EI-8, no. 1 p.10-11 (1973).

35. Chiu, C., "A Luminescent and Fluorescent Region Associated with Prebreakdown and Breakdown in n-hexane" J. Phys. D: Appl. Phys., Vol. 9 p. 851 (1976).

36. Cohen, A.C. "Maximum Likelihood Estimation in the Weibull Distribution Based on Complete and Censored Samples", Technometrics, Vol. 7, no. 4, p. 579 (1965).

37. Cox, D.R., "Renewal Theory", Methuen & Co. Ltd. p. 109 (London) (1962).

38. Cramér, H., "Mathematical Method of Statistics" Princeton University Press p. 249 (1966).

39. Cress, P.; Dirksen, P; Graham, J.w., "Fortran IV With Watfor and Watfiv" Prentice-Hall Inc. (1970).

40. Devins, J.C.; Rzad, S.J.; Schwabe, R.J., "Pre-Breakdown Phenomena in Liquids: Electronic Processes", J. Phys. D: Appl. Phys., Vol.9, p.L87 (1976).

41. Endicott, H.S.; Weber, K.H., "Electrode Area Effect for the Impulse Breakdown of Transformer Oil", T.A.I.E.E. Vol. 76 p. 393 (Aug.) (1957).

42. Epstein, B.; Brooks, H., "The Theory of Extreme Values and Its Implications in the Study of the Dielectric Strength of Paper Capacitors", J. of Appl. Phys. Vol. 19, p. 544 (1948).

43. Farrell, O.; Ross, B. "Solved Problems in Analysis" Dover Publications Inc. p. 39 (1971).

44. Fischer, P.; Rohl, P., "Application of Statistical Methods to the Analysis of Electrical Breakdown in Plastics", Simiens-Forsch-n Entwickl. Ber. Vol.3 no. 2 p. 125 (1973)

45. ibid. p. 128

46. ibid. p. 126

47. Freund, J.E., "Mathematical Statistics" Prentice-Hall Inc. p. 322 (1962).

48. ibid. p.98

49. Freudenthal, A.M.; Gumbel, E.J., "Minimum Life in Fatigue (#7)", Am. St. Ass. J. p. 515 (Sept.) (1954).

50. Gallagher, T.J., "Simple Dielectric Liquids", Clarendon Press p. 105 (Oxford) (1975).

51. ibid. p. 51

52. Goodwin, D.W.; MacFadyen, K.A., "Electrical Conduction and Breakdown in Liquid Dielectrics", Proc. Phys. Soc. Vol. 66B, p. 85 (1953).

53. Gumbel, E.J., "Statistics of Extremes", Columbia University Press (1958).

54. ibid. p. 118

55. ibid, p. 251

56. ibid. p. 156

57. Gumbel, E.J.; Goldstein, N. "Analysis of Empirical Bivariate Extremal Distributions", Am. Stat. Ass. J. p.794 (Sept.) (1964).

58. ibid. p.20

59. Gzowski, O.; Limo, J.; Piltkowska, J. "Triggering of Electrical Breakdown in n-hexane", Phénomènes de Conduction Dans les Liquids Isolants, no.179 Editions du Centre National de la Recherche Scientifique p.140 (Grenoble) (1968).

60. ibid. p. 143

61. Hancox, R.; Tropper, H., "The Breakdown of Transformer Oil Under Impulse Voltages", Proceed. of IEE Vol. 105, Part A, p. 250-57 (1958)

62. Heiman, F.; Sibillot, P.; Coelho, R., "New Observations of Prebreakdown Events in n-hexane in a Point Plane Configuration", J. Phys. D: Appl. Phys. Vol. 9, p. 95-98 (1976).

63. Hakim, R.M., "Distribution of Relaxation Times of Insulating Oil" IEEE Trans. on Elect. Insul. Vol. EI-6, no. 4, p. 39, (1971).

64. Hakim, R.M.,"The Properties of an Insulating Oil and Its Fractions at Low Temperatures", IEEE Trans. on Elect. Insul., Vol. EI-10, no. 4, p.124 (1975).

65. Heller, B.; Veverka, A., "Analysis of Relations Between Different Distribution Functions of Breakdown Voltage", Acta Technica Csac., Vol. 20, no. 4 p. 375 (1975).

66. Holmes, M.C., "Insulation Variability" J. Franklin Inst. Vol. 245 p. 159 (feb.) (1948).

67. Johnson, N.L.; Kotz,S., "Continuous Univariate Distributions -1", Houghton Mifflin Co. p. 251 (1970.

68. ibid. p. 273

69. Kaneko,R.; Sugiuama, K., "Dependence on Impulse Breakdown Strength on Cable Length", Elect. Eng. in Jap. Vol. 93, no. 3 p. 62, 98,(May-June) (1974).

70. Kao, J.H. K. "A Graphical Estimation of Mixed Weibull Parameters in Life-Testing of Electron Tubes", Technometrics, Vol. 1, no. 4, p. 389 (1959).

71. Kao, J.H.K., "Computer Methods for Estimating Weibull Parameters in Reliability Studies", I.R.E. Trans. Reliability and Quality Control, Vol. 13 p. 15, (1958).

72. Kao, K.C., "Theory of High-Field Electrical Conduction in Dielectric Liquids", IEEE Trans. on Elect. Insul. Vol. EI-11, no. 4, p. 121 (1948).

73. Kawaguchi, Y; Murata, H.; Ikeda, M., "Breakdown of Transformer Oil", IEEE Trans. on Power Systems and Apparatus, Vol. PAS 91, p. 9, (1972).

74. ibid. p. 13

75. Kielpinski, T.J.; Nelson W.; "Optimum Censored Accelerated Life Tests for Normal and Log-normal Distributions", IEEE Trans. on Reliability, Vol. R-24, no. 5, p. 310, (1975).

76. King, J.R., "Probability Charts for Decision Making" Industrial Press Inc. p. 29 (New York) (1971).

77. ibid. p. 66

78. ibid. p. 177

79. ibid. p. 179

80. ibid. p. 181

81. Kok, J.A., "Electrical Breakdown of Insulating Liquids", Interscience Publishers Inc. (1961).

82. ibid. p. 62

83. ibid. p. 63

84. Krasucki, Z., "Breakdown of Liquid Dielectrics", Proc. Roy. Soc., Vol. 294A, no. 143B, p. 393 (1966).

85. ibid. p. 396

86. ibid. p. 401

87. Landau, L.D.; Lifshitz, E.M., "Fluid Mechanics", Pergamon Press (1959).

88. Lewis, T.J., "The Statistical Basis of Impulse Testing", IEE Proc. Vol. 105, Part C,p.27, (1957).

89. Lewis, T.J.; Ward, B.W.,"A statistical Interpretation of the Electrical Breakdown of Liquid Dielectrics" Proc. Royal Soc. Vol. 269A, p. 233 (1966).

90. Lindgren, B.W.; McElrath, G.W., "Introduction to Probability and Statistics", The MacMillan Co. (New York) (1966).

91. ibid. p. 91

92. MacFadyen, K.A., "Some Researches into the Electrical Conduction and Breakdown of Liquid Dielectrics" Brit. J. of Appl. Phys. Vol. 6, p.1 (1955)

93. McCool, J.I., "Inference on Weibull Percentiles and Shape Parameter From Maximum Likelihood Estimates", IEEE Trans. on Reliability, Vol. R-19, no. 1, p. 2 (1970).

94. Meeker, Q.W.; Nelson V. "Optimum Accelerated Life-tests for the Weibull and Extreme Value Distributions" IEEE Trans. on Reliability, Vol. R-24, no. 5, p. 321 (1975).

95. Metzmacher, K.D.; Brignell, J.E., "Application of the Statistical Model for Liquid Breakdown" Phénomènes de Conduction dans les Liquides Isolants, No. 179 Editions du Centre National de la Recherche Scientifique p. 145-153 (Grenoble) (1970).

96. Midoz,J. "Cables,Haute Tension au Polyéthylène, Contribution à L'étude de la Fiabilité des Câbles Electriques", Revue Générale de L'électricité, Vol. 85, no. 10, p. 793 (1976).

97. Monsanto Compnay, "The Aroclor Polychlorinated Polyphenyls", Technical Bulletin O-FF/1(EX).

98. Morikawa, E. "Optical Observation of Prebreakdown Phenomena in Dielectric Oil", Electr. Engin. in Japan Vol. 92 no. 1, p. 11-17 (1972).

99. Nelson, J.K. "Statistical Effects of Environmental Factors on Liquid-Breakdown Measurement", Proc. IEE Vol. 118 no. 11 p. 1675 (1971).

100. ibid. p. 1678

101. ibid. p. 1677

102. Nelson, J.K., "Evidence for Transitions in the Prebreakdown Mechanism of Liquid Dielectrics", Proc. of Inst. of Elect. Engrs. (London) Vol. 122 no. 12 (Dec,) p. 1439 (1975).

103. ibid. p. 1441

104. Nelson, J.K.; McGrath, P.B., "The Effect of Stress-Induced Motion on the Conduction, Current Statistics of Liquid Dielectrics", J. Phys. D - Appl. Phys. Vol. 5, no. 6, p. 1111 (1972).

105. Nelson, J.K.; Salvage, B.F., "Electric Strength of Transformer Oil for Large Electrode Areas", Proc. IEE Vol. 118, no. 2, p. 388-393 (1971)

106. Nelson, W. "Graphical Analysis of Accelerated Life Test Data With the Inverse Power Law Model", IEEE Trans. on Reliability, Vol. R-21, no. 1, p.2 (Feb.) (1972).

107. Nelson, W. "Analysis of Accelerated Life Test Data- Least Squares Methods for the Inverse Power Law Model", IEEE Trans. on Reliability, Vol. R24 no. 2, p. 103 (June) (1975).

108. Németh, E.; Csaki, E., "Methods of Mathematical Statistics for Evaluating Electric Breakdown Measuring Series", Periodica Polytechnica, Electr. Eng. Vol. 7, p.9 (1963).

109. Nitta, Y.; Aihara, Y., "Polarity Effect on Breakdown Voltage in Organic Liquids", IEEE Trans. on El. Insulation Vol. EI-11 no. 3, p. 91 (1976).

110. Nosseir, A. "Effect of Dissolved Gases, Stress, and Gap Spacing on High Field Conductivity in Liquid Insulants", IEEE Trans. on Elect. Insulation Vol. EI-10, no. 2, p. 58 (1975).

111. Occhini, E. "A statistical Approach to the Discussion of the Dielectric Strength in Dielectric Cables", IEEE Trans. on Power Apparatus and Systems, Vol. 90 p. 2671 (1971).

112. ibid. p. 2672

113. ibid. p. 2675

114. Otnes, R.K.; Enochson, L., "Digital Time Series Analysis", John Wiley and Sons, p. 372 (1972).

115. Oudin, J.M., "Evaluation de la Fiabilité des Reseaux de Câbles Isolés à Partir Dessais Statistiques de Claquage Sur Échantillons", Revue Générale de Electricité", Vol. 80, no. 4, p. 330 (1971).

116. Oudin, J.M.; Rerolle, Y.; Thévenon, H., "Theorie Statistique du Claquage Electrique", Vol. 77, no. 4 p. 430 (1968).

117. Palmer, S.; Sharpley, W.A., "Electrical Strength of Transformer Insulation", Proc. IEE, Vol. 116, p. 2029 (1969).

118. Papadopoulos, A.S.; Tsokos, C.P., "Bayesian Confidence Bounds for the Weibull Failure Model", IEEE Trans. on Reliability, Vol. R-24, no. 1, p. 21 (1975).

119. Pedersen, B., "Gassing of Insulating Oils Under the Influence of an Electric Discharge", The Brown Boveri Review, Vol. 55 no. 4/5 p. 222 (1968)

120. Posner, E.C., "The Application of Extreme Value Theory to Error-Free Communications", Technometrics Vol. 7, no. 4 p. 518 (1965).

121. Qureishi, A.S., "The Discrimination Between Two Weibull Processes", Technometrics, Vol. 6, no.1, p. 17 (1964).

122. Rademaker, A.W.; Antle, C.E., "Sample Size for Selecting The Better of Two Weibull Populations", IEEE Trans. on Reliability, Vol. R-24, no. 1, p. 17 (1975).

123. Saums, H.L.; Pendleton, W.W., "Materials for Electrical Insulating and Dielectric Functions" Hayden Book Co. (1973).

124. ibid. p. 308

125. ibid. p. 309

126. ibid. p. 311

127. ibid. p. 371

128. Schied, F., "Theory and Problems of Numerical Analysis", McGraw-Hill Book Co. (1968).

129. Seikii, Y.; Yoda, B., "Statistical Investigation of Fatigue Deteriroration of Rubber and Plastic Insulated Cables Caused by Impulse Voltage", Elect. Eng. in Japan, Vol. 91, no. 4, p. 161 (1971).

130. Shiga, T; Kawashima, M; Inagaki, Y., "Application of the Theory of Extreme Value Distribution to the Breakdown Voltage of Cables", Sumitomo Electric Technical Review, no. 13, p. 17 (Jan.) (1970).

131. Sie, T.H.; Wohlfarht,O.F., "Contribution to the Measurement of the Impulse Withstand Voltage of Oil-Paper Insulation Systems", Trans. IEEE Vol. PAS-88 no. 6, p. 862 (1969).

132. Sie, T.H.; Wohlfarht, O., "Transference of Test Results from Experiments on Small Models to n Times Larger Test Objects with Insulation Oil", T.A.I.E.E. Vol. 81 p. 601 (Dec.) (1962).

133. Simo, E., "Large Scale Dielectric Test of Transformer Oil with Uniform Field Electrodes", IEEE Trans. on Electr. Insul., Vol. EI-5, no. 4, p. 121 (1970).

134. Simoni, L., "A New Approach to Voltage Endurance Test on Electrical Insulation", IEEE Trans. on Elect. Insul. Vol. EI-8, no.3, p. 76 (1973).

135. Singh, B.; Chadband, N.G.; Smith, W.C.; Calderwood J.H., "Prebreakdown Processes in Electrically Stressed Insulating Liquids", J. Physics 'D': Appl. Phys. Vol. 5 p. 1457 (1972).

136. ibid. p. 1463

137. ibid. p. 1459

138. Smith, C.W.; Calderwood, J.H., "Studies of Pre-Breakdown Phenomena in Liquid Dielectrics Using an Image Intensifier", Phénomènes de Conduction Dans les Liquides Isolants, no.179 Editions du Centre National de la Rechereche Scientifique p.161 (Grenoble) (1970).

139. ibid. p. 166

140. Spitzer, F.R.J., "Prebreakdown Conduction Current in Insultaing Liquids". Ph.D. Thesis, University of London p. 179 (1967).

141. ibid. p.16

142. ibid. p.178

143. ibid. p. 143

144. Streeter, V.L., "Handbook of Fluid Dynamics", McGraw Hill, 5th Edition (1971).

145. Theophilus, G.D.; Srivastava, K.D.; Van Heeswijk, R.G. "In-Situ Observation of Microparticles in a Vacuum Insulated Gap Using a Scanning Electron Microscope", J. of Appl. Phys., Vol. 47, no. 3, p. 897 (1976).

146. Tsumoto, M.; Okiai, R., "A New Application of Weibull Distribution to Impulse Breakdown of Oil-Filled Cable", IEEE Trans. on Power Apparatus and Systems, Vol. PAS-93, no. 1, p. 360 (1974).

147. Tsutsumi, Y.; Higaki, M., "Number of Solid Impurities in Transformer Oil", Elect. Eng. in Japan, Vol. 91, no. 6, p. 86 (1971).

148. Volkov, V.N.; Mit'kin, Y.A. "Formation of Bridges in a Liquid Placed in an Electric Field", Fluid Mech. -Soviet Research, Vol. 3, no. 1, p. 7, (1974).

149. Ward, B.W.; Lewis, T.J., "A New Statistical Theory for the Breakdown of Liquid Hydrocarbons", J. of the Electrochem. Soc., Vol. 107, no.3, p. 191, (1960)

150. ibid. p. 192

151. ibid. p. 193

152. Weber, K.H.; Endicott, H.S., "Area Effect and its Extremal Basis for the Electric Breakdown of Transformer Oil", AIEE Trans., Vol.75, p. 371 (1956).

153. Weber, K.H.; Endicott, H.S., "Extremal Area Effect for Large Area Electrodes for the Electric Breakdown of Transformer Oil", Trans. AIEE Vol. 76, p. 1091 (1957).

154. Weast, R.C., "Handbook of Chemistry and Physics", Forty-ninth Edition,The Chemical Rubber Co. (1968).

155. Weibull, W., "Fatigue Testing and the Analysis of Results", Permagon Press, p. 192 (Oxford) (1961).

156. Zaky, A.A.; Nosseir, A.; Megahed, I.Y.; Evangelou, C. "Electrical Breakdown of Mineral Oil Under Non-Uniform Fields", J. Phys. D. Appl. Phys., Vol. 9, p. 198, p. 2287 (1976).

157. Zaky, A.A.; Nosseir, A.; Megahed, I.Y.; Evangelou, C. "Effect of Polarity and Gap Length on the Breakdown Characteristics of Mineral Oil for Non-Uniform Fields", J. Phys. D. Phys. Vol. 9, p.L77 (1976).

158. Zaky,A.A.; Megahed, I.Y.; Evangelou, C.E.; "The Effect of Organic Additives on the Breakdown and Gassing Properties of Mineral Oil", J. Phys. D. Appl. Phys. D. Appl. Phys. Vol. 9, p. 841 (1976)

159. ibid. p. 849

160. ibid. p. 848

161. This Thesis, Chapter 3, p. 83

****